THE AMERICAN PHYSICAL SOCIETY

OFFICERS OF THE SOCIETY

[illegible]	Ernest G. Gunn	University of Chicago, Chicago, Ill.
[illegible]	W. F. G. Swann	Bartol Research Foundation, Philadelphia, Pa.
[illegible]	W. S. [illegible]	Columbia University, New York City
[illegible]	G. B. Pegram	Columbia University, New York City
[illegible]	James T. Tate	University of Minnesota, Minneapolis, Minn.
[illegible] Secretary for Pacific Coast	L. B. Lamb	University of California, Berkeley, Calif.

THE PHYSICAL REVIEW

[illegible]ished by the American Physical Society at 449 Atwater St., Menasha, Wis. Executive [illegible] University of Minnesota, Minneapolis, Minn. Two volumes annually, twelve issues per [illegible].

[illegible] series. From July 1, 1893, to January 1, 1913, the Review was conducted by Edward [illegible], Ernest Merritt and Frederick Bedell, with the financial support of Cornell University. [illegible] four volumes were issued annually; subsequent volumes, semi-annually; thirty-five [illegible] in all.

[illegible] series. On January 1, 1913, the Review was transferred to the American Physical [illegible] as announced on the first page of the new series which was then begun. Since then it has [illegible] conducted by a Board of Editors elected by the Society. Semi-annual volumes begin in [illegible] and July. Since July 1, 1920, the Review has been issued twice a month.

[illegible]ubscriptions are referred to page 2 of the advertisements for further information.

Annual Subscription, throughout the Postal Union, $10.00 in advance.

Single copies of current volume, $1.00.

[illegible] Index, 1893-1920, $4.00, in advance.

[illegible] Volumes, $4.00 per volume; Back Numbers, $1.00 per copy for issues prior to July 1, [illegible] (Vols. 1-32), $.50 per copy for issues subsequent thereto. Postage is free if remittance [illegible] with order; otherwise postage is extra. No bound volumes can be supplied. The Review [illegible] to purchase a limited number of First Series, Vol. 1, No. 1 (at $2.00 each); Second Series, [illegible] Vol. 1, No. 1, January 1916; Vol. 7, No. 2, February 1916; Vol. 7, No. 4, April 1916; and Vol. 7, [illegible], May 1916 (at $1.00 each).

[illegible] advertisements. Rates will be supplied by the Editor on request. Copy for each number [illegible] be received at Minneapolis two weeks prior to the date of issue; old copy is used until new [illegible] received. Send electrotypes direct to the publishers, George Banta Publishing Co., Menasha, [illegible].

[illegible] of the payment is allowed subscription agencies and members of the American Physical [illegible].

[illegible] of address and Complaints of failure to receive the Review, in the case of members [illegible] Physical Society, should be addressed to the Treasurer in the case of other subscribers to [illegible] St., Menasha, Wis.; or to the Editor. New copies can be sent free in response to [illegible] of non-delivery only if notice of non-delivery is received within three months of date [illegible].

[illegible] Communications should be addressed to the Physical Review, University of Minne[illegible], Minn.

[illegible] at the postoffice at Menasha, Wis., as second class matter. [illegible] for mailing at special rate of postage provided for in section 1103, Act of October 3, 1917, authorized November 6, 1918.

Second Series *July 15, 1930* *Vol. 36, No. 2*

THE

PHYSICAL REVIEW

THE INCOMPLETE PASCHEN-BACK EFFECT

By J. B. Green

Mendenhall Laboratory of Physics, Ohio State University

(Received May 23, 1930)

Abstract

Darwin's calculations for the Zeeman effect have been applied to the most noted examples of discrepancy between the older quantum theory and experiment, those of the Cu $^2P^2D$ multiplet, and the Mg and Be $^3P^3S$ multiplets. The positions and intensities of the lines calculated are in very good agreement with the experiment. The distorted Zeeman patterns of $^3P^3D$ of Mg and $^2P^2D$ of Na are attributed to the action of the magnetic field on ^3P and ^2P separations.

HEISENBERG and Jordan,[1] and Darwin[2] have applied the new quantum mechanics to the calculation of the standard Zeeman effect at all field-strengths. This had previously been done only for weak and strong fields, but not for intermediate field-strengths. Kronig[3] and Fowler[4] have also given rules for intensities. Mensing[5] has applied these results to the case of the $^2P^2D$ multiplet of sodium, and to the $^3P^3D$ multiplet of Mg, and has shown that the observed intensities are in excellent agreement with the theory.

In both of these cases, however, the D separation is practically zero, and we therefore have the case of a very strong field for the D separation while it is a very weak field for the P separation. In this paper the author has sought for some intermediate cases in which the field-strength gives separations of the same order of magnitude as the Zeeman separation.

I. The Spectrum of Copper

The most conspicuous example of this sort is given by the excellent work of Back[6] on the $^2P^2D$ multiplet of copper, λλ5220, 5218, 5153. In this case, the ^2D separation is 6.90 cm^{-1} while the Zeeman separation is 1.76 cm^{-1}. From Darwin's work we get the formula for the positions of the levels in the magnetic field, W

[1] Heisenberg and Jordon, Zeits. f. Physik **37**, 263 (1926).

[2] Darwin, Proc. Roy. Soc. **A115**, 1 (1927); see also K. Darwin, Proc. Roy. Soc. **A118**, 264 (1928).

[3] Kronig, Zeits. f. Physik **31**, 885 (1925).

[4] Fowler, Phil. Mag. **1**, 1079 (1925).

[5] Mensing, Zeits. f. Physik **39**, 24 (1926).

[6] Back, Ann. d. Physik **70**, 333 (1923).

$$- a_{m_l-1,\,m_s+1}\beta(l - m_l + 1)(s + m_s + 1)$$
$$+ a_{m_l,m_s}[W - \beta \cdot 2m_s m_l - \omega(m_l + 2m_s)]$$
$$- a_{m_l+1,\,m_s-1}\beta(l + m_l + 1)(s - m_s + 1) = 0.$$

The a's are numerical coefficients related to the intensities. We write down this equation for every permitted value of m_s and m_l and group the equations thus found into sets in which $m_s+m_l=m$, is the same. The determinant of each group thus found gives us the values of W for that particular value of m. For the intensity formulae, the reader is referred to Darwin's work.

In the case of the Cu multiplet, the value of $\beta=6.90/5=1.38$ cm^{-1} for the ^2D levels, and $248.3/3=82.77$ cm^{-1} for the P levels, while $\omega=1.76$ cm^{-1}. The results are given in Table I.

TABLE I

Position of undisturbed line	Observed position in magnetic field	Calculated new theory (1)	Calculated old theory (2)	Obs. Int.	Calc. Int. (1)	Cal. Int. (2
	18.764	8.835	8.863	1	1	1
	.735	.770	.800	6	3	3
	.704	.715	.737	7	5	5
	.670	.673	.673	8	8	8
	.279	.276	.295	7	7	7
	.205	.205	.232	10	10	10
5218.200	.137	.137	.168	10	9.5	10
	.085	.090	.105	7	6	7
	17.729	7.727	.727	8	8	8
	.644	.647	.663	7	4.5	5
	.560	.573	.600	1	2	3
		.508	.537	0	.5	1
	20.857	20.864	20.837	2	1	3
	.600	.615	.585	5	4	4
	.433	.474	.459	8	4	10
	.282	.354	.332	4	1	3
5220.080	.148	.235	.206	1	1	1
	19.959	19.985	19.954	1	2	1
	.845	.846	.828	4	3	3
	.727	.726	.701	10	10	10
	.608	.604	.575	5	4	4
	.367	.356	.323	3	3	3
	53.652	3.652*	3.660	7	7.5	7.5
	—	.599	.598	0	2.5	2.5
5153.26	.292	.291	.291	10	10	10
	.228	.229	.229	10	10	10
	52.909	2.921	2.922	4	2.5	2.5
	2.850	.850	2.862	9	7.5	7.5

(The multiplet $^3P^2D$ of Cu, H = 37,000 g)
* See text.

A study of the table shows that the newer theory gives much better agreement with experiment than the older theory for 5218 and 5220 except in one component 5220.433. All the other exceptions are very faint lines, which are too difficult to measure with any degree of accuracy. The distortion of intensities is also in the direction indicated by the newer theory.

5153 according to the new theory should be shifted 0.029A to the red. This amount has been subtracted from all the calculated wave-lengths to show the distortion of the pattern, in almost complete agreement with the experiment.

II. The Spectrum of Beryllium

Beryllium furnishes a very good example for the theory, since the ^3P separation is very small, much smaller, in fact, in comparison with the field-strengths available, than the ^2D separations of copper. We are, however, faced with a difficulty, in that the theory has been worked out for the "standard" Zeeman effect. This means that the coupling between the l and s vectors must be such that the ordinary Landé g and γ rules are obeyed. In the case of Be, we should expect the ratio $\Delta\nu_{21}/\Delta\nu_{10}=2:1$ whereas Back[6] has found 3.58:1. The total separation is 3.02 cm^{-1} and if we take β for the P_{21} separa-

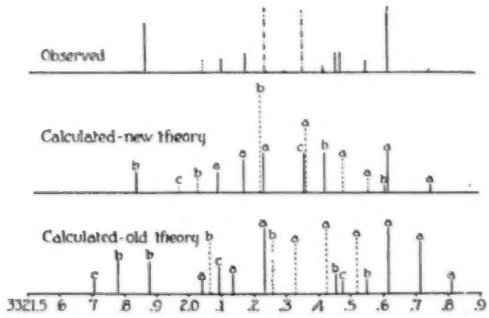

Fig. 1. The Zeeman effect of the Be $^3P^3S$ triplet. Lengths of lines indicate intensities. Dotted lines indicate parallel polarization, full lines perpendicular polarization, dot-and-dash lines double polarization. *a* indicates components of 3322.423. *b* indicates components of 3322.162. *c* indicates components of 3322.090.

tion, we get 0.59 cm^{-1} while for the P_{10} separation it is 0.33 cm^{-1}. Goudsmit[7] has shown, however, that the γ-sum is independent of the l-s coupling and hence β has been chosen as $3.02/6=0.503$ cm^{-1}.

The results are shown graphically in Fig. 1 for the $^3P^3S$ triplet at λ3322. While they are not so satisfying as the results for Cu, they are still seen to be very good indeed. Two discrepancies in polarization are apparent, and the author has no explanation for these. The presence of a σ-component of 3322.455 is not accounted for by the theory. Back[6] has attempted to account for the double polarization of the component of 3322.358 by saying that a σ-component of the line *b* has "crossed" a π component of the line *a*. The new theory shows no need for such an explanation, the double polarization being predicted.

III. The Spectrum of Magnesium

The $^3P^3S$ triplet of magnesium, λλ 5183, 5172, 5167 has been chosen as an example. Here, the ^3P separation yields $\beta=10.09$ cm^{-1}, and from Back's

[7] The Structure of Line Spectra, McGraw-Hill Company, 1930.

observations $\omega = 1.88$ cm^{-1}. The results are indicated in Table II. The intensities are relative only within one line and not from line to line. The calculated shifts of the lines are in general in the correct direction, while the intensities are in excellent agreement with experiment.

TABLE II.

	Observed	Calculated (1)	Calculated (2)	Obs Int.	Calc Int. (1)	Calc Int. (2)
	84.545	84.548	84.540	1	1	2
	.309	.300	.295	8	3.5	8
	.055	.049	.049	10	8	10
	83.821	83.808	83.803	7	7	8
5183.558	.576	.566	.558	10	10	10
	.326	.317	.312	9	7.5	8
	.076	.067	.067	10	7.5	10
	82.834	82.826	82.821	8	4	8
	.589	.584	.576	3	1.5	2
	73.691	73.681	73.658	4	3	5
	.418	.408	.413	5	4	5
5172.680	72.932	72.919	72.924	8	8	8
	.441	.430	.435	8	7.5	8
	71.954	71.941	71.946	5	4	5
	.737	.724	.701	6	5	5
	68.299	68.245	68.318	3	2.5	2
5167.342	67.326	67.269	67.342	4	4	4
	66.342	66.293	66.366	1	1.5	2

Back[8] has also measured the Zeeman effects of the $^3P^3D$ multiplet in magnesium, in which the ^3D separation has disappeared. Here, too, the patterns are distorted, and not so simple as one is at first led to believe. The photographs in Back-Landé, "Zeemaneffekt und Multiplett-struktur" show this effect very clearly, and it is to be attributed to the fact that the magnetic field is beginning to affect the ^3P separations as it does in the above example. In the $^2P^2D$ multiplet of sodium a similar effect is also taking place, and the pictures show a markedly distorted Zeeman pattern.

[8] Back, Zeits. f. Physik **33**, 379 (1925).

FINE STRUCTURE OF THE *K*-RADIATION OF THE LIGHTER ELEMENTS

By Lawrence Y. Faust
Randal Morgan Laboratory of Physics, University of Pennsylvania

(Received May 19, 1930)

Abstract

A vacuum spectrograph of simple construction is described in which it is possible to maintain bombarding currents of 150 milliamperes. With a line grating on glass (1179 lines per mm) photographs, some measurable in the second and third orders have been obtained of the soft x-radiation from beryllium, boron, oxygen and carbon, also from tungsten and certain heavier elements. Under analysis with a thermo-electric densitometer the *K* lines of the lighter elements, excepting oxygen, were found to be complex. The *K*-radiation of boron compounds contained 13 components, that of "pure" boron four, that of carbon nine whereas the beryllium radiation was still more complex. The relative intensities of these components was shown to depend on the energy used in stimulating them. The representative wave-length selected for the $K\alpha$ line was for oxygen 23.7A, for boron 69.3A, for carbon 45.3 while for beryllium the radiation embraced more than 15A with maxima at 107.2, 113.2 and 118.7A. The complex structure is thought to be partly a true fine structure and partly a system of satellites due to interaction with associated dissimilar atoms. A possible hypothesis is suggested in explanation of these results.

Introduction

THE possibility of diffracting soft x-rays from line gratings at small glancing angles was first pointed out by Professor A. H. Compton,[1] in 1923. Since that time important advances have been made, especially by Thibaud,[2] in the technique of this method, resulting in a number of valuable contributions to our knowledge of the frequencies and inter-relations of spectral lines in the soft x-ray region. Thibaud[3] has measured the *K* lines of carbon, oxygen, nitrogen and boron and the *L*, *M*, and *N* radiations of several elements of high atomic number. Other investigators including Hunt,[4] Osgood,[5] Weatherby[6] and Howe[7] have concentrated on the measurement of the *K* line of carbon in view of its possible value as a calibrating or reference line. Söderman[8] has made careful measurements of the *K* lines of the elements between magnesium and beryllium with the exception of neon. In addition to these wave-length measurements Bazzoni[9,10] Faust and

[1] A. H. Compton, Phil. Mag. **45**, 1121 (1923).
[2] Thibaud, Journ. de Phys. et le Rad. **1**, 13 (1927).
[3] Thibaud, Comptes Rendus, Jan., 1926. Thibaud, Phys. Zeits. **28**, 241 (1928).
[4] Hunt, Phys. Rev. **30**, 227 (1927).
[5] Osgood, Phys. Rev. **30**, 567 (1927).
[6] Weatherby, Phys. Rev. **32**, 707 (1928).
[7] Howe, Proc. Nat. Acad. Sci. Mar., 1928.
[8] Söderman, Zeits. f. Physik **52**, 795 (1929).
[9] Bazzoni, Faust and Weatherby, Nature, May 11 (1929) p. 717.
[10] Bazzoni, Faust and Weatherby, Abstract, Am. Phys. Soc., Washington Meeting, Apr., 1929, Phys. Rev. **33**, 1101 (1929).

Weatherby have studied the fine structure of the K lines of carbon and boron by densitometric methods.

It is evident that the line grating offers amongst other advantages the best means for investigating the K-radiation and associated K-absorption edges of the light elements. There is some reason to suspect that with the light elements the proximity of the K level to the exterior of the atom may cause a deviation from the simplicity of structure characteristic of K lines of the heavier elements. However, the researches listed above were for the most part carried out with too low resolving powers to bring out any fine structure in the K lines if such structure existed. The single exception to this statement is in the work of Bazzoni, Faust and Weatherby who densitometered the lines obtained in the first, second and third orders from a grating of 1179 lines per mm. These workers reported that the K line of carbon contains four components lying between 44.2, 44.9, 45.4 and 46.2A and that the K line of boron is of still more complex construction.

The investigation reported on in the present paper was undertaken to check in greater detail the measurements reported by these last mentioned authors and to extend such measurements to other elements of low atomic number.

The Apparatus

The apparatus consisted of a special vacuum spectrograph constructed of brass pipe in a design similar to that of Weatherby.[11] This apparatus differed from Weatherby's in several particulars. In the first place it was of larger diameter permitting the use of a photographic plate 5″ long at a distance of 40 cm from the grating. In the second place the anode-cathode structure was altered to make closer adjustment of clearances possible and to obtain a higher electron current. Both anticathode and filament were mounted on standards attached to a single plate which was wax-sealed to the spectrograph. A spiral filament was centered in an adjustable steel focusing ring coaxial with the anticathode. This ring, which formed one of the filament leads, was earthed and was separately water-cooled by a jacket surrounding the anticathode and insulated therefrom by a Pyrex tube. The other filament lead and the anticathode itself were also each water-cooled and were suitably isolated electrically by Pyrex insulation. The maximum clearance between the cathode and anticathode structure did not exceed 1/8 inch. This design incorporates the advantages of Dershem's[12] tube but is much simpler.

In order to prevent the fogging of the photographic plate as much as possible, carbon paper was introduced into the path of the direct and reflected beams. Considerable scattering resulted from the use of carbon paper, and later aluminum foil was substituted. This substitution resulted in producing clearcut, sharply measurable images of the direct and reflected beams.

[11] Weatherby, reference 6.

[12] Dershem, Journ. Optical Society of America **18**, 127 (1929).

Eastman x-ray plates were used in all the work with exposures varying from 15 minutes to six hours, three hours being the average.

The current to the anticathode was usually approximately 60 m.a. The driving potential was obtained from d.c. generators in series. A vacuum as low as 10^{-4} mm could be obtained in the spectrograph during operation by the action of a set of diffusion pumps.

The width of the two slits used in collimating the x-ray beam was 0.1 mm or less. The width of the grating used was 2 mm.

At this point attention may be called to the fact that Thibaud[2] has investigated the collimating properties of a grating at grazing angles. He obtains a formula for the variation of diffraction angle with the grazing angle.

$$\frac{di}{d\theta} = \frac{\theta/2}{(2n\lambda/d + (\theta/2)^2)^{1/2}}.$$

Thus when $\theta = 0$ the diffracted beam is parallel. The maximum variation of θ in this work due to the width of the grating and the width of the slits was $\Delta\theta = 5'$. Whence for a grating of 1179 lines per mm with an angle 3° at 50A, $di/d\theta = 0.2$. Thus corresponding to $5'$ for $\Delta\theta$ we have $1'$ change in i which corresponds at 50A to about 0.08A or about the experimental limit of accuracy. In general the values of θ and $\Delta\theta$ were about half the above values whence the error would be roughly 0.02A which is well within experimental error. It is therefore apparent that in the apparatus as used in this work errors due to lack of perfect collimation of the beams were negligible.

Measurements

The determination of the wave-length of a line is dependent (Fig. 1) on the measurement of the angles α and θ and the grating constant d used in the formula:

$$n\lambda = 2d \sin(\alpha/2) \sin(\alpha + \theta)/2.$$

The constant d, obtained by the usual procedure employing the 5461 line of the Hg arc was found to be 8481.8A corresponding to a ruling of 1179 lines per mm. The grating used was furnished by Professor R. W. Wood, to whom we hereby acknowledge indebtedness. Tan θ can be obtained by

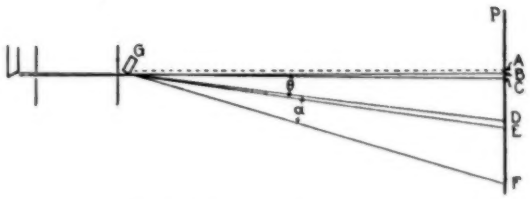

Fig. 1. Diagram of apparatus.

dividing the distance between the direct beam (*BC*. Fig. 1.) of x-rays passing by the grating and the beam (*DE*) reflected from the surface of the grating by the perpendicular distance (*GA*) from the effective center of the grating to the photographic plate.

The measurement of the distance GA was made on a comparator by comparison with a standard meter. The accuracy of this measurement was within 0.05 mm in 40 cm. Since care was taken to insure that the entire face of the grating was in the path of the incident beam, this measurement should correspond to the equivalent distance between grating and plate.

The distance BC to DE was found from a direct measurement on a Hilger traveling micrometer microscope of the extreme edges of the direct and reflected beams corresponding to the distance BE. This distance divided by the distance, GA, of the plate from the grating was taken as the corrected value for $\tan\theta$. An examination of Fig. 1 shows the justification of this procedure. BC is the direct beam image as found on the plate. In the absence of the grating this beam would extend from C to A. Thus AB is the position of the direct beam cut off by the grating and is therefore the effective direct beam. Then $BD+AB/2+DE/2$ represents the real distance between the reflected beam and effective direct beam. The distance AB is measured by DE since the width of DE is due to the divergence of the direct beam. Whence $BD+AB/2+DE/2=BE$.

Having determined θ we find α by measuring $\alpha+\theta$. $\mathrm{Tan}(\alpha+\theta)$ is equal to $BF+AB/2$ divided by the plate distance GA. In order to get $BF+AB/2$ it is necessary to add to BE which has been found already, the distance $EF+DE/2$.

Since the measurement of fine structure requires wave-length determinations for each component in the image F, the measurement of $EF+DE/2$ was carried out directly on the vacuum thermocouple densitometer. The width of the entrance slit in the diaphragm over the plate under investigation was 0.05 mm and this was therefore made the distance between successive plate settings in the line density measurements of the plates. To the moving part of the densitometer was attached a bar with fiducial mark which could be followed with the micrometer microscope and thus used to measure the distance that the plate moved.

In making a measurement the reflected line was placed in front of the densitometer slit. The plate was moved until the peak of the reflected line was found and the corresponding position of the fiducial mark was read on the micrometer. The plate was moved on its carriage until the diffracted line to be measured was near the slit. Readings on the galvanometer were taken every 0.05 mm from this point across the width of the diffracted line. Whenever the readings indicated a peak in the line, the position of the fiducial mark was read with the micrometer. The wave-length of each of these peaks was determined thus independently of the others in every case.

Curves produced by plotting the galvanometer deflections against wave-length proved to be reproducible in independent runs, thus suggesting the absence of any serious errors in this part of the work.

With the procedure described, measurements have been completed for the K lines of carbon, boron, oxygen and beryllium. These have been obtained in some cases in three orders. The combined effect of intensity of the line image and variation in dispersion for the different orders determined in

each case which order would give the best resolution of the fine structure under densitometer analysis.

CARBON

The lines of carbon were present on every plate although no carbon was placed on the anticathode. The source of this carbon is probably the grease vapor present at all times in the apparatus. In the 40 plates taken in this particular phase of the study (serial numbers 79 to 119) about 20 carbon lines were studied under the densitometer, the others being either too weak or too strong to give good resolution of the fine structure. Under visual observation most of the carbon lines appeared as continuous broad bands with maximum intensity on the short wave side. However, in several instances where small grazing angles were used, the first order carbon line appeared as a doublet, the shorter wave component being considerably the stronger.

A plot of the densitometer results obtained from a typical carbon line is shown in Fig. 2. Here the peaks indicate diminished transmission through the plates, i.e., the intensity maxima of x-radiation. It is apparent that here

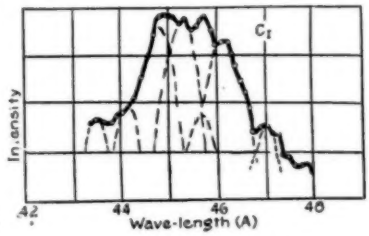

Fig. 2. Plot of densitometer results obtained from a typical carbon line.

we have a complex curve made up of several components. An attempt has been made to analyze this net curve into its constituents, a possible combination being shown in Fig. 2. An examination of this curve shows a rapid rise in intensity from the short-wave side to the first peak at 44.70A. A number of peaks follows with a gradual decrease in intensity to 46.20 where the curve again breaks in a sharp descent followed by a number of less prominent maxima. The small change of slope in the curve at 44.2A is a real effect and can be observed on all the curves of the carbon line. This demonstrates that the densitometer yields results sufficiently reproducible to attach a meaning even to a change of slope in the curve. The resolved lines shown in the figure are of course arbitrary to some degree. The position and magnitude of these components as shown do not represent the only way in which this curve could be built up. But little weight can be placed on the relative intensities of the minor components since that depends to a large degree on the method of choosing them.

The intensity of the line was found to depend on applied voltage. Although in general in soft x-ray spectroscopy the line intensity increases with

[13] Dershem, Phys. Rev. **34**, 1015 (1929).

the voltage and with increasing plate current, we find in the case of carbon that there is a decrease in line intensity with increase of these factors. This is in accord with the observations of Dershem[13] who explained the effect as due to the burning off of the carbon from the anticathode by the greater energy used. Thus only faint carbon lines appeared at 2700 volts.

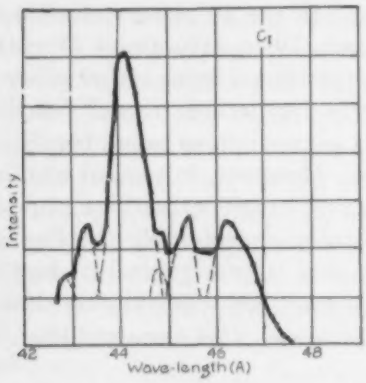

Fig. 3. Densitometer curve of the first order carbon line on a plate taken at 2300 volts.

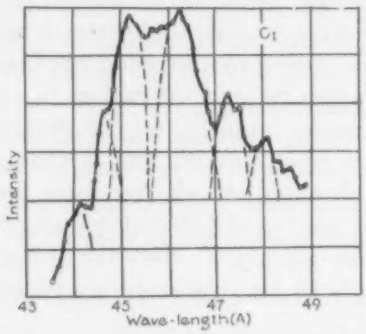

Fig. 4. Densitometer curve of the first order carbon line on a plate taken at 1500 volts.

It was found that the relative intensities of the components of the lines are dependent on the driving potential, the shorter wave components increasing in intensity relative to the long wave components at higher voltages. This interesting relation was specifically investigated by taking two series of plates under similar conditions excepting that the driving voltage for the one series was 1500 to 1600 volts and for the other series 2300 to 2800 volts.

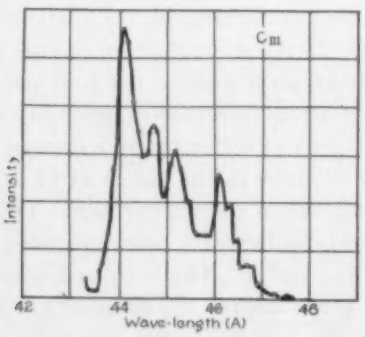

Fig. 5. Densitometer curve of a third order carbon line on a plate taken at 2500 volts.

Curves in Figs. 3 and 4 illustrate the different intensity distributions obtained in these tests. Fig. 3 is the densitometer curve of the first order carbon line on a plate taken at 2300 volts. This line under visual observation appeared as a doublet. A clearly defined peak is seen here at 43.3A. The curve then rises to a sharp maximum at 44.10A and shows two more distinct

peaks at 45.40A. Comparison with Fig. 2 shows that the small change of slope in that curve has now risen to the chief peak, the longer wave peaks being of less intensity. This is the case for all curves of lines taken at voltages of 2300 volts or more and therefore shows a shift of the maximum to the short wave side with increasing voltage.

Fig. 4 is a first order carbon line taken at 1500 volts. The principal peak is now at 45.3A with a second peak at 46.25. The short wave maxima have become reduced in intensity to mere kinks in the curve.

Fig. 5 is a densitometer curve of a third order carbon line showing unusually good resolution of the four principal maxima of the curve. This plate was taken at 2500 volts.

TABLE I

Plate No.	Order	Voltage	Wave-lengths of components of carbon.									
94	I	2300	42.70	43.23	44.10	44.70	45.4	46.25				
94	III	2300	42.90	43.24	44.00	44.65	45.25	46.00				
95	II	2300	42.60	43.06		44.48	45.28	46.20				
112	I	1900		43.45	44.05	44.62	45.35	46.20	46.55			
112	II						45.31		46.80			
97	I	1900				44.68	45.41	46.25		47.20	48.11	(weak)
113	II	1900			44.25	44.70	45.26	46.20	46.57	47.00		
114	I	1800			44.27	44.75	45.28	46.20		47.18	47.79	
114	II	1800			44.30	44.70	45.25					
116	I	1500			44.17	44.60	45.41	46.25		47.35	48.15	(weak)
115	I	1700				44.61	45.34	46.23		47.12	47.80	
115	II	1700	42.55	42.96	43.95	44.68	45.33	46.03		47.00		
93	I	2300	42.50	43.40	44.12	44.70	45.30					
96	I	1900			44.33							
79	III	2500		43.30	44.01	44.71	45.11	46.11	46.45	46.90	47.50	
87	I	1600	42.70	43.20	44.10	44.75	45.40	46.32	46.60	47.00		
Ave. values			42.66	43.23	44.05	44.66	45.33	46.20	46.60	47.21	47.70	

Taking all of the curves together there appears to be sufficient reason for concluding that the carbon K line contains 9 components centered about 42.7, 43.2, 44.0, 44.7, 45.3, 46.2, 46.6, 47.2, and 47.7A. We may also conclude that the relative prominence of these components and therefore the apparent position in the frequency scale of the unresolved line depends on the driving voltage, the maximum being 45.3A at 1500 volts and at near 44.0A at 2500 volts.

There is some uncertainty in the assignment of the title "$K\alpha$" to any particular component because of this shift in the maximum from 44.0 to 45.3A. Whatever the reason for the shift may be, it seems probable that the rate of decrease in intensity with decreasing voltage will be greater for the minor components than for the principal K line. Now since the 45.3A component was the maximum at 1500 volts, the lowest voltage at which lines could be obtained, it is perhaps justifiable to assign to the $K\alpha$ line of carbon the wave-length 45.33A.

No explanation can be offered at this time as to the significance of the fine structure here shown. Dr. C. B. Bazzoni has suggested that there is a possibility that the energy due to the excitation potentials of the other elements in combination with carbon interacts with the K-radiation of carbon to produce the satellite lines. The elements here in combination with the carbon are supposedly hydrogen and oxygen. It can be shown that the fre-

quency differences between the principal line and the various satellites are at least in qualitative agreement with this idea. There is also an agreement between the number of satellites observed and the number predicted from this consideration.

Boron

Boron lines were secured on 25 plates using boric acid, borax or boron on the anticathode. Fifteen of these lines were suitable for use in the densitometer. Second order boron overlapped the third order carbon line so that only the first order of boron could be measured.

The anticathodes of the boron compounds were prepared by fusing the compound on the anticathode. The line of pure boron was obtained by placing amorphous metallic boron obtained from Kahlbaum in a net-work of slots on the face of the anticathode.

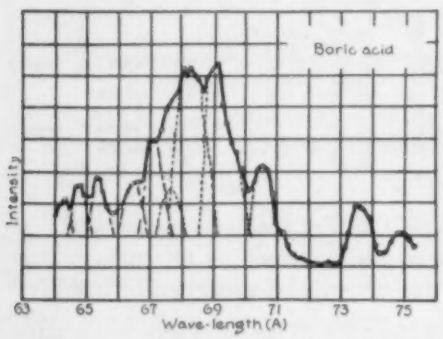

Fig. 6. Densitometer curve of a boron line taken with fused boric acid.

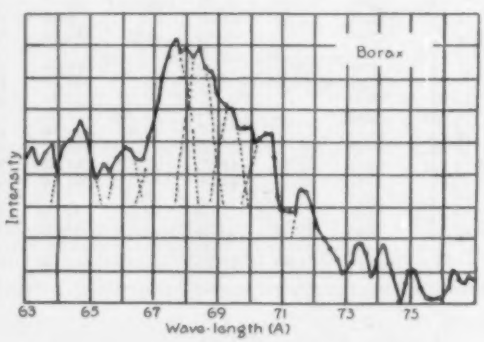

Fig. 7. Densitometer curve of a boron line taken with fused borax.

Under visual observation the $K\alpha$ line of boron appears as a continuous band broader than that of carbon. In several cases with small glancing angles the line appears to be just resolved into a doublet. The maximum of the line in general is on the short wave side. Two attendant lines on each side of the boron line are also visible to the eye in the spectra of boric acid and of borax. These attendant lines are absent in the spectrum of pure boron. This point was investigated carefully and plates from pure boron were obtained with lines even denser than the lines of the compounds with however no trace of satellites.

For given conditions of exposure the more intense lines of boron were obtained at higher voltages. Most of the lines of boron were obtained at 2300 volts more.

Fig. 6 shows a densitometer curve of a boron line taken with fused boric acid. This curve was resolved into components in a manner similar to that described for carbon. Fig. 7 is the plot of a line taken with fused borax on the anticathode. The conditions under which these plates were taken and the values of the resolved components are given in Table II

TABLE II.

Plate No.	Material	Voltage	Plate Distance	Wave-lengths of components of boron											
81	Borax	2500	30cm	64.85		66.43	67.37	68.28	69.30	70.30	71.63		73.26	73.90	75.00	76.60
83	"	2300	30	64.50			67.30	68.12	69.15	70.22	71.20	72.67		73.75	74.90	
102	"	1870	30	64.81		66.40	67.30	68.30	69.33	70.00	71.26	72.24	73.10		74.90	77.00
102(2)	"	1870	30			66.89	67.40	68.30	69.35	70.00	71.25	72.00				77.10
88	"	1850	30	64.72		66.70	67.70	68.40	69.38	70.20	71.20					76.46
68	Boric acid	2500		64.85	65.25	66.57	67.87		69.33	70.40	71.24	72.05	73.28	74.08	75.0	77.00
71	"	2500		64.75		66.40	67.52	68.10	69.30	70.40	71.25	72.00	73.28	74.13	75.0	
72	"	2500		64.40	65.69	66.49	67.40	68.11	69.07	70.51	71.20					
96	"	1900	30	64.40		66.52		68.14	69.10	70.20	71.50	72.17	73.36			76.45
97	"	1900	30		65.30	66.00	67.70		69.40			71.90	73.19	74.38		
73	Boron	2500	40				67.87		69.00							
74	"	2500	30				67.80	68.49	69.16	70.74						
94	"	2300	30				67.40	68.16	69.41	70.42						
95	"	2300	30				67.70	68.34	69.42	70.41						
114	"	1800	40				67.76	68.38	69.45	70.30						
Averages				64.68	65.45	66.55	67.61	68.38	69.33	70.36	71.32	72.03	73.20	74.00	74.95	76.75

No marked difference is observed between the fine structure of the borax lines and the boric acid lines. The densitometer curves of pure boron are shown in Figs. 8 and 9. It is seen that but four components remain in the lines in this case. It would appear, therefore, that the presence of the attendant lines may be due to the association of the boron with other elements.

The curve of Fig. 8 is for a line taken at 2300 volts while Fig. 9 shows a curve of a line taken at 1800 volts. As in the case of carbon, a definite shift of the maximum to the short wave side occurs with increasing voltage. Reasoning in a manner similar to that used in selecting the wave-length of the $K\alpha$ line of carbon it would appear justifiable to assign a wave-length 69.33A to the $K\alpha$ line of boron.

The results in Table II seem to show that there are 13 components in the lines obtained from the boron compounds located at 64.68, 65.45, 66.55, 67.61, 68.38, 69.33, 70.36, 71.32, 72.03, 73.20, 74.00, 74.95, and 76.75A and that the spectrum of the K-radiation of the boron used contains four components at 67.61, 68.38, 69.33 and 70.36A. All of these figures are uncertain in the second decimal place.

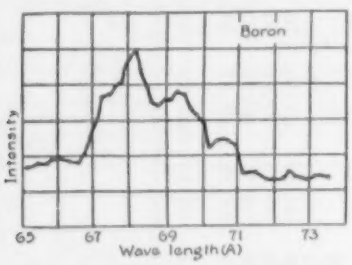

Fig. 8. Densitometer curve of pure boron line taken at 2300 volts.

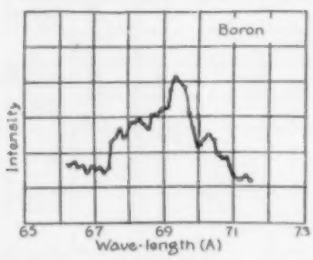

Fig. 9. Densitometer curve of pure boron line taken at 1800 volts.

It should be noticed that although the amorphous boron was "metallic" undoubtedly it contained appreciable percentages of oxide, hydride and probably nitride.

The explanation of the fine structure through the hypothesis of the development of addition and subtraction quanta through the interaction of the boron radiation with excited or neutral atoms associated in the molecular lattice is more difficult than for carbon. If we accept these results as showing that the K-radiation of boron is composed of four components, then to predict the fine structure of the compounds of boron on the above hypothesis, it is necessary to calculate these addition and subtraction quanta for each of the four compounds. Boron is associatd with oxygen in fused boric acid and with sodium and oxygen in fused borax.

These calculations being carried out the number of satellites predicted is found to be substantially the same as the number observed. Also in many cases a close concordance between predicted and observed wave-length is found. However, due to the fact that the lines predicted due to sodium are in all cases coincident within 0.1A with oxygen lines or original component lines no definite conclusions can be formulated at this time.

There can be no doubt that these attendant lines are associated with the $K\alpha$ of boron. They do not seem to be due to any other element. In no case was it found possible to secure the attendant lines in the absence of the boron line. It is of some significance that in every case where the attendant lines appeared the oxygen line was present also.

Oxygen

The $K\alpha$ line of oxygen appears on all plates of the boron compounds and on many others. Although several densitometer curves were taken of this

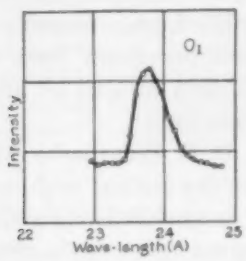

Fig. 10. Densitometer curve of a typical oxygen line.

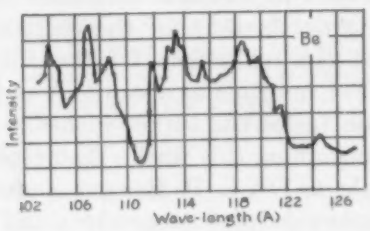

Fig. 11. Densitometer curve of the lines of beryllium.

line, only a single component appeared. Fig. 10 shows a curve of a typical oxygen line. The wave-length assigned to $K\alpha$ oxygen is 23.77 ± 0.06A.

Beryllium

A target of pure beryllium obtained from the Beryllium Company of America was used in the measurements of this element. Only faint traces of the presence of a line with three components could be obtained at 1800 volts using currents as large as 150 milliamperes for six hours. At 2700 volts beryllium lines of more intensity could be obtained using 40 milliamperes for two and a half hours. The line appears as a broad band with two distinct maxima. On the short wave side of this band a distinct line appears of the same intensity as the band.

Fig. 11 shows a densitometric curve of the lines of beryllium. Only four plates have been taken of this element of which three are suitable for use in the densitometer. It is not believed to be justifiable, therefore, to deduce values for the fine structure of the lines, but only for the three principal peaks. These maxima occur at 107.2 ± 0.4A, 113.2 ± 0.3A and 118.7 ± 0.2A. The great breadth, approximately 15A, of this line is peculiar to this element and should be remarked.

Discussion

It will be observed that the value we obtain for oxygen (23.77 ± 0.06A) is in good agreement with the value found by Söderman (23.77 ± 0.08A). Our value for beryllium (113.2 ± 0.3A) also checks with Söderman's value (113.4 ± 0.3) measured to the easily distinguishable maximum of this line.

The method of measurement used in our work in which a single component is selected from a group would seem to explain the divergence of our values for carbon and boron from those obtained by other investigators. Thus a visual measurement to the middle of the carbon line yields a value of 44.65A, in good agreement with the value of Söderman (44.70) and of Howe (44.62). The value (45.33) however, which we have finally selected based on a study of the components agrees very closely with the determination of Weatherby (45.4A). Similarly in the case of boron, a visual measurement to the middle of the line gives 67.8, in good agreement with Söderman's value (67.80 ± 0.2A) and with that of Thibaud (68.0A) while the value here selected for the principal maximum is considerably higher, namely 69.33A.

The great breadth of the carbon, boron and beryllium lines must be accepted as a real effect, for the $K\alpha$ line of oxygen at 23.77A and the N doublets of tungsten at about 56A and 60A are fine lines.

In conclusion the author wishes to thank Dr. B. B. Weatherby who aided him in beginning this work. And especially does the author wish to express his thanks to Dr. C. B. Bazzoni under whom this work was carried out and whose many helpful suggestions and keen interest are largely responsible for the success of these measurements.

THE SPARK SPECTRA OF SILVER AND PALLADIUM (Ag II AND Pd II)—AN EXTENSION

By H. A. Blair
Palmer Physical Laboratory, Princeton, N. J.

(Received June 9, 1930)

Abstract

An attempt was made to excite the $4f$ electron spectrum of Ag II in the Schüler tube with helium. Failure is discussed assuming the excitation process Ag normal atom $+He^+$. Some little extension was made to the lower spectrum. The Schüler tube was also used to extend the $4d^9 6s$ and $5d$ configurations of Pd II. About forty terms were added. A complete list of lines arising from high levels is given.

Ag II

AN ATTEMPT was made, using the Schüler tube, to excite the spectrum connected with the $4f$ electron in Ag II. By Hund theory this should consist of the set of terms ^{3} and ^1P, D, F, G, H in combination with the terms associated with the $5d$ electron. From analogy with other spectra the lines should lie in the lower half of the visible spectrum. Some fifty lines were measured in this region which could be allotted to the Ag II spectrum with reasonable certainty, but comparatively few were strong. About one quarter of these correspond to lines given in Kayser's Handbuch without displacement of wave-length. This lack of displacement further identifies these lines as being due to transitions from the $4f$ state for the following reason:—As is well known the lines due to transitions from high levels, which are diffuse when excited in the electric spark, are sharp when excited in the Schüler tube and besides have greater wave numbers by about two units. This means that the levels from which they arise are displaced by that amount toward their series limits. Since, however, the $4f$ levels will likely have a displacement similar to that known in the $5d$ it is to be expected that the lines due to transitions between them will not be displaced.

Among the lines observed some of the $5d$ differences were found, but it was not possible to identify any of the $4f$ terms with certainty on account of the fewness of the combinations. It appears that the Schüler tube is not well adapted to the excitation of this spectrum. This will be considered later in connection with the results in Pd II as well.

The spectral region from 2000 to 3000A which contains the lines of existing classifications of the silver spark, the most recent of which is due to Shenstone,[1] was also measured from Schüler tube plates. Shenstone's classification included all the predicted terms arising from the structures $d^9 5s$, $6s$, and $5d$, but the terms $5d^3P_0$ and $5d^1S_0$ were doubtful. The present measures gave about twenty new lines, some of which permitted these terms to be determined more reasonably, although the $^1S_0$ is much higher than expected

[1] Shenstone, Phys. Rev. **31**, 317 (1928).

TABLE I. *Ag II terms.*

$d^9 5d\,^3P_0$	89366.9	$d^9 5d\,^1S_0$	95287.5

These new terms are given in Table I. To correspond with the other terms as previously given by Shenstone about 2 cm^{-1} should be subtracted.

In Table II are given the new lines as well as the few old ones whose allocations have been changed. In each case the wave number and wave-length are from Schüler tube measurements. From each of these also should 2 cm^{-1} be subtracted that they may fit Shenstone's terms. In the case of the old lines the authors and intensities are given.

TABLE II. *Ag II lines.*

Wave-length	Author	*I*	*I*	Wave number	Designation
3329.71	F	3*u*	10	30023.9	$5p\,^1D_2^0 - 6s\,^3D_2$
3146.10	B		8	31776.2	$5p\,^1F_3^0 - 6s\,^3D_2$
2801.93	B		4	35679.2	$5p\,^1P_1^0 - 5d\,^3S_1$
2752.19	B		4	36324.0	$5p\,^1D_2^0 - 5d\,^3D_3$
2743.78	B		15	36435.3	$5p\,^3D_1^0 - 5d\,^3P_1$
2728.73	B		3	36636.3	$5p\,^1D_2^0 - 5d\,^3D_2$
2656.59	E	10*u*	10	37631.0	$5p\,^1F_3^0 - 5d\,^3P_2$
2617.01	B		12	38200.1	$5p\,^3D_1^0 - 5d\,^3P_0$
2587.24	B		3	38639.7	$5p\,^1P_1^0 - 5d\,^3P_0$
2435.07	B		2	39434.8	$5p\,^3P_0^0 - 5d\,^3S_1$
2506.91	B		1	39877.8	$5p\,^3F_3^0 - 5d\,^3P_2$
2454.20	B		4	40734.2	$5p\,^3P_2^0 - 6s\,^3D_2$
2411.59	B		20	41453.8	$5p\,^3D_1^0 - 5d\,^1D_2$
2317.26	B		1	43141.1	$5p\,^3P_1^0 - 5d\,^3P_2$
2265.85	B		3	44120.5	$5p\,^3D_1^0 - 5d\,^1S_0$
2243.44	S	9*U*	40	44560.6	$5p\,^1P_1^0 - 5d\,^1S_0$
2240.47	B		3	44619.6	$5p\,^3F_2^0 - 5d\,^3D_1$
2226.02	S	10*U*	15	44909.2	$5p\,^3P_1^0 - 5d\,^3P_0$
2210.32	B		4	45228.2	$5p\,^3P_2^0 - 6s\,^1D_2$
2120.81	B		2	47136.9	$5p\,^3P_1^0 - 5d\,^1P_1$

S—Shenstone F—Frings. E—Exner & Haschek. B—Author.

Some of the previously classified lines were greatly enhanced with the Schüler tube. These are λ3372 from 1 to 50, λ3269, 1 to 40, λ3223, 3 to 40, λ3184, 1*u* to 50, λ3129, 1*u* to 20. No reason can be given for these marked changes of intensity. The remainder of the lines in the group to which they belong, the 6*s*, although in most cases stronger, were not greatly different.

PD II

The spectrum arising from the electron configurations $4d^9$, $4d^8\,5s$ and $5p$ of Pd II has been very completely analyzed by Shenstone.[2] He was also able to classify a considerable number of the diffuse lines giving several of the $4d^8 6s$ and $5d$ terms. The present work is an extension of the analysis of the lines arising from the latter configurations.

Method of excitation. As with the silver, the Schüler tube was used for the excitation of the spectrum. The cathode used in each case was cylindrical, open at both ends, and measured 0.5 inches in diameter, and 1.5 inches in

[2] Shenstone, Phys. Rev. **32**, 1 (1928).

length. Helium was used to carry the current. It was purified by continuous circulation through a Misch metal discharge, and through chabazite cooled with liquid air. All gaseous impurities but hydrogen were soon removed by this method. A current of about 200 m.a. was used, the line voltage being 750 d.c. The gas pressure was kept between 3 and 4 mm, a much lower pressure, i.e., about 2 mm being found, as usual, to give the spark spectrum weakly compared with the arc. The photographs were made with the Hilger E1 quartz spectrograph. The extent of excitation is discussed later.

The data. In Table III is given a list of all the lines obtained, both classified and unclassified. The unassigned lines were included since the accuracy of measurement is probably sufficient to render a repetition of the

TABLE III. *Pd II lines.*

Wave-length	Author	I_1	I_2	Wave number	Designation
3382.57	S	1	10	29554.8	$ap^3F_{2\frac{1}{2}}^0-6s^4F_{2\frac{1}{2}}$
3377.35	B		2	29600.5	
3371.69	B		3	29650.2	
3365.99	B		2	29700.4	
3355.93	B		5	29789.5	
3352.19	B		3	29822.7	
3348.46	B		1	29855.9	$ap^2D_{2\frac{1}{2}}^0-ed^4F_{2\frac{1}{2}}$
3348.11	B		1	29859.0	
3315.64	B		1	30151.4	
3282.96	B		1	30451.6	$kp^3H_{4\frac{1}{2}}^0-ed^3F_{3\frac{1}{2}}$
3280.65	B		4	30473.0	
3278.05	B		3	30497.2	$cp^3F_{3\frac{1}{2}}^0-ed^4D_{3\frac{1}{2}}$
3276.24	B		1	30514.0	
3274.96	B		3	30525.9	
3261.72	B		2	30649.9	
3241.79	B		3	30838.3	
3237.44	B		1	30879.7	$ep^2P_{\frac{1}{2}}^0-6s^4P_{\frac{1}{2}}$
3221.12	B		1	31036.2	
3220.46	B		2	31042.5	$ep^2P_{\frac{1}{2}}^0-6s^2P_{\frac{1}{2}}$
3212.70	B		1	31117.5	
3210.48	B		6	31139.0	$ep^2D_{2\frac{1}{2}}^0-ed3_{2\frac{1}{2}}$
3206.88	B		3	31174.0	$ep^2S_{\frac{1}{2}}^0-6s^2P_{1\frac{1}{2}}$
3206.39	B		1	31178.7	$cp^2F_{3\frac{1}{2}}^0-ed^4F_{4\frac{1}{2}}$
3201.04	B		3	31230.9	
3189.34	B		4	31345.4	
3184.59	B		5	31392.1	$ap^4P_{1\frac{1}{2}}^0-6s^4F_{2\frac{1}{2}}$
3154.62	B		1	31690.4	
3153.16	S	2*u*	10	31705.1	$ep^2P_{\frac{1}{2}}^0-6s^2P_{1\frac{1}{2}}$
3149.83	B		1	31738.6	
3147.39	B		1	31763.2	
3146.51	B		1	31772.1	
3144.16	B		4	31795.8	
3138.33	B		3	31854.9	
3137.33	B		8	31865.0	$bp^4S_{1\frac{1}{2}}^0-6s^4P_{1\frac{1}{2}}$
3136.67	B		5	31871.7	
3135.41	S	10*ua*	3	31884.5	$bp^4D_{3\frac{1}{2}}^0-ed3_{3\frac{1}{2}}$
3123.61	B		3	32005.0	
3122.98	B		3	32011.4	
3117.70	B		1	32065.7	
3105.17	S	8*uA*	15	32195.1	$ap^4F_{3\frac{1}{2}}^0-6s^4F_{3\frac{1}{2}}$
3098.68	B		1	32262.4	$ep^2S_{\frac{1}{2}}^0-ed8_{\frac{1}{2}}$
3098.69	B		1	32263.3	
3091.28	B		1	32339.7	
3087.34	B		1	32381.0	

TABLE III (*continued*)

Wave-length	Author	I_1	I_2	Wave number	Designation
3086.26	S	3*u*	4*d*	32392.3	$ap^2F_{3\frac{1}{2}}^0-6s^2F_{2\frac{1}{2}}$ $ap^2F_{3\frac{1}{2}}^0-6s^4F_{2\frac{1}{2}}$
3083.18	B		1	32424.6	
3081.60	B		4	32441.3	
3079.97	B		2	32458.4	
3078.44	B		2	32474.6	
3077.01	B		6	32489.7	$bp^4D_{2\frac{1}{2}}^0-ed3_{2\frac{1}{2}}$
3072.11	B		1	32541.5	
3068.88	E	3*uA*	8	32575.7	$ap^2D_{2\frac{1}{2}}^0-6s^4F_{2\frac{1}{2}}$
3055.07	S	10*uA*	35	32723.0	$kp^2G_{4\frac{1}{2}}^0-6s^2G_{4\frac{1}{2}}$
3053.87	B		4	32735.8	$kp^2G_{4\frac{1}{2}}^0-6s^2G_{3\frac{1}{2}}$
3040.16	B		2	32883.5	$cp^2D_{2\frac{1}{2}}^0-ed3_{2\frac{1}{2}}$
3026.09	S	10*uA*	25	33036.3	$kp^2G_{3\frac{1}{2}}^0-6s^2G_{3\frac{1}{2}}$
3024.81	B		1	33050.3	$ap^2D_{1\frac{1}{2}}^0-6s^4F_{2\frac{1}{2}}$
3024.27	B		2	33056.2	
3020.86	B		1	33093.5	$bp^4D_{1\frac{1}{2}}^0-ed4_{\frac{1}{2}}$
3018.95	B		3	33114.5	$bp^4S_{1\frac{1}{2}}^0-6s^2D_{2\frac{1}{2}}$
3014.72	S	5*ua*	4	33160.9	$bp^4P_{2\frac{1}{2}}^0-6s^2F_{2\frac{1}{2}}$
3013.59	S	5*ua*	4	33173.4	$bp^4P_{1\frac{1}{2}}^0-6s^2F_{2\frac{1}{2}}$
2997.49	B		8	33351.5	$kp^2F_{2\frac{1}{2}}^0-6s^2D_{2\frac{1}{2}}$
2989.61	B		1	33439.5	
2955.28	S	2*uA*	5	33827.9	$ap^2G_{3\frac{1}{2}}^0-6s^2F_{2\frac{1}{2}}$
2951.66	B		2	33869.4	$cp^2D_{1\frac{1}{2}}^0-ed4_{\frac{1}{2}}$
2946.44	S	2*uA*	3	33929.4	$ep^2P_{1\frac{1}{2}}^0-6s^2P_{\frac{1}{2}}$
2944.53	B		1	33951.4	
2939.45	S	3*uA*	4	34010.1	$ep^2S_{\frac{1}{2}}^0-6s^2P_{\frac{1}{2}}$
2934.84	E	20*uA*	15	34063.5	$ap^4F_{2\frac{1}{2}}^0-6s^4F_{2\frac{1}{2}}$
2925.28	E	10*uA*	15	34174.8	$ap^2F_{2\frac{1}{2}}^0-6s^2F_{2\frac{1}{2}}$
2920.36	E	5*uA*	5	34232.3	$ap^2D_{1\frac{1}{2}}^0-6s^4F_{1\frac{1}{2}}$
2911.03	E	1*uA*	6	34344.1	$ep^2D_{2\frac{1}{2}}^0-6s^2P_{1\frac{1}{2}}$
2910.69	B		2	34346.1	
2900.25	E	2*u*	4	34469.7	
2889.97	E	2*u*	4	34592.3	$ep^2P_{1\frac{1}{2}}^0-6s^2P_{1\frac{1}{2}}$
2880.32	E	3*uA*	4	34708.2	$ep^2D_{2\frac{1}{2}}^0-6s^2P_{\frac{1}{2}}$
2877.88	E	100*uA*	20	34737.6	$ap^4F_{4\frac{1}{2}}^0-6s^4F4_{\frac{1}{2}}$
2871.20	E	100*uA*	25d	34818.5	$ap^2F_{3\frac{1}{2}}^0-6s^2F_{2\frac{1}{2}}$ $ap^2F_{3\frac{1}{2}}^0-6s^4F_{2\frac{1}{2}}$
2870.16	E	1*uA*	4	34831.0	$ap^2D_{1\frac{1}{2}}^0-6s^2F_{2\frac{1}{2}}$
2854.03	B		1	35027.9	
2853.51	S	10*uA*	10*d*	35034.3	$ap^4F_{3\frac{1}{2}}^0-6s^2F_{2\frac{1}{2}}$ $ap^4F_{2\frac{1}{2}}^0-6s^4F_{2\frac{1}{2}}$
2850.73	E	5*uA*	6	35068.4	$ap^2F_{3\frac{1}{2}}^0-ed^4D_{2\frac{1}{2}}$
2837.48	E	20*uA*	25	35232.2	$cp^2F_{2\frac{1}{2}}^0-ed3_{2\frac{1}{2}}$
2837.12	S	5*uA*	40	35336.7	$ap^2F_{2\frac{1}{2}}^0-ed^4F_{2\frac{1}{2}}$
2826.33	E	3*uA*	4	35371.2	$ep^2D_{1\frac{1}{2}}^0-6s^2P_{1\frac{1}{2}}$
2822.94	E	10*uA*	8*d*	35413.6	$ap^2D_{3\frac{1}{2}}^0-6s^2F_{3\frac{1}{2}}$ $ap^2D_{2\frac{1}{2}}^0-6s^4F_{2\frac{1}{2}}$
2821.68	E	30*uA*	15	35429.4	$ap^4\ F_{4\frac{1}{2}}-6s_4\ F_{3\frac{1}{2}}$
2815.31	B		1	35509.6	
2808.75	B		1	35592.6	$bp^4D_{3\frac{1}{2}}^0-ed9_{2\frac{1}{2}}$ $ep^2D_{2\frac{1}{2}}^0-6s^2D_{2\frac{1}{2}}$
2808.30	E	5*uA*	10	35598.3	$kp^2F_{3\frac{1}{2}}^0-6s^2G_{3\frac{1}{2}}$
2807.34	E	5*uA*	25	35610.4	$ap^2G_{3\frac{1}{2}}^0-6s^2F_{2\frac{1}{2}}$
2805.31	B		3	35636.2	
2800.74	B		10	35694.4	$bp^4D_{2\frac{1}{2}}^0-6s^4P_{1\frac{1}{2}}$
2800.44	E	5*uA*	20	35698.2	$ap^4G_{3\frac{1}{2}}^0-6s^4F_{2\frac{1}{2}}$
2792.68	B		1	35797.4	$ap^4F_{1\frac{1}{2}}^0-6s^4F_{2\frac{1}{2}}$
2791.62	B		2	35811.0	$bp^4D_{1\frac{1}{2}}^0-6s^4P_{1\frac{1}{2}}$
2791.32	B		1	35814.8	$cp^2P_{\frac{1}{2}}^0-ed4_{\frac{1}{2}}$
2791.11	B		4	35817.5	
2787.73	E	100*uA*	50	35860.9	$ap^2G_{4\frac{1}{2}}^0-6s^2F_{3\frac{1}{2}}$
2781.48	B		5	35941.5	$ep^2D_{2\frac{1}{2}}^0-6s^2P_{1\frac{1}{2}}$

TABLE III (*continued*)

Wave-length	Author	I_1	I_2	Wave number	Designation
2781.32	B		1	35943.6	
2776.63	E	150*uA*	50	36004.3	$ap^4G_{3\frac{1}{2}}^0-6s^4F_{4\frac{1}{2}}$
2770.00	B		1	36090.5	
2765.83	B		4	36144.9	
2762.95	B		3	36182.5	
2751.55	B		3	36332.4	$bp^4D_{2\frac{1}{2}}^0-6s^2D_{1\frac{1}{2}}$
2751.06	E	4*uA*	8	36338.9	$bp^4D_{3\frac{1}{2}}^0-6s^2D_{2\frac{1}{2}}$
2750.51	S	1*uA*	4	36346.2	
2745.48	B		1	36412.7	
2732.36	B		3	36587.6	$cp^2D_{1\frac{1}{2}}^0-6s^4P_{1\frac{1}{2}}$
2732.07	B		5	36591.5	$cp^2D_{2\frac{1}{2}}^0-ed9_{2\frac{1}{2}}$
2731.61	B		7	36597.6	$ap^2D_{2\frac{1}{2}}^0-6s^4F_{1\frac{1}{2}}$
2731.36	B		4	36600.9	$ap^2F_{3\frac{1}{2}}^0-6s^2F_{2\frac{1}{2}}$
2726.78	E	5*uA*	20	36662.4	$kp^2F_{3\frac{1}{2}}^0-6s^2G_{4\frac{1}{2}}$
2709.82	B		5	36891.9	$ep^2P_{\frac{1}{2}}^0-fd$ 14
2707.29	S	1*u*		36926.4	
2703.21	E	5*uA*	4	36982.0	$ap^4F_{1\frac{1}{2}}^0-6s^4F_{1\frac{1}{2}}$
2696.18	E	5*u*	6*d*	37078.5	$\left\{\begin{array}{l} ap^4G_{3\frac{1}{2}}^0-6s^2F_{2\frac{1}{2}} \\ ap^4G_{2\frac{1}{2}}^0-6s^4F_{2\frac{1}{2}} \end{array}\right.$
2693.72	E	10*uA*	35	37112.4	$kp^2H_{4\frac{1}{2}}^0-6s^2G_{4\frac{1}{2}}$
2680.67	S	1*u*	3	37293.0	$bp^4D_{2\frac{1}{2}}^0-6s^2P_{1\frac{1}{2}}$
2678.95	E	5*uA*	12	37317.0	$ap^4G_{4\frac{1}{2}}^0-6s^4F_{4\frac{1}{2}}$
2677.48	B		5	37337.4	$cp^2D_{2\frac{1}{2}}^0-6s^2D_{2\frac{1}{2}}$
2676.86	E	5*uA*	10	37346.1	$ap^4D_{2\frac{1}{2}}^0-6s^4F_{3\frac{1}{2}}$
2660.19	E	1*u*	5	37580.1	$ap^4F_{1\frac{1}{2}}^0-6s^2F_{2\frac{1}{2}}$
2653.57	B		2	37673.9	
2651.09	E	5*uA*	5	37709.1	$ap^4F_{2\frac{1}{2}}^0-ed^4D_{2\frac{1}{2}}$
2650.38	B		5	37719.3	$cp^2P_{\frac{1}{2}}^0-ed8_{1\frac{1}{2}}$
2644.07	B		3	37809.2	$kp^2F_{3\frac{1}{2}}^0-fd14$
2641.67	B		8	37843.6	
2636.37	B		1	37919.6	$\left\{\begin{array}{l} ap^2G_{4\frac{1}{2}}^0-ed^4D_{3\frac{1}{2}} \\ ap^2F_{3\frac{1}{2}}^0-ed^4G_{4\frac{1}{2}} \end{array}\right.$
2636.17	B		1	37922.5	
2633.41	B		1	37962.3	$\left\{\begin{array}{l} cp^2P_{1\frac{1}{2}}^0-6s^4P_{\frac{1}{2}} \\ ap^2F_{3\frac{1}{2}}^0-ed^4F_{3\frac{1}{2}} \end{array}\right.$
2632.33	E	2*u*	2	37977.8	$ap^4F_{2\frac{1}{2}}^0-ed^4F_{2\frac{1}{2}}$
2630.78	B		3	38000.9	$bp^4S_{1\frac{1}{2}}^0-fd13_{2\frac{1}{2}}$
2630.16	E	20*uA*	25	38009.2	$ap^4G_{4\frac{1}{2}}^0-6s^4F_{3\frac{1}{2}}$
2628.85	E	5*uA*	5	38028.1	$ap^4D_{1\frac{1}{2}}^0-6s^4F_{2\frac{1}{2}}$
2625.08	M	2*uA*	30	38082.7	$ap^2F_{2\frac{1}{2}}^0-ed^4G_{3\frac{1}{2}}$
2624.63	E	2*uA*	3	38089.3	$ap^2D_{2\frac{1}{2}}^0-ed^4D_{2\frac{1}{2}}$
2620.38	E	2*uA*	4	38151.0	$ap^4D_{\frac{1}{2}}^0-6s^4F_{\frac{1}{2}}$
2618.86	M	4*uA*	12	38173.2	$bp^4P_{2\frac{1}{2}}^0-ed3_{2\frac{1}{2}}$
2618.01	S	2*uA*	4	38185.6	$\left\{\begin{array}{l} bp^4P_{1\frac{1}{2}}^0-ed3_{2\frac{1}{2}} \\ cp^2D_{1\frac{1}{2}}^0-6s^2P_{1\frac{1}{2}} \end{array}\right.$
2615.12	S	1*u*	25	38227.8	
2612.89	B		4	38260.4	$ap^4G_{2\frac{1}{2}}^0-6s^4F_{1\frac{1}{2}}$
2606.20	E	2*uA*	6	38358.6	$ap^2D_{2\frac{1}{2}}^0-ed^4F_{2\frac{1}{2}}$
2600.79	B		1	38438.3	$cp^2P_{1\frac{1}{2}}^0-6s^2D_{2\frac{1}{2}}$
2597.52	B		1	38486.7	$ap^2F_{3\frac{1}{2}}^0-ed^2F_{3\frac{1}{2}}$
2594.41	B		1	38532.9	$cp^2P_{\frac{1}{2}}^0-6s^4P_{1\frac{1}{2}}$
2594.17	E	10*uA*	10*d*	38536.4	$\left\{\begin{array}{l} ap^4G_{3\frac{1}{2}}^0-6s^2F_{2\frac{1}{2}} \\ ap^4G_{2\frac{1}{2}}^0-6s^4F_{2\frac{1}{2}} \end{array}\right.$
2592.09	M	1*u*	2	38567.4	$cp^2F_{2\frac{1}{2}}^0-ed8_{1\frac{1}{2}}$
2588.58	B		1	38619.6	$bp^4D_{\frac{1}{2}}^0-ed4_{\frac{1}{2}}$
2587.15	E	3*uA*	50	38641.0	$kp^4G_{4\frac{1}{2}}^0-gd^2F_{3\frac{1}{2}}$
2586.52	B		2	38650.4	$bp^4S_{1\frac{1}{2}}^0-fd14$
2583.02	B		6	38702.8	$kp^2G_{3\frac{1}{2}}^0-gd^2D_{2\frac{1}{2}}$
2582.20	B		1	38715.1	
2580.23	B		1	38744.6	
2572.65	E	1*uA*	2	38858.8	$ap^4G_{2\frac{1}{2}}^0-6s^2F_{2\frac{1}{2}}$
2568.85	B		1	38916.2	$kp^2H_{4\frac{1}{2}}^0-6s^2G_{4\frac{1}{2}}$

TABLE III (*continued*)

Wave-length	Author	I_1	I_2	Wave number	Designation
2568.02	E	4*u*	10	38928.8	$kp^2H_{4\frac{1}{2}}^0-6s^2G_{3\frac{1}{2}}$
2567.20	B		3	38941.3	$cp^2F_{3\frac{1}{2}}^0-ed8_{2\frac{1}{2}}$
2565.92	B		1	38960.7	$ap^4F_{3\frac{1}{2}}^0-ed^4D_{3\frac{1}{2}}$
2565.72	B		1	38963.7	
2564.51	E	3*uA*	40	38982.1	$kp^2G_{3\frac{1}{2}}^0-gd^2F_{2\frac{1}{2}}$
2563.33	S	2*uA*	2	39000.0	
2561.67	B		4	39025.3	
2561.43	B		2	39029.0	
2553.74	E	1	20	39146.4	
2552.26	B		2	39169.2	$cp^2P_{\frac{1}{2}}-6s^2D_{1\frac{1}{2}}$
2551.54	B		4	39180.3	
2543.35	B		3	39306.4	$cp^2P_{\frac{1}{2}}^0-6s^4P_{\frac{1}{2}}$
2541.99	E	10*uA*	30	39327.4	$kp^2G_{4\frac{1}{2}}^0-gd^2G_{4\frac{1}{2}}$
2539.30	E	50*uA*	10	39369.1	$ap^4D_{3\frac{1}{2}}^0-6s^4F_{4\frac{1}{2}}$
2535.94	E	1	10	39421.3	
2534.11	E	5*uA*	35	39449.7	
2533.94	B		10	39452.4	
2532.21	E	1*u*	15	39479.3	
2526.76	B		4	39564.5	
2525.19	E	4*u*	10	39589.1	
2521.30	E	2*u*	5	39650.2	$bp^4D_{3\frac{1}{2}}^0-6s^2G_{4\frac{1}{2}}$
2520.59	E	1	1	39661.3	$bp^4D_{3\frac{1}{2}}^0-6s^2G_{3\frac{1}{2}}$
2518.13	E	7*uA*	40	39700.0	$kp^2G_{3\frac{1}{2}}^0-gd^2G_{3\frac{1}{2}}$
2515.33	E	5*uA*	20	39744.2	$bp^4P_{2\frac{1}{2}}^0-6s^4P_{2\frac{1}{2}}$
2513.11	B		1	39779.4	$ep^2P_{1\frac{1}{2}}^0-fd14$
2511.22	B		2	39809.3	$ap^4D_{1\frac{1}{2}}^0-6s^2F_{2\frac{1}{2}}$
2508.92	E	10*uA*	8	39845.7	$ap^4F_{3\frac{1}{2}}^0-ed^4F_{3\frac{1}{2}}$
2508.06	E	3*uA*	15	39859.5	$ep^2S_{\frac{1}{2}}^0-fd14$
2500.11	S	1*u*	12	39986.2	
2499.11	E	5*uA*	6	40002.1	$ap^4F_{3\frac{1}{2}}^0-ed^4G_{4\frac{1}{2}}$
2498.22	E	5*uA*	15	40016.4	$cp^2F_{2\frac{1}{2}}^0-6s^2D_{1\frac{1}{2}}$
2491.02	B		1	40132.1	$cp^2P_{\frac{1}{2}}^0-6s^2P_{1\frac{1}{2}}$
2488.62	B		1	40170.8	
2487.78	B		8	40184.4	$ap^4D_{2\frac{1}{2}}^0-6s^4F_{2\frac{1}{2}}$
2484.01	E	1	2	40245.3	
2482.60	E	1	1	40268.2	$bp^4D_{2\frac{1}{2}}^0-6s^2G_{3\frac{1}{2}}$
2481.75	E	2*u*	12	40281.9	
2479.03	E	20*uA*	12	40326.2	$ap^4F_{4\frac{1}{2}}^0-ed^4D_{3\frac{1}{2}}$
2478.84	B		4	40329.2	$\begin{cases} ap^2G_{3\frac{1}{2}}^0-ed2_{2\frac{1}{2}} \\ ap^2D_{1\frac{1}{2}}^0-ed4_{\frac{1}{2}} \end{cases}$
2478.57	B		2	40333.6	
2477.46	E	2*uA*	6	40351.7	$ap^2D_{1\frac{1}{2}}^0-ed^4F_{1\frac{1}{2}}$?
2476.57	B		20	40366.2	
2476.11	B		1	40373.8	
2475.89	B		2	40377.3	
2473.52	B		5	40416.0	
2472.96	B		1	40425.2	
2471.45	B		1	40449.8	
2469.77	B		6	40477.3	$ep^2D_{2\frac{1}{2}}^0-fd13_{2\frac{1}{2}}$
2469.06	B		2	40489.0	
2468.68	B		1	40495.2	$ap^4G_{3\frac{1}{2}}^0-ed^4D_{3\frac{1}{2}}$
2467.92	E	1	2	40507.7	$ap^2F_{3\frac{1}{2}}^0-ed^4G_{3\frac{1}{2}}$
2465.42	B		2	40548.8	
2463.97	E	1*uA*	4	40572.6	
2462.60	B		1	40595.2	
2461.89	B		4	40606.9	
2459.72	E	3*u*	7	40642.8	
2457.02	B		3	40687.4	
2456.31	B		2	40699.2	
2453.49	E	2*u*	6	40745.9	$ap^4F_{4\frac{1}{2}}^0-ed^4H_{5\frac{1}{2}}$
2452.76	B		4	40758.1	$ap^2F_{3\frac{1}{2}}^0-6s^4P_{2\frac{1}{2}}$
2452.39	E	3*u*	20	40764.2	

TABLE III (*continued*)

Wave-length	Author	I_1	I_2	Wave number	Designation
2451.04	B		8	40786.2	
2450.95	E	10*uA*	8	40788.2	
2449.92	S	2*u*	4	40805.3	
2444.20	E	20*uA*	12	40900.7	$ap^2F_{3\frac{1}{2}}^{\circ}-ed^4F_{2\frac{1}{2}}$
2443.88	B		1	40906.0	
2443.45	E	5*uA*	5	40913.3	$ap^2F_{3\frac{1}{2}}^{\circ}-ed^2F_{3\frac{1}{2}}$
2442.01	B		2	40937.4	
2441.81	B		1	40940.8	
2440.01	B		6	40969.9	
2437.81	E	10*uA*	10	41007.9	$ap^4F_{4\frac{1}{2}}^{\circ}-ed^4F_{4\frac{1}{2}}$
2436.39	E	20*uA*	25	41031.8	$ap^4F_{4\frac{1}{2}}^{\circ}-ed^4G_{5\frac{1}{2}}$
2432.72	B		1	41093.8	$bp^4D_{3\frac{1}{2}}^{\circ}-fd12_{3\frac{1}{2}}$
2431.46	B		25	41115.0	$ap^4F_{3\frac{1}{2}}^{\circ}-ed^4F_{3\frac{1}{2}}$
2426.71	B		3	41195.6	
2426.08	E	8*uA*	30	41206.2	
2425.74	B		6	41212.0	$ap^4F_{4\frac{1}{2}}^{\circ}-ed^4F_{3\frac{1}{2}}$
2425.02	B		3	41224.2	$bp^4D_{3\frac{1}{2}}^{\circ}-fd13_{3\frac{1}{2}}$
2422.62	E	4*uA*	12	41265.0	$kp^2F_{3\frac{1}{2}}^{\circ}-gd^2D_{2\frac{1}{2}}$
2422.37	B		8	41269.3	$ap^2D_{2\frac{1}{2}}^{\circ}-1_{2\frac{1}{2}}$
2421.95	E	2*uA*	4	41276.4	$ap^4G_{3\frac{1}{2}}^{\circ}-ed^4F_{4\frac{1}{2}}$
2420.22	B		1	41306.0	$bp^4D_{3\frac{1}{2}}^{\circ}-fd10_{3\frac{1}{2}}$
2419.41	E	2*uA*	4	41319.9	$ap^2F_{3\frac{1}{2}}^{\circ}-ed2_{2\frac{1}{2}}$
2418.56	B		3	41334.4	
2418.33	B		3	41337.2	$bp^4P_{2\frac{1}{2}}^{\circ}-6s^4P_{1\frac{1}{2}}$
2417.09	B		3	41359.5	
2416.57	E	6*uA*	20	41368.3	$ap^4D_{2\frac{1}{2}}^{\circ}-6s^4F_{1\frac{1}{2}}$ $ap^4F_{4\frac{1}{2}}^{\circ}-ed^4G_{4\frac{1}{2}}$
2416.32	B		2	41372.7	
2415.21	E	1*uA*	22	41391.6	
2414.95	B		2	41396.1	$ap^2F_{3\frac{1}{2}}^{\circ}-ed7_{3\frac{1}{2}}$
2413.91	B		8	41414.0	$ap^2D_{1\frac{1}{2}}^{\circ}-6s^4P_{2\frac{1}{2}}$
2413.20	B		1	41426.1	
2411.67	E	5*uA*	15	41452.5	$ap^2G_{3\frac{1}{2}}^{\circ}-ed6_{3\frac{1}{2}}$
2410.55	B		15	41471 6	
2408.47	B		1	41507.5	$ap^2D_{2\frac{1}{2}}^{\circ}-ed^2F_{3\frac{1}{2}}$
2406.34	B		60	41544.2	$kp^2F_{3\frac{1}{2}}^{\circ}-gd^2F_{3\frac{1}{2}}$
2405.99	E	1	2	41550.3	$ap^2G_{4\frac{1}{2}}^{\circ}-ed^4G_{5\frac{1}{2}}$
2401.38	E	30*uA*	40	41630.1	
2401.13	B		12	41634.4	
2400.97	E	5*uA*	12	41637.1	$ap^2G_{3\frac{1}{2}}^{\circ}-ed^2G_{4\frac{1}{2}}$
2400.31	E	1	2	41648.5	
2399.38	B		4	41664.6	
2398.72	B		25	41676.2	
2397.49	B		1	41697.6	$cp^2D_{2\frac{1}{2}}^{\circ}-fd10_{1\frac{1}{2}}$
2398.38	B		1	41699.4	$bp^4D_{2\frac{1}{2}}^{\circ}-fd12_{2\frac{1}{2}}$
2396.40	B		4	41716.5	$ap^2G_{4\frac{1}{2}}^{\circ}-1_{3\frac{1}{2}}$
2396.11	B		7	41721.6	
2394.55	B		8	41748.8	
2391.35	E	1	8	41804.6	
2391.06	B		3	41809.6	$cp^2D_{2\frac{1}{2}}^{\circ}-fd11_{1\frac{1}{2}}$
2390.71	E	2*uA*	15	41815.8	$bp^4D_{1\frac{1}{2}}^{\circ}-fd12_{2\frac{1}{2}}$
2389.89	E	1	2	41830.5	$bp^4D_{2\frac{1}{2}}^{\circ}-fd13_{2\frac{1}{2}}$
2387.55	B		5	41871.1	
2386.25	B		20	41894.0	$bp^4P_{1\frac{1}{2}}^{\circ}-ed8_{2\frac{1}{2}}$
2385.01	E	3*uA*	8	41915.6	$ap^2D_{2\frac{1}{2}}^{\circ}-ed2_{2\frac{1}{2}}$
2383.43	E	4*uA*	15	41943.6	$ap^4F_{3\frac{1}{2}}^{\circ}-ed^4F_{3\frac{1}{2}}$
2383.25	B		2	41946.6	$bp^4D_{1\frac{1}{2}}^{\circ}-fd13_{2\frac{1}{2}}$
2382.70	B		7	41956.4	$ap^2G_{4\frac{1}{2}}^{\circ}-ed^2F_{3\frac{1}{2}}$
2382.46	E	30*uA*	35	41960.5	
2382.26	B		2	41964.1	
2382.10	B		1	41966.9	$ap^4D_{2\frac{1}{2}}^{\circ}-6s^2F_{2\frac{1}{2}}$
2381.78	B		2	41972.6	$bp^4P_{1\frac{1}{2}}^{\circ}-6s^2D_{1\frac{1}{2}}$

TABLE III (*continued*)

Wave-length	Author	I_1	I_2	Wave number	Designation
2379.51	B		15	42012.6	$ap^4G_{5\frac{1}{2}}^0-ed^4H_{4\frac{1}{2}}$
2379.31	B		10	42016.2	
2378.55	E	2*uA*	30	42029.5	
2376.77	B		2	42061.1	$bp^4D_{1\frac{1}{2}}^0-fd11_{1\frac{1}{2}}$
2374.97	B		3	42092.9	$cp^2D_{2\frac{1}{2}}^0-fd12_{2\frac{1}{2}}$
2374.23	B		4	42106.1	$bp^4S_{1\frac{1}{2}}^0-gd^2D_{2\frac{1}{2}}$
2373.97	E	1	8*d*	42110.6	$bp^4P_{1\frac{1}{2}}^0-6s^4P_{1\frac{1}{2}}$
2372.96	E	2	4	42128.6	
2369.07	B		4	42197.8	$cp^2D_{1\frac{1}{2}}^0-fd10_{1\frac{1}{2}}$
2368.54	B		4	42207.2	$ap^2D_{1\frac{1}{2}}^0-ed3_{2\frac{1}{2}}$
2367.59	B		4	42224.0	$ap^2F_{3\frac{1}{2}}^0-ed5_{3\frac{1}{2}}$
2365.46	E	0*uA*	20	42262.2	$kp^2H_{4\frac{1}{2}}^0-gd^2G_{3\frac{1}{2}}$
2364.75	E	3*uA*	7	42274.9	$ap^4G_{5\frac{1}{2}}^0-ed^4F_{4\frac{1}{2}}$
2364.61	B		7	42277.3	
2364.07	B		7	42287.0	
2363.91	B		6	42289.9	
2363.41	E	5*uA*	18	42298.8	$ap^4G_{4\frac{1}{2}}^0-ed^4G_{5\frac{1}{2}}$
2362.95	B		8	42307.0	
2362.83	B		1	42309.2	$cp^2D_{1\frac{1}{2}}^0-fd11_{1\frac{1}{2}}$
2361.23	E	1*uA*	15	42337.9	$ap^4F_{2\frac{1}{2}}^0-ed^4F_{1\frac{1}{2}}$
2360.97	B		30	42342.5	$kp^2F_{3\frac{1}{2}}^0-gd^2D_{2\frac{1}{2}}$
2360.76	B		1	42346.2	
2359.14	E	4*uA*	75	42375.3	$ap^4G_{5\frac{1}{2}}^0-5d^4H_{6\frac{1}{2}}$
2358.95	B		3	42378.8	
2357.43	B		3	42406.1	
2355.57	E	3*uA*	20	42439.5	$ap^4F_{2\frac{1}{2}}^0-ed5_{3\frac{1}{2}}$
2355.34	B		3	42443.7	$ap^2F_{3\frac{1}{2}}^0-ed6_{3\frac{1}{2}}$
2350.72	E	1*uA*	10	42527 1	
2349.38	B		2	42551.3	
2349.02	E	2*uA*	8	42557.9	
2347.76	B		25	42580.6	$kp^2F_{3\frac{1}{2}}^0-gd^2F_{3\frac{1}{2}}$
2347.38	B		1	42587.5	
2347.17	E	8*uA*	10	42591.4	$ap^4F_{3\frac{1}{2}}^0-ed^4G_{3\frac{1}{2}}$
2345.52	B		8	42621.4	$kp^2F_{3\frac{1}{2}}^0-gd^2F_{2\frac{1}{2}}$
2344.77	B		1	42635.0	$ap^4G_{4\frac{1}{2}}^0-ed^4G_{4\frac{1}{2}}$
2342.50	B		1	42676.3	
2341.93	E	1	6	42686.8	
2340.26	B		3	42717.2	$ap^2D_{2\frac{1}{2}}^0-ed^4F_{1\frac{1}{2}}$
2339.95	E	1	15	42722.9	$cp^2D_{1\frac{1}{2}}^0-fd13_{2\frac{1}{2}}$
2339.65	B		1	42728.3	
2338.10	E	1*u*	2	42756.7	$ap^4F_{3\frac{1}{2}}^0-1_{3\frac{1}{2}}$
2335.57	B		5	42802.9	
2335.43	B		3	42805.5	
2334.04	E	1*uA*	2	42831.0	$ap^2G_{3\frac{1}{2}}^0-ed7_{2\frac{1}{2}}$
2333.32	B		3	42844.2	
2332.81	B		2	42853.6	
2332.47	E	4*uA*	8	42859.8	$ap^4D_{2\frac{1}{2}}^0-ed^4D_{2\frac{1}{2}}$
2331.94	B		1	42869.5	
2329.96	E	3*uA*	5	42906.0	$ap^4G_{4\frac{1}{2}}^0-ed^4D_{3\frac{1}{2}}$
2329.76	B		1	42909.7	$cp^2P_{1\frac{1}{2}}^0-fd11_{1\frac{1}{2}}$
2328.56	E	3*uA*	4	42931.8	$ap^4G_{2\frac{1}{2}}^0-1_{3\frac{1}{2}}$
2327.35	M	3*uA*	8	42954.1	
2326.11	E	1	7	42977.0	$bp^4P_{2\frac{1}{2}}^0-6s^2P_{1\frac{1}{2}}$
2325.12	E	3*uA*	3*d*	42995.3	$cp^2F_{3\frac{1}{2}}^0-6s^2G_{4\frac{1}{2}}$
2324.07	E	3*uA*	8	43014.7	
2323.34	E	2*uA*	12	43028.2	$ap^2F_{3\frac{1}{2}}^0-6s^2D_{1\frac{1}{2}}$
2322.79	B		3	43038.4	$ap^2D_{2\frac{1}{2}}^0-ed6_{2\frac{1}{2}}$
2320.56	B		5*d*	43079.7	$ap^4F_{1\frac{1}{2}}^0-ed4_{2\frac{1}{2}}$
2319.40	E	4*uA*	10	43101.4	$ap^4F_{1\frac{1}{2}}^0-ed^4F_{1\frac{1}{2}}$
2318.12	B		1	43125.1	$bp^4D_{1\frac{1}{2}}^0-fd14$
2317.96	E	2*uA*	5	43128.1	$ap^4D_{2\frac{1}{2}}^0-ed^4F_{3\frac{1}{2}}$
2317.23	B		1	43141.7	

TABLE III (*continued*)

Wave-length	Author	I_1	I_2	Wave number	Designation
2315.65	B		5	43171.2	$ap^4G_{2\frac{1}{2}}^0-ed^2F_{3\frac{1}{2}}$
2314.73	B		1	43188.2	
2314.47	E	1	4	43193.2	$cp^2P_{1\frac{1}{2}}^0-fd12_{2\frac{1}{2}}$
2313.80	B		4	43205.7	
2312.29	B		6	43233.9	$ep^2P_{1\frac{1}{2}}^0-gd^2D_{2\frac{1}{2}}$
2310.57	B		10	43266.0	$ap^2G_{4\frac{1}{2}}^0-ed5_{3\frac{1}{2}}$; $kp^2F_{3\frac{1}{2}}^0-gd^2G_{4\frac{1}{2}}$
2307.40	E	20*uA*	25	43325.4	$ap^4G_{4\frac{1}{2}}^0-ed^4H_{5\frac{1}{2}}$
2306.99	B		2	43333.2	
2306.71	B		2	43338.4	
2305.70	E	1	10	43357.3	
2304.89	S	1*u*	3	43372.7	$cp^2D_{1\frac{1}{2}}^0-fd14$
2304.35	B		7	43382.8	
2303.47	B		1	43399.3	$ap^4F_{2\frac{1}{2}}^0-6s^4P_{2\frac{1}{2}}$
2303.28	B		1	43402.9	$ap^4F_{3\frac{1}{2}}^0-ed2_{2\frac{1}{2}}$
2302.14	B		3	43424.4	
2295.71	B		4	43546.1	
2295.51	E	3*uA*	12	43549.9	$ap^2D_{1\frac{1}{2}}^0-ed8_{2\frac{1}{2}}$
2294.02	B		4	43578.1	$ap^4G_{2\frac{1}{2}}^0-ed2_{2\frac{1}{2}}$
2293.52	E	5*uA*	10	43587.7	$ap^4G_{4\frac{1}{2}}^0-ed^4F_{4\frac{1}{2}}$
2292.97	B		2	43598.1	
2290.72	B		1	43640.8	$ap^2F_{2\frac{1}{2}}^0-6s^2D_{2\frac{1}{2}}$
2287.55	B		10	43701.3	
2286.78	B		8	43716.1	$kp^2H_{5\frac{1}{2}}^0-gd^2G_{4\frac{1}{2}}$
2283.40	E	3*uA*	3	43780.9	
2283.09	B		3	43786.8	
2282.87	E	3*u*	5	43790.9	$ap^4G_{4\frac{1}{2}}^0-ed^4F_{3\frac{1}{2}}$
2282.40	E	2	12	43800.9	$ap^2D_{2\frac{1}{2}}^0-6s^4P_{2\frac{1}{2}}$
2281.37	E		4*d*	43819.7	$ap^2D_{1\frac{1}{2}}^0-6s^4P_{1\frac{1}{2}}$; $ap^2F_{3\frac{1}{2}}^0-ed7_{2\frac{1}{2}}$
2280.43	B		25	43837.8	
2277.33	E	4*ua*	3	43897.4	
2275.92	E	5*ua*	10	43924.7	
2274.70	E	2*ua*	3	43948.3	$ap^4G_{4\frac{1}{2}}^0-ed^4G_{4\frac{1}{2}}$
2272.13	B		1	43998.0	
2270.11	E	6*uA*	40	44037.1	$ap^4F_{2\frac{1}{2}}^0-ed7_{2\frac{1}{2}}$
2269.11	B		1	44046.5	
2268.42	B		1	44069.9	
2266.43	B		2	44108.6	$ap^4D_{1\frac{1}{2}}^0-ed^4F_{2\frac{1}{2}}$
2265.69	B		4	44123.0	$ap^4F_{4\frac{1}{2}}^0-1_{3\frac{1}{2}}$
2264.68	B		3	44142.6	$cp^2P_{1\frac{1}{2}}^0-fd10_{1\frac{1}{2}}$
2263.63	B		2	44163.2	$ap^4F_{1\frac{1}{2}}^0-6s^4P_{2\frac{1}{2}}$
2262.30	B		15	44189.0	
2261.72	E	2*uA*	20	44200.4	
2261.29	B		20	44208.8	
2260.45	E	6*uA*	18	44225.2	$ap^4G_{3\frac{1}{2}}^0-ed^4G_{3\frac{1}{2}}$
2259.32	S	1*u*	5	44247.2	$ap^4D_{1\frac{1}{2}}^0-ed4_{1\frac{1}{2}}$
2259.03	S	1*u*	3	44253.1	$cp^2P_{1\frac{1}{2}}^0-fd11_{1\frac{1}{2}}$
2257.06	B		1	44291.7	$ep^2D_{1\frac{1}{2}}^0-gd^2F_{2\frac{1}{2}}$
2254.30	B		20	44345.8	
2253.74	B		2	44357.0	
2252.98	B		1	44371.8	
2252.60	S	2*u*	5	44379.3	$ap^4G_{3\frac{1}{2}}^0-ed^4F_{1\frac{1}{2}}$
2247.40	S	3	3	44482.0	$ap^4G_{2\frac{1}{2}}^0-ed5_{3\frac{1}{2}}$
2245.11	S	1*u*	3	44527.3	$ap^4D_{1\frac{1}{2}}^0-ed2_{2\frac{1}{2}}$
2243.47	B		4	44559.8	
2243.29	B		1	44563.5	
2243.17	S	0*u*	2	44565.8	
2242.54	B		7	44578.3	
2242.34	B		1	44582.3	$ep^2D_{2\frac{1}{2}}^0-gd^2D_{2\frac{1}{2}}$
2241.51	B		4	44598.9	$ap^2D_{2\frac{1}{2}}^0-ed8_{3\frac{1}{2}}$
2240.57	S	1*u*	2	44617.7	$ap^4G_{3\frac{1}{2}}^0-ed^4F_{2\frac{1}{2}}$

TABLE III (*continued*)

Wave-length	Author	I_1	I_2	Wave number	Designation
2237.42	B		1	44680.5	$ap^4D_{2\frac{1}{2}}^0 - 6s^2F_{2\frac{1}{2}}$
2235.05	B		3	44727.7	
2234.25	B		15	44743.8	
2232.63	B		4	44776.2	
2231.36	B		10	44801.8	$ap^4F_{1\frac{1}{2}}^0 - ed7_{2\frac{1}{2}}$
2230.75	B		2	44814.0	
2230.43	B		4	44820.5	$ap^4D_{1\frac{1}{2}}^0 - ed^23_{2\frac{1}{2}}$ $ep^2D_{2\frac{1}{2}}^0 - gd^2F_{3\frac{1}{2}}$
2229.76	B		4	44833.9	$kp^2H_{4\frac{1}{2}}^0 - gd^2F_{3\frac{1}{2}}$
2229.55	B		1	44838.1	
2228.68	B		1	44855.5	
2228.40	B		5	44861.2	$ep^2D_{2\frac{1}{2}}^0 - gd^2F_{2\frac{1}{2}}$
2224.91	B		1	44931.5	
2224.14	B		2	44947.1	
2223.63	S	25*ua*	25	44957.5	$ap^4D_{3\frac{1}{2}}^0 - ed^4D_{3\frac{1}{2}}$
2223.57	B		2	44958.6	
2222.20	S	25*ua*	25	44986.3	
2220.40	B		1	45022.9	
2220.20	S	0	5	45026.9	
2216.49	B		4	45102.2	$cp^2F_{2\frac{1}{2}}^0 - fd11_{1\frac{1}{2}}$
2212.50	B		1	45183.7	
2210.57	S	0*u*	2	45223.1	
2206.32	B		4	45310.1	
2205.95	B		1	45317.8	$cp^2P_{\frac{1}{2}}^0 - fd14$
2205.41	S	0*u*	25	45328.9	$bp^4D_{3\frac{1}{2}}^0 - gd^2D_{2\frac{1}{2}}$
2204.80	B		2	45341.4	
2204.55	S	0*u*	4	45346.5	
2201.97	B		1	45399.6	
2200.09	B		2	45438.4	
2196.16	S	1*u*	20	45519.7	$kp^2H_{4\frac{1}{2}}^0 - gd^2G_{4\frac{1}{2}}$
2193.88	S	0*u*	15	45567.0	$bp^4D_{3\frac{1}{2}}^0 - gd^2F_{3\frac{1}{2}}$
2193.47	S	3*u*	4	45575.5	
2192.69	B		7	45591.8	$kp^2F_{2\frac{1}{2}}^0 - gd^2G_{3\frac{1}{2}}$
2192.11	B		1	45603.8	
2191.92	B		3	45607.8	$bp^4D_{3\frac{1}{2}}^0 - gd^2F_{2\frac{1}{2}}$
2190.55	B		4	45636.3	
2190.45	S	10*ua*	7	45638.7	$ap^4D_{3\frac{1}{2}}^0 - ed^4F_{4\frac{1}{2}}$
2184.34	S	0*u*	2	45766.1	
2181.54	B		1	45824.7	
2180.72	S	0*u*	2*d*	45841.9	$ap^4D_{2\frac{1}{2}}^0 - ed^4F_{3\frac{1}{2}}$
2178.30	B		5	45892.9	$ap^4F_{4\frac{1}{2}}^0 - ed6_{3\frac{1}{2}}$
2172.92	B		3	46006.7	
2171.38	S	3*u*	1	46039.2	$ap^4D_{2\frac{1}{2}}^0 - 1_{3\frac{1}{2}}$
2166.36	B		3	46145.9	
2166.04	B		1	46152.6	$ap^4D_{\frac{1}{2}}^0 - ed8_{1\frac{1}{2}}$
2164.41	B		3*d*	46187.4	
2163.18	B		2	46213.7	$bp^4D_{2\frac{1}{2}}^0 - gd^2F_{3\frac{1}{2}}$
2161.35	B		3	46252.9	$bp^4D_{3\frac{1}{2}}^0 - gd^2G_{4\frac{1}{2}}$
2158.74	S	0*u*	2*d*	46308.6	
2157.85	B		1	46327.6	$cp^2D_{2\frac{1}{2}}^0 - gd^2D_{2\frac{1}{2}}$
2155.91	B		2	46369.5	
2141.28	S	1*u*	1	46686.2	
2140.69	B		3	46699.1	
2124.33	S	1*u*	2	47058.8	$bp^4P_{\frac{1}{2}}^0 - fd11_{1\frac{1}{2}}$

E—Exner & Naschek
M—Meggers
S—Shenstone
B—Author
u—Diffuse
A—strong in arc
a—weak in arc.
Wave numbers measured, wave-lengths calculated.

I_1—Meggers' intensities except for Shenstone's lines.
I_2—Author's estimates from Schüler tube.
Author—Original observer.

work unnecessary. The standards used were the corrected Pd II sharp lines from Shenstone's classification. In general no greater variation than 0.5 cm^{-1} was necessary in satisfying the combination principle with new terms. All the normally diffuse lines were included, even when they had been previously given by Shenstone, since the accuracy of measurement is here much greater, since some of the classifications have been altered and since the usual displacement of the diffuse lines by 2–3 cm^{-1} prevents a consistent scheme. The complete line list of Pd II is obtainable by adding that here given to that of Shenstone's sharp lines.

TABLE IV. *Origin of high terms of Pd II.*

Pd III Config.	Term	Added Electron	Terms Theoretical	Terms Empirical
$4d^8$	^3F	$6s$	$^{4,2}F$	$6s^{4,2}F$
		$5d$	$^{4,2}P, D, F, G, H$	ed^4 D, F, G, H parts of
	^3P	$6s$	$^{4,2}P$	$6s^{4,3}P$ parts doubtful.
		$5d$		None identified.
	^1S	$6s$		None identified.
		$5d$		None identified.
	^1D	$6s$	^3D	$6s\,^3D$
		$5d$	$^3S, P, D, F, G$	fd Not nameable.
	^1G	$6s$	^3G	$6s\,^3G$
		$5d$	$^3D, F, G, H, I$	$gd\,^3D, F, G.$

In Table IV are given the electron configurations of the high terms, the predicted terms and those thought to have been found. The lettering corresponds to that in the list of high terms given in Table V. Where a term could not be reasonably placed in a group it was left unlettered.

The $6s$ **group.** It was found possible to complete the $6s$ group satisfactorily, except for the $^2P_{\frac{1}{2}}$ term, and possibly the $^4P_{1\frac{1}{2}}$ term, the former being particularly doubtful, as it requires the crossing over of the components of the doublet.

The convergence of the terms is odd in part. The $^4F_{4\frac{1}{2}}$ $^4F_{3\frac{1}{2}}$ separation has decreased from 2013.3 to 692.2 in going from the $5s$ to the $6s$ group, and these terms appear to be approaching the same limit as would be expected with the inverted type of convergence pointed out by Shenstone,[3,4] i.e., where equal J values do not cross. The $^4F_{2\frac{1}{2}}$ and $^2F_{3\frac{1}{2}}$ however, which are also expected to have the same limit have already crossed over each other, although just by one cm^{-1}. It would be interesting to find what would happen in the next series member as well as to investigate the "strong field" Zeeman pattern of the present one. The lines are too diffuse to do this with a source in air, but it might be accomplished at low pressure. The $^4F_{1\frac{1}{2}}$ and $^2F_{2\frac{1}{2}}$ have converged considerably, again as expected. The doubtful validity of two of the P terms renders a discussion of their convergence profitless. The ^2D has converted from -1227.2 to -612.9 while the ^2G which in the first member had an interval of only 108.2 has closed to 12.5. The indication is that each doublet is going to its own limit.

[3] Shenstone, Nature **122,** 727 (1928).
[4] Hund, Zeits. f. Physik **52,** 601 (1928).

TABLE V. *High terms of Pd II.*

No.	Term	Designation
*61	79535.0	$6s^4F_{4\frac{1}{2}}$
*62	80227.2	$6s^4F_{3\frac{1}{2}}$
*63	83065.0	$6s^2F_{2\frac{1}{2}}$
*64	83066.0	$6s^4F_{2\frac{1}{2}}$
*65	84249.0	$6s^4F_{1\frac{1}{2}}$
*66	84847.5	$6s^2F_{2\frac{1}{2}}$
*67	85123.5	$ed^4D_{2\frac{1}{2}}$
68	85543.5	$ed^4H_{5\frac{1}{2}}$
69	85740.9	$ed^4D_{3\frac{1}{2}}$
*70	85805.6	$ed^4F_{4\frac{1}{2}}$
71	85829.3	$ed^4G_{4\frac{1}{2}}$
72	85905.8	$ed^4H_{6\frac{1}{2}}$
*73	86009.3	$ed^4F_{3\frac{1}{2}}$
74	86166.0	$ed^4G_{4\frac{1}{2}}$
75	88754.7	$ed^4G_{3\frac{1}{2}}$
76	88920.4	$1_{2\frac{1}{2}}$
77	89147.2	$ed^4F_{2\frac{1}{2}}$
78	89160.0	$ed^2F_{2\frac{1}{2}}$?
79	89566.6	$ed\ 2_{2\frac{1}{2}}$
*80	89859.2	$ed\ 3_{2\frac{1}{2}}$
81	90345.9	$ed\ 4_{\frac{1}{2}}$
82	90368.7	$ed^4F_{1\frac{1}{2}}$
83	90470.5	$ed\ 5_{3\frac{1}{2}}$
84	90690.2	$ed\ 6_{3\frac{1}{2}}$
85	91430.6	$6s^4P_{2\frac{1}{2}}$
86	92068.7	$ed\ 7_{2\frac{1}{2}}$
87	92251.1	$ed\ 8_{1\frac{1}{2}}$
88	93063.6	$6s^4P_{1\frac{1}{2}}$?*
89	93567.5	$ed\ 9_{2\frac{1}{2}}$
90	93700.7	$6s^2D_{1\frac{1}{2}}$
91	93837.4	$6s^4\ P_{\frac{1}{2}}$
92	93999.6	$6s^2\ P_{\frac{1}{2}}$??
93	94313.6	$6s^2D_{2\frac{1}{2}}$
94	94662.6	$6s^2P_{1\frac{1}{2}}$
*95	97625.0	$6s^2G_{4\frac{1}{2}}$
96	97637.5	$6s^2G_{3\frac{1}{2}}$
97	98674.0	$fd10_{1\frac{1}{2}}$
98	98785.1	$fd11_{1\frac{1}{2}}$
99	99068.6	$fd12_{2\frac{1}{2}}$
100	99199.3	$fd13_{2\frac{1}{2}}$
101	99849.0	$fd14$
102	103304.2	$gd^2D_{2\frac{1}{2}}$
103	103542.6	$gd^2F_{3\frac{1}{2}}$
104	103583.5	$gd^2F_{2\frac{1}{2}}$
105	104228.3	$gd^2G_{4\frac{1}{2}}$
106	104301.5	$gd^2G_{3\frac{1}{2}}$

* Previously given by Shenstone, reference 2.

Intervals

$6s^4F$	692.2	2838.8	1183.0
$6s^2F$	1782.5		
ed^4D	617.4	—	—
ed^4H	−362.5	—	—
ed^4F	203.7	3137.9	1221.5
ed^4G	336.7	2588.7	—
$6s^4P$	1633.0	773.8	
$6s^2D$	−612.9		
$6s^2G$	12.5		
gd^2F	40.9		
gd^2G	73.2		

The 5*d* group. The terms built on the $d^8\,{}^3F$ of Pd III should be found in three groups with separations similar to those of the components of the ${}^3F$. This ${}^3F$ of Pd III has not been found, but the $d^8s^2\,{}^3F$ of Pd I which is known should have separations of about the same magnitudes. Its intervals are 3100 and 1500. The terms here designated "*ed*" which are considered to be those built on the ${}^3F$ of Pd III are sharply divided into but two groups. The second group does in fact start at about 3,000 above the first but it shows no definite division within itself. This is to be expected, however, considering the narrowness of the interval.

The lower "*ed*" group which is quite distinct, which shows the proper quantum numbers to be based on the ${}^3F_4$, and in which the naming of the terms was possible from intensities of combination is composed entirely of quartets of high inner quantum numbers. This apparent separation of the quartets and doublets seems to indicate the inverted type of convergence. In Ni I Russell[5] found this situation with the quintets and triplets of the $d^8s \cdot 4p$ configuration, but it was not general throughout the spectrum.

The combinations made by the remainder of the "*ed*" group indicate a coupling in which the L vector is losing its identity. The "*fd*" group which is quite probably based on the ${}^1D$ of the ion from its position, had to be left nameless also for this reason. The "*gd*" group gave much more complete combinations, and these terms could be assigned L values quite definitely. The "*gd*" ${}^2H$ and ${}^2I$ could not be found although the ${}^2H$ at least should make sufficient combinations. It is noteworthy that the "*gd*" group lies at about 19,000 above the beginning of the "*ed*" just as does the $5s^2G$ above the $5s^4F$.

The unassigned lines. The type of coupling makes it difficult to find new terms by the method of differences as the expected differences frequently do not occur. The labor involved in a method of trial of lines is probably not warranted until more idea of the positions of the missing terms can be obtained. The several unassigned strong lines are quite likely due to missing terms of high L and J whose combinations will be very few.

Excitation limit with helium. The extent of excitation of these two spectra and the points of maximum excitation are in agreement with the discussion of these points by R. A. Sawyer.[6] He has found that with metals of high melting point as cathodes where the presence of the atoms of the cathode substances in the discharge is due to sputtering rather than vaporization, that the principal processes of excitation start from the normal state of the atom. Thus the highest levels excited to any great extent will be those which lie at the energy of the helium ion, 24.48 volts, 198, 290 cm^{-1} above the normal state of the metal atom. Further, there should be an intensity maximum at this energy as well as at 19.75 volts, the metastable potential of helium. Neither of the spectra here considered was measured in the region where the excitation maximum due to the metastable potential would occur, but they may be considered as regards the energy of the helium ion.

[5] H. N. Russell, Phys. Rev. **34**, 821 (1929).

[6] Sawyer, Bulletin, Am. Phys. Soc **5**, No. 2, Abstract 22, April (1930).

In the case of silver the lowest term of the ion $d^{10}\ {}^1S_0$ is at $-39{,}163.9$ cm^{-1} from the $4d^9 5s\ {}^3D_3$ which has been used as the zero level. The ionization potential of Ag I is 59,370 cm^{-1}. Subtracting these energies from that of the helium ion leaves about 99,750 cm^{-1} available for excitation, on the scale used. This is much too low for the $4f$ electron levels which from analogy with other spectra are to be expected to lie about 20,000 cm^{-1} above the $5d$, i.e., at about 110,000.

In the case of palladium the lowest term $4d^9\ {}^2D$ is at $-25{,}081$ cm^{-1}, while the ionization potential of Pd I is about 67,060. About 106,150 cm^{-1} is thus available for excitation, and there should be an intensity maximum of the lines arising from terms in this neighborhood. The "gd" doublet terms at 104,000 do in fact give rise to the group of lines which, compared to the ordinary spark, is enhanced most in intensity and which is quite as strong as even the lowest of the high set of terms. Nothing can be said about the limit of excitation as no higher spectrum than the $5d$ was sought, and it is probably just within the available energy.

The author wishes to express his thanks to Professor A. G. Shenstone, under whose direction the work was done, and to the Carnegie Foundation through whose generosity the laboratory was enabled to procure a calculating machine which greatly facilitated the calculation of the wave-numbers from the measurements.

THE RESONANCE (*B-A*) BAND SYSTEM OF THE HYDROGEN MOLECULE

By Hugh H. Hyman
Physical Laboratory, Union College

(Received June 3, 1930)

Abstract

Part I. Experimental procedure. A three meter focal length vacuum spectrograph, designed by Professor J. J. Hopfield, has been constructed at the University of California and used to photograph the extreme ultraviolet hydrogen band spectra. A description of the type of mounting and method used to focus the instrument is given. The greater dispersion and resolving power has made possible the measuring of additional lines. New tables of frequencies are given.

Part II. Lines in sixty-eight bands have been given quantum assignments. On the basis of the old quantum theory the moment of inertia of the hydrogen in the normal (A level) state is found to be 0.4673×10^{-40} g cm^2 and the nuclear separation to be 0.7500×10^{-8} cm. In the first electronic excited state (B level) the moment of inertia is 1.4225×10^{-40} g cm^2 and the nuclear separation 1.308×10^{-8} cm. Comparison of the present results with those obtained by Richardson and Davidson in their study of bands found in the visible leaves no doubt but that the ultraviolet B state also is the lower state of the bands studied by them. This, then, verifies the assumption made by Birge and leads to the conclusion that the ionization potential of H_2 must be 15.34 volts to within a few hundredths of a volt.

Bands connected with vibrational levels A_0 A_1 and A_2 are not observed. In order to obtain the best possible value of I_0, data from all available sources were correlated and averaged. Birge and Jeppesen calculated accurate values of B_0 and B_1, for the normal level, from Rasetti's data on the Raman effect of gaseous hydrogen. Values for B_1 by the two methods agree to one part in seven thousand but their value for B_0 is 0.27 percent higher than the value given by the present method. This discrepancy points to an irregularity in the moment of inertia of hydrogen in the $v=0$ state of the normal electronic level, as has been pointed out by Birge and Jeppesen.

Introduction

INVESTIGATIONS of the fine structure of bands found in the extreme ultraviolet have been handicapped greatly by the low dispersion and resolving power of the instruments used in the photographic work. Professor J. J. Hopfield of the University of California has designed a vacuum spectrograph using a three inch grating, 15000 lines per inch, with a three meter focal length. It has been found that the instrument has a resolving power of 0.1A and a dispersion of 2.76A per millimeter in the second order. The spectrograph has been built in the shop of the Physics Laboratory of the University of California by Mr. W. R. Stamper and his assistants, following the plans furnished by Professor Hopfield.

The hydrogen bands of the extreme ultraviolet were photographed by the writer, this being the first vacuum work completed on the instrument.

Previous to the present work Dieke and Hopfield,[1,2] by obtaining ab-

[1] Dieke and Hopfield, Zeits. f. Physik **40**, 229 (1926).
[2] Dieke and Hopfield, Phys. Rev. **30**, 400 (1927).

sorption and emission spectrograms, were able to give a complete analysis of the vibrational levels of the three known lower electronic states of the hydrogen molecule. These three states are known as the A, B, and C levels, the A level being the normal state of the molecule.

Schumann,[3] Lyman,[4] Witmer,[5,6] Werner,[7] Hori,[8] and others had photographed and measured H_2 bands in the extreme ultraviolet. The bands photographed and measured by Werner constitute the C-A system, as given by Dieke and Hopfield. The Lyman-Witmer bands now are known to form the B_3-A_v transitions of the B-A system. These B_3-A_v bands are obtained when the discharge tube is filled with a mixture of argon and hydrogen. These same bands appear when only hydrogen is used in the tube, but generally are weaker, some of them being almost completely blended by more intense bands of the B-A system. Richardson, and his students,[9] in a series of papers, have identified a great number of electronic levels of the hydrogen molecule. Birge[10] assumed that the lower level of the Richardson "A" and "B" band systems[11] was identical with the B state of the bands in the ultraviolet. With a Ritz formula for the Richardson band system, Birge found the ionization potential of H_2 to be 15.34 volts. In the same paper a summary of the quantum levels and constants of the hydrogen molecule is given. Starting with the vibrational analysis as given by Dieke and Hopfield,[1,2] Hori[8] has obtained an analysis of the fine structure of the C-A bands. In the same paper he gave a preliminary analysis of the Lyman-Witmer progression (B_3-A_v), based on the assumed presence of R, Q, and P branches. For the latter work Hori used Witmer's measurements.

Part I. Experimental Procedure

The instrument designed by Professor J. J. Hopfield and used for obtaining the spectrogram shown in Fig. 2 is so made that it is possible to obtain on the photographic plate any region of the spectrum. The plates are of such size that a span of 1200 Angstroms, in the first order can be photographed with one exposure. Arrangements have been made so that thirteen exposures may be taken on one plate. However, it has been found that limiting the number to five is more practical.

Type of mounting.

As the space to be evacuated needed to be kept a minimum, a modified form of the Eagle mounting[12] was used, instead of the Rowland type. The

[3] W. Schumann, Werner Anzerger **29,** 230 (1892).
[4] T. Lyman, Spectroscopy of Extreme Ultraviolet, (1914).
[5] Witmer, Proc. Nat. Acad. Sci. **12,** 238 (1926).
[6] Witmer, Phys. Rev. **28,** 1223 (1926).
[7] Werner, Proc. Roy. Soc. **113A,** 107 (1929).
[8] T. Hori, Zeits. f. Physik **44,** 11, 834 (1927).
[9] Richardson and Davidson, Proc. Roy. Soc. **125A,** 23 (1929), and article referred to in this paper.
[10] R. T. Birge, Proc. Nat. Acad. Sci. **14,** 12 (1928).
[11] Richardson and Davidson, Proc. Roy. Soc. **115A,** 528 (1927).
[12] A. Eagle, Astrophys. J. **31,** 120 (1910).

slit, the photographic plate, and the grating were all placed in a cast iron tube three meters long. Five sylphons served as a means for making the adjustments of the plate-holder and grating. These adjustments could be made after a vacuum had been obtained. A grating to be used in this manner must be capable of motion along the tube, and also of rotation about a vertical axis. Fig. 1*A* shows how this was accomplished. The grating is fastened to the carriage *C* which is mounted on the rails *R*. Rods *D* and *E* served to move the grating.

The position of the grating is shown by two dials placed at *A* and *B*. The plate-holder *F-G* is pivoted such that the line of rotation passes through the line of the slit and the radius of curvature of the holder is one-half the radius of curvature of the grating. The slit is at *S*.

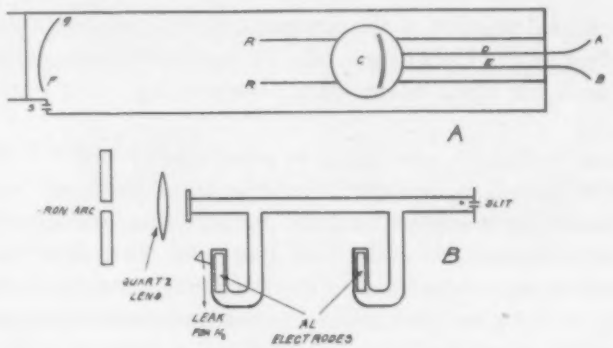

Fig. 1. Diagram of apparatus.

It is well known that in order to obtain the best definition with a concave grating the slit and the grating must be on a circle whose diameter is equal to the radius of curvature of the grating, and, in this case, all the spectral lines are focused on this same circle. The method of mounting fulfills these requirements. It can be seen that the exact position of four variables must be determined to obtain the focus.

Adjustment of the instrument.

The first work to be done was to focus the instrument for all regions of the spectrum. In the case of the Rowland mounting there is a standard method of procedure but in the mounting considered here the method is not so well established.

The first step in the adjustment was the leveling of the grating so that the images would all fall upon the horizontal opening over the plate. Once this position for the grating had been determined, this variable was eliminated.

The second step in the adjustment was to find the approximate settings of the plate, the grating, and the slit with respect to one another, for a definite region of the spectrum.

For convenience, a portion of the visible spectrum of the mercury arc was used. For approximate settings, the eye was used to examine the image

which was assumed to be formed on a photographic plate. When the adjustments were found sufficiently close to serve as a starting point, a photograph of the known lines of mercury was taken and examined for the purpose of determining the course of procedure. Upon examining these plates it was found that certain parts of the spectrum were in much better focus than others. This indicated that the angle of the plate-holder was not correct.

The question, then, was one of determining what changes were necessary in order to bring in focus all the spectrum that fell on this plate. This necessitated the determination of the angle of the plate, the angle of the grating and the distance of the grating from the slit.

To obtain these relations, the central part of the grating was covered. By covering the central part, each individual line appears as double, if not in focus.

With the central portion of the grating covered, photographs were taken and the doubling of the lines observed. At least three exposures were taken on one plate with the plate-holder fixed, the grating being moved along the tube.

One of these exposures was taken at what was considered the best focus for some part of the plate, and the other two on opposite sides of this point. On at least two of these exposures doubling occurred. By carefully measuring the distance between these doubled lines and then drawing graphs, the position of the grating for the focus of the line being considered was found. At least two lines on the plate, preferably at extreme ends, were used and from data obtained the position of the grating for the focus of a line that would fall on the slit was calculated. To determine the amount of rotation of the plate it was necessary to know, in addition to the above, the pitch of the screw that moved the grating and also the distance of the lines on the plate from the slit. It must be remembered that the focus moves in and out twice as fast as the grating moves.

If P_0 is the position of the grating for focus on the slit, P_a the position for the focus of the line being considered, k the pitch of the screw moving the grating, and d the distance of the line from the slit, then the grating must be moved approximately

$$\frac{2k(P_a - P_0)}{d} \times 57 \text{ degrees}.$$

By repeated trials the angle of the plate was determined as well as the position of the grating in the tube. Thus the four variables were determined that fixed the focus for the one region. This same process was repeated for each section of the spectrum. Allowance has been made for sufficient overlapping from one region to another.

After obtaining the focus from λ1000 to λ6000, photographs of the iron arc were taken (λ2300 to λ6000) and many of the lines identified and marked on the plates. These plates are on file for use as an easy method of identifying the exact region given by any one position.

Vacuum technique.

Perhaps one of the greatest difficulties to be overcome was the obtaining of a vacuum suitable for photographic work in the ultraviolet. The volume to be evacuated was approximately one hundred eighty liters. The surface of the iron pipe alone was over two and three-quarters square meters. The ends of the spectrograph were sealed with rubber gaskets and held firm by heavy bolts. The opening for inserting plates was sealed in the same manner. Five sylphons, three windows and two outlets also were potential sources of trouble. Several holes were found in the casting.

At first one mercury vapor pump backed by a large General Electric Company vacuum pump was used to evacuate the system. It was found that this was inadequate. A second mercury vapor pump was then inserted in parallel with the first.

The pressure inside the spectrograph under working conditions varied between 0.005 mm and 0.010 mm of mercury, as measured by a McLeod gauge.

Photographic work.

A π-shaped discharge tube, made of Pyrex with aluminum electrodes, was used. As the region photographed reached beyond the limit of transmission of quartz or fluorite, the discharge tube was fastened directly to the spectrograph. Current from a 11,500 volt transformer was used, and a water rheostat in series with the tube was so adjusted as to give a maximum of intensity without melting the tube. Approximately 0.5 of an ampere was run through the tube. Considerable difficulty was found in eliminating the continuous spectrum found when exposing the plate in the second order, but by grinding the inside of the tube until a rough surface was obtained, much of the continuous spectrum was found to disappear.

The hydrogen was generated electrolytically, passed through a drying tube of P_2O_5, then through a capillary leak directly to the discharge tube. As the gas was being removed by a Cenco pump and also through the slit, it was necessary to have a continuous flow of hydrogen.

The evacuating pumps and the flow of hydrogen were started at least two hours before the photographic work, thus insuring a thorough flushing out of the discharge tube. Any trace of air was noticeable at once in the visible spectrum. The best plates obtained show no trace of known impurities. Schumann plates made by Hilger Company were used.

To make sure that no first order hydrogen lines were being photographed the discharge tube was run under the same conditions as were used for the good plates except that a quartz window was placed between the slit and the source of light.

In general, investigators in the extreme ultraviolet have been handicapped not only by low dispersion and low resolving power, but also by lack of suitable standards. As the measurements in this investigation were from plates showing the second order H_2 lines it was found possible to measure them using first order iron arc lines as standards.

TABLE I. *B-A. Bands of hydrogen.* (*indicates known blend).

Band	*R*-branch I	*m*	cm⁻¹	*P*-branch I	*m*	cm⁻¹
B_0-A_3	2	0	78,462			
	2	1	439	4	1	78,332*
	1B	?	356*	1	2	160
	3	3	203*	5	3	77,937
	0	4	77,996*	4	4	654*
	3	5	733*	4	5	317
				2	6	76,943*
				4	7	496*
				2	8	020*
B_0-A_4	3	0	74,992			
	6	1	973	6R	1	74,856*
	5	2	898	5	2	706
	5	3	767	6	3	501
	1B	4	579*	4B	4	243
	4B	5	343*	8	5	73,937*
	3	6	040*	1	6	562
				2	7	135*
				000	8	72,674*
B_0-A_5	1	0	71,749*			
	4	1	738*	5	1	71,621*
	3	2	674*	4	2	481
	4	3	560*	6	3	293
	1	4	396	3	4	059
	2	5	187	5	5	70,779*
		6		1	6	458*
	00B	7	70,631	2	7	098
B_0-A_6	1	0	68,737			
	5B	1	729	4	1	68 614*
	2	2	678*	1	2	486*
	4	3	581*	4	3	315*
	0	4	441*	5	4	102*
	1	5	258*	3	5	67 851*
				000	6	564*
B_0-B_7	3	0–1	65,953*	1	1	65,836*
	2	2	893*	00	2	721*
	1	3	836*	2	3	567*
	00	4	721	00	4	379*
	2	5	567	1	5	156
	00	6	379	1	6	64,908*
B_0-A_8	3	0–1	63,410*	0	1	63,303*
	0	2	383	1	2	195*
	1	3	314	1B	3	057
		4		1	4	62,862
	4B	5	134*	00	5	717
B_0-B_9	000	1	61,126*	3	1	61,017*
	4	2	112*	2	2	60,919*
				3	3	814*
B_1-A_3	4B	0	79,772*			
	1	1	752*	2	1	79,642
		2		2	2	476
	2	3	503*	4	3	251*
	0B	4	288	2	4	78,965
	3	5	010*	3	5	623
	2	6	78,656*	00	6	228
				1B	7	77,776
B_1-A_4	2	1	76,283	1B	1	76,171
	1	2	204	2	2	020*
	2	3	066	1	3	75,812
				3	4	550
				0	5	237
				2	6	74,873*
B_1-A_5	0	0	73,050			
	00	1	029	2	1	72,928*
	2	2	72,988	0	2	809*
	2	3	849*	1	3	615*
	000	4	674*			
	3	5	458*	2	5	078*
	1	6	186*	1	6	71,749*
B_1-A_6	1	0	70,053			
	4	1	043	3	1	69,933
	2	2	69,984	2	2	802
	3	3	881*	3	3	626*
	2	4	730*	1	4	408
	2	5	540*	4	5	151
	6	6	278	000	7	68,514

Band	*R*-branch I	*m*	cm⁻¹	*P*-branch I	*m*	cm⁻¹
B_1-A_7	5B	0–1	67,268*	5	1	67,156*
	2	2	221	4	2	038*
	4	3	133*	5	3	66,880*
	00	4	011*	4	4	686*
	1	5	66,845	4	5	456*
				00	6	196
B_1-A_8	5	0–1	64,729*	3	1	64,619*
	1	2	696	2	2	513
	3	3	619*	1	3	362*
	0	4	526	000	4	204
	1	5	392*	4B	5	003*
B_1-A_9	2	0	62,442			
	1	1	434*	3	1	62,325*
	5	2	421*	000	2	230
	2	3	357*	1	3	115
	3	4	298*	5	4	61,968*
	4B	5	206	1	5	809
	3	6	048*	3	6	612
B_2-A_2	3	1	81,631	1	1	80,934*
	1	2	80,934*	0	2	754
	1	3	768	00B	3	528
		4		1	4	241*
	3B	5	267	3	5	79,982
				3	7	010
B_2-A_4	4	1	77,562	3	1	77,456
		2		1	2	299
	1	3	329*	5	3	087
				1	4	76,820*
				4	5	496*
B_2-A_5	4B	0	74,343*			
	6	1	327	4	1	74,221*
	1	2	252	4	2	078*
	2	3	125	8	3	73,883
	8	4	73,937*	2	4	637*
	0	5	717*	4	5	344
	0B	6	411*	00	6	008
B_2-A_6	000	0	71,337			
	3	1	319*	2	1	71,212*
	000	2	257	1	2	081
	2	3	146	3	3	70,903*
	0	4	70,994*	1	4	680*
	5	5	779*	1	5	408*
B_2-A_7		1		0	1	68,441*
	1	2	68,492*	4	2	315
	1	3	401*	5	3	168*
	5	5	102*	0	5	67,721*
	1	6	67,906*			
B_2-A_8	5	0–1	66,006*	3B	1	65,901
	1	2	65,967	3	2	793*
	2	3	893*	6	3	650*
	3	4	793*	3	4	475
	6	5	650*	4	5	270
				5	6	040*
B_2-A_9	4B	0–1	63,718*	4	1	63,614*
	1	2	693	2	2	518*
	3	3	638	4	3	396
	000	4	556*	3	4	243*
	1	5	447	4	5	074*
B_2-A_{10}	3	0	61,689*			
	4	1	699	4	1	61,595
	3	2	689*	3	2	513
	3	3	654	3	3	411
	0	4	601		4	
	00	5	527	2	5	154*
				00	6	60,993*
				3	7	814*
B_3-A_3		1		0	1	82,171*
	0	2	82,171*	000	3	81,767
B_3-A_4	00B	0	78,831			
	3	1	808	3	1	78,708*
	3	2	708*	1	2	551*
	3	3	568	4	3	332
	3	4	356*	3	4	062*

TABLE I. *B-A. Bands of hydrogen (Continued).*

Band	R-branch I	R-branch m−½	R-branch cm⁻¹	P-branch I	P-branch m−½	P-branch cm⁻¹
	1	5	075	3	5	77,733*
				2	7	76,931
B_3A_3	2	0	75,591			
	0	1	569	2	1	75,468
	1	2	492*	1	2	323*
	2	3	358	5	3	125*
				2	4	74,873*
				1B	5	579*
				4	6	221*
				0	7	73,821*
B_3A_4				3	1	72,458*
				2	3	146
				1	5	71,649*
				3	6	319*
B_3A_7	1	0	69,794			
	4	1	784	3	1	69,684*
	2	2	730*	2	2	562*
	2	3	633	4	3	399
	2	4	493	2	4	196*
	00	5	312	3	5	68,955
	00	6	092*	2	6	678*
B_4A_4	0B	0–1	67,248*	4	1	67,133
	000	2	205	4	2	038*
				5	3	66,880*
				4	4	686*
B_4-A_3	3	1	64,961	1B	1	64,859
	2	2	932	2	2	782*
	2	3	871	3	3	638*
	2	4	782*	0	4	486
	2	5	653*	3	5	307
				000	6	106
B_4-A_{10}	1	0	62,934			
	5	1	942	6	1	62,842
	3	2	926	5	2	758
	4	3	887	5	3	653*
	0	4	826	3	4	529
	2	5	745	3	5	387
	5	6	653*	000	6	230
				3	7	048*
B_4-A_{11}	4	1	61,224	000	1	61,126*
		2		1	2	045
	2	3	197	4	3	60,965*
	2	4	154	2	4	871
	4	5	112*	2	5	768
B_5-A_5	0		83,500			
	0	1	477	1	1	83,382*
	1	2	382*	2	2	212
	1	3	200*	2	3	82,976*
	0	4	82,966	000	4	679
				2	5	320*
B_5-A_6	1B	0	80,045			
	2	1	017	3	1	79,921*
	3	2	79,921*	1	2	752*
	4B	3	772*	4	3	544*
	4	4	544	3	4	264*
	3	5	264*	2	5	78,937*
	0B	6	78,887	1	6	551*
				0B	7	127
B_6-A_3	1	0	76,820*			
	2	1	781*			
B_6-A_6	0	0	73,789			
	4	1	770	3	1	73,672
	0	2	699	2	2	538
	2B	3	579	5	3	354
	0	4	411	1	4	124
	3	5	185	2	5	72,849*
B_6-A_7	0	0–1	70,994*	3	1	70,903*
		2		5	2	779*
		3		1	3	608
	1	4	680*	1	4	408
	1	5	458*	000	5	153
				3	6	69,881
				2	7	562*

Band	R-branch I	R-branch m−½	R-branch cm⁻¹	P-branch I	P-branch m−½	P-branch cm⁻¹
B_6-A_8	2	0–1	68,458*	1	1	68,360
	1	2	401*	1	2	250*
	4	3	315*	5	3	102*
	5	4	168*	1	4	67,906*
	1	5	004	2	5	704
	2	6	67,737	000	6	409
B_6-A_9	4	0–1	66,171*	4	1	66,073*
	1	2	137	1	2	65,976*
	4	3	073*	2	3	847*
	1	4	65,976*	0	4	691
	2	5	847*	00	5	530
B_6-A_{10}	00	0–1	64,156*	0	1	64,054
	000	3	088	1	3	63,863
	4B	4	003*	00	4	734
	0	5	63,934	1	5	586*
				1	6	436*
				3	7	243*
B_6-A_{11}	3	0	62,421*			
	1	1	434*	3	1	62,325*
	5	2	421*	3	2	258
	3	3	397	4B	3	174*
	2	4	357*	3	4	076
	2	5	298*	5	5	61,968*
				5	6	859
				3B	7	736*
B_6-A_{12}	00	0	60,993*			
	3	1	61,017*	2	1	60,919*
	2B	2	034*	2	2	871*
	2B	3	034	3	3	814*
	2B	4	034	000	4	753*
	00	5	993*	1	5	691*
B_7A_3	1	1	84,655	1	1	84,560*
	1	2	560*	0	2	390
	0	3	368	4	3	153
		4		000	4	83,851
	4	5	83,806	0	5	487*
				4	7	82,551
B_7-A_4				1	2	80,934*
	1	3	80,934*	1	3	719
B_7-A_5	0	0	77,996*			
	2	1	957	1	1	77,863*
	2	2	870*	1	2	712
	1	3	725	5	3	508
				2	4	251
				2	5	76,943*
				00	6	583
B_8-A_4	2	0	74,973*			
	4	1	946	6R	1	74,856*
	2	2	873	0	2	717*
	2	3	746	3	3	531
	1B	4	579	00	4	295
	4B	5	343	3	5	018*
				0	6	73,717*
				3	7	314*
B_8-A_7	0	0	72,186*	2	1	72,078*
				1	3	71,785
	1	5	71,649*	3	5	319*
				0	6	033
B_8-A_8	2	0–1	69,633*	2	1	69,540*
	0	2	584	0	2	428
	0	3	480*	6	3	278
	000	4	367*	00	4	092*
	2	5	196*	2	5	68,871
				4	6	614*
B_8-A_9				5B	1	67,268*
				5	2	156*
	0B	3	67,248	4	3	038*
	4	4	133*	2B–	4	66,865*
				4	5	686*
B_9-A_{10}	3	0–1	65,327*	3	1	65,235
	1	2	304	1	2	149
	2	3	255*	5	3	040*
				1	4	64,908*
				2	5	755*

TABLE I. *B-A. Bands of hydrogen (Continued)*

Band	*R*-branch I	*R*-branch m−½	*R*-branch cm⁻¹	*P*-branch I	*P*-branch m−½	*P*-branch cm⁻¹
B_8-A_{11}	000	0	63,599			
	4	1	614*	2	1	63,518*
	1	2	586*	1	2	436*
	000	3	562*	0	3	350*
	2	4	518*	3	4	247*
	2	5	460	4B	5	134*
				4	6	62,995*
B_8-A_{12}	4B	0	62,174*	6	1	62,100
	3	1	191	3	2	048*
	4B	2–3	206*	5	3	61,989
	3	4	191*	4	4	925
	4	5	149	1	5	821
	1	6	061	3B	6	736*
B_9-A_8	000	0	85,835	00	1	85,706
	000	1	797	2	3	296
	00B	3	501	1	4	84,993
B_9-A_9	1	0	82,375			
	2	1	320*	1	1	82,234
	1	2	234*			
B_9-A_{10}	3	0	79,148			
	2	1	103*	3	1	79,010
	3	2	010*	3	2	78,864*
	3	3	78,864*	2	3	656*
	2	4	656*	3	4	393
				1	5	082
				3	6	77,733*
B_9-A_{11}	3	1	73,314*	3	1	73,224
	00	2	248*	00	2	090
	2	3	135*	2	3	72,928*
	1	4	72,988	000	4	714
				3	5	458*
				1	6	186*
B_9-A_{12}	5	0–1	70,779*	1	1	70,680*
	00B	3	631*	1	3	408*
	1	4	458			
$B_{10}-A_9$	1	0–1	68,492*	1	1	68,401
	0	2	441*	1	2	300
	2	3	378*	5	3	168
	1	4	258	1	4	67,986*
	000	5	132	2B	5	812*
$B_{10}-A_{10}$		2	66,456*	1B	1	66,377
				4	3	171*
$B_{10}-A_{11}$	2	0–1	64,755*	2	1	64,653
	5	2	729*	1	2	583*
	1	3	701	2	3	496
	3	4	638*	1	4	392*
	1	5	583*	3	5	273
$B_{10}-A_{12}$	000	0	63,339	6	1	63,261
	0	1–2–3	350*	4	2	217
				4B	3	134*
B_7-A_6	1	1	86,991	1	3	86,410
B_7-A_7	0	0	83,487*			
	000	1	455	0	1	83,363
	0	2	338	1	2	200*
		3		1	3	82,976*
	1	4	82,951	000	4	697
				0	5	346
B_7-A_8	1	0	80,241*			
	2	1	214	1B	1	80,131
		2		0B	2	79,972
	3	3	79,943	2	3	772
		4	752	2	4	503*
		5	476	0	5	189
B_7-A_9	0	1	77,199	00	1	77,113
				2	3	76,784*
				0B	5	257
B_7-A_{10}	000	0	74,446			
	2	1	426	4B		74,343*
	4	3	221*	3	3	040*
	4	4	078*	0	4	73,821*
	0	5	73,850	1	5	562*

Band	*R*-branch I	*R*-branch m−½	*R*-branch cm⁻¹	*P*-branch I	*P*-branch m−½	*P*-branch cm⁻¹
B_7-A_6	3	0	69,626*			
	0	1	603	1	1	69,516
	2	2	562*	0	2	428*
	0	3	480*			
	000	4	367*	000	4	111
B_7-A_{10}	1	1	67,584	3	1	67,496*
	000	2	564*	000	2	409*
	2	3	496*	2	3	296*
	000	4	490*	5	4	156*
	2	5	296*	00	5	011*
B_7-A_{11}	1B	1–2–3	64,449*	1	1	64,362*
	5	5	373	3	2	307*
				3	3	245
				000	5	106
B_8-A_8	1	0	84,560*			
	0	1	526	000	1	84,446
	000	2	432	0	2	280
	1	3	240	2	3	046
	2	4	026	000	4	83,775
	1	5	83,713	1	5	410
				00B	6	004
B_8-A_9	2	0	78,310			
	1	1	286	3	1	78,203*
	3	2	203*	3	2	062*
	3	3	062*	1	3	77,863*
	2	4	77,870	0	4	622
	4	5	654*	1	5	329*
				1	7	76,634
B_8-A_7	1	1	75,492*			
	1	3	323*	5	3	75,125*
B_8-A_8	1	0–1	72,988*	0	1	72,886
	0	3	809*	1	3	615
B_8-A_{10}	1	0–1	68,666*	4	1	68,581*
	000	3	572	1	2	49?*
	1	4	486*	2	3	378*
	2	5	378*	1	4	250*
B_8-A_{11}	2	0–1	66,942*	2B	1	66,865
	000	2	906	4	3	686*
	0	3	892	000	4	561
B_8-A_{12}	000	1	65,541	000	1	65,392
	00	2–3	530*	3	2	327*
	2	4	507	2	3	255
B_9-A_8	00	0	79,343			
	1B	1	338	4	1	79,251*
	000	2	235	2	2	103*
	2	3	103*	0	3	78,920
				2	4	656*
B_9-A_9	3	0	74,040*			
	3	1	018*	8	1	73,937*
	8	2	73,937*	0	2	821*
	0	3	850	2	3	637*
				00	5	248*
B_9-A_9	1	0	71,749*			
	4	1	738*	1	1	71,649*
	3	2	674*	4	2	560*
	5	3	621*	1	3	410
				2	4	212*
				1	5	070
B_9-A_{10}	2	0	69,730	1	1	69,649
	3	1	684*	2	2	540*
				0	3	428*
				6	4	278*
				000	5	111
B_9-A_{11}	1	0–1	67,986*	1B	1	67,920*
	1B	3	920*	2B	2	812*
	1	4	906*	0	3	721*
	3	5	851*	2	5	496*
				000	6	409*
				2	7	296*

An iron arc (see Fig. 1*B*) was used as the source of light for the comparison spectrum. The lens and the window shown were of quartz. The iron arc was run for five minutes before starting the hydrogen source and also for five minutes after stopping the discharge, thus enabling one to detect any shift in the lines while making the exposures.

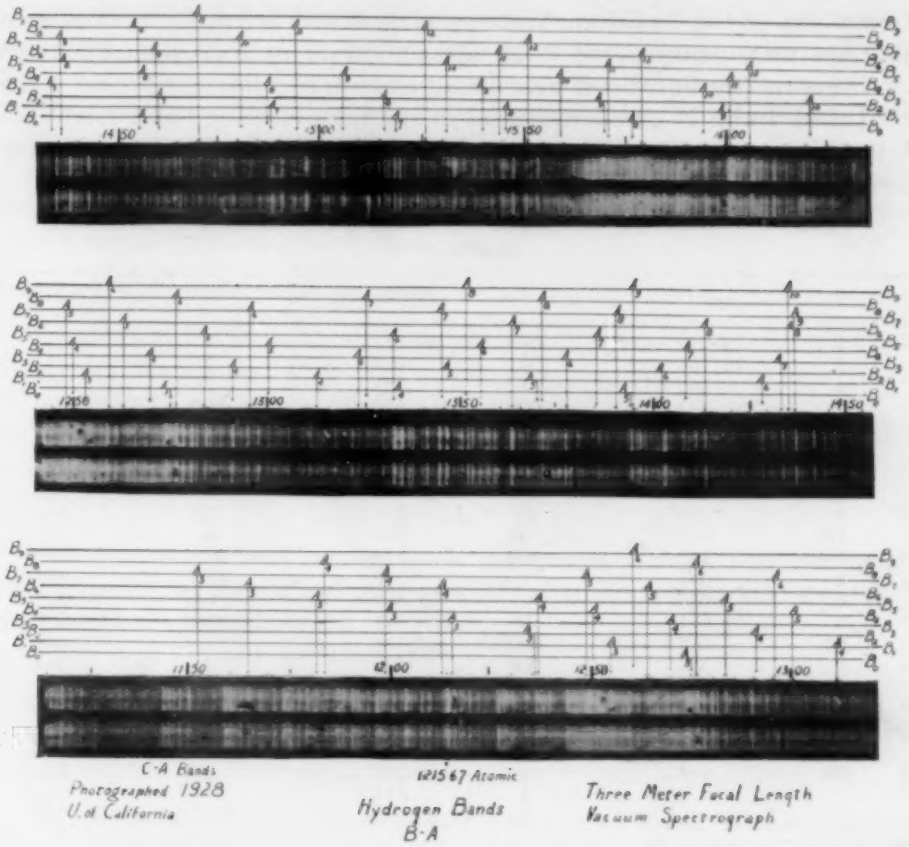

Fig. 2.

The shutter over the plate was so arranged that by turning a screw the iron lines did not cover all the plate that had been exposed to the hydrogen light. The iron lines may be seen in Fig. 2 and are easily distinguished from the hydrogen lines. On the same plate is found also an exposure showing only hydrogen lines.

Only plates that showed no displacement of the iron lines were used for measurement. It was found that the instrument was very sensitive to temperature changes. No special provisions had been made for maintaining a constant temperature, but care was taken in keeping the room as nearly as possible at one temperature while making the exposures.

Many iron lines suitable for standards were found between 2600A and

3300A.[13] For the H_2 lines below 1300A, hydrogen lines were measured in the third order against iron lines as standards and these hydrogen lines were then used as standards in the second order. The iron lines used as standards were spaced approximately 100A or less apart.

The measurements were made on a 200 millimeter comparator purchased by Professor R. T. Birge through the generosity of the Rumford Grant Committee of the American Academy of Arts and Sciences. It is believed that the measurements are in all cases accurate to approximately 0.05A.

In general the lines listed were measured from two different plates.

Tables I and II give frequencies of the lines measured and intensities. Intensities are merely visual estimates. Table I also gives the quantum assignments as discussed in Part II.

TABLE II. *Frequencies of lines between λ1260A and λ1640A measured but not identified in this work.*

I	cm^{-1}	*I*	cm^{-1}	*I*	cm^{-1}
1	79,990	000	72,752	2	65,765
3	78,766	0	629	2	743
1	666	1	431	2	627
1	527	000	419	000	593
1	512	000	396	3	226
3	495	000	272	3V	63,884
0	375	1B	051	000	843
000	260	000	71,635	2	806
1	248	0	534	2B	800
1B	182	00	436	0	795
1−	153	000	378	000	505
1	093	1	110	000	490
0	038	0	70,863	00	62,802
0	77,674	0	68,855	23	670
00	615	000B	68,756	2	408
0	356	000	523	1	313
1	188	00	326	2	270
00	149	00	67,398	1	126
00	73,741	000	185	1	120
1	664	1	66,993	1	61,795
00	418	1	413	2B	034
		1	355		
		1	65,985		

The focusing of the instrument was carried out in cooperation with Dr. C. A. Pulskamp, to whom the writer is indebted for his valuable aid in adjusting the instrument. The writer also wishes to express his thanks to Professor J. J. Hopfield, who suggested the problem and under whose direction the experimental work was started.

PART II. ROTATIONAL DATA

While the work on the fine structure of the hydrogen resonance bands was in progress Kemble and Guillemin[14] published an article in which they concluded, on theoretical grounds, that the *B-A* system must consist of *R* and *P* branches only.

[13] H. Kayser, and H. Konen, Handbuch der Spectroscopie, Vol. 7, (1924).

[14] Kemble and Guillemin, Proc. Nat. Acad. Sci. **14**, 782 (1928).

Richardson and Davidson[11] have completed the fine structure analysis of certain bands found in the visible. It will be shown that there is a definite connection between this band system and the *B-A* system.

Schaafsma and Dieke[15] have published rotational energy data, based on H_2 plates obtained by Dieke with Hopfield's 50 cm vacuum spectrograph at the University of California. The quantum assignments in the present paper were made entirely independent of their work. Data from their work have been used, with other data available, in calculating the moment of inertia of the molecule in the normal state.

Two brief accounts of the preliminary work on the *B-A* bands have been published in short articles to Nature.[16,17]

The vibrational analysis as given by Dieke and Hopfield[1,2] serves as a starting point for this work. All results are given in terms of the old quantum theory unless specified otherwise.

Verification of combination principle.

The lines of the three possible branches, *P*, *Q* and *R* of the usual quantum theory are defined as follows[18]

$$R_J = F'_{J+1} - F_J'' \tag{1}$$

$$Q_J = F_J' - F_J'' \tag{2}$$

$$P_J = F'_{J-1} - F_J''. \tag{3}$$

The *Q* branch is not observed in the *B-A* bands. Kemble and Guillemin[13] have given as the theoretical reason for this that the *B-A* bands represent a transition from the $2^1\Sigma$ level to the $1^1\Sigma$ level.

From Eqs. (1) and (3) it follows[19]

$$R_J - P_J = F'_{J+1} - F'_{J-1} = 2\Delta F_J' \tag{4}$$

$$R_{J-1} - P_{J+1} = F''_{J+1} - F''_{J-1} = 2\Delta F_J''. \tag{5}$$

Eq. (4) shows that the values of $2\Delta F'_j$ may be obtained from any band if the *R* and *P* branches are known and the relative rotational quantum numbering of the lines has been found. The values of $2\Delta F_J'$ should be identical, within the limit of experimental error, for all bands of the *A* or n'' progression; that is, these values should be the same for all bands having the same upper level (*B*).

In the same manner, the values of $2\Delta F_J''$ should be the same for all bands having the same lower level. These facts are illustrated in Fig. 3.

[15] Schaafsma and Dieke, Zeits. f. Physik **55,** 164 (1929).

[16] Hyman and Birge, Nature **123,** 277 (1929).

[17] Hyman and Jeppesen, Nature **125,** 462 (1930).

[18] R. T. Birge, Chapter 4, p. 144 of Report of Committee on Radiation in Gases, Molecular Spectra in Gases, Bulletin No. 57 of the National Research Council, (1926). This bulletin is referred to hereafter as the "Report." In general the nomenclature in this paper is that used in the Report.

[19] Report, p. 145.

The combination principle was first verified by choosing three bands such that two have the same B level and two the same A level, and finding differences between R and P lines such that equations (4) and (5) were satisfied.

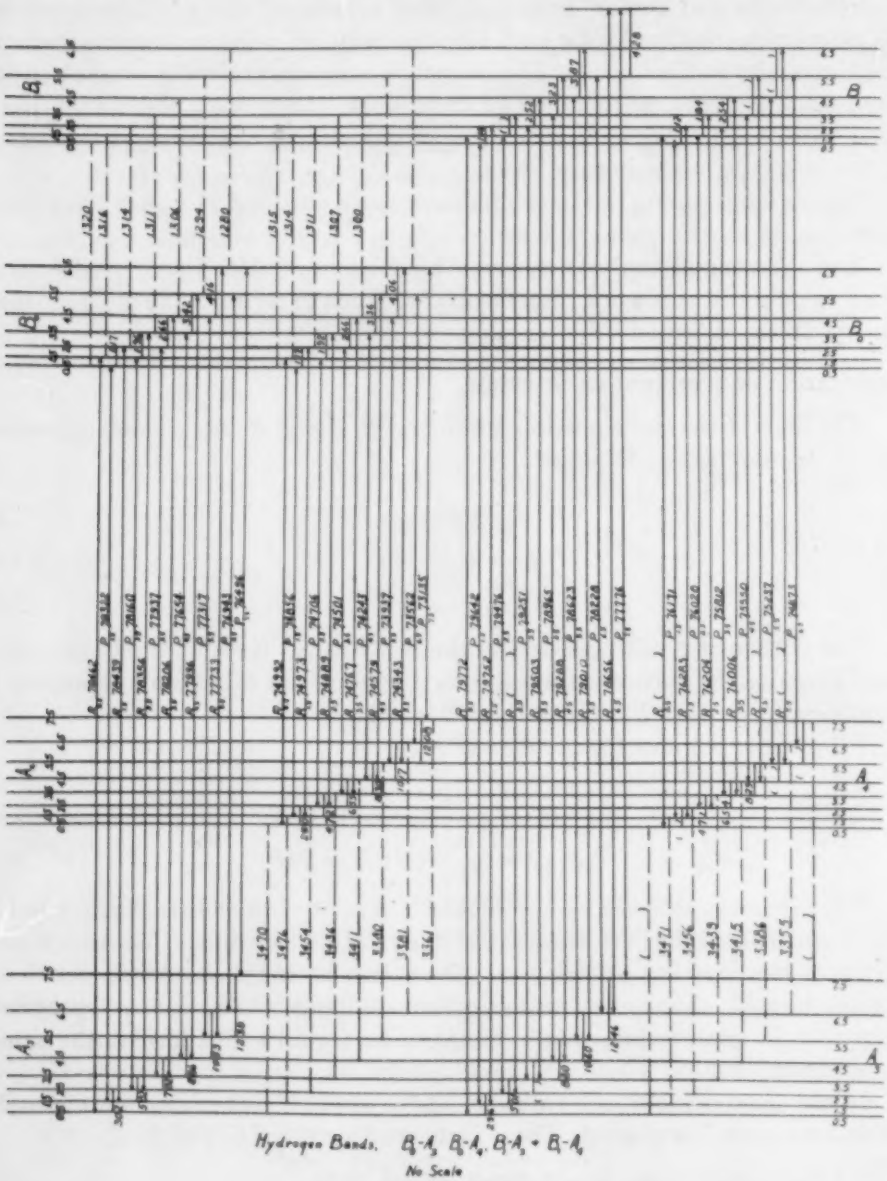

Fig. 3. Energy level diagram.

The vibrational analysis had been found by Dieke and Hopfield.[2] It was not necessary to know the true numbering of the lines in the bands. The method of obtaining this numbering will be explained later. The lines of the individual band were separated into R and P branches by the usual method of second differences.

After verifying the combination principle for these three bands, the work was extended to other bands. The results are collected in Tables I, III, and IV. Lines connected with sixty-eight bands were found. The results show alternating intensity of lines as is to be expected since the H_2 molecule is symmetrical.

TABLE III. *Average values of* $2\Delta F'$.

k	1.5	2.5	3.5	4.5	5.5	6.5
B_0	116.4	192.9	266.3	338	411	475
B_1	111	184	254	324	390	434
B_2	104	176	242	314	375	403
B_3	100	169	234	296	350	419
B_4	97	165	225	279	318	331
B_5	93	155	215	274	324	
B_6	93	146	208	246	315	
B_7	86	138	187	254	287	
B_8	85	146	197	242	312	
B_9	86	115	202	223		

TABLE IV. *Average values of* $2\Delta F''$.

k	1.5	2.5	3.5	4.5	5.5	6.5
A_3	295	502	702	881	1060	1249
A_4	285	475	652	830	1011	1217
A_5	268	445	617	780	923	
A_6	253	416	577	731	869	1033
A_7	230	386	533	679	802	896
A_8	214	364	493	607	755	
A_9	200	324	452	558	681	
A_{10}	175	289	400	500	581	694
A_{11}	169	260	341	426	501	558
A_{12}	148	271	335	414		

TABLE IVa. *Values of* $2\Delta F''$ *from Witmer and Hori.*

k	1.5	2.5	3.5	4.5	5.5
A_3(H)		529			
A_2 (W)	321	531			
A_1 (H)		557	764	991	1231
A_1 (W)	345	562			
A_0 (W)	356	588			

To find m, the effective rotational quantum number, the $2\Delta F'$ values are plotted and extrapolated to $\Delta F = 0$. m is now to be chosen so that ΔF equals zero when m equals zero and it is found that this condition is satisfied, at least to a close approximation, by assuming half integer values for m. Richardson and Davidson[11] referring to the lower level of bands analyzed by them, state "$m_0 = 0.50013$ and remains very close to 1/2 throughout the vibrational levels." This level is now known to be identical with the B state as described in this paper.

Continuing the study of the B state later, it will be shown, by using the analytic method,[23] that the value of m is found to be a half-integer to

[20] Report, p. 173.

within 0.005, that is,[21] α is zero or practically zero. At present we assume[22] $m=k=J-0.5$.

A second check on the assignment of the lines to the R and P branches was found by comparing the values[23] of $\omega_v(m)$ for the B level as obtained by

TABLE V. *B-state. Average values of* $\omega_v(m)$ *(From both R and P lines). Values in parentheses are those obtained by Richardson and Davidson from bands in the visible.*

m	0.5	1.5	2.5	3.5	4.5	5.5	6.5
B_1-B_0	1318.5 (1318.345)	1315.8 (1316.41)	1312.4 (1312.55)	1307.0 (1306.94)	1300.6 (1299.68)	1289.8 (1290.99)	1279.9 (1280.94)
B_2-B_1	1282.0 (1281.475)	1280.0 (1279.84)	1276.7 (1276.6)	1272.1 (1271.815)	1265.7 (1265.59)	1260.0 (1258.04)	1245 (1249.32)
B_3-B_2	1244 (1246.71)	1244 (1245.25)	1240 (1242.38)	1238 (1238.12)	1234 (1232.61)	1223 (1225.89)	1217 (1218.02)
B_4-B_3	1214 (1213.015)	1212 (1211.76)	1211 (1209.06)	1207 (1205.17)	1200 (1200.10)	1196 (1193.86)	1190 (1186.75)
B_5-B_4	1179 (1179.95)	1180 (1178.77)	1176 (1176.33)	1174 (1172.74)	1167 (1168.03)	1164 (1162.25)	1160 (1155.5)
B_6-B_5	1147 (1147.50)	1152 (1146.32)	1145 (1144.00)	1140 (1140.64)	1139 (1136.15)	(1130.77)	(1124.8)
B_7-B_6	1115 (1115.5)	1112 (1114.32)	1112 (1112.04)	1105 (1108.7)	1102 (1104.3)		
B_8-B_7	1086	1080	1079 (1081.29)	1078–	1068	1071	
B_9-B_8	1052	1047	1038	1030	1028		

using the different A vibrational states as the base level. In a similar manner, but using different B vibrational states as base levels the values of $\omega_v(m)$ for the A level were found. Tables V and VI give the average values found. In making these averages the numbers obtained from the differ-

TABLE VI. *A-state. Averae values of* $\omega_v(m)$.

m	0.5	1.5	2.5	3.5	4.5	5.5
A_4-A_3	3470.0	3467.2	3454.7	3435.1	3413.5	3392
A_5-A_4	3241.5	3236.0	3223.5	3207.3	3184.5	3153
A_6-A_5	3012	3008.5	2995.8	2979.9	2956	2928
A_7-A_6	2785.3	2774.9	2753.7	2746.1	2720	2692
A_8-A_7	2543.7	2536.8	2524.5	2513	2513	2450
A_9-A_8	2288	2288	2265	2241	2202	
$A_{10}-A_9$	2029	2018	2006	1984	1956	1918
$A_{11}-A_{10}$	1726	1720	1715	1689	1659	1627
$A_{12}-A_{11}$	1423	1414	1380	1358	1324	1303

ences of two frequencies neither of which was from blended lines were given weighted values. Fig. 3 also shows the values of $\omega_v(m)$. The numbers on this diagram are obtained by using P lines. Table V also gives (in parenthesis) the values as obtained by Richardson and Davidson[11] from their analysis of

[21] Report, p. 137 gives $m=J-\frac{0}{1}=J-0.5-\alpha=k-\alpha$, where J is an integer and k a half-integer. This is in terms of the old quantum theory as used in this paper. In the new mechanics J is one unit less.

[22] It is to be remembered that the value of $m-1/2$ is the value of J for the new mechanics.

[23] Report, p. 113.

bands in the visible. The Richardson and Davidson measurements are from plates taken using a larger grating and the bands measured are in the visible. Their values of $\omega_v(m)$ are presumably the more trustworthy. It is to be remembered that an error of one-tenth Angstrom in the ultraviolet region considered here represents an error of between six and nine frequency units.

The values of $\Delta F'$ as obtained from the rotational energy function[24] also agree almost identically with those obtained by Richardson and Davidson from their data. They give a value of D_0 (their C) smaller than the theoretical value. The D_0 used in the present report is found theoretically and represents the best known method for obtaining this constant, while Richardson and Davidson have obtained the value empirically. More will be said about these constants later.

Birge[10] in his summary of the quantum levels and resulting constants of the hydrogen molecule has taken the B state of the ultraviolet bands to be also the lower state of the Richardson "A" and "B" bands. This seemed justifiable at that time as the result of the close agreement of the vibrational data of Dieke and Hopfield[2] and of Richardson.[11]

The far more accurate data of the present work confirms the assumption beyond all doubt, since the agreement of the spacings of all levels, both vibrational and rotational, is within the very small limits of experimental error. This verification of the assumption by Birge leads to the conclusion that the ionization potential of H_2 must be 15.34 volts to within a few hundredths of a volt, as given by Birge at that time.

Mention has been made of the rotational energy function

$$F = B_0 m^2 + D_0 m^4 + F_0 m^6 + \cdots . \tag{6}$$

It is from this equation that the actual spacings of the rotational energy levels are found. The value of B_0 is inversely proportional to the moment of inertia for no vibration and infinitely slow rotation.

Birge, in the Report,[25], gives three methods of handling the data obtained. Method one is purely empirical and is not to be considered here.

Method two is a rapid semigraphical method for evaluating B_0.

From the rotational energy function, by assuming $m = k - \alpha$, one obtains, to a very close approximation when α is small.

$$\frac{\Delta F}{k} = 2B_0 - \frac{2B_0\alpha}{k} + 4D_0k^2 + 6F_0k^4. \tag{7}$$

In the present work α is zero, or at least very small. If we assume the value of F_0 to be small[26] we have

$$\frac{2\Delta F}{k} = 4B_0 + 8D_0k^2. \tag{8}$$

This equation represents a parabola with the vertex at $k = 0$.

[24] Report, p. 141.

[25] Report, pp. 169–173.

[26] Richardson and Davidson gave α equal to 0.0013, $F_0 = 1.3 \times 10^{-5}$.

The values of $2\Delta F/k$ for the B_0 state are

k	1.5	2.5	3.5	4.5
$\frac{2\Delta F}{k}$	77.60	77.16	76.09	75.11

These latter values were plotted against k and from this a fairly accurate value of $4B_0$ found directly.

D_0 is theoretically related to B_0 by the relation

$$D_0 = \frac{-4B_0^3}{\omega_0^2}. \tag{9}$$

ω_0 is found by double extrapolation of the values of $\omega_v(m)$ to find the value of $\omega_0(0)$.

The final result of this extrapolation is that $\omega_0(0) = 1337.82\ \text{cm}^{-1}$.

Method three is strictly analytic and is the most accurate method of handling the data.

From the rotational energy function the following result is obtained, where $m = k - \alpha$

$$2\Delta\overset{*}{F} = 2\Delta F - 8D_0k^3 - 12F_0k^5 - 16H_0k^7 = (4B_0 + 8D_0)(k - \alpha) \tag{10}$$

if the values of F_0 and H_0 are zero.

The value of $2\Delta\overset{*}{F}$ may be called the reduced value of $2\Delta F$. The values of $2\Delta F$ are found directly. Values of F_0 and H_0 are assumed to be equal to zero. The value, $D_0 = -0.01647$, is found by using the approximate value of $B_0(19.46\ \text{cm}^{-1})$ found by method two in the theoretical Eq. (9).

In the equation $2\Delta\overset{*}{F} = 2\Delta F - 8D_0k^3$ the following values are found:

$2\Delta F$	k	$8 - D_0k^3$	$2\Delta\overset{*}{F}$
116.4	1.5	0.4447	116.845
192.9	2.5	2.059	194.959
266.3	3.5	5.649	271.949
338.0	4.5	12.007	350.009

The plot of $2\Delta\overset{*}{F}$ against k is a straight line, as predicted by the above theory.

The least squares solution of the equation

$$2\Delta\overset{*}{F} = (4B_0 + 8D_0)(k - \alpha) \tag{11}$$

accordingly gives the most probable values of B_0 and of α.

The solution gives

$$B_0 = 19.445\ \text{cm}^{-1}; \quad \alpha = -0.005\ \text{cm}^{-1}.$$

It is believed B_0 has a true probable error not exceeding one part in one thousand. The probable error in α is such that the true value may be zero.

Richardson and Davidson have found $B_0 = 19.455_5$.

The moment of inertia is found from the relation

$$I_0 = \frac{h}{8\pi^2 B_0 c} = \frac{27.66 \times 10^{-40}}{B_0} \text{g cm}^2 \qquad (12)$$

$$= (1.4225 \pm 0.003) \times 10^{-40} \text{g cm}^2.$$

The error in B_0 is also to be found in the value of the moment of inertia. In addition there is a small probable error in the constant[27] 27.66×10^{-40}.

The nuclear separation r_0, in centimeters, is given by the relation

$$r_0 = (I_0/\mu)^{1/2} \quad \text{where}$$

$$\mu = 1.6490 \times 10^{-24} \frac{m_1 m_2}{m_1 + m_2} \quad \text{and}$$

m_1 and m_2 are the atomic weights of the two atoms.[28]

The resulting value for the nuclear separation is

$$1.3084 \times 10^{-8} \text{ cm}.$$

The rotational energy function becomes

$$F = 19.445m^2 - 0.01647m^4 \qquad (14)$$

$$m = \tfrac{1}{2}, 1\tfrac{1}{2}, 2\tfrac{1}{2} \text{ etc.}$$

The following is a comparison of the values of F obtained with those given by Richardson and Davidson:

Richardson and Davidson from bands in visible	$B-A$ bands found in ultraviolet
(cm^{-1})	(cm^{-1})
38.85	38.81
77.30	77.22
115.06	114.85
151.685	151.06
186.955	186.13

In the solution, Richardson and Davidson have used $D = -0.0152$ cm^{-1} instead of -0.01647.

Constants for the normal level.

The evaluation of the moment of inertia of H_2, for the normal electronic level, has been carried out with the cooperation of Mr. C. Rulon Jeppesen, and the results have been reported briefly.[17] In this case the values of $2\Delta F''$, as given in Table IV, begin at the vibrational level $v = 3$. For $v = 0$, 1, and 2, the less accurate and extensive data of Hori,[8] and Witmer,[6] were used. These

[27] Birge, Phys. Rev. Supplement **1**, 63 (1929) gives

$$h/8\pi^2 c = (27.65_{82} \pm 0.04) \times 10^{-40} \text{g cm}. \qquad (13)$$

[28] Constants used are those given by Birge, reference 27.

data are listed in Table IVa. In order to obtain the best possible value of I_0, data from all available sources were correlated and averaged. These sources include Schaafsma and Dieke,[15] in addition to those already quoted.

The various values of $2\Delta F/k$, resulting from the observations of the different observers, were plotted against k, on a large scale. In this case Eq. (7) becomes

$$\frac{2\Delta F_v}{k} = 4B_v + 8D_v k^2 + 12F_v k^4 \tag{15}$$

and the resulting curve, for each value of v, should be approximately a parabola with its vertex at $k=0$. Smooth curves were drawn through the plotted points, so as to satisfy, roughly, the form of Eq. (15). From these curves we obtain first approximate values of $4B_v$. These values were then plotted against v, and found to form a reasonably smooth curve. What appeared to be the best smooth curve was then drawn, and from this, smoothed values of $4B_v$ were obtained. These smoothed values were now used to calculate theoretical values of D_v, using the theoretical relation[29]

$$D_v = D_e - \beta(v + \tfrac{1}{2}) \tag{16}$$

where[30]

$$\frac{\beta}{D_e} = -\frac{\omega_e}{24B_e}\left(\frac{\alpha}{B_e}\right)^2 - 5\left(\frac{\alpha}{B_e}\right) + 8x_e. \tag{17}$$

The value of ω_e(4368.6 cm^{-1}) was obtained from a smooth curve, using data by Witmer.[6] Still later work[31] has led to 4371 cm^{-1} as the best value of ω_e, but the change is immaterial in connection with β. For B_e we used 60.16 cm^{-1}, as obtained by extrapolating our smooth $B_v v$ curve to $v=-\frac{1}{2}$. The slope of this curve, at $v=-\frac{1}{2}$, gives the value of α (2.68 cm^{-1}).

We could now calculate theoretical values of $8D_v k^2$, in Eq. (15). In order to calculate the final term in Eq. (15), we assumed[32] that

$$F_v = F_e = \frac{D_e^2}{B_e}\left(2 - \frac{\alpha\omega_e}{6B_e^2}\right) \tag{18}$$

The true theoretical expression for F_v, as a function of v, has not yet been derived, but the last term in Eq. (15) is so small that any change of F_v with v is immaterial, for not too large values of k.

[29] In this case, the new mechanics relations have been used. In equations like (9), one *should* use D_e, B_e, and ω_e (values for $v=-1/2$) in place of D_0, B_0, and ω_0, but numerically the change is insignificant.

[30] This theoretical expression for β/D_e is equivalent to that given by Pomeroy (Phys. Rev. **29**, 59 (1927)), but is much simpler in actual use. It was suggested to us by Professor R. T. Birge.

[31] R. T. Birge and C. R. Jeppesen, Nature **125**, 463 (1930).

[32] Compare "Report," p. 237, Eq. (198).

With these calculated values of D_v and F_v, we now obtained a value of $4B_v$ from selected points on the $2\Delta F_v/k : k$ curve, using Eq. (15). A weighted average of the resulting values of $4B_v$, for each value of v, was thus obtained. This process is equivalent to drawing a smooth curve through the plotted $2\Delta F_v/k$ points, having the theoretical *shape*, leaving only the constant term to be evaluated. Such curves, as actually drawn, were found to be quite as satisfactory as the original empirical curves. This is a most gratifying verification of theory, since the "distortion" of the H_2 molecule, with both rotation and vibration, is relatively large.

The new values of B_v were again plotted against v, and found to lie much more closely on a smooth curve than the original approximate values. The changes were, however, so small that it was deemed unnecessary to calculate *new* theoretical values of D_v (method of successive approximations). Since we had used the *finite* differences $2\Delta F_v$, the value of the constant term in Eq. (15) is, strictly, not $4B_v$, but[33] $4B_v+8D_v$. The final smoothed values of B_v, obtained after this correction, are given in Table VII. They were then fitted, by least squares, to a third degree rational integral function, the result being

$$B_v = 60.587 - 2.7938(v+\tfrac{1}{2}) + 1.0500\times 10^{-2}(v+\tfrac{1}{2})^2 - 24.058\times 10^{-4}(v+\tfrac{1}{2})^3. \qquad (19)$$

TABLE VII.

v''	B_v'' smoothed observed values	B_v'' calc. values
0	59.19	59.192
1	56.415	56.411
2	53.63	53.630
3	50.835	50.834
4	48.01	48.008
5	45.14	45.138
6	42.20	42.210
7	39.20	39.209
8	36.145	36.120
9	32.92	32.930
10	29.52	29.624
11	25.39	26.187
12	20.565	22.606

The calculated values, according to Eq. (19), are also given in Table VII. In this equation, the absolute term gives the value B_e for the hypothetical state of zero vibration ($v=-1/2$), according to the new mechanics. It corresponds to $I_e=0.4565\times10^{-40}$ g cm^2 and $r_e=0.7412\times10^{-8}$ cm. This is quite different[34] from Hori's value of $I_e=0.467\times10^{-40}$. The value of B_0.

[33] See Eq. (145), p. 174 of "Report."

[34] See reference 17 for a discussion of this point.

corresponding to $v=0$, is 59.192 cm^{-1}, giving $I_0=0.4675\times10^{-40}$, $r_0=0.7500\times10^{-8}$. These latter are the constants for the actual normal level of hydrogen.

As already noted, accurate data for $2\Delta F''$ values extend only from $v=3$ to 12, inclusive (Table IV). As can be seen from Table VII, Eq. (19) fits the data in a satisfactory manner only up to $v=9$. In fact, the B_v values for $v=10$, 11, 12, were not used in obtaining this equation, since they deviate sharply from any smooth curve. These higher values of v are close to dissociation, and the fact that the corresponding moments of inertia are appreciably larger than those given by the equation is not surprising.

The values of B_0, B_1, and B_2 are not so trustworthy, but they do, perhaps accidentally, fit in very well with the values B_3 to B_9. It would therefore appear that our final value of B_0 is reliable to about 0.2 percent. After this work was completed, Birge and Jeppesen[31] calculated accurate values of B_0 and B_1, from Rasetti's data[35] on the Raman effect in gaseous hydrogen. Their value of B_1 (56.4035 cm^{-1}) is in remarkable agreement with our value of 56.411 cm^{-1}, as given by Eq. (19), but their value of B_0 (59.354 cm^{-1}) is 0.27 percent greater than our value of 59.192 cm^{-1}. This discrepancy points to a real irregularity in the moment of inertia of hydrogen in the $v=0$ state, as discussed by Birge and Jeppesen. They discuss also an apparent irregularity in the frequency of vibration for this same level.

The final conclusion is then that Eq. (19), or Table VII, last column, gives reliable values of B_v'' from $v=1$ to 9 inclusive, but that the true value of B_0 is that given by Birge and Jeppesen, namely $B_0=59.354$ cm^{-1}, corresponding to $I_0=0.4660\times10^{-40}$ g cm^2 and $r_0=0.7489\times10^{-8}$ cm^{-1}. Because of the irregularity in the value of B_0, it is impossible to give a reliable value of B_e, but it seems best, in calculating theoretical values of D_e and other derived constants, to use the value given by Eq. (19).

The experimental work and part of the theoretical work, of this investigation, were carried out at the University of California and the writer wishes to express his sincere thanks to Professor R. T. Birge of the University of California not only for the very obliging and valuable assistance that was given while the writer was at the University of California but also for the interest and advice he has given during the past year. He is also indebted to Mr. C. R. Jeppesen for his help in deriving the constants for the normal level.

[35] F. Rasetti, Phys. Rev. **34**, 367 (1929).

THE LUMINESCENCE OF ZINC SULPHIDE UNDER THE ACTION OF ALPHA, BETA AND GAMMA-RAYS

By George S. Gessner

Randal Morgan Laboratory of Physics, University of Pennsylvania

(Received May 21, 1930)

Abstract

The luminescence of zinc sulphide under the action of α, β and γ-rays was studied with an especially designed brass capsule. The zinc sulphide was exposed to the α-rays or β and γ-rays, or α, β and γ-rays from radium or its products, while the luminescent material and the exciting agent were kept separate. In this way the effect of these rays upon the luminescent material was observed, separately and collectively. The experiment was made under practically constant temperature. The luminosity time curves for the three types of capsules were consistent in characteristics. It was found that for a time there was a definite increase in brightness; then the luminescence decreased under the constant action of the rays and rose again to a second maximum. This was followed by gradual decrease with time as long as observations were taken. The decay of luminescence of zinc sulphide, after the removal of the radio active source, showed that the decay curve is not of the type whose ordinate can be expressed by a single exponential term.

Introduction

THE action of α, β and γ-rays from radium or its products, upon luminous compounds has been studied by several experimenters[1] during the last two decades and theories have been formulated to explain their results.

Przibram[2] and his students found that the luminescence of some minerals increased under the action of β-rays and then gradually decayed after passing through a maximum. Smith[3] found an increase in brightness at room temperature of chemically pure barium bromide.

Studies in luminosity of luminescent zinc sulphide under the action of α, β and γ-rays from radium or its products, up to this time, have been made using mixtures of the luminescent material and the radioactive exciting agent. One of the features of the presentr esearch was to keep the radioactive source separate from the luminescent material, thus avoiding the possible formation of complex products. Another feature was the use of a source of radiation which remained constant during the period of the experiment. Thus it was possible to observe the brightness as soon as the luminescent material was brought in contact with the radioactive source. This was not done in previous experiments on zinc sulphide because of the

[1] E. Rutherford, Proc. Roy. Soc. **83A,** 561 (1909–10), E. Marsden, Proc. Roy. Soc. **83A,** 548 (1909–10), Patterson, Walsh and Higgins, Proc. Phys. Soc. of London **4,** 215 (1917).

[2] K. Przibram and E. Kara-Michailova, Akad. Wiss. Wien, Ber **131,** 2A 285 (1923), **132,** 2A, 261 (1924).

[3] L. E. Smith, Phys. Rev. **28,** 431 (1926).

time taken for the source of rays to become constant. It was also thought desirable to use a strong source of radiation, hoping thereby to hasten the decay.

Not only were the radioactive source and the luminescent material kept separate but the luminescent material was kept inclosed in a capsule so that it could be studied before bringing it in contact with the radioactive source or after its removal.

Apparatus and Procedure

In order to keep the luminescent material separate from the radioactive source, brass capsules were prepared, as shown in Fig. 1, each consisting of five major parts. On a gold plate fitted snugly in a depression on the face of part (5) was placed a layer of radium sulphate in equilibrium

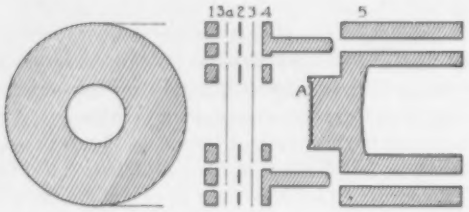

Fig. 1. Brass capsule.

with its decay products and covered with a coat of varnish. Such a plate furnishes a constant source of radiation permitting the α as well as the β and γ-rays to pass through. Part (4), serving to hold parts (1) and (5) together consists of a thin brass washer to which are fastened several legs fitting snugly into holes in part (5). Part (1) is a brass washer to which can be fastened part (2), an aluminum washer; a thin sheet of mica is

Table I.

Capsule	Radium content	Rays emitted
1	0.293 mg	α β γ
2	0.522	α β γ
3	0.910	α β γ
4	0.815	α β γ
A	2.40	α β γ
B	.16	β γ
C	2.8	α β γ
D	Pol.	

placed between the brass washer and the aluminum washer and parts (1) and (2) are fastened together by means of small screws. The luminescent material was placed in the opening in the aluminum washer (2) and the sample as well as the aluminum washer were covered with a piece of very thin mica (3). Against this mica disk part (4) was fastened by means of small screws. Thus the sample was separated from the radioactive source and also protected from contamination by radium and its products.

Three different kinds of capsules were prepared: (A) where the mica disk (3) was thin enough to allow α as well as β and γ-rays to pass through (in some cases the mica was replaced by aluminum foil); (B) were the mica (3) was thick enough to allow only the β and γ-rays to pass through; (C) where the layer of radium sulphate was replaced by a polonium plate, giving off chiefly α-rays. Thus it was possible to study the effect of α-rays or β and γ-rays or α, β and γ-rays upon the sample of zinc sulphide.

The luminosities of the different samples were measured by means of a Nutting polarization photometer. The arrangement of apparatus is shown in Fig. 2. The apparatus is so arranged that by changing the distance between the standard lamp and the ground glass screen, its illumination of the screen can be controlled. The standard lamp S is supplied by means of storage batteries and its voltage maintained constant by a potentiometer arrangement, and a ballast lamp to stabilize the current for small variations in the battery voltage. Light from the standard lamp is reflected by the rhomb shown in Fig. 2, thus passing through the polarizing Nicol NP and the photometer cube C. Light from the sample B is reflected by the prism D thus passing into the photometer cube C, and is again reflected as shown in Fig. 2.

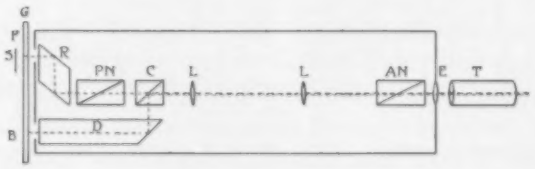

Fig. 2. Diagram of photometer.

In making an observation, the telescope is focused on the photometer cube and the field appears as two strips of reflected light from the sample B with the transmitted light from the standard lamp between them. By varying the intensity due to the standard lamp by means of the Nicol prism AN, the central strip is made alternately lighter and darker than the strips illuminated by the sample B until an intensity match is obtained. With the exception of the improvement in design of the capsule the apparatus is the same as that used by Smith[3] in his study of barium bromide. The reference lamp S was a 110 volt incandescent carbon filament lamp operated at 60 volts. This lamp was compared with a lamp standardized by the Bureau of Standards. A green filter F was interposed to produce a better color match.

The brightness of the samples was readily calculated from the scale readings of the photometer and the constants of the apparatus. The photometer was graduated in logarithms of the ratio of the illuminating power of the standard lamp to that of the sample. If K is the transmission coefficient of the filter, C_1 the candle power of the standard lamp, C_2 the candle power of the sample, d_1 and d_2 their respective distances from the ground glass screen G,

$$\log_{10}(KC_1/d_1^2) - \log_{10}(C_2/d_2^2) = x \text{ (reading on photometer)}.$$

If A is the area of the exposed luminous portion of the sample, the brightness B in apparent candle power per square cm is

$$B = (KC_1d_2^2)/(d_1^2 10^x A).$$

The sample of luminescent zinc sulphide approximately 0.020 cm in thickness was prepared and sufficient time allowed for the decay of the luminosity due to exposure to light in preparing. The sample was slipped on part (5) Fig. 1 and its luminosity read at intervals of a few minutes for the first hour, then at slightly longer intervals for the first day. All measurements were made at room temperature.

Results

This study has shown that for crystalline zinc sulphide, there is first an initial growth to maximum value, then a decrease in luminosity followed by a second growth to a maximum, and then a very slow decay.

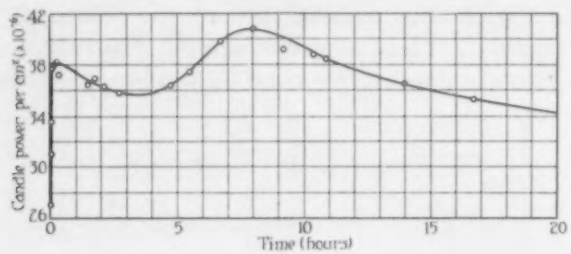

Fig. 3a. Luminosity curve, capsule (4), α, β, γ-rays. Zinc sulphide screen.

Figs. 3a and 3b show the variation of luminosity with time for two samples (4) and (A) (radium content given in Table I); from these curves will be seen that the maxima as well as the time required to reach these maxima are dependent upon the amount of radium present. Capsule (4) containing less radium than capsule (A) requires a longer time to reach the maximum values

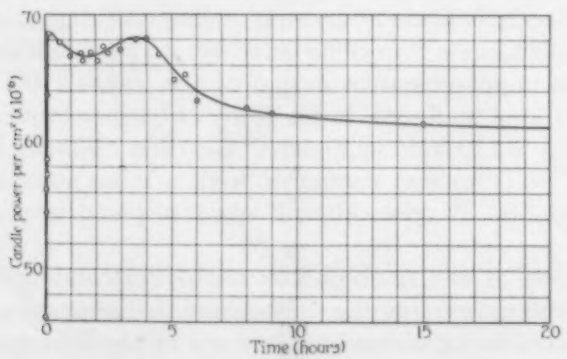

Fig. 3b. Luminosity curve, capsule (A), α, β, γ-rays. Zinc sulphide screen.

and these maxima are lower time to reach the maximum values and these maxima are lower than for capsule (A). Similar results were found for capsules (1), (2), and (3). Capsule (1) for example, containing 0.293 milli-

grams of radium, required about 5 hours to reach the first maximum and about 15 hours to reach the second maximum. The maximum brightness for capsule (1) was 1.65×10^{-6} candle power per square cm. In all the above cases the sample of zinc sulphide was bombarded by α, β, and γ-rays.

Fig. 4 is a luminosity time curve for capsule (C). In this case the luminescent material was bombarded by β and γ-rays only. This curve also shows

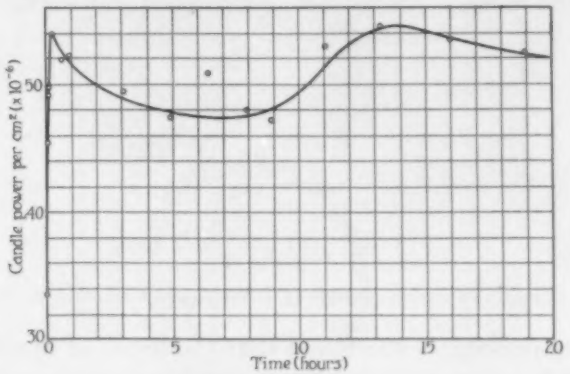

Fig. 4. Luminosity curve, capsule (C), β, γ-rays. Zinc sulphide screen.

the two maxima but the time required to reach the first maximum value was about 20 minutes and the second maximum about 13 hours.

Fig. 5 shows the curves of Fig. 3a, 3b and 4 plotted over a longer period of time. From this curve we can see that the rate of decay for capsule (A) after reaching its second maximum is greater than that of capsule (4). The

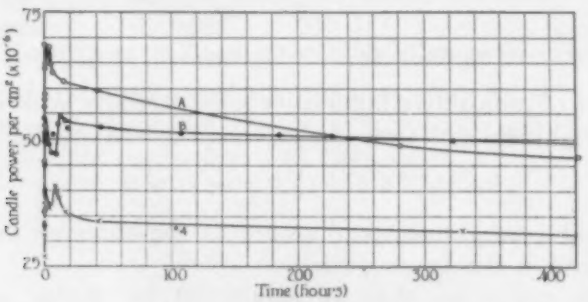

Fig. 5. Curves of Figs. 3a, 3b and 4 plotted over long periods of time.

decay of capsule (A) was not nearly so rapid as was expected from consideration of the amount of radium present in the two cases. It must also be noted that decay of luminescence for capsule (C) (which emits only β and γ-rays) after reaching the second maximum is much slower than for capsule (A).

The initial part of the luminosity time curve for capsule (D) is shown in Fig. 6. In this capsule the radium sulphate was replaced by a polonium plate so that the sample of zinc sulphide was bombarded chiefly by α-rays. Here also is seen the initial growth, decay and second maximum, followed by a gradual decay.

Fig. 7 shows the variation of luminosity with time for capsule (4) over a period of 400 days. Only one maximum is shown on this curve, this is due to the small time scale used in plottings. From this curve and similar curves

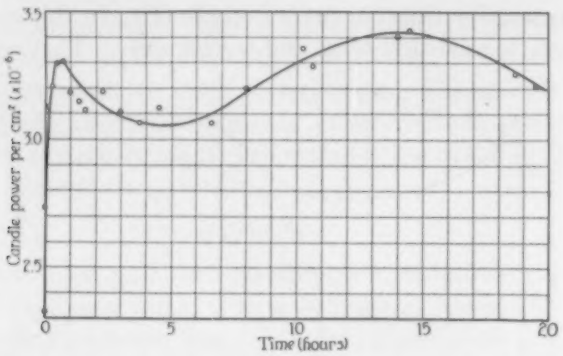

Fig. 6. Luminosity curve, capsule (D), Po α-rays. Zinc sulphide screen.

drawn over long periods, it was found that the decay of luminosity was not hastened as much as was expected by using a strong radium source.

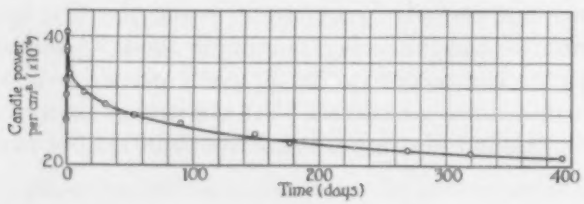

Fig. 7. Variation of luminosity with time for capsule (4) over a period of 400 days.

The theory of radioactive luminosity formulated by Walsh,[4] in which the variation in brightness with time was expressed by the equation

$$\log\left[(B/(b+B)\right] + a + kt = 0$$

where a, b, and k are constants, does not fit the observed decay curves of brightness found in this investigation.

Neither do the other theories mentioned by Walsh on radioactive luminescence explain the initial growth or the appearance of the second maximum, which was characteristic of all the curves plotted, whether the material was bombarded by α or β and γ, or α, β and γ-rays.

Since the luminescent material and the radioactive source were kept separate, it was possible to study the decay of the luminescent material after the radioactive source was removed. The screens containing the luminescent material were placed in contact with the exciting agent until the maximum brightness was reached and then the radioactive source was removed and the rate of decay of luminosity with time was studied. Fig. 8

[4] J. W. T. Walsh, Proc. Phys. Soc. of London **39**, 318 (1926–27).

shows the relation of brightness to time. The broken curve (with ordinates on the right) shows the relation between logarithms of intensity and time. From this curve it can readily be seen that the luminosity time curve, for a sample after the exciting agent was removed, is not of the type whose ordinate can be expressed by a single exponential term.

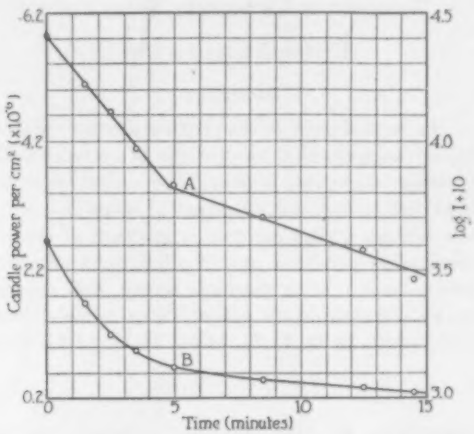

Fig. 8. Curve A = relation between logarithms of intensity and time.
Curve B = luminosity vs. time.

The fact that the decay of the zinc sulphide after removal of the exciting agent is not a single exponential may be an important factor in the formulation of a theory explaining the initial part of the brightness curves found in this investigation.

In conclusion the writer wishes to express his appreciation to Professor D. H. Kabakjian who suggested the problem, prepared the radium samples and under whose direction the work was carried out, and to Dr. E. E. Witmer for many helpful suggestions and discussions.

A SECOND IONIZATION POTENTIAL IN POTASSIUM VAPOR

By A. L. Hughes and C. M. Van Atta
Washington University, Saint Louis

(Received June 11, 1930)

Abstract

The occurrence of a second peak in the photoionization curve of potassium vapor (Lawrence and Edlefsen) suggests that there might be a related peak (or discontinuity) in the curve for ionization by electron impact. The ionization in potassium vapor was investigated by Hertz' method of neutralization of space charge by positive ions. It was found that there was an abrupt increase in gradient of the ionization curve, indicating a second ionization potential at 0.97 ± 0.05 volt above the first one corresponding to the series limit. With mercury vapor, the apparatus indicated the presence of Lawrence's ultraionization potentials in mercury vapor, together with three new ones (10.40, 10.62, 10.88, 11.28, 11.40, 11.77, 12.16, 12.46).

Introduction

CERTAIN peculiarities in the photoionization curve of potassium in the vicinity of the series limit led to these experiments. Lawrence and Edlefsen[1] found that the photoionization of potassium is a maximum at the series limit (2856A), diminishes to a minimum at 2700A, and then rises to a second higher maximum at 2340A. Mohler and Boeckner,[2] however, find that the ionization starts at the series limit and increases steadily. This curve resembles Lawrence's[3] earlier results except for the fact that in the latter case the effect began at 2600A. The peculiar form of the curve obtained by Lawrence and Edlefsen suggests that in ionization by electron impact something of a similar nature might be revealed. The only work which we can find on the ionization potential of potassium by electron impact is that done thirteen years ago by Tate and Foote,[4] who identified roughly the ionization potential with the theoretical value corresponding to the series limit. They were interested only in establishing this approximate identity and made no attempt to study the shape of the ionization curve above the ionization potential. Another result which suggests that a careful study of the ionization curve for potassium might reveal peculiarities is Lawrence's discovery of the ultraionization potentials of mercury vapor (i.e., discontinuities in the ionization curve at 0.20, 0.89, 1.30 and 1.66 volts above the theoretical ionization potential corresponding to the series limit).

Apparatus and Results

The method used for investigating the ionization potential was that originally used by Hertz. An oxide coated platinum filament, F, 11 mm long,

[1] E. O. Lawrence and N. E. Edlefsen, Phys. Rev. **34**, 1056 (1929).
[2] F. L. Mohler and C. Boeckner, Bureau of Standards, Journal of Research **3**, 303 (1929).
[3] E. O. Lawrence, Phil. Mag. **50**, 345 (1925).
[4] J. T. Tate and P. D. Foote, Washington Acad. Sci. Jour. **7**, 517 (1917).

was mounted in a rectangular box of monel metal, *B*, 25×30×15 mm. A second oxide coated filament, *C*, was located just outside the box, opposite a small slit 0.6 mm in width. The slit was at right angles to the filament,

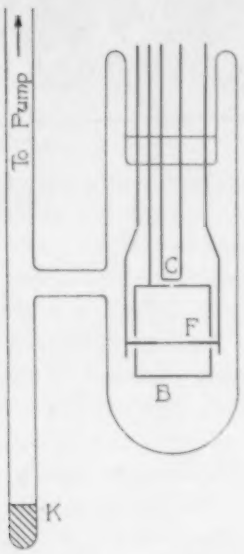

Fig. 1. Diagram of tube.

so that only those electrons coming from a nearly equipotential region of the filament, *C*, were allowed to enter the box. The potassium was dis-

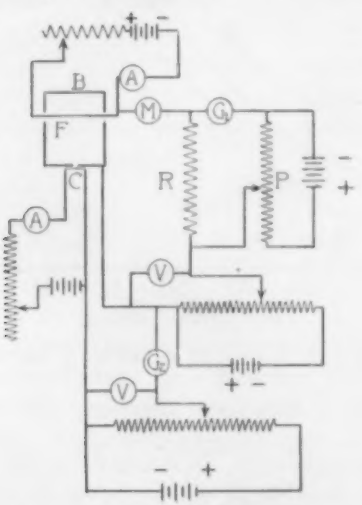

Fig. 2. Arrangement of balancing circuit.

tilled into a side tube, *D*. The whole of the apparatus, including part of the tube leading to the pump, was surrounded by a furnace, the temperature of which could be controlled.

To measure the change in the space charge limited current from F, caused by ionization inside the box, we used a balance arrangement, shown in Fig. 2. The thermionic current from the filament, F, passed through a resistance R. The voltage drop across R was balanced by an opposing potential from the potentiometer, P, through the galvanometer, G. Any change in the space charge limited current, far too small to be measured

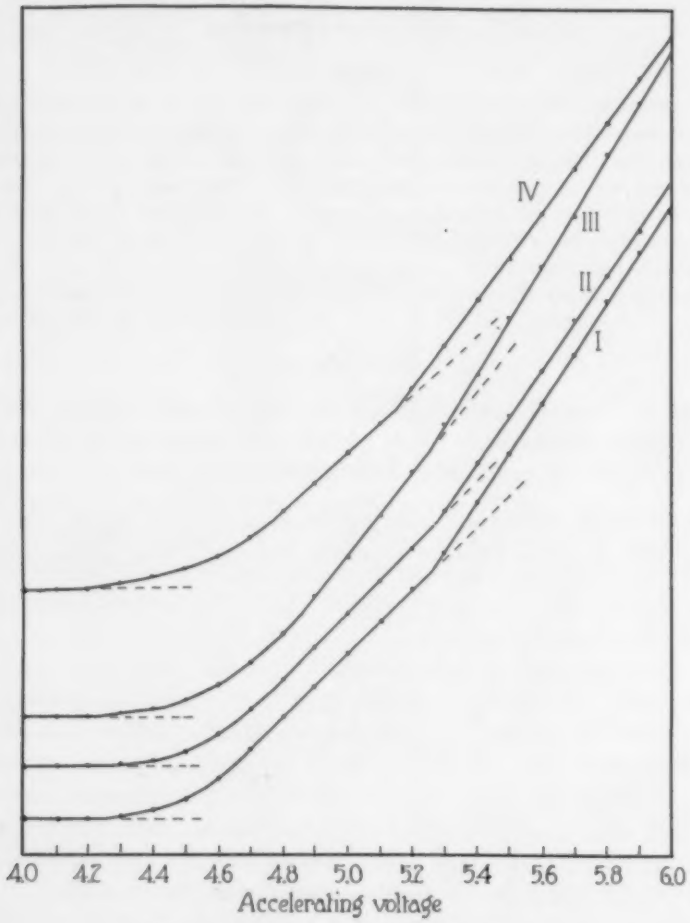

Fig. 3. Ionization curves for K vapor.

Curve:	I	II	III	IV
Temp.:	189	200	197	197°C

accurately on the micro-ammeter, M, could be easily read on the galvanometer. To secure steady conditions, batteries of large capacity were used.

In order that almost every electron from C entering the box should collide with a potassium atom, the apparatus was kept between 180°C and 205°C. This temperature range corresponds to a range of electronic mean free paths from 6 mm to 2 mm, and of vapor pressures from 0.0018 to 0.005 mm of mercury.

Under our final conditions, the space charge limited current from F was independent of the heating current for temperatures well below the rated limit of the filament. The presence of potassium in the apparatus increased the emission from filament C so much that sufficient electrons to cause measurable ionization were given off at a temperature below visible redness. Thus the velocity range of the emitted electrons due to temperature was small.

Some typical curves are shown in Fig. 3. Only relative values of the ionization potentials, of course, are given accurately by this method, since we had no easy way of correcting for the contact differences of potential involved. We have assumed that the initial rise in the curve corresponds to the ionization potential, which from spectroscopic data is 4.32 volts for potassium. All the curves show a second distinct discontinuity nearly one volt above the point at which ionization begins. The average of the separations between the first and second breaks for twenty-three curves is 0.97 ± 0.05 volts. It is interesting to note that just above the first break the curves merge into the horizontal axis asymptotically, making it difficult to determine the exact point at which ionization begins; whereas the second break is very sharp. The sharpness of the second break indicates that the velocity range of the ionizing electrons was small enough to show the true shape of the ionization curve. Thus we conclude that the rounding off of the first break is a true representation showing a slow increase in the ionization probability in the neighborhood of the ionization potential.[6]

As a check on the apparatus we also attempted to verify Lawrence's results on the ultraionization potentials of mercury vapor, before beginning the work on potassium vapor. We found that the discontinuities in mercury vapor were considerably more difficult to reproduce time after time than the single discontinuity in potassium. However, we obtained the following values for the ultraionization potentials of mercury, which are not wholly in agreement with those found by Lawrence.[7]

Lawrence's values	10.40	10.60		11.29		11.70	12.06	
Our values	10.40	10.62	10.88	11.28	11.40	11.77	12.16	12.76

Discussion

We may regard the discontinuity in the ionization curve at 0.97 volts above the first ionization potential as indicating the onset of an additional kind of ionization. This may be considered as a second ionization potential at $4.32+0.97=5.29$ volts. It is tempting to seek a correlation between the

[6] Simultaneously with the measurement of the change in the space charge limited current by galvanometer G_1, the total emission from filament C was measured on galvanometer G_2. We found that the emission from C did not vary over 10 percent over the range of accelerating potentials used in producing the curves. Furthermore, the emission from C was a smooth, almost linear, function of the accelerating potential. Thus the discontinuity in the ionization curves above the ionization potential cannot be due to any abrupt change in the number of electrons entering the box.

[7] E. O. Lawrence, Phys. Rev. **28**, 947 (1926).

second ionization potential by electron impact and the short wave-length peak in Lawrence's work. We should expect to find the onset of a second type of photoionization at 2334A, corresponding to 5.29 volts. However, in Lawrence's experiment, the second type of photoionization begins at 2700A and rises to a maximum at 2340A. Now the second break in our curves corresponds much more closely to the latter value, although we should have expected correlation with the former.

Until recently it was customary[8] to associate the presence of the second ionization potential in photoionization in potassium with an effect on the molecule. Such evidence as we have as to the association in potassium vapor indicates that for every molecule, there are perhaps 5,000 atoms. Therefore, in order to account for the results, it has been suggested that, for light, the molecule has a much larger absorption coefficient than the atom. Since the change in slope at the second ionization potential in our ionization by electron impact curves is of the same order as the change in slope at the first, it would also mean a very large effective cross section for the molecule for electron impact as compared with the atom. Since this line of argument seems to lead to a conclusion which is difficult to believe, we are inclined to associate the second discontinuity with the onset of a second type of ionization in the atom, for which we have no theory.

A close correlation between the effects of light and electron impact is not to be expected. We know, for example, that in the excitation of an atom by light, the fit between the wave-length of the exciting light and the energy changes in the aton must be exact. However, in the case of electron impact, the colliding electron need have only *sufficient* energy. Similarly, in the field of ionization, we could hardly expect an exact parallelism between the effect of light and the effect of electron impact.

[8] E. O. Lawrence, Phil. Mag. **50**, 345 (1925), R. W. Ditchburn and F. L. Arnot, Proc. Roy. Soc. **A123**, 516 (1929).

ABSORPTION AND COLLISION BROADENING OF THE MERCURY RESONANCE LINE

By M. W. Zemansky*
Palmer Physical Laboratory, Princeton, N. J.

(Received June 9, 1930)

Abstract

Radiation emitted by a mercury resonance lamp. It is shown how an approximate expression for the frequency distribution of the radiation from a resonance lamp can be arrived at, and that it can be represented approximately by a Gauss error curve with a half-breadth depending upon the geometry of the lamp and upon the vapor density, and in general greater than that of the absorption line.

Absorption coefficient and ratio of emission to absorption line breadth. Assuming that all five components of the mercury resonance line are alike both in emission and in absorption, and that any one component of the emission and of the absorption line is a Gauss error curve of half-breadth $\Delta\nu_E$ and $\Delta\nu_D$ respectively ($\Delta\nu_D$ = Doppler breadth), the absorption of a slab of thickness l is calculated as a function of $\kappa(\nu_0)l$, where $\kappa(\nu_0)$ is the absorption coefficient for the center of any one of the components. From experimental values of the absorption, $\kappa(\nu_0)$ is found to be consistent with the theoretical value $1.41\times10^{-13}N$ (where N is the number of Hg atoms per cc) provided $\Delta\nu_E/\Delta\nu_D$ is taken to be 1.21 in these experiments, 1.46 in Orthmann's, 1.50 in Hughes and Thomas', 1.15 in Kunze's, and 1.15 in Kopfermann and Tietze's.

Lorentz collision broadening of the absorption line. A theoretical expression is obtained for the absorption coefficient when collision broadening is superimposed upon Doppler broadening, and is evaluated for different values of the frequency and of $\Delta\nu_C/\Delta\nu_D$ where $\Delta\nu_C$ is the Lorentz collision breadth and $\Delta\nu_D$ is the Doppler breadth. With $\kappa(\nu_0)l$ and $\Delta\nu_E/\Delta\nu_D$ equal to the values found for these experiments, the absorption is calculated as a function of $\Delta\nu_C/\Delta\nu_D$. From experimental values of the absorption of mercury vapor in the presence of H_2, N_2, A, CO, NH_3, He, CH_4, and C_3H_8, $\Delta\nu_C$ is found as a function of the pressure of each gas. The curves of $\Delta\nu_C$ against pressure yield the effective broadening radius of each molecule, which is found to be directly proportional to the square root of the molecular diamagnetic susceptibility. On the basis of the Langevin theory this means that the effective broadening area of a molecule varies at the product of the number of outer electrons and the mean square radius of all the electronic orbits. The same result is obtained from the experiments of Füchtbauer, Joos and Dinkelacker.

Absorption Coefficient and Ratio of Emission to Absorption Line Breadth

THE transmission through mercury vapor of the radiation emitted by a mercury resonance lamp has been measured many times under apparently similar conditions, and yet the results have varied very markedly. The resulting values of absorption coefficient have differed from one another by as much as several hundred percent. In an investigation of the quenching of mercury resonance radiation by foreign gases which has been in progress for

* National Research Fellow.

the last two years it was found necessary to know the absorption coefficient of mercury vapor for mercury resonance radiation very accurately. Consequently, this quantity was studied rather carefully with a view to discover, if possible, the causes for the existing discrepancies. The present paper, it is hoped, will clear up those difficulties which have not already been solved by others, and will give a summary of all the work that has been done since 1925, as well as a new set of measurements of the absorption coefficient.

The Radiation Emitted By a Mercury Resonance Lamp

It has been shown by Wood[1] that the mercury resonance line ($\lambda = 2537$) emitted by a mercury arc consists of five components of approximately equal intensity, and that all of these components are absorbed approximately equally by a column of mercury vapor. This has been substantiated by very careful measurements of the Zeeman effect of the mercury resonance line in a recent paper by Schein.[2] The intensity distribution of the radiation emitted by a mercury resonance lamp, however, is not known accurately as a function of the vapor density, the type of resonance lamp, dimensions, etc. It was assumed by Orthmann,[3] Kunze,[4] and Schein that the radiation emitted by a mercury resonance lamp was similar in intensity distribution to radiation whose half-breadth was equal to that of the absorption line but which had been absorbed slightly by passing through a thin layer of mercury vapor on its way out of the resonance lamp. This assumption was used by Orthmann and Kunze to calculate a correction factor which was applied to all the experimental values of the absorption. Schein, however, recognized that this assumption implies that the radiation emitted by a resonance lamp has a half-breadth slightly larger than that of the absorption line, and, by graphical means, estimated that, in his experiments, the ratio was 1.23.

The original supposition, namely, that the radiation emitted by a mercury resonance lamp is similar to that which results when a line of half-breadth equal to that of the absorption line passes through a thin absorbing layer, is only partly true, for when the vapor density in the resonance lamp approaches zero, the intensity should approach zero, whereas, according to the above assumption, it approaches a constant. A more satisfactory picture of the situation can be made on the basis of the following approximations:

1. The original stimulating radiation from the arc has a breadth that is so wide in comparison to the absorption line breadth of the vapor in the resonance lamp that it can be regarded as a continuous spectrum in the limited range of frequencies under consideration. Call this intensity A.

2. The radiation that is re-emitted in the body of the resonance lamp is a fraction ϵ of that amount of A which is absorbed in a column of average thickness l_1. Call this radiation $A_1(\nu)$.

[1] R. W. Wood, Phil. Mag. **50**, 761 (1925).
[2] M. Schein, Helv. Phys. Act. Vol. II, Sup. I (1929).
[3] W. Orthmann, Ann. d. Physik **78**, 601 (1925).
[4] P. Kunze, Ann. d. Physik **85**, 1013 (1928).

3. The radiation that finally emerges from the resonance lamp is the radiation $A_1(\nu)$ after it has passed through a column of vapor of average thickness l_2. Call this radiation $A_2(\nu)$.

The situation is represented graphically in Fig. 1.

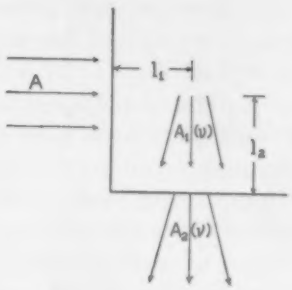

Fig. 1. Schematic representation of a resonance lamp.

Let us consider only one component of the mercury resonance line, inasmuch as all the components behave the same way. We have

$$A_1(\nu) = \epsilon A(1 - e^{-\kappa(\nu) l_1})$$

$$A_2(\nu) = A_1(\nu) e^{-\kappa(\nu) l_2}$$

where $\kappa(\nu)$ is the absorption coefficient of the vapor in the resonance lamp for the frequency range between ν and $\nu + d\nu$. Let us make the usual assumption:

$$\kappa(\nu) = \kappa(\nu_0) e^{-[2(\nu-\nu_0)/\Delta\nu_A]^2 \log_e 2}$$

where $\kappa(\nu_0)$ is the absorption coefficient for the center of the line of frequency ν_0, and $\Delta\nu_A$ is the half-breadth of the absorption line. Calling $2(\nu-\nu_0)/\Delta\nu_A (\log_e 2)^{\frac{1}{2}} = \omega$, we have then

$$\kappa(\omega) = \kappa(0) e^{-\omega^2}.$$

Let us further assume that the geometry of the resonance lamp has been so arranged that l_1 is very nearly equal to l_2. This is not essential, but it simplifies matters somewhat. Then, after substitution, we have

$$A_2(\omega) = \epsilon A(1 - e^{-x e^{-\omega^2}}) e^{-x e^{-\omega}} \qquad (1)$$

where $x = \kappa(\nu_0) l_1 = \kappa(\nu_0) l_2$.

Plotting this expression for different values of x, it is found that it resembles a Gauss error curve fairly well with a half-breadth greater than that for the curve $e^{-\omega^2}$, that is, greater than the half-breadth of the absorption line. Calling this new half-breadth $\Delta\nu_E$, $\Delta\nu_E/\Delta\nu_A$ was found graphically to be 1.16 when $x = 0.25$ and 1.33 when $x = 0.50$. As the vapor density approaches zero, x approaches zero, and Eq. (1) approaches $x\epsilon A e^{-\omega^2}$, which is correct, because the intensity approaches zero, and the half-breadth approaches the absorption line breadth.

Burger and van Cittert[5] considered the broadening of a spectral line by absorption and obtained an expression for the breadth as a function of x. Unfortunately, however, their results can not be applied to the case of a resonance lamp.

If there were some way of estimating x for a particular resonance lamp it might be worth while to use the expression given by Eq. (1) in what is to follow. Since, however, there is no way of knowing how accurately x can be estimated, it is better to replace Eq. (1) by a Gauss error curve of half-breadth $\Delta\nu_E$ where $\Delta\nu_E$ is to be determined by experiment.

Two types of resonance lamp have been used to obtain resonance radiation. In the first one, the resonance radiation is taken off the incident window at about 45° to the incident beam,[6] and in the second, it emerges from a separate window at an angle of 90° to the incident beam.[7] It is obvious that the second type can be designed to correspond to a much smaller value of x than the first. It is therefore to be expected that the experiments conducted with the 90° type will involve a smaller value of $\Delta\nu_E$ than those performed with one of the 45° type.

The Absorption of Radiation

When radiation of frequency between ν and $\nu+d\nu$ and intensity $K(\nu,0)$ passes through an absorbing slab of thickness l with absorption coefficient $\kappa(\nu)$, then the transmitted radiation, $K(\nu, l)$ is given by[8]

$$K(\nu, l) = K(\nu, 0)e^{-\kappa(\nu)l}.$$

Let us suppose, as usual, that the emission and absorption lines are Gauss error curves with half-breadths $\Delta\nu_E$ and $\Delta\nu_A$ respectively. Then

$$K(\nu, 0) = K(\nu_0, 0)e^{-[2(\nu-\nu_0)/\Delta\nu_E]^2\log_e 2}$$
$$\kappa(\nu) = \kappa(\nu_0)e^{-[2(\nu-\nu_0/\Delta\nu_A]^2\log_e 2}$$

and the absorption, A, is

$$A = 1 - \frac{\int_{-\infty}^{\infty} e^{-[\omega^2+\kappa(\nu_0)le^{-(\Delta\nu_E/\Delta\nu_A\omega)^2}]}d\omega}{\int_{-\infty}^{\infty} e^{-\omega^2}d\omega}$$

where

$$\omega = \frac{2(\nu-\nu_0)}{\Delta\nu_E}(\log_e 2)^{1/2}.$$

For values of $\kappa(\nu_0)l \leqq 1.5$, the series expansion of Eq. (2) is satisfactory for numerical computation

[5] H. C. Burger and P. H. van Cittert, Zeits. f. Physik **51**, 638 (1928).
[6] A. L. Hughes and A. R. Thomas, Phys. Rev. **30**, 466 (1927).
[7] P. Kunze, reference 4.
[8] A. v. Malinowski, Ann. d. Physik **44**, 935 (1914).

$$A = \kappa(\nu_0)l \cdot \frac{1}{\left(1+\left(\frac{\Delta\nu_E}{\Delta\nu_A}\right)^2\right)^{1/2}} - \frac{[\kappa(\nu_0)l]^2}{2!} \cdot \frac{1}{\left(1+2\left(\frac{\Delta\nu_E}{\Delta\nu_A}\right)^2\right)^{1/2}} + \cdots$$

$$\cdots + (-1)^n \frac{[\kappa(\nu_0)l]^n}{n!} \cdot \frac{1}{\left(1+n\left(\frac{\Delta\nu_E}{\Delta\nu_A}\right)^2\right)^{1/2}} + \cdots$$

$$A = 1 - \frac{\int_{-\infty}^{+\infty} e^{-[\omega^2+\kappa(\nu_0)le^{-(\Delta\nu_E/\Delta\nu_A\omega)^2}]}\, d\omega}{\int_{-\infty}^{\infty} e^{-\omega^2}\, d\omega}.$$

TABLE I. *Values of A.*

$\kappa(\nu_0)l$ \ $\frac{\Delta\nu_E}{\Delta\nu_A}$	0	.50	1.0	1.27	2.0	3.0
0.25	0.221	0.200	0.160	0.140	0.102	0.0723
.50	.393	.360	.291	.256	.188	.133
1.0	.632	.588	.486	.428	.316	.226
1.5	.777	.736	.619	.550	.400	.287
2.0	.865	.832	.711	.630	.472	.348
3.0	.950	.925	.820	.738	.564	.414
4.0	.982	.967	.878	.805	.622	.461
4.5	.989	.977	.897		.640	.480

For values of $\kappa(\nu_0)l > 1.5$ it was found more convenient to evaluate A graphically. The values of A for different values of $\kappa(\nu_0)l$ and $\Delta\nu_E/\Delta\nu_A$ are given in Table I, and are plotted in Fig. 2. Curves of A against $\kappa(\nu_0)l$ for various values of $\Delta\nu_E/\Delta\nu_A$ are shown in Fig. 3. DeGroot[9] has given curves of the same character as those of Fig. 2, but in a form that is not very convenient for the purpose at hand.

When $\Delta\nu_E/\Delta\nu_A$ is kown, a curve of A against $\kappa(\nu_0)l$ can be drawn, and from experimental values of A and l, $\kappa(\nu_0)$ can be obtained. Values of $\kappa(\nu_0)$ for mercury vapor at a density corresponding to 20° C obtained by different authors under different conditions are given in Table II.

It will be seen from Fig. 3 that, if a curve of A against $\kappa(\nu_0)l$ for $\Delta\nu_E/\Delta\nu_A = a$, where a is any number, be used in a situation which really requires the use of a curve for $\Delta\nu_E/\Delta\nu_A > a$, the resulting values of $\kappa(\nu_0)l$ will be too small. It is to be expected, therefore, that the smallest values of $\kappa(\nu_0)$ will correspond to the largest values of $\Delta\nu_E/\Delta\nu_A$. This is seen to be the case, for it was pointed out in the beginning that the 45° type of resonance lamp yields a broader line than the 90° type.

There is another important error that can result in a final value of $\kappa(\nu_0)$ that is too small, namely, the reception by the photoelectric cell of scattered

[9] W. de Groot, Physica **9**, 263 (1929).

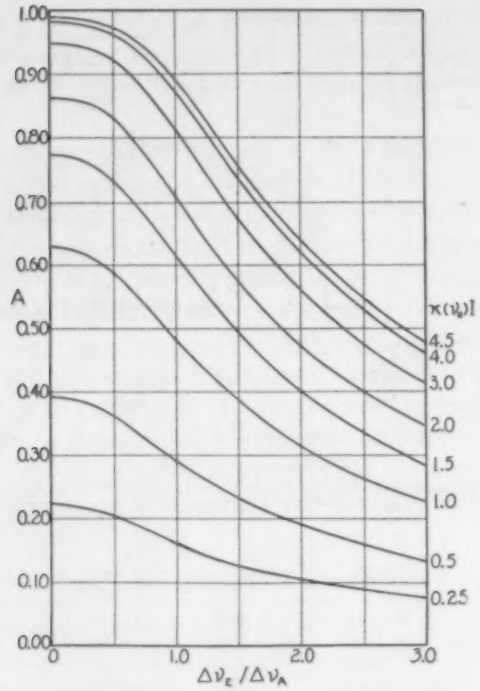

Fig. 2. Values of A for different values of $\kappa(\nu_0)l$ and $\Delta\nu_E/\Delta\nu_A$.

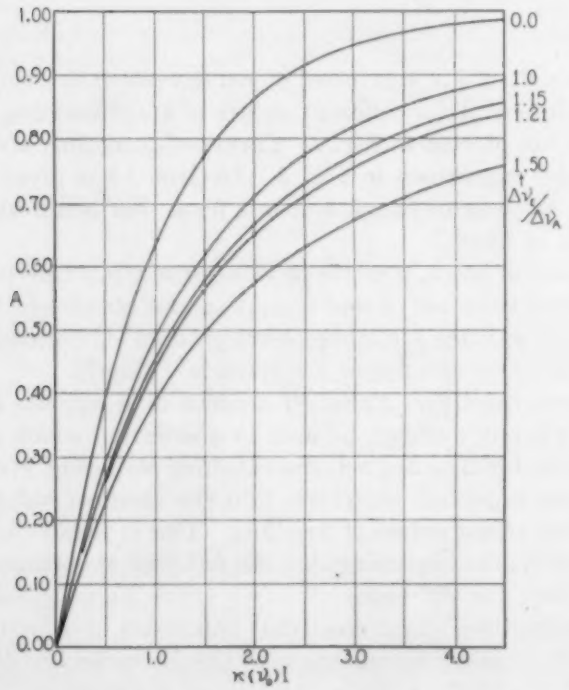

Fig. 3. Curves of A against $\kappa(\nu_0)l$ for various values of $\Delta\nu_E/\Delta\nu_A$

TABLE II.

	Type of Resonance Lamp	Method of computing $\kappa(\nu_0)l$ from A	at 20°C
Orthmann[3]	45°	Used curve of A against $\kappa(\nu_0)l$ for $\Delta\nu_E/\Delta\nu_A=1$ and applied a correction factor to A to take into account absorption in the resonance lamp.	3.1
Hughes and Thomas[6]	45°	Used exponential law of absorption which is equivalent to assuming $\Delta\nu_E/\Delta\nu_A=0$	1.24
Schein[2]	90°	Used curve of A against $\kappa(\nu_0)l$ for $\Delta\nu_E/\Delta\nu_A=1.23$ but computed $\Delta\nu_E/\Delta\nu_A$ inaccurately.	3.77
Kunze[4]	90°	Same as Orthmann	5.2
Kopfermann and Tietze[10]	90°	Used formula due to Ladenburg for a situation in which the emitting and absorbing slabs are both infinitesimally thin.	5.2
Author	90°	Used curve of A against $\kappa(\nu_0)l$ for $\Delta\nu_E/\Delta\nu_A$ equal to that value which makes $\kappa(\nu_0)l$ vary linearly with Nl. This value was found to be 1.21.	5.61

radiation along with the transmitted radiation. If the photoelectric cell is placed close to the emerging window, and if the diaphragm which limits the incident beam is in front of the incident window, then a portion of the scattered radiation emitted by the *whole* emerging face is received by the photoelectric cell, resulting in a smaller value of A. It has been found by experiment that no scattered radiation reaches the photoelectric cell if the following conditions are adhered to:

1. The diaphragm limits the incident beam to a diameter of about 1 cm, and is placed over the *emerging* window.
2. The photoelectric cell is no nearer than 7 cm from the diaphragm.

It is believed that, in the experiments of Orthmann and in those of Hughes and Thomas, this was a possible source of error when the mercury vapor density was high enough to give rise to appreciable scattering. In all of the previous experiments, it is believed, an incorrect curve of A against $\kappa(\nu_0)l$ was used to compute the absorption coefficient.

APPARATUS

There is nothing essentially new in the apparatus used in these experiments, so that we shall limit ourselves to a very brief description.

Arc. Quartz mercury arc made by Cooper Hewitt, water-cooled and magnetically deflected.

Resonance lamp. 90° type with crystalline quartz windows cemented on with picein wax. Between it and the mercury diffusion pump there was a trap which was kept surrounded by ice. The drop of liquid mercury in a side tube was also kept in an ice bath. The exciting radiation from the arc illu-

[10] H. Kopfermann and W. Tietze, Zeits. f Physik **56**, 604 (1929).

minated about 5 mm of the incident window and the resonance radiation was taken off an area of the emerging window about 5 mm in diameter.

Absorption cell. A disk of heavy Pyrex glass about 4.5 cm inside diameter, and 0.792 cm in length was cut as shown in Fig. 4. Two crystalline quartz windows were cut in the same way and cemented on with picein wax. This was then cemented to a Pyrex tube about 10 cm long and 2 cm in diameter in which was placed a drop of mercury. There was thus a large opening between the tube containing the drop of mercury and the absorption cell proper, which enabled equilibrium conditions to be obtained rapidly.

The absorption cell was connected to the pumps through a glass spiral about a foot in diameter, which had sufficient flexibility to allow the cell to be moved in and out of the path of the light beam. A diaphragm with an

Fig. 4. Absorption cell.

aperture of about 1 cm remained fixed in space on the emerging side of the cell.

The photoelectric cell. The cell was made of fused quartz and had a platinum plate. It was first thoroughly cleaned and baked out, and then about 5 cm of H_2 was admitted. A discharge was passed through the H_2 by a small induction coil and then the H_2 was pumped out. This was repeated a few times until the platinum became slightly discolored. About 4 mm of H_2 was then introduced and the cell was sealed off. It was run on about 200 volts and a sensitive Compton electrometer was used to measure the current. The linearity of the cell at various voltages was tested with calibrated screens.

Method

With liquid air on the absorption cell the transmission of the quartz windows was measured and compared with the transmission of a piece of

cellophane which was mounted beside the cell and which came in front of the diaphragm when the cell was moved aside. The cellophane was used to cut down the intensity of the incident light by a known amount when it was measured. The mercury vapor in the absorption cell was maintained at constant density by a suitable substance contained in a Dewar flask which moved with the cell. Melting Benzol was used for the temperature 4.2°C and melting paraxylene for 12.1°C. Water was used for temperatures between 15 and 20°C. The absorption cell proper was always at room temperature which was held as near 20°C as possible. In calculating the number of mer-

TABLE III.

(1)	(2) Thickness l in cm	(3) Temp. °C	(4) Nl $\times 10^{-13}$	(5) Absorption A	(6) $\frac{\Delta\nu_E}{\Delta\nu_A}$	(7) $\kappa(\nu_0)l$ from Exp. plus Eq. (2)	(8) $\kappa(\nu_0)l$ Theor. Eq. (4)
Orthmann	0.85	2.7	0.706	0.346	1.46	0.82	0.995
		6.1	.970	.419		1.10	1.37
		11.5	1.60	.571		1.91	2.26
		12.0	1.68	.582		2.00	2.37
		15.5	2.28	.700		3.22	3.22
		18.0	2.85	.723		3.52	4.02
		19.3	3.18	.763		4.25	4.49
Hughes and Thomas	1.62	−13	.244	.202	1.50	.43	.344
		−8	.431	.309		.72	.608
		−3	.745	.440		1.23	1.05
		2	1.27	.554		1.83	1.78
		7	2.01	.660		2.79	2.84
		12	3.20	.755		4.32	4.51
Kunze	.301	0	.191	.161	1.15	.27	.269
		10	.494	.356		.72	.696
		15	.776	.489		1.12	1.09
		20	1.20	.620		1.70	1.69
Kopfermann and Tietze	.54	−11	.102	.115	1.15	.19	.144
		0	.343	.291		.55	.483
		10	.886	.539		1.31	1.25
		15	1.39	.661		1.95	1.96
		20	2.15	.741		2.60	3.03
Author	.792	0	.503	.370	1.21	.77	.71
		4.2	.752	.490		1.18	1.06
		12.1	1.58	.681		2.26	2.23
		15.4	2.11	.753		2.94	2.98
		20.0	3.15	.840		4.45	4.44

cury atoms per cc the vapor pressure was obtained from the International Critical Tables and the Knudsen correction was applied. In determining the transmission at a particular temperature, readings were taken through the cell and then through the cellophane at least six times.

Liquid air was put on the resonance lamp and the sensitivity of the photoelectric cell was increased by increasing the voltage. The absorption of the radiation emitted by the resonance lamp was then measured and found to be less than the radiation emitted by the lamp at 0°C. This was due to diffuse reflection in the resonance lamp of the edges of the broad 2537 line

from the arc. Other wave-lengths did not affect the photoelectric plate, for the reason that platinum treated with hydrogen has a long wave-length limit only a little above 2537. It was estimated that about 1 percent of the radiation from the resonance lamp at 0°C consisted of unabsorbable radiation. Every reading was therefore corrected to take account of this.

The results, along with those of others, are shown in Table III, and plotted in Fig. 5.

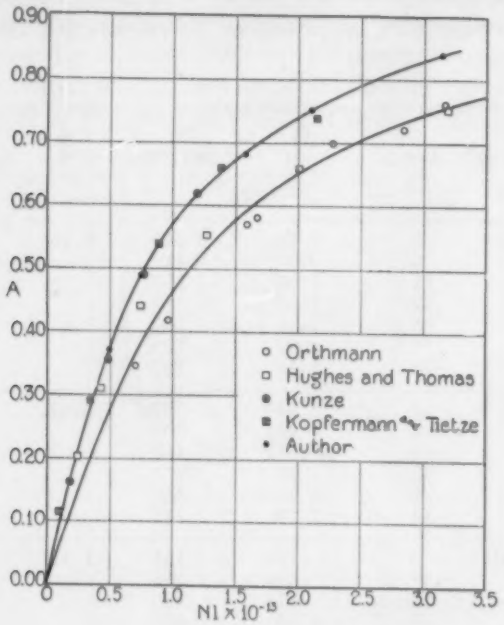

Fig. 5. A as a function of Nl.

It will be seen in Fig. 5 that all the measurements fall into two groups. those taken with the 90° type of resonance lamp, and those taken with the 45° type, the former yielding much larger values of the absorption. Both groups, however must correspond to the same values of $\kappa(\nu_0)l$. Inasmuch as it is impossible to calculate accurately $\Delta\nu_E/\Delta\nu_A$, the particular curve of A against $\kappa(\nu_0)l$ for each group is not immediately at hand. It must be chosen by appeal to theory as follows:

It is a well-known result that:[11]

$$\int_0^\infty (\kappa\nu)d\nu = \frac{h\nu_0 N}{4\pi} B_{1\to 2}$$

where N = no. of absorbing atoms per cc

ν_0 = frequency of center of line

$B_{1\to 2}$ = Einstein coefficient defined in terms of light intensity, and where the integration is to be taken over all the fine structure components of the absorption line. Using the Einstein relations

[11] E. A. Milne, M.N. of R.A.S. **85**, 111 (1924).

$$\frac{A_{2\to1}}{B_{1\to2}} = \frac{2h\nu^3}{c^2}\cdot\frac{q_1}{q_2}$$

and $A_{2\to1} = 1/\tau$, we have

$$\int_0^\infty \kappa(\nu)d\nu = \frac{\lambda_0^2}{8\pi\tau}\cdot\frac{q_2}{q_1}\cdot N$$

and substituting $\lambda_0 = 2.537\times10^{-5}$ cm, $\tau = 10^{-7}$ sec.[12] and $q_2/q_1 = 3$, we get

$$\int_0^\infty \kappa(\nu)d\nu = 7.68\times10^{-4}N.$$

Since each component of the absorption line obeys

$$\kappa(\nu) = \kappa(\nu_0)e^{-[2(\nu-\nu_0)/\Delta\nu_A]^2\log_e 2}$$

and since there are five components,

$$\int_0^\infty \kappa(\nu)d\nu = 5\left(\frac{\pi}{4\log_e 2}\right)^{1/2}\kappa(\nu_0)\Delta\nu_A$$
$$= 5\times1.07\kappa(\nu_0)\Delta\nu_A$$

whence finally

$$\kappa(\nu_0)l = \frac{1.44\times10^{-4}}{\Delta\nu_A}\cdot Nl. \tag{3}$$

In none of the experiments did the mercury vapor pressure ever become high enough to involve Lorentz collision broadening or Holtzmark coupling broadening of the absorption line. $\Delta\nu_A$ therefore, is the Doppler breadth $\Delta\nu_D$, and since the temperature of the absorption cell proper was always at 20°C, $\Delta\nu_D$ is constant. The Doppler breadth of a line is known to be $7.16\times10^{-7}\,\nu_0(T/M)^{1/2}$ sec^{-1} where T is the absolute temperature and M is the molecular weight. For mercury at 20°C, $\Delta\nu_D = 1.02\times10^9$ sec^{-1}, and consequently Eq. (3) becomes

$$\kappa(\nu_0)l = 1.41\times10^{-13}Nl. \tag{4}$$

In Fig. 6, Eq. (4) is shown as a heavy line. The individual points were obtained as follows:

A curve between $\kappa(\nu_0)l$ and A was sought which, in conjunction with the author's values of A, would give values of $\kappa(\nu_0)l$ that varied linearly with Nl. It was found that the curve corresponding to $\Delta\nu_E/\Delta\nu_A$ equal to 1.21 achieved this, and at the same time, agreed well with Eq. (4). Curves of $\kappa(\nu_0)l$ and A were then sought which, in conjunction with the other experimental values of A, would give values of $\kappa(\nu_0)l$ that agreed best with Eq. (4). In this way the curves corresponding to the values of $\Delta\nu_E/\Delta\nu_A$ given in Table III,

[12] R. Ladenburg, Naturwiss. **14**, 1208 (1926), H. W. Webb and H. A. Messenger, Phys. Rev. **33**, 319 (1929). For other references see M. W. Zemansky, Phys. Rev. **29**, 519 (1927).

column (6) were obtained, and the values of $\kappa(\nu_0)l$ in column (7) were obtained from these curves and experimental values of A. The values of $\kappa(\nu_0)l$ in column (8) were computed from Eq. (4). The agreement with theory is shown in Fig. 6.

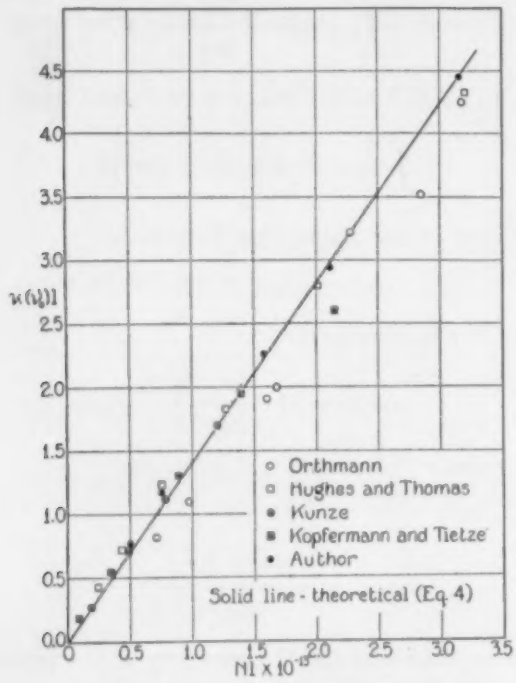

Fig. 6. $\kappa(\nu_0)l$ as a function of Nl.

Lorentz Collision Broadening

When an absorption line is broadened by Doppler broadening only, the absorption coefficient is given by

$$\kappa(\nu) = \kappa(\nu_0)e^{-[2(\nu-\nu_0)/\Delta\nu_D]^2 \log_e 2}$$

where $\Delta\nu_D$ = Doppler breadth. Under the influence of collision broadening, the absorption coefficient varies with the frequency according to a curve of the type

$$\frac{1}{1+\left[\dfrac{2(\nu-\nu_0)}{\Delta\nu_C}\right]^2}$$

where $\Delta\nu_C$ = collision breadth = no. of impacts per sec./π. With collision broadening superimposed on Doppler broadening

$$\kappa(\nu) = \frac{2\kappa(\nu_0)}{\pi\Delta\nu_C}\int_{-\infty}^{\infty}\frac{e^{-(2\delta/\Delta\nu_D)^2\log_e 2}}{1+\left[\dfrac{2}{\Delta\nu_C}(\nu-\nu_0-\delta)\right]^2}\,d\delta$$

$$= \frac{2\kappa(\nu_0)}{\pi\Delta\nu_C}\int_{-\infty}^{\infty}\frac{e^{-[2/\Delta\nu_D(\nu-\nu_0-\delta)]^2\log_e 2}}{1+\left(\frac{2}{\Delta\nu_C}\delta\right)^2}d\delta$$

where $\kappa(\nu_0)$ =abs. coeff. of center of line when Doppler broadening only is effective, i.e., for zero pressure of foreign gas. Call

$$\frac{2(\nu-\nu_0)}{\Delta\nu_D}(\log_e 2)^{1/2} = q \quad \text{and} \quad \frac{\Delta\nu_C}{\Delta\nu_D}(\log_e 2)^{1/2} = p$$

and let

$$x = \frac{2\delta}{\Delta\nu_D}(\log_e 2)^{1/2}.$$

Then

$$\frac{\kappa(\nu)}{\kappa(\nu_0)} = \frac{p}{\pi}\int_{-\infty}^{\infty}\frac{e^{-(q-x)^2}}{p^2+x^2}dx$$

$$= \frac{2p}{\pi}e^{-q^2}\int_0^{\infty}\frac{e^{-x^2}\cos 2iqx}{p^2+x^2}dx.$$

Now

$$\frac{1}{p^2+x^2} = \int_0^{\infty}e^{-(p^2+x^2)u}du$$

whence

$$\frac{\kappa(\nu)}{\kappa(\nu_0)} = \frac{2p}{\pi}e^{-q^2}\int_0^{\infty}e^{-p^2u}du\int_0^{\infty}e^{-(1+u)x^2}\cos 2iqxdx$$

$$= \frac{2p}{\pi}e^{-q^2}\int_0^{\infty}e^{-p^2u}du\,\frac{1}{2}\left(\frac{\pi}{1+u}\right)^{1/2}e^{q^2/1+u}.$$

Let $1+u = t^2/p^2$, and we have, finally

$$\frac{\kappa(\nu)}{\kappa(\nu_0)} = \frac{2}{(\pi)^{1/2}}e^{p^2-q^2}\int_p^{\infty}e^{-t^2+(p^2q^2/t^2)}dt. \tag{5}$$

When there is no collision broadening, $p=0$, and

$$\kappa(\nu) = \kappa(\nu_0)e^{-q^2}\frac{2}{(\pi)^{1/2}}\int_0^{\infty}e^{-t^2}dt = \kappa(\nu_0)e^{-q^2}.$$

At extremely high foreign gas pressures p is very large, and the original expression for $\kappa(\nu)/\kappa(\nu_0)$ can be shown to reduce to $1/(\pi)^{1/2}\cdot p/p^2+q^2$. It can readily be verified that, for all values of p,

$$\int_0^{\infty}\kappa(\nu)d\nu = \left(\frac{\pi}{4\log_e 2}\right)^{1/2}\kappa(\nu_0)\Delta\nu_D$$

which is required by the constancy of the Einstein B coefficient.

In order to evaluate the integral in Eq. (5), we proceed as follows:[13] Expanding $e^{p^2q^2/t^2}$ we have

$$\frac{\kappa(\nu)}{\kappa(\nu_0)} = \sum_{n=0}^{\infty} I_n(p)\frac{e^{-q^2}q^{2n}}{n!}$$

where

$$I_n(p) = \frac{2}{(\pi)^{1/2}}e^{p^2}p^{2n}\int_p^{\infty} e^{-t^2}\frac{dt}{t^{2n}}.$$

Integrating by parts (starting with (dt/t^{2n})) we obtain a convenient means for computing successively all the $I_n(p)$,

$$I_n(p) = \frac{p}{2n-1}\left(\frac{2}{\pi^{1/2}} - 2pI_{n-1}(p)\right)$$

and

$$I_0(p) = e^{p^2}\frac{2}{(\pi)^{1/2}}\int_p^{\infty} e^{-t^2}dt$$

which can be obtained from tables.

$\kappa(\nu)/\kappa(\nu_0)$ was evaluated for different values of p and q and the results are given in Table IV.

$$\frac{\kappa(\nu)}{\kappa(\nu_0)} = \frac{2}{\pi^{1/2}}e^{p^2-q^2}\int_p^{\infty} e^{-t^2+(p^2q^2/t^2)}dt$$

$$p = (\log_e 2)^{1/2}\frac{\Delta\nu_C}{\Delta\nu_D}, \qquad q = (\log_e 2)^{1/2}\frac{2(\nu-\nu_0)}{\Delta\nu_D}$$

TABLE IV. *Values of* $\kappa(\nu)/\kappa(\nu_0)$.

q \ p	0	0.5	1.0	1.5
0	1.0000	0.6157	0.4276	0.3216
0.2	.9608	.6015	.4215	.3186
.4	.8521	.5613	.4038	.3097
.6	.6977	.5011	.3766	.2958
.8	.5273	.4294	.3425	.2779
1.0	.3679	.3549	.3047	.2571
1.2	.2369	.2846	.2662	.2349
1.4	.1409	.2233	.2292	.2123
1.6	.0773	.1728	.1954	.1902
1.8	.0392	.1333	.1657	.1695
2.0	.0183	.1034	.1402	.1504

The absorption is given, as before, by

$$A = 1 - \frac{K(\nu_0, 0)\int_0^{\infty} e^{-[2(\nu-\nu_0)/\Delta\nu_E]^2\log_e 2}\cdot e^{-\kappa(\nu)l}d\nu}{K(\nu_0, 0)\int_0^{\infty} e^{-[2(\nu-\nu_0)/\Delta\nu_E]^2\log_e 2}d\nu}$$

[13] I am indebted to Dr. T. H. Gronwall for the method of evaluating Eq. (5), and to Professor H. P. Robertson for valuable help throughout the calculation.

which becomes

$$A = 1 - \frac{\int_{-\infty}^{\infty} e^{-[(q/\Delta\nu_E/\Delta\nu_D)^2 + \kappa(\nu)/\kappa(\nu_0) \cdot \kappa(\nu_0) l]} dq}{\int_{-\infty}^{\infty} e^{-(q/\Delta\nu_E/\Delta\nu_D)}\, dq}$$

and which can be evaluated graphically for any situation in which $\kappa(\nu_0)l$ and $\Delta\nu_E/\Delta\nu_D$/are known. This was done for these experiments at 20 °C for which $\kappa(\nu_0)l = 4.44$ and $\Delta\nu_E/\Delta\nu_D = 1.21$, and for Orthmann's experiments at 15.5°C for which $\kappa(\nu_0)l = 3.22$ and $\Delta\nu_E/\Delta\nu_D = 1.46$. The results are given in Table V and Fig. 7.

$$A = 1 - \frac{\int_{-\infty}^{\infty} e^{-[(q/\Delta\nu_E/\Delta\nu_D)^2 + \kappa(\nu)/\kappa(\nu_0) \cdot \kappa(\nu_0) l]} dq}{\int_{-\infty}^{\infty} e^{-(q\Delta\nu_E/\Delta\nu_D)^2} dq}$$

$$\frac{\kappa(\nu)}{\kappa(\nu_0)} = \frac{2}{\pi^{1/2}} e^{p^2 - q^2} \int_p^{\infty} e^{-t^2 + (p^2 q^2/t^2)} dt.$$

TABLE V.

$\kappa(\nu_0)l$	$\frac{\Delta\nu_E}{\Delta\nu_D}$	p	$\frac{\Delta\nu_C}{\Delta\nu_D}$	A
4.44	1.21	0	0	0.840
		0.5	0.6	.833
		1.0	1.2	.775
		1.5	1.8	.707
3.22	1.46	0	0	.700
		.5	.6	.687
		1.0	1.2	.630
		1.5	1.8	.562

From the curves in Fig. 7 it is possible to obtain the collision breadth of the mercury absorption line merely by measuring the absorption. The advantage of this is that low enough foreign gas pressures may be used so that the five fine structure components of the mercury resonance line will not merge into one another, as was the case in the experiments of Füchtbauer Joos and Dinkelacker[14] who broadened the line by foreign gases at pressures up to fifty atmospheres. There is one disadvantage, however, in that the asymmetry in the line broadening predicted by theory and observed by Minkowski[15] in the case of sodium cannot be taken into account. It will be seen later how this affects the final results. Nevertheless it is believed that this method of measuring the magnitude of the collision breadth

[14] C. Füchtbauer, G. Joos, and O. Dinkelacker, Ann. d. Physik **71**, 204 (1923).
[15] R. Minkowski, Zeits. f. Physik **55**, 16 (1929).

of a line is superior to the photographic method, because it enables one to separate the collision breadth from the Doppler breadth easily. A spectrogram of an absorption line which has been broadened only slightly by a foreign gas could be used to obtain the collision breadth provided one plotted

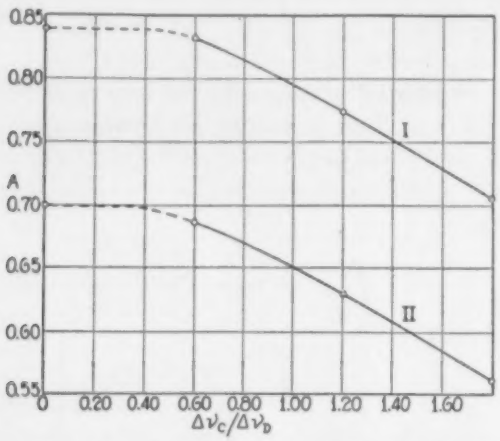

Fig. 7. A as a function of $\Delta\nu_E/\Delta\nu_D$. Curve I, $\kappa(\nu_0)l=4.44$, $\Delta\nu_E/\Delta\nu_D=1.21$. Curve II, $\kappa(\nu_0)l=3.22$, $\Delta\nu_E/\Delta\nu_D=1.46$.

measured values of $\kappa(\nu)/\kappa(\nu_0)$ against frequency, and compared these curves with those obtained from Eq. (5). A correction would have to be made, of course, for the frequency shift due to asymmetrical broadening. It is doubtful whether existing experimental data on absorption lines are sufficiently ac-

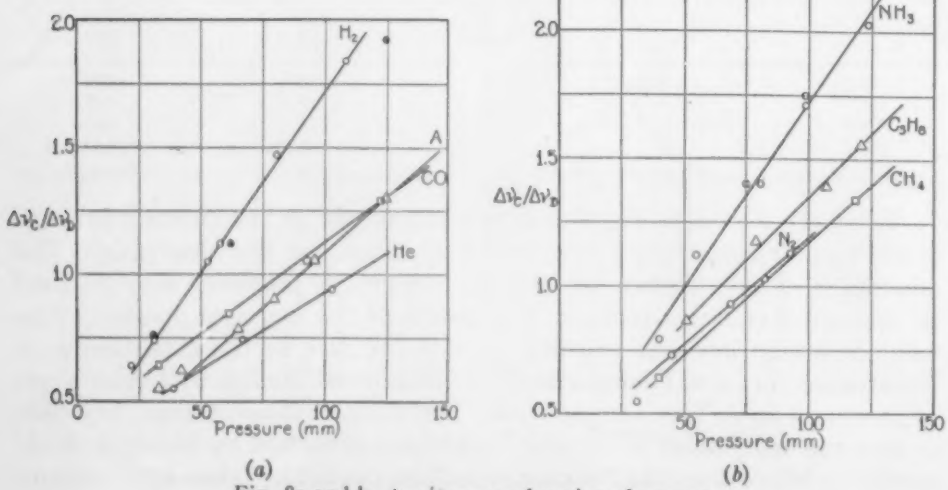

Fig. 8a and b. $\Delta\nu_C/\Delta\nu_D$ as a function of pressure.

curate for this purpose. The spectrograms of the 2537 absorption line obtained by Füchtbauer, Joos and Dinkelacker at very high foreign gas pressures yield values of the collision breadth that are somewhat in doubt be-

cause of the fact that the fine structure of the line has been completely wiped out. Nevertheless the values obtained by them are very interesting and will be referred to later.

TABLE VI.

Gas	Pressure in mm p'	Absorption A	$\frac{\Delta\nu_C}{\Delta\nu_D}$ from Fig. 7
H_2	0	0.840	0
	22	.830	.64
	31	.821	.74
	53	.790	1.05
	58	.783	1.12
	81	.746	1.47
	109	.702	1.84
H_2	0	.700	0
(Orthmann)	31	.674	.76
	62	.638	1.12
	125	.548	1.92
N_2	0	.840	0
	31	.836	.55
	45	.822	.73
	69	.802	.93
	83	.792	1.03
	93	.782	1.13
A	0	.840	0
	33	.836	.55
	42	.831	.62
	65	.817	.78
	80	.806	.90
	96	.790	1.05
	125	.764	1.30
CO	0	0.840	0
	33	.830	.64
	61	.812	.84
	93	.790	1.05
	123	.766	1.29
He	0	.840	0
	39	.836	.55
	67	.821	.74
	103	.802	.94
NH_3	0	.840	0
	40	.817	.79
	55	.783	1.12
	75	.754	1.40
	81	.754	1.40
	99	.717	1.71
	99	.712	1.75
	124	.680	2.03
CH_4	0	.840	0
	40	.830	.64
	119	.760	1.34
C_2H_2	0	.840	0
	51	.810	.86
	79	.777	1.17
	107	.755	1.39
	121	.736	1.55

A number of foreign gases were used to broaden the line, and the results are given in Table VI and in Fig. 8. It is seen in Fig. 8 that the collision breadth plotted against the pressure of the foreign gas does not yield a straight line passing through the origin, as it should according to the relation:

$$\Delta\nu_C = \frac{\text{no. of impacts per sec.}}{\pi}$$

It is believed that this is due to the failure to take into account the asymmetry in line broadening, but that the error will not be large if the linear portions of the curves are considered. The three points for H_2 shown in Fig. 8 obtained by Orthmann five years ago under entirely different conditions as to mercury vapor density, thickness of cell, type of resonance lamp, etc., agree well enough to constitute an excellent check on the method as a whole.

Calling Z the number of impacts per mercury atom per sec, we have from kinetic theory

$$Z = 2\sigma_E^2 \frac{9.71 \times 10^{18} p'}{T}\left(2\pi kT\left(\frac{1}{m}+\frac{1}{M}\right)\right)^{1/2}$$

where T is the absolute temperature, p' the pressure in mm, k Boltzmann's constant, m the mass of a mercury atom, M the mass of a foreign gas molecule, and σ_E the effective distance between centers.
Since $\Delta\nu_C = Z/\pi$,

$$\frac{Z}{p'} = \pi\Delta\nu_D \frac{\Delta\nu_C/\Delta\nu_D}{p'} = \pi \times 1.02 \times 10^9 \times \text{slope of line in Fig. 8} \quad (6)$$

and

$$\frac{Z}{\sigma_K^2 p'} = \frac{2 \times 9.71 \times 10^{18}}{T}\left(2\pi kT\left(\frac{1}{m}+\frac{1}{M}\right)\right)^{1/2} \quad (7)$$

from which σ_E^2 can be calculated.[16] The values of Z/p', $Z\sigma^2_E p'$, and σ^2_E obtained from these experiments along with those from the work of Füchtbauer, Joos, and Dinkelacker are given in Table VII.

TABLE VII.

	Gas	$\frac{Z}{p'}\times10^{-7}$ from Eq. (6)	$\frac{Z}{\sigma_E^2 p'}\times10^{-22}$ from Eq. (7)	$\sigma_E^2\times10^{16}$	$\sigma_E\times10^8$	$(\sigma_E\times1.80)\times10^8$	$-\chi_M\times10^6$	$(-\chi_M)^{1/2}\times10^3$
Author	He	1.94	1.29	15.0	3.88	2.08	1.87	1.37
	H_2	4.48	1.83	24.5	4.95	3.15	3.94	1.99
	CO	2.32	.521	44.5	6.68	4.88	10.6	3.26
	N_2	2.66	.521	51.0	7.15	5.35	11.8	3.44
	A	2.76	.448	61.5	7.85	6.05	18.0	4.24
	NH_3	4.65	.653	71.2	8.45	6.65	19.0	4.36
	CH_4	2.84	.671	42.3	6.51	4.71	12.2	3.50
	C_3H_8	3.17	.431	73.5	8.58	6.78	40.5	6.37
F. J. and D.	H_2	5.09	1.83	27.8	5.27	3.47	3.94	1.99
	N_2	3.38	.521	64.8	8.05	6.25	11.8	3.44
	A	3.98	.448	88.9	9.44	7.64	18.0	4.24
	CO_2	5.40	.431	125	11.2	9.40	18.7	4.32
	H_2O	4.37	.638	68.5	8.28	6.48	13.0	3.61
	O_2	3.20	.491	65.1	8.07	6.27	para.	

DISCUSSION

It is seen from Table VII that all the values of σ_E^2 are larger than the normal ones, which vary from about 9 to 12×10^{-16} cm, in agreement with the ideas of Kallmann and London.[17] The most striking result, however, is obtained if we adopt the point of view that, in the collision process, the mercury atom has a constant radius equal to the gas-kinetic radius (1.80×10^{-8} cm) and that each broadening gas has its own effective radius. The effective radius of each gas is then obtained by substracting 1.80×10^{-8} from σ_E. Values of $\sigma_E - 1.80\times10^{-8}$ are given in Table VII along with values of

[16] The values of σ_E^2 obtained from these experiments are to be regarded as lower limits because of the error in neglecting asymmetry. Relative values, however, are probably quite reliable.

[17] Kallmann and London, Zeits. f. Phys. Chem. Abt. B, 2 (1929).

the molecular diamagnetic susceptibility, χ_M. All the values of χ_M are experimental ones[18] except that for CO which was obtained by adding the susceptibilities of C and O. The justification for this is that it yields a result almost equal to that of N_2 which is known to be similar to CO in most of its properties.

In Fig. 9 the effective radius is plotted against the square root of the susceptibility, and very good straight lines are obtained for both Füchtbauer's and these results. The agreement between the two lines is no less remarkable than the lines themselves, inasmuch as the two methods are so radically different. It is possible that the correct line lies between the two

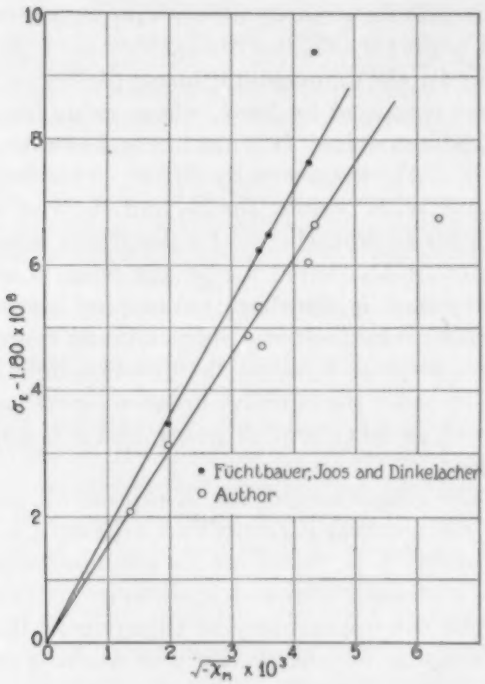

Fig. 9. σ_E as a function of $(-X_M)^{1/2}$.

because of the error that is peculiar to each method. The Langevin theory of diamagnetism allows us to give a meaning to this linear relation. According to the simple theory of diamagnetism for an atom, the atomic susceptibility is given by $-(e^2/6mc^2)\, n\overline{r^2}$ where n is the number of outer electrons of the atom, and $\overline{r^2}$ is the mean square radius of all the electronic orbits. Applying this relation to all the molecules in question, we get the result that the effective cross-section of a molecule for collision broadening is proportional to the number of outer electrons and to the mean square radius of the electronic orbits, a result that is quite interesting.

[18] A. P. Wills and G. Hector, Phys. Rev. **23**, 209 (1924), G. Hector, Phys. Rev. **24**, 418 (1924), F. Bitter, Phys. Rev. **33**, 389 (1929), Stoner "Magnetism and Atomic Structure."

According to this result, oxygen, although it is strongly paramagnetic, and cannot be plotted in Fig. 9, ought to behave like N_2 or CO, because O_2 has 16 electrons and a gas-kinetic radius of 1.47×10^{-8} cm, whereas N_2 and CO have each 14 electrons and radii equal to 1.58×10^{-8} cm and 1.60×10^{-8} cm respectively. The effective broadening radius of O_2, according to Füchtbauer's results is 6.27×10^{-8} cm in good agreement with Füchtbaur's value for N_2, 6.25×10^{-8} cm. The author did not use O_2 as a broadening agent for fear that at such high O_2 pressures, the inside walls of the absorption cell would become covered with HgO, which would lower their transmission and completely obscure any slight change in the absorption of the mercury vapor.

The only points that lie seriously off their respective straight lines in Fig. 9 are Füchtbauer's point for CO_2 and the author's for C_3H_8. There is a possibility that the value for the diamagnetic susceptibility of CO_2, -18.7×10^{-6} is too small. It was measured by Soné, whose value for N_2 is considerably smaller than the accepted value. It is not likely, however, that the value for the susceptibility of C_3H_8, measured by Bitter, is too large, because it was based on Hector and Wills' values for N_2 and H_2, and also because it fits in well with the higher hydrocarbons. Its departure from the line in Fig. 9 is much too great to be accounted for on the basis of experimental error. There is a possibility that, in the time that elapsed between its preparation and its use, it became contaminated. Unfortunately there was not sufficient time at the author's disposal to settle the question definitely. It would be very interesting to measure the effective broadening radius of all the gaseous hydrocarbons, as well as other organic gases, and it is quite likely that this will be done next year.

In conclusion, the author would like to express his indebtedness to Mr. L. J. Buttolph of the General Electric Vapor Lamp Co. for the loan of a mercury arc, and to Dr. J. R. Bates for his kindness in supplying methane and propane. It is a pleasure also to acknowledge my debt to the National Research Council for the opportunity of engaging in this research and to Professor K. T. Compton for the privilege of working in Palmer Physical Laboratory.

THE EFFECT OF SMALL ANGLE SCATTERING ON THE ELECTRON ABSORPTION COEFFICIENT

By Metta Clare Green
Department of Physics, University of California

(Received June 7, 1930)

Abstract

An indirect study of the scattering of electrons by gas molecules has been made by measuring electron absorption coefficients in an apparatus containing a Faraday cylinder of variable aperture. A straight path method was used in which electrons from an oxide-coated filament were given a desired velocity and made to traverse a 7.5 cm path to the collector. A retarding potential between the cylinder and its shield kept out all electrons which had suffered inelastic collisions as well as those which had been scattered outside of the collector opening. Measurements were made in argon, helium, hydrogen, and mercury vapor at accelerating potentials ranging from 11 to 196 volts. The radius of the cylinder aperture varied from one one-hundredth to one tenth of the path length. No consistent variation of the absorption coefficient with opening was found in any case. Theoretical calculations based on scattering laws obtained from inverse square or fifth power laws of force predicted relatively large variations. Calculations made assuming uniform scattering or the Sommerfeld law indicated small changes of the same order of magnitude as the deviations between individual values obtained in this experiment.

INVESTIGATIONS have recently been made by Dymond[1] and Watson,[2] Harnwell,[3] and Arnot[4] of the distribution of electrons scattered by gas molecules. The experimental curves showing the relation between the intensity of the scattered current per unit solid angle and the scattering angle all indicate relatively large scattering at small angles for both elastic and inelastic collisions. The initial steepness of the slopes of the curves increases with increasing initial electron velocity. Dymond and Watson's curve for elastic scattering of 210 volt electrons in helium gives very rough agreement with Born's[5] theoretical curve calculated for slower electrons in hydrogen, but, as they point out, this fact is not very significant. Harnwell's original curves for elastic scattering in molecular and monatomic hydrogen compared total scattering between θ and $\theta+d\theta$ with scattering per unit solid angle given by the theoretical equation of Born. When corrected for this error,[6] his experimental values of scattered intensity per unit solid angle are no longer in agreement with the theoretical values. Arnot found that the curve for elastic scattering of 82 volt electrons in mercury vapor had a steeper initial slope than that of Dymond and Watson's helium curve for electrons of the same

[1] E. G. Dymond, Phys. Rev. **29**, 433 (1927).
[2] E. G. Dymond and E. E. Watson, Proc. Roy. Soc. Lon. **122**, 571 (1929).
[3] G. P. Harnwell, Phys. Rev. **33**, 559 (1929), **34**, 661 (1929).
[4] F. L. Arnot, Proc. Roy. Soc. **A125**, 660 (1929).
[5] M. Born, Göttinger Nachrichten, p. 146 (1926).
[6] G. P. Harnwell, Phys. Rev. **35**, 285 (1930).

initial velocity. The experimental curves all indicate much less rapid change of scattered intensity with scattering angle at small angles than that given by the theoretical scattering law obtained from an inverse square law of force between the electron and the scattering particle.

Indirect evidence on the angular distribution of electrons scattered by molecules is given by measurements of electron absorption coefficients in gases and vapors. An electron beam is diminished in intensity by collision with molecules of a gas through which it passes, according to the equation, $I = I_0 e^{-\alpha p x}$, where I is the electron current reaching the end of the path, I_0 is the initial current, x, the path length, and α, the absorption coefficient.

Determinations of α all involve measuring the variation of the logarithm of the ratio of the final to the initial current with path length or gas pressure. The rate of variation of α with the diameter of the aperture of the Faraday cylinder used for collecting the final beam should depend on the angular distribution of the scattered electrons. Comparison of data so far collected with different experimental arrangements of apparatus indicates that α is practically constant for relatively large ranges of cylinder aperture. Brode[7]

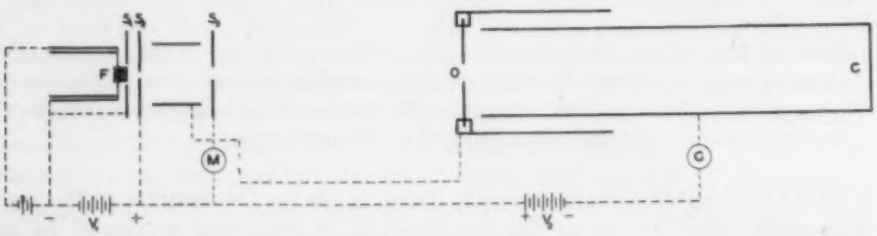

Fig. 1. Diagram of apparatus.

obtained very good agreement between values of α for cadmium vapor taken in very different types of apparatus. However, quantitative information cannot be obtained by direct comparison of other existing data.

Accordingly a direct experimental study of this question has been made in an apparatus in which a beam of electrons from a hot oxide-coated filament was given a definite velocity and then made to travel a straight path through gas at known pressure to a collector of variable opening.

The experimental arrangement is shown in Fig. 1. F is a small oxide-coated nickel cylinder which is welded to a tungsten wire and is a practically equipotential source of electrons.[8] S_1, S_2 and S_3 are circular holes of 5, 2, and 3 mm diameter respectively. C is a Faraday cylinder 9 cm long and 2 cm in diameter, whose shield has a magnetically-operated shutter-opening, O, similar to that of a camera. The diameter of O varied from 2.3 to 17 mm. The distance from S_2 to O is 7.7 cm. Accelerating and retarding potentials, V_1 and V_2, were applied between the filament and second nickel plate and the Faraday cylinder and its shield, respectively. Galvanometers G and M measured the final electron current and the total emission through S_2. The

[7] R. B. Brode, Phys. Rev. **35**, 504–508 (1930).

[8] G. Hertz, and R. K. Kloppers, Zeits. f. Physik **31**, 463 (1925).

metal parts were all made of nickel and the inside of the tube enclosing the whole apparatus was sputtered with nickel and grounded through M. The earth's magnetic field was neutralized by large Helmholz coils.

Absorption coefficients were measured in argon, helium, molecular hydrogen and mercury vapor. Electron velocities corresponding to 13, 27.5, and 97 volts accelerating potential were used in argon, helium and hydrogen; in argon 47 and 196 volt electrons were also studied. 40 volt electrons were used in mercury.

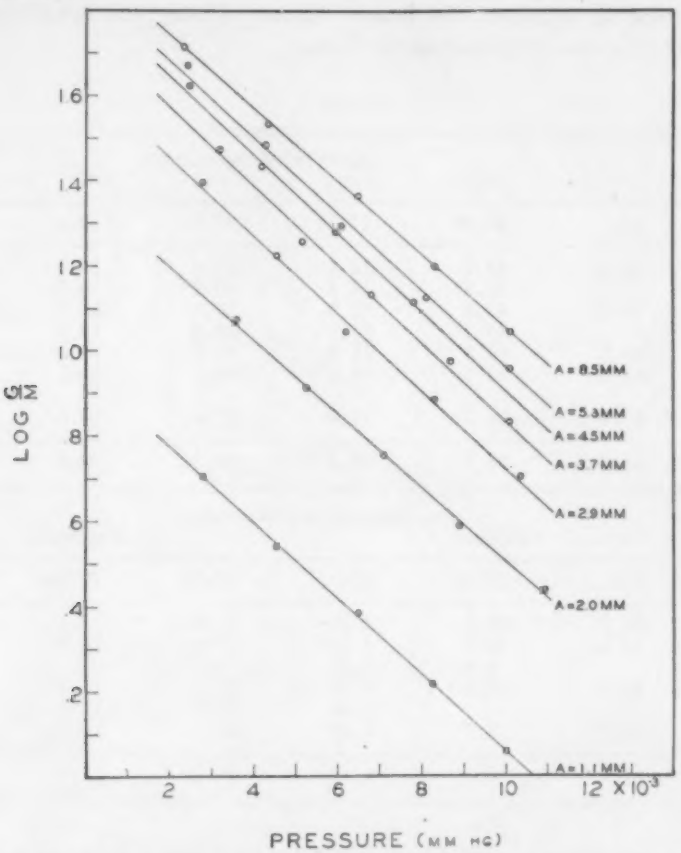

Fig. 2. Logarithm of ratio of current, G, at end of path to total current, M, as a function of pressure and aperture radius, A, for 97 volt electrons in argon.

The argon was purified in a calcium arc and the helium and hydrogen were passed through charcoal cooled in liquid air.

With constant accelerating potential, readings of G and M were made for from three to five different pressures for each cylinder aperture. From four to seven different apertures were used for each accelerating potential. The total electron current varied from 2 to 8×10^{-7} amperes, while the currents to the Faraday cylinder were from 2 to 100×10^{-9} amperes. Curves were obtained showing the variation of the final current with the total emission through S_2 for fixed values of pressure, aperture, and accelerating potential.

Readings were always taken in the region where the two currents were proportional to each other.

The true value of the electron velocity was determined by retarding potential curves. Each current, G, was taken as the difference between galvanometer scale deflections for a retarding potential about ten percent less than and one equal to the accelerating potential. The apparent size of the beam was determined by plotting values of G/M against aperture. The opening for which the G/M ratio fell to half its limiting value for wide openings was used to measure the beam radius. Under the conditions of this experiment this was approximately 3 mm.

TABLE I.

Aperture radius	Absorption coefficient, α Argon					Mercury
(mm)	13v	27.5v	47.5v	96.5v	196v	37.5v.
1.1	64.8	43.2	34.4	30.4	18.3	94.5
2.0		43.5	37.5	30.1	20.2	84.5
2.9	70.9	43.9	35.8	30.6	19.9	82.4
3.7		43.2	35.2	31.0	19.8	84.5
4.5	68.6	43.5	35.8	31.4	22.0	89.0
5.3	67.4	42.9	33.8	30.7	21.7	
6.2						94.5
8.5	67.4	44.3	34.0	27.6	20.6	
Av. α	67.8	43.5	35.2	30.3	20.4	91.1

Aperture radius	Absorption coefficient, α Helium			Hydrogen		
(mm)	13v	27.5v	97v	11.5v	27.5v	97v
1.1	14.9	10.8	3.21	27.0	15.1	11.2
2.9	15.2	10.8	3.54	27.0	16.5	10.5
3.7		9.6	4.05			
4.5	13.5	10.1	4.05	27.7	16.2	11.1
6.2			3.88	24.6	15.5	10.8
8.5	14.5	8.3	4.55	25.3	16.0	9.1
Av. α	14.5	9.9	4.12	26.3	15.9	10.5

The gas pressures varied from 2 to 12×10^{-3} mm for argon and helium, from 10 to 50×10^{-3} mm for hydrogen, and from 5 to 25×10^{-4} mm for mercury.

The value of the absorption coefficient was determined in each case by plotting the values of the logarithm of G/M (assumed to be proportional to log I/I_0) against the gas pressure and dividing the slope of the straight line so obtained by the path length. The latter was not clearly defined in the apparatus, but it was assumed to be 7.5 cm. Correction was made for room temperature so that the values of α are in cm^2/cm^3 of gas at 1 mm pressure and 0° C. In Fig. 2 are shown the observed values of the log G/M plotted as a function of the pressure in argon at 97 volts: it appears that the relationship is linear.

Table I summarizes the experimental results for the variation of the electron absorption coefficients with aperture diameter. Figs. 3 and 4 represent these results graphically for some of the accelerating potentials in argon and hydrogen.

These values of α have a consistent tendency, except in the case of the low velocity measurements in hydrogen, to be higher than those recently obtained by Normand[9] in this laboratory with a magnetic deflection method.

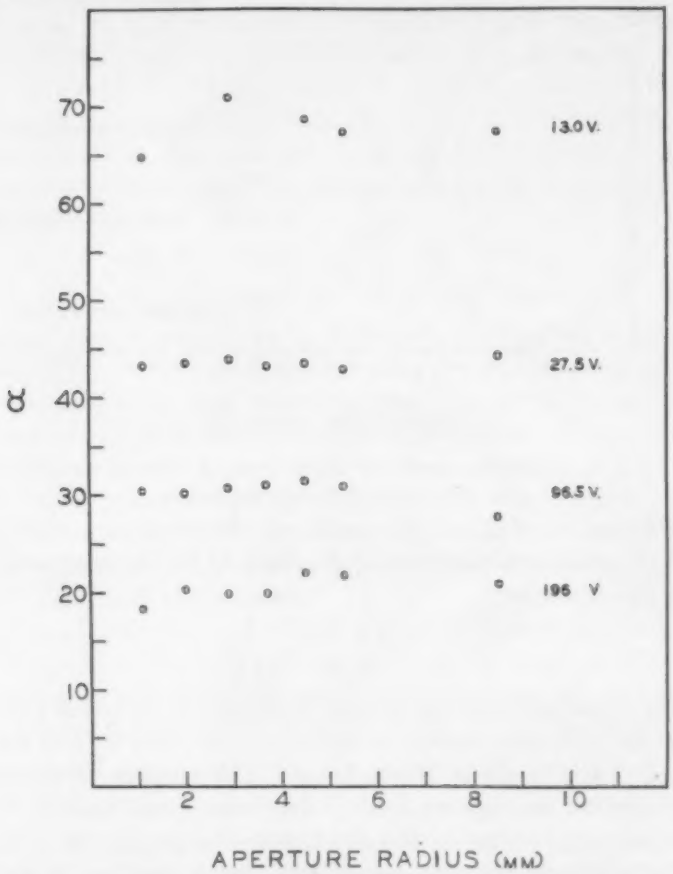

Fig. 3. Electron absorption coefficient α, as a function of aperture radius and accelerating potential in argon.

In helium this might be partly due to impurities, but it can hardly be ascribed to contamination in the case of argon, since most of the probable impurities would have lower values of α than argon. The difference has not been explained, but it is of interest to note that Jones[10] got consistently higher values of α in mercury with a straight path method than with the magnetic deflection method.

As seen from the table of results, there is no consistent tendency for α to vary with aperture within the limits of error of these measurements.

[9] C. E. Normand, Phys. Rev. **35**, 1217 (1930).
[10] T. J. Jones, Phys. Rev. **32**, 459 (1928).

Theoretical Discussion

Assuming an inverse square law of force between the electron and the scattering center one obtains with classical mechanics an expression for the

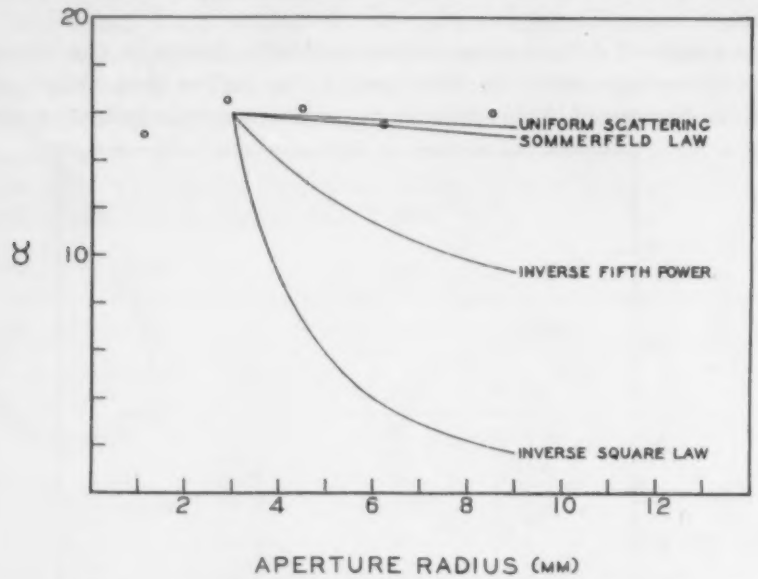

Fig. 4. Absorption coefficient for 27.5 volt electrons in hydrogen. Circles indicate observed values.

variation of intensity of elastically scattered electrons with scattering angle which is identical in form with that of Rutherford for the scattering of alpha-particles by heavy nuclei:

$$\frac{1}{n}\frac{dN}{dA} = \left(\frac{e^2Z}{4Er}\right)^2 \frac{1}{\sin^4 \theta/2}$$

where θ is the angle between the original direction of the beam and the radius vector from the scattering center to the scattered particle, n is the intensity per unit area of the incident beam, dN/dA, the number of electrons which have been deflected through an angle θ and fall on unit area at a distance r from the scattering center, e, the electronic charge, E, the initial kinetic energy of the scattered particle, and Z, the atomic number of the scatterer.

Taking into consideration the polarization of the scattering particle by the passing electron Zwicky[11] obtained an inverse fifth power law of attraction which would give the scattering formula:

$$\frac{1}{n}\frac{dN}{dA} = \frac{K}{r^2} \frac{1}{(\cos^2 \theta/2 \sin^5 \theta/2)^{1/2}}.$$

This is an approximate expression which is valid only for small angle scattering. K is a constant and the other symbols have the above meanings.

The scattering law derived by Sommerfeld[12] on the basis of the wave mechanics considers the interaction of the electron with the "electron cloud"

[11] F. Zwicky, Phys. Zeits. **24**, 171 (1923).

[12] A. Sommerfeld, Atombau und Spectrallinien, Wellenmechanischer Ergänzungsband, p. 231.

surrounding the nucleus of the scattering atom. The "electron cloud" is formed by the electrons outside the nucleus, all of which are assumed to be in the K-shell. The derivation neglects any disturbance of the electronic charge distribution of the atom by the field of the passing electron. The equation thus derived is:

$$\left|\frac{\psi_1}{\psi_0}\right|^2 = \left(\frac{e^2Z}{4Er}\right)^2 \times \frac{1}{(\sin^2\theta/2 + \alpha^2)^2}$$

In this formula, $|\psi_1/\psi_0|^2$ is the ratio of the intensity of the scattered to the initial beam per unit area and $\alpha = \lambda Z/2\pi a$ where λ is the wave-length of the electron in terms of Planck's constant, h, and its momentum, mv, and a is the radius of the first Bohr orbit of the atom. If α is very small, that is, for very fast electrons, this becomes the Rutherford formula. For slow electrons, of long wave-length, $\sin^2\theta/2$ becomes negligible in comparison with α^2 and the formula becomes, merely:

$$\left|\frac{\psi_1}{\psi_0}\right|^2 = \left(\frac{e^2Z}{4Er}\right)^2 \frac{1}{\alpha^4} = \left(\frac{h^2}{4\pi^2me^2Z}\right)^2 \frac{1}{r^2}.$$

This indicates uniform scattering in all directions. The above considerations would predict that the intensity of scattering per unit angle would show less variation with angle for slow electrons than that given by the Rutherford formula, but would approach it at higher velocities. That this has been found experimentally has been previously mentioned.

The scattering laws can be applied to determine the theoretical variation of the absorption coefficient with collector aperture by a double integration which takes into account all electrons scattered outside the aperture from every point in the path of the beam.

In the case of the scattering resulting from an inverse square law of force, if $\theta = \tan^{-1} a/(L\text{-}x)$ is the angle subtended by the aperture radius at the point of collision, the current scattered beyond the opening per unit intensity of the incident beam per scattering center is given by the expression:

$$\frac{dI}{I} = -K\int_{\tan^{-1}a/(L-x)}^{\pi} \frac{\sin\theta d\theta}{\sin^4\theta/2} = -2K\left(\frac{(a^2 + (L-x)^2)^{1/2} + (L-x)^2}{a}\right)^2$$

a is the radius of the aperture, x, the distance from the beginning of the path to the point of collision, L, the path length, and $k = 2\pi(e^2Z/4E)^2$. The same meanings will be attached to these symbols whenever they occur in the following discussion.

Multiplying by $N\,dx$ to get the effect of all the scattering particles, N being the number of molecules per cc, and integrating from $x = 0$ to $x = L$, this equation becomes

$$\log\frac{I}{I_0} = -2KN\left(L + \frac{2}{3}\frac{L^3}{a^2} - \frac{2}{3}a^3 \pm \frac{2}{3}\frac{(a^2 + L^2)^{3/2}}{a^2}\right)$$

I_0 is the current when $x = 0$. When a is very small in comparison with L, this may be simplified to:

$$\log\frac{I}{I_0} = -2KN\frac{4}{3}\frac{L^3}{a^2}$$

Since

$$\log \frac{I}{I_0} = -\alpha L p$$

$$\alpha = \frac{8KN}{3p} \frac{L^2}{a^2}.$$

That is, α should vary inversely as the square of the aperture radius. This theoretical variation of α is plotted for 27.5 volt electrons in hydrogen in the lower curve of Fig. 4. The constant K has been chosen arbitrarily to give the theoretical curve the experimental value at the point $a = 3$ mm, this being the point at which the size of the collector opening equals that of the beam.

The above derivation, as well as those that follow, is approximate in that it considers only the scattering due to elastic collisions. At 27.5 volts in hydrogen, however, the fraction of inelastic scattering at small angles is small, as indicated by the work of Dymond and Watson and that of Harnwell on velocity and angular distribution of the two types of scattering. Further, this treatment neglects scattering due to collisions after the first and takes no account of space charge in the beam, nor of finite width of the beam. The effect of the size of the electron beam has been recently calculated by Beeck[13] for the case of uniform scattering. Similar calculations for the scattering resulting from an inverse square law of force show that the effect of the size of the beam is to make the theoretical variation of α with aperture greater and thus to increase the discrepancy between the theoretical and the experimental curves.

The effect of aperture on α can be obtained for an inverse power law of force from the fact that $\tan \theta = CP/E$ where P is the potential energy of the electron at the point of nearest approach to the scattering particle and E is its initial kinetic energy. C is a factor of proportionality which depends on the power discussed. The above energy relation holds only for small angles of deflection. For an inverse n^{th} power law $\tan \theta = C'/(p^{n-1}V)$, V being the accelerating potential corresponding to the kinetic energy of the electron, and p, the distance of nearest approach. Noticing that all the electrons coming within a circle of radius, p, are scattered at angles greater than θ, one can write immediately for the total current of electrons scattered in all angles greater than θ from a volume of the beam dx cm long at a distance x from the beginning of the path,

$$-dI = I\pi p^2 N dx.$$

If for p^2 is substituted its value from the energy relation and for $\tan \theta$, its value, $a/(L-x)$, the expression becomes, on integration from $x = 0$ to $x = L$

$$\log \frac{I}{I_0} = -\frac{K'}{a^{2/(n-1)}} L^{2/(n-1)+1}$$

$$\alpha = K'' \left(\frac{L}{a}\right)^{2/(n-1)}$$

Thus, for an inverse square law α varies inversely with a^2 as previously found. For the inverse fifth power law, $\alpha = k'''(L/a)^{\frac{1}{2}}$. A curve representing this

[13] O. Beeck, Zeits. f. Physik **61**, 251 (1930).

variation of α with a is plotted in Fig. 4. This curve was also arbitrarily made to have the experimental value $\alpha = 16$ for $a = 3$ mm.

Uniform scattering is obtained from the Sommerfeld formula by neglecting $\sin^2\theta/2$ with respect to α^2. The α in Sommerfeld's notation should not be confused with the α used as a symbol for the absorption coefficient. When the electron wave-length is long in comparison with the radius of the first Bohr orbit, the expression for the scattering at any distance x from the beginning of the path is:

$$\frac{dI}{I} = -\frac{2\pi}{\alpha^4}\left(\frac{e^2Z}{4E}\right)^2 N dx \int_{\tan^{-1}a/(L-x)}^{\pi} \sin\theta d\theta = C\left[1 + \frac{L-x}{(a^2+(L-x)^2)^{1/2}}\right].$$

From this, by integrating over the path one obtains:

$$\log\frac{I}{I_0} = -C(L - a + (a^2 + L^2)^{1/2})$$

or

$$\alpha = \frac{C}{Lp}(L - a + (a^2 + L^2)^{1/2}).$$

For small values of a compared to L

$$\alpha = C'(2 - (a/L)).$$

For molecular hydrogen the coefficient C' is arbitrarily chosen so that $C'(2-a/L)$ is equal to 16 for a 3 mm aperture. The resulting variation of α with aperture for uniform scattering is shown in Fig. 4.

For the numerical case chosen in Fig. 4 the value of Sommerfeld's α is about 0.7. In the above case $\sin^2\theta/2$ is neglected in comparison with α^2. When both terms are retained, the dependence of the absorption coefficient on aperture may be found by graphical integration. Fig. 4 shows the curve obtained from the Sommerfeld scattering law adjusted in the same manner as the other curves.

An examination of Fig. 4 shows that the dependence of α on aperture is greatest if an inverse square law of force is assumed and least in the case of uniform scattering as is to be expected. The variation of the experimental points is less than that predicted by the power laws and of the same order of magnitude as that given by the Sommerfeld or the uniform scattering law. The theoretical treatment given here deals only with absorption due to change in the direction of motion of the electron without change in energy. There is also some inelastic scattering which increases the absorption coefficient by an undetermined amount. If an arbitrary constant is added to the coefficients obtained from the scattering laws, any one of the curves can be made to lie within the limits of variation of the experimental points. To do this, however, assuming only scattering due to either an inverse square or fifth power law of force would assume that the scattering was largely inelastic, which is not the case, as we know from previous results. We may conclude, therefore, that the small angle scattering more nearly follows the Sommerfeld law than the inverse power laws, but may be a combination of uniform scattering with that due to some power law.

I am indebted to Professor R. B. Brode for proposing this study and for his continued assistance and interest throughout its progress.

THE RATE AT WHICH IONS LOSE ENERGY IN ELASTIC COLLISIONS

By Austin M. Cravath*
Palmer Physical Laboratory, Princeton University

(Received May 16, 1930)

Abstract

The rate of energy loss of ions (including electrons) moving through a gas is rigorously calculated on the assumption that the ions and molecules are smooth elastic spheres with no attraction at a distance, having Maxwellian velocity distributions corresponding to the temperatures T_i and T_m respectively. The result is

$$f = \frac{8}{3}\frac{mM}{(m+M)^2}\left(1-\frac{T_m}{T_i}\right)$$

where m and M are the masses of ion and molecule respectively, T_i and T_m are their temperatures, and f is the average energy loss per collision expressed as a fraction of the average ionic energy.

THERE are a number of problems in which ions (including electrons) move through a gas with an approximately Maxwellian velocity distribution corresponding to a temperature higher than that of the gas, and an expression for the rate at which the ions lose energy in elastic collisions is required. For instance, Compton[1] required it for his electron mobility equation. He deduced an approximate expression as follows. First he calculated the average energy loss for ions of given velocity striking molecules at rest at all angles from grazing to head on. He then corrected this for the motion of the molecules by finding how the energy loss for head on collisions was altered by a (one dimensional) molecular velocity distribution, and multiplying the expression for molecules at rest by this factor. The velocity distribution of the ions was not considered at all. Indeed there *is* no ion velocity distribution if one is merely interested in the average fraction of *its own* energy which an ion loses per collision. What was actually needed, however, was the average energy loss in all collisions expressed as a fraction, f, of the average energy (of all the ions in a given volume). The result obtained was

$$f = 2\frac{m}{M}\left(1-\frac{\Omega}{\omega}\right)$$

where m and M are the masses and ω and Ω the average energies of the ions and molecules respectively.

The present paper gives the rigorous calculation of the energy loss on the assumption that ions and molecules are smooth elastic spheres with no attraction at a distance, having Maxwellian velocity distributions.

* National Research Fellow.

[1] Compton, Phys. Rev. **22**, 333 (1923).

The symbols which will be used are:

m = mass of ion.
M = " " molecule.
σ = sum of radii of ion and molecule.
T_i = absolute temperature of ions.
T_m = " " " molecules.
k = Boltzmann's constant.
n = number of ions per cm³.
N = " " molecules per cm³.
$\boldsymbol{V}$ = initial vector velocity of ion.
$\boldsymbol{U}$ = " " " " molecule.
$\mu = M/(m+M)$.
$\boldsymbol{W} = (1-\mu)\boldsymbol{V}+\mu\boldsymbol{U}$ = velocity of center of mass.
$\boldsymbol{R} = \boldsymbol{V}-\boldsymbol{W} = \mu(\boldsymbol{V}-\boldsymbol{U})$ = initial velocity of ion relative to center of mass.
$\boldsymbol{D}$ = unit vector giving direction of line of centers, from ion to molecule, at collision.
Q = total energy loss of all ions in 1 cm³ in 1 sec.
$f = Q/\{$(no. collisions per cm³ per sec) (average ionic energy)$\}$ = average fraction of average energy lost per collision.

To find the total energy loss, Q, we have simply to find the loss in each type of collision and then integrate over all the collisions in 1 cm³ in 1 sec. A given type of collision is specified by given values of $\boldsymbol{V}$, $\boldsymbol{U}$, and $\boldsymbol{D}$. In a collision, that component of $\boldsymbol{R}$, the velocity of the ion relative to the center of mass, which is parallel to the line of centers, $\boldsymbol{D}$, is reversed, and the perpendicular component is unaltered. Hence the final velocity of the ion is

$$\boldsymbol{V}' = \boldsymbol{V} - 2\boldsymbol{R}\cdot\boldsymbol{D}\boldsymbol{D}$$

and the energy lost by the ion is

$$\tfrac{1}{2}m\boldsymbol{V}^2 - \tfrac{1}{2}m\boldsymbol{V}'^2 = \tfrac{1}{2}m\{4\boldsymbol{V}\cdot\boldsymbol{D}\boldsymbol{R}\cdot\boldsymbol{D} - 4(\boldsymbol{R}\cdot\boldsymbol{D})^2\} = 2m\boldsymbol{R}\cdot\boldsymbol{D}\boldsymbol{W}\cdot\boldsymbol{D}$$

where $\boldsymbol{W}$ is the velocity of the center of mass.

The number of ions per cm³ with velocity components between V_x and V_x+dV_x, V_y and V_y+dV_y, V_z and V_z+dV_z is

$$dn = n(m/2\pi kT_i)^{3/2}e^{-mV^2/2kT_i}dV_xdV_ydV_z \ .$$

where n is the number of ions per cm³ and T_i is their temperature. Similarly, the number of molecules per cm³ with given velocity is

$$dN = N(M/2\pi kT_m)^{3/2}e^{-MU^2/2kT_m}dU_xdU_ydU_z.$$

The number of collisions per cm³ per sec. between ions and molecules of the above velocities in which the line of centers at impact lies within the solid angle $d\omega$ about the direction $\boldsymbol{D}$ is

$$dndN(\boldsymbol{V}-\boldsymbol{U})\cdot\boldsymbol{D}\sigma^2d\omega = dndN(1/\mu)\boldsymbol{R}\cdot\boldsymbol{D}\sigma^2d\omega$$

where σ is the sum of the radii of ion and molecule. The energy loss per cm³ per sec. in these collisions of the given type is

$$(2m\boldsymbol{R}\cdot\boldsymbol{DW}\cdot\boldsymbol{D})\left\{n(m/2\pi kT_i)^{3/2}e^{-mV^2/2kT_i}dV_x dV_y dV_z\right\}$$
$$\times\left\{N(M/2\pi kT_m)^{3/2}e^{-MU^2/2kT_m}dU_x dU_y dU_z\right\}(\sigma^2/\mu)\boldsymbol{R}\cdot\boldsymbol{D}d\omega.$$

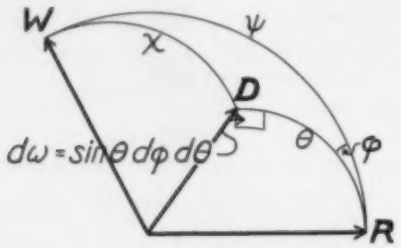

Fig. 1.

$\boldsymbol{D}$ may be expressed in polar coordinates ϕ and ϑ (Fig. 1) with the axis parallel to $\boldsymbol{R}$ and the plane $\phi = 0$ containing $\boldsymbol{W}$. Then

$$d\omega = \sin\theta d\phi d\theta$$
$$\boldsymbol{R}\cdot\boldsymbol{D} = R\cos\theta$$
$$\boldsymbol{W}\cdot\boldsymbol{D} = W\cos\chi = W(\cos\theta\cos\psi + \sin\theta\sin\psi\cos\phi)$$

and the total energy loss per cm³ per sec. becomes

$$Q = \int_{-\infty}^{\infty}\int_{-\infty}^{\infty}\int_{-\infty}^{\infty}\int_{-\infty}^{\infty}\int_{-\infty}^{\infty}\int_{-\infty}^{\infty}\int_{0}^{2\pi}\int_{0}^{\pi/2}(2mnN\sigma^2/\mu)(m/2\pi kT_i)^{3/2}(M/2\pi kT_m)^{3/2}$$
$$e^{-mV^2/2kT_i - MU^2/2kT_m}R^2W\cos^2\theta\sin\theta$$
$$(\cos\theta\cos\psi + \sin\theta\sin\psi\cos\phi)d\theta d\phi dV_x\,dV_y\,dV_z\,dU_x\,dU_y\,dU_z$$

in which R, W, and ψ are all functions of $V_x \cdots\cdots U_z$.

The integrations with respect to θ and ϕ may be performed immediately. For the remaining six integrations, $\boldsymbol{V}$ and $\boldsymbol{U}$ are replaced by $\boldsymbol{R}$ and $\boldsymbol{W}$, expressed in polar coordinates. The result is

$$Q = 8(2\pi)^{1/2}nN\sigma^2k^{3/2}\left\{mM(mT_m + MT_i)\right\}^{1/2}(m+M)^{-2}(T_i - T_m).$$

Finally, f, the average energy loss per collision expressed as a fraction of the average energy of the ions, is equal to Q divided by the number of collisions per cm³ per sec. all divided by the average energy:

$$f = Q\Big/\left\{\left[nN\pi\sigma^2\left(\frac{8kT_i}{\pi m}\right)^{1/2}\left(\frac{m}{M}\,\frac{T_m}{T_i}+1\right)^{\frac{1}{2}}\right]\left[\frac{3}{2}kT_i\right]\right\}$$
$$= \frac{8}{3}\,\frac{mM}{(m+M)^2}\left(1-\frac{T_m}{T_i}\right).$$

METHOD OF ENHANCING THE SENSITIVENESS OF ALKALI METAL PHOTOELECTRIC CELLS

By A. R. Olpin
Bell Telephone Laboratories

(Received June 6, 1930)

Abstract

A technique is described for sensitizing alkali metal photoelectric cells to light by introducing onto the metal surface small amounts of dielectrics, as oxygen, water vapor, sulphur vapor, sulphur dioxide, hydrogen sulphide, air, sodium bisulphite, carbon bisulphide, etc., or some organic compound as methyl alcohol, acetic acid, benzene, nitrobenzene, acetone, etc., or some organic dye as tropaeolin, rosaniline base, eosin, cyanine, kryptocyanine, dicyanine, neocyanine, etc. The marked increase in electron emission from the cathodes of cells so treated is due primarily to an increase in response to red and infrared light. Vacuum sodium cells have been produced, yielding photoelectric currents as high as 7 microamperes per lumen of white light of color temperature 2848°K and caesium cells yielding far greater currents.

The response of these cells is proportional to the intensity of the exciting light even for light of longer wave-lengths than that to which the cell responded before treatment.

Spectral response curves are similar for all cells using the same metal as cathode. These curves differ from the curves for the pure metal by the appearance of a new selective maximum at lower frequencies. This newly appearing maximum resembles the regular maximum for the untreated metal and is always separated from it by the frequency of a well-known line in the vibration-rotation spectrum of the dielectric molecules, usually the 1.5μ line so characteristic of oxygen-hydrogen, carbon-hydrogen or nitrogen-hydrogen linkages. The long wave limit shifts an amount agreeing with the separation of the maxima.

With a cell so designed that the cathode could be sensitized in a side chamber and then slipped into its proper place (thus keeping the anode free from light-sensitive materials), stopping potentials were obtained for electrons, liberated by monochromatic light, from a sodium cathode before and after treating it with sulphur vapor and air. For light of wave-lengths ranging from λ3500A to λ8000A falling on the treated cathode, the electron retarding potentials are found to vary linearly with the frequency of the exciting light, thus establishing the validity of Einstein's photoelectric equation for composite surfaces. From the slope of the straight line depicting this relationship, the value of Planck's constant h is found to be 6.541×10^{-27}, significant to three figures. An almost identical value is obtained for untreated sodium. The apparent stopping potentials, or voltages at which the photoelectric currents become zero are the same before and after the sulphur and air treatment. The voltage at which the current just saturates is always greater after treatment than before. This is a measure of the change in contact potential of the cathode due to the presence of the sulphur and air. Changes of approximately 0.8 volts are common.

The validity of Einstein's equation precludes the possibility of explaining the new maximum in the spectral response curve for a treated surface by a "Raman shift" of the incident light frequencies, even though the separation of these maxima is equal to certain well-known vibration-rotation frequencies of the dielectric molecules. It may be that the natural frequency of the alkali metal atom is diminished by the vibration frequency of the complex atom in which it is incorporated.

The Lindemann formula for the frequency of the selective photoelectric maximum $[2\pi\nu = (ne^2/mr^3)^{1/2}]$, primitive though it seems in the light of modern theory, has always given values for the pure metals in close agreement with experimental determinations. The n term is determined by the valence of the substance, a choice of unity being used for the monovalent alkali metals corresponding to an electron revolving around a singly charged ion. A choice of 2, 3,—for divalent, trivalent,—substances corresponds to electrons revolving around doubly, triply—charged ions. Under certain conditions the alkali metals manifest different valencies, such for instance, as those exhibited in the oxide series Na_2O_2, Na_2O, Na_2O, Na_4O. These compounds can be prepared in vacuum and are light-sensitive. Spectral response curves for such cells exhibit all the selective maxima called for by the Lindemann formula when the value of n is chosen to agree with the valence of the metal. Data are presented showing this condition to be general for the alkali metals, a maximum response to red or infrared light being dependent upon the formation of a subvalent compound, as a suboxide.

Attention is called to seemingly analogous phenomena in the fields of photoelectricity, photography, fluorescence and absorption.

THE work which culminated in the results to be reported in this paper was inspired by the simple inference that, since photoelectric emission from potassium is greatly increased by a non-conducting hydride film on the surface,[1,2] some other dielectric film might be still more effective in the same sense. As will be seen the consequences were far-reaching. Not only have far more sensitive photoelectric cells been developed but their characteristics have been studied sufficiently to throw some light on the cause of the increase. Moreover, the results of the rather extensive research suggest plausible explanations of various phenomena in the fields of absorption, photoelectricity, fluorescence and photography.

A. Apparatus for Measuring Photoelectric Currents

The response of photoelectric cells to unresolved light was always measured on a high sensitivity Leeds and Northrup galvanometer, a system of external shunts being used to lower the sensitivity as the magnitude of the photoelectric currents increased. Currents as small as 10^{-10} amperes could be conveniently determined in this way with the instrument on which the largest currents obtainable were measured.

The photoelectron emissions for highly resolved light, represented by the ordinates of the spectral response curves which follow, were measured by a Compton quadrant electrometer using a resistance leak of the order of 10^4 megohms. By suitably adjusting the needle voltage, steady deflections were easily readable for currents as small as 10^{-14} amperes.

The source of light was usually a glowing tungsten filament of horizontal candle power about 70 and color temperature 2848°K. To resolve or disperse this light, a high precision Hilger monochromator was used. Proper corrections for the dispersion of the prism were made. All data plotted in the spectral response curves of this paper represent current per unit energy of the incident light, unless otherwise specified.

[1] Elster and Geitel, Phys. Zeits. **11**, 257 (1910).
[2] K. Moers, Zeit. Anorg. Chem. **113**, 179 (1920).

The ordinate values for any one figure are not directly comparable with those of any other.

B. Sensitization of Cells with Vapors from Sulphur

1. *Potassium surfaces.* The first experiment with dielectric films on light sensitive cathodes was performed by admitting sulphur vapor to a potassium surface in vacuum. The technique involved in the manufacture of these cells is given here as typical of that for all the cells made and used throughout the series of tests herein reported, except where otherwise specified.

A glass bulb of the shape shown in Fig. 1. was connected to a vacuum pump by means of a distilling tube, in a side chamber of which was a slug of previously distilled potassium. In the center of the cells was a metallic

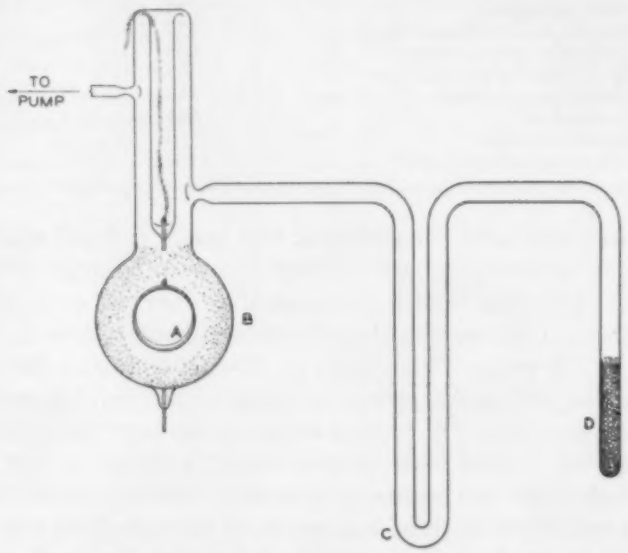

Fig. 1. Experimental type photoelectric cell. *A*-Ring-shaped anode. *B*-Bulb coated on inside with alkali metal to form cathode. *C*-Liquid air trap. *D*-Side arm containing dielectric.

ring *A* with a wire leading through the glass walls to form an anode. A lead-in wire came through the bottom of the cell to make contact with the potassium when it was deposited on the glass walls. A small glass tube *D* containing ordinary commercial flowers of sulphur was sealed onto the stem of the bulb. The U-shaped section *C* of this tube could be immersed in liquid air to trap the vapors coming from the sulphur.

After thorough evacuation of the system, the potassium in the distilling tube was melted and then distilled against the suction of the pump into the glass bulb and a coating made on the inner walls *B*. With a point flame a clear space about one inch in diameter for admitting the exciting light was made on the side of the bulb. As the light fell on the potassium surface, a galvanometer in series with the cell showed that a steady, though limited, emission of electrons was going on. The side tube containing sulphur was then heated and a very small amount sublimed onto the potassium coating.

The pump was left running during this treatment. The galvanometer registered an increased emission of electrons almost immediately and this continued until a certain critical amount of sulphur vapor had come in contact with the surface after which the number of electrons liberated by the light, began rapidly to decrease.

Table I gives a typical history of the treatment of a potassium surface with sulphur vapor, showing the relative current values for two different polarizing voltages at every stage in the process.

TABLE I.

Cathode History	P.E. Current at Cathode Voltages −8	−50
Freshly distilled potassium	34.	38.
After admitting a trace of sulphur vapor	179.	217.
After admitting more sulphur vapor	905.	424.
Incident light diffused by ground glass	542.	542.
Slightly more sulphur admitted	840.	386.
Sulphur tube sealed off	846.	418.
Very low pressure of Argon	1360.	2280.
Argon pressure increased to 0.1 mm	1470.	4120.

It was noted that once the dielectric film began to build up, as shown by a change in the surface color, the current values were larger at low voltages than at high. This has been quite generally observed with this type cell, the voltage-current curves showing a maximum sometimes at cathode voltages as low as −5 volts. This maximum disappeared with the introduction of argon into the cell, and a general increase in measurable current even at low voltages was noted. A typical series of voltage current curves for a potassium surface treated with sulphur vapor is shown in Fig. 2. Another series for a rubidium cell similarly treated is reproduced in Fig. 3. The irregularities exhibited in these curves could be smoothed out by focusing the incident light on the side of the cell rather than the back, or by passing it through a diffusing glass. This suggested that they were due to the shape or design of the tube, an interesting observation which will be further discussed in a later section of this paper.

TABLE II.

Color of exciting light	EK filter used	KSH cell	KS cell	KH cell
White	None	374	374	374
Violet	#76	11	11	20
Blue	#78	93	101	132
Green	#60	59	85	44
Yellow	#16	120	72	9
Red	#29	58	11	1

It developed early in the work that the photoelectric emissions from potassium surfaces treated as described above were not only greater than those of potassium hydride cells for unresolved light, but the response to red light was decidedly larger. Even more striking results of this character were

obtained in some cases by flashing hydrogen on the surface treated with sulphur. Table II illustrates the relative sensitivities to colored light on a scale in which the emissions under the action of total light are made equal. The letters used to describe the cells refer to the elements known to be present at the cathode surface.

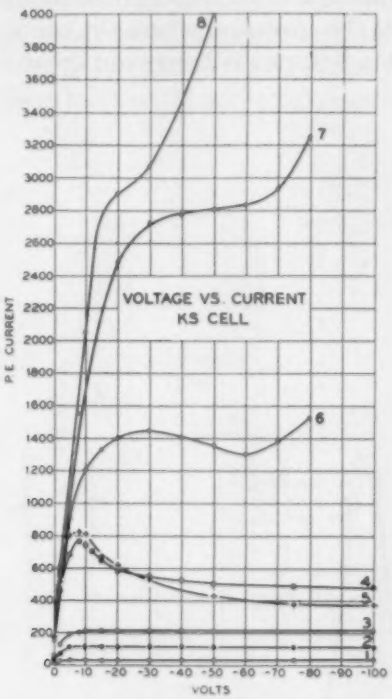

Fig. 2.

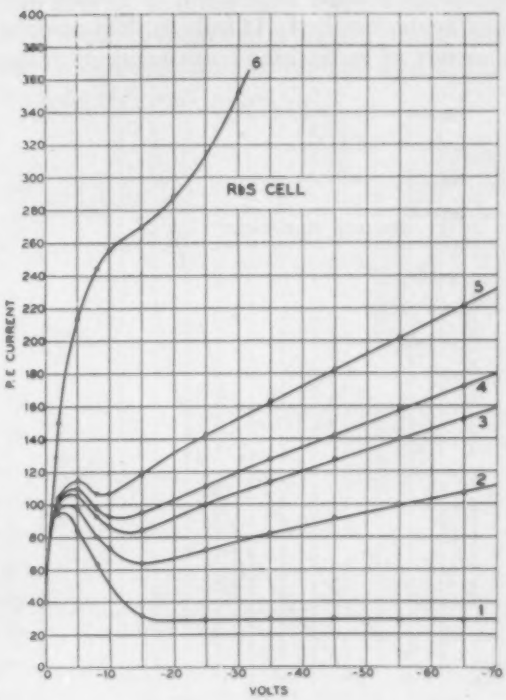

Fig. 3.

Fig. 2. Voltage-current curves for different stages in the manufacture of a potassium-sulphur vapor photoelectric cell. 1—For pure potassium cathode. 2–5—After successive treatments with sulphur vapor. 6–8—After successive admission of increasing pressures of argon.

Fig. 3. Voltage-current curves for a rubidium-sulphur vapor photoelectric cell containing different pressures of argon. 1 Vacuum condition. 2–6 Argon pressure gradually increased.

The color temperature of the constant light source used in the preparation of this table was not known, but Fig. 4 shows the relative sensitivities of KH and KS cells to white light of color temperature 2848°K. The new cells were very stable and showed little change in emission upon aging, the tendency being rather frequently to increase slightly in sensitivity during the first few days after sealing off the pump. In Fig. 5 are plotted some curves showing relative sensitivities throughout the spectrum. These curves, taken with spectrally resolved light, are corrected so that the ordinates, representing current per unit of light energy incident on the surface, are equal at the selective maxima.

It will be noted that the large selective maximum for each of these curves lies in the blue-violet region of the spectrum but that the maximum for the potassium-sulphur cell is slightly displaced toward shorter wave-lengths. The long wave end of the curves for this cell can be represented as an amplified sensitivity curve for pure potassium plus an additional curve representing a new maximum symmetrically drawn about 6200A. This maximum could be greatly enhanced by proper treatment and its importance should not be overlooked. It falls in that portion of the spectrum where the energy content of radiations from most illuminating systems is large, and its pres-

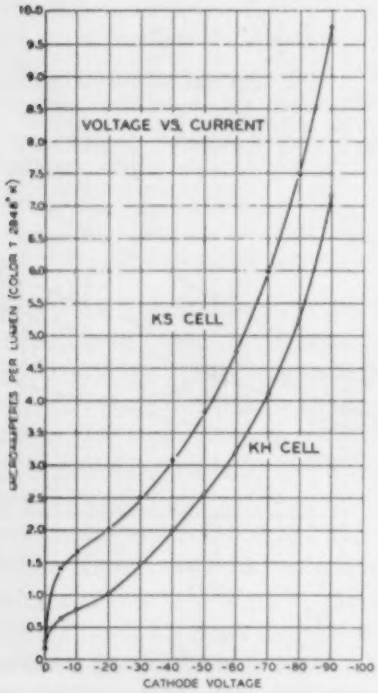

Fig. 4.

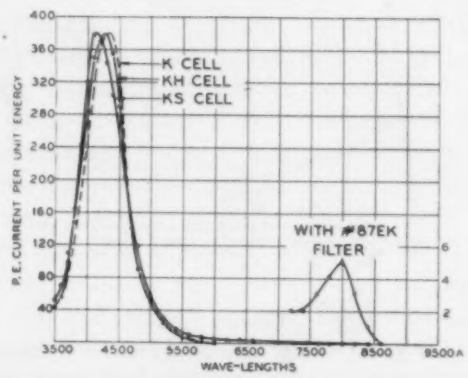

Fig. 5.

Fig. 4. Relative sensitivities of potassium-sulphur vapor and potassium-hydride photoelectric cells.
Fig. 5. Spectral response curves for potassium, potassium-hydride and potassium-sulphur vapor photoelectric cells.

ence figured strongly in increasing the response of a cell to white light. Further discussion of this part of the curve will be reserved for a subsequent section of this paper.

2. *Rubidium and caesium surfaces.* Encouraged by the increase in response to red light manifested by potassium cells treated with sulphur vapor, the same treatment was applied to rubidium and caesium. Since the selective maxima[3] and the long wave limits[4] for these two alkali metals are or-

[3] F. Gross, Zeits. f, Physik **7**, 316 (1921).
[4] B. Gudden, "Lichtelektrische Erscheinungen" p. 40 Julius Springer, Berlin (1928).

dinarily found at greater wave-lengths than for potassium, it was thought that surfaces of these metals, treated as above, should yield electrons more freely than potassium when excited by red or infrared light. However, disappointment in this respect attended all early efforts, presumably because the low melting points and high vapor pressures of rubidium and caesium would not permit the formation of a definite surface structure. The results illustrated for a treated caesium film in Fig. 6, differ only from what would be expected with a pure caesium film by the presence of a maximum between 5000A and 5500A. This is the wave-length region at which caesium in bulk form has been observed to manifest a selective maximum.[5]

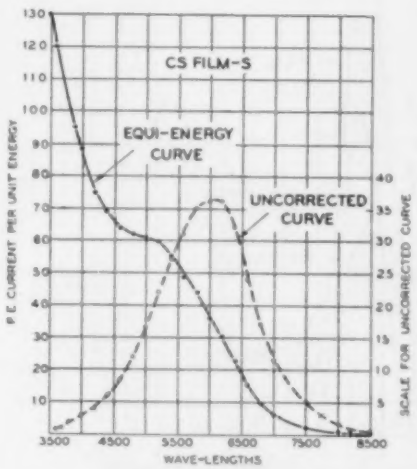

Fig. 6.

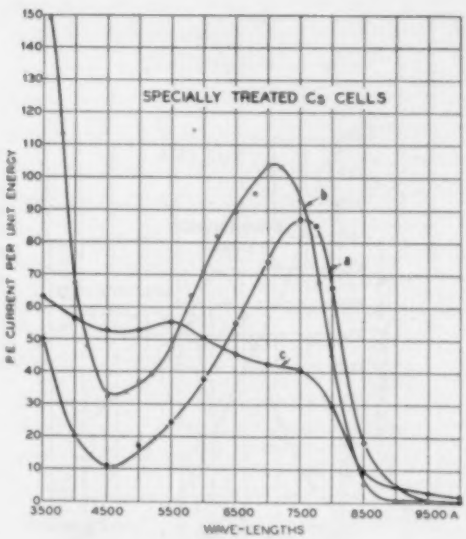

Fig. 7.

Fig. 6. Spectral distribution of sensitivity for a caesium film on magnesium plus sulphur vapor.

Fig. 7. Spectral distribution of sensitivity for a specially treated caesium photoelectric cell. Curves (a) and (b) were obtained from cells treated to give maximum response to red light. Curve (c) was obtained on a similar cell having less red sensitivity.

Early difficulties in treating caesium surfaces effectively with gases have in great measure been overcome by subsequent development of a technique for controlling the amounts of the various constituents which make up the cathode, so as to form the proper compounds. The rather remarkable results obtained with these cells supplement the data contained in this paper and will constitute the subject of a later publication. Suffice it to say that the photoelectric yield for properly treated caesium cathodes is almost entirely due to a marked response to deep red and infrared light, as shown in Fig. 7.

[5] E. F. Seiler, Astrophys. J. **52**, 3, 129 (1920).

3. *Sodium surfaces.* The difficulties which arose in connection with the manufacture of rubidium and caesium cells suggested the advisability of using sodium as the photosensitive material. It was found in fact that when sodium was treated similarly with sulphur vapor, photoelectric cells were evolved having much greater sensitivity than the potassium-sulphur cells previously described. Moreover, the cause of this was found to be increased response to light at the long wave end of the visible spectrum and in the infrared.

Fig. 8 shows a typical curve giving photoelectric current per unit of exciting light energy for such a cell throughout the spectrum. The maxi-

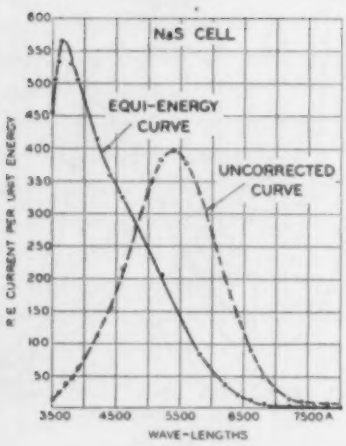

Fig. 8.

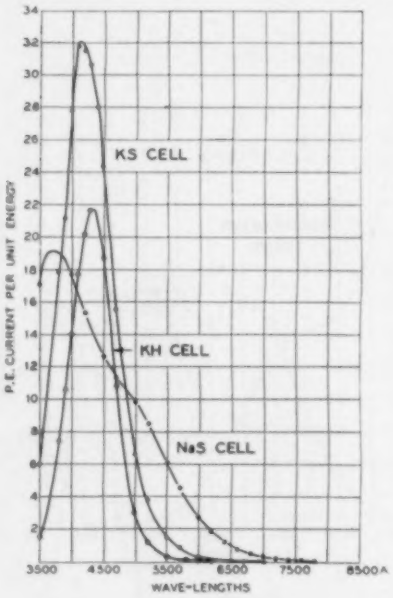

Fig. 9.

Fig. 8. Spectral response curve for a sodium-sulphur vapor cell. The broken curve is a plot of actual electrometer readings.

Fig. 9. Relative sensitivity of potassium hydride, potassium-sulphur vapor and sodium-sulphur cells throughout the spectrum.

mum at λ3600A should probably appear at a slightly shorter wave-length as it is likely that some absorption of the incident light by the glass walls of the cell occurs below λ3800 or 4000A. However, the fact that Richardson and Compton[6] found this maximum at λ3600A, and Pohl and Pringsheim[7] at λ3400A shows that the peak had not been shifted appreciably by the treatment with sulphur vapor. It was the appearance of a new maximum at approximately λ4800A that was most significant. In Fig. 9 are found three curves comparing the spectral response of a sodium-sulphur cell with that of two types of potassium cell.

[6] O. W. Richardson and K. T. Compton, Phil. Mag. **26**, 549 (1913).
[7] R. Pohl and P. Pringsheim, Verh. d. D. Phys. Ges. **14**, 46 (1912).

By applying a point flame momentarily near the edge of the cell window and temporarily producing a vapor of the sodium and the gas occluded on it, a startling increase in sensitivity was brought about. The response of the surface to white light of color temperature 2848°K after this last treatment was about double that observed before. Moreover, the increase was again chiefly in the red and infrared regions, as shown in Fig. 10. The new spectral emissivity curve could be broken up into a regular curve for sodium greatly amplified plus a new curve with a pronounced maximum at approximately

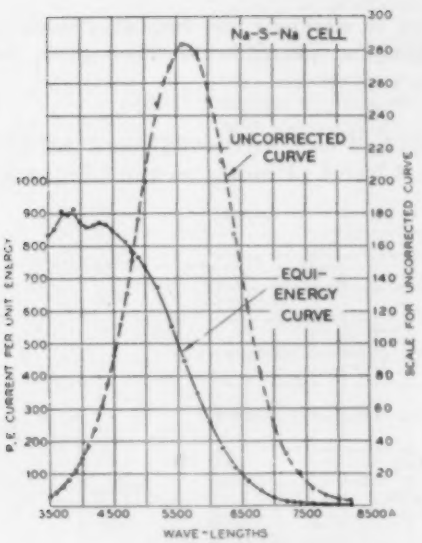

Fig. 10.

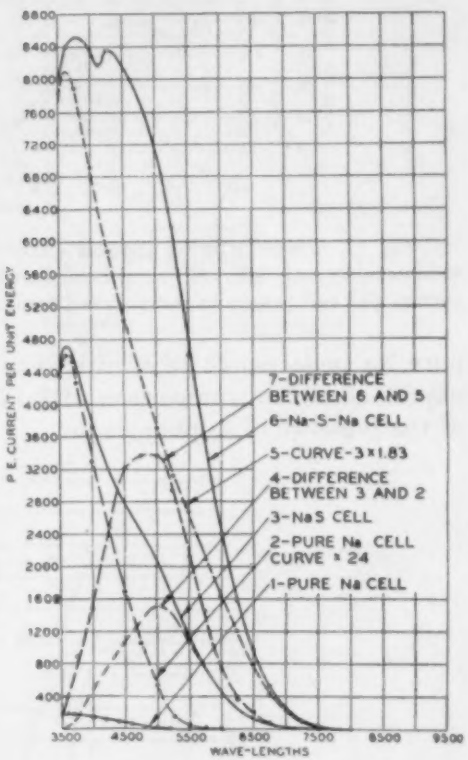

Fig. 11.

Fig. 10. Spectral response curve for sodium-sulphur vapor cell after deposition of a film of the mixture on the surface.

Fig. 11. Curves analyzing the increased sensitivity of sodium-sulphur vapor cells throughout the spectrum.

λ4800A. In Fig. 11 is found a record of the spectral distribution of emissions for each step in the sensitizing process.

At this stage in the development of these cells, air at atmospheric pressure was admitted onto the surface. Upon re-evacuation the cell showed absolutely no response to light of any color. By applying a point flame near the edge of the cell window momentarily and producing a vapor of sodium plus the adsorbed gases, a film deposited on the cathode surface which was strikingly sensitive to light. This experiment has been repeated with many

cells and the same effect always occurs. It appears that the effect is a broadening of the new selective maximum on the long wave side with a shift of the long wave limit to approximately 1μ, as shown in Fig. 12. Fig. 13 shows that

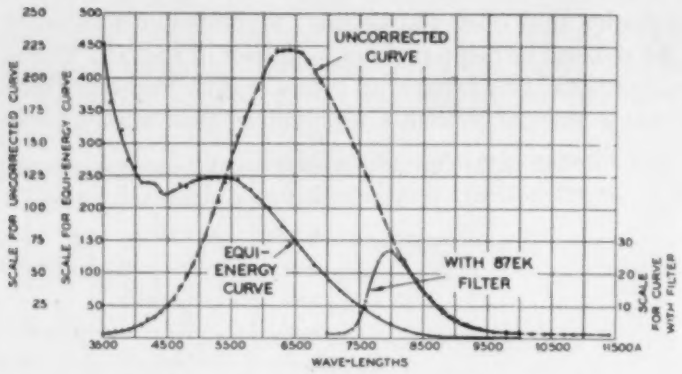

Fig. 12. Curves showing spectral distribution of sensitivity and long wave limits for sodium-sulphur-air cell. Actual electrometer readings are plotted in the broken curve, and current per unit energy in the so-called equi-energy curves.

pure Na surfaces can be sensitized to light of long wave-lengths by air and oxygen alone, but comparison with Figs. 12 and 14 indicates the advantage of the presence of sulphur vapor.

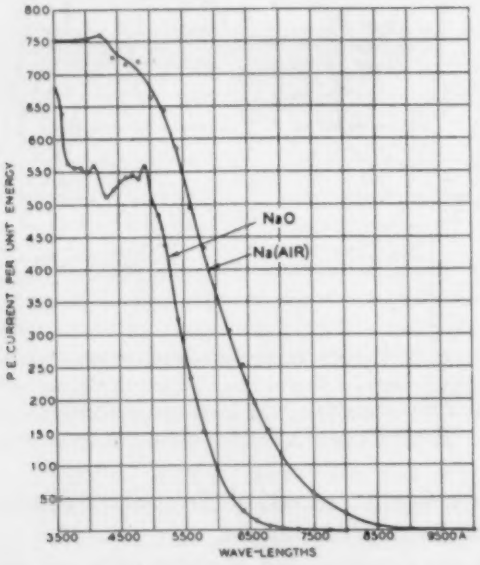

Fig. 13. Spectral response curves for sodium photoelectric cells treated with oxygen and air alone.

In Fig. 15 are given voltage-current curves for a typical potassium cell treated with sulphur vapor, a sodium cell similarly treated, another such

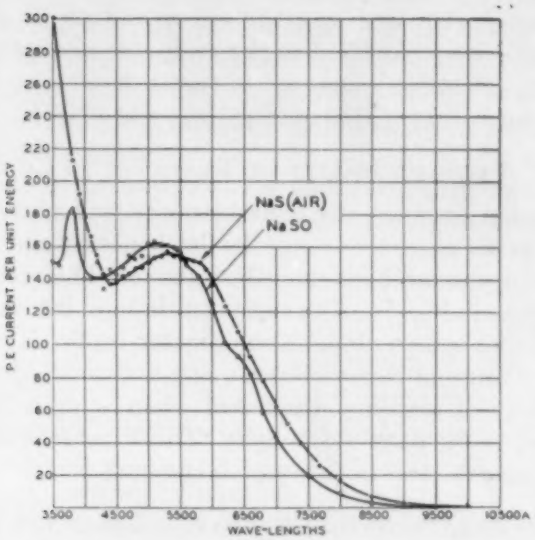

Fig. 14. Spectral distribution of sensitivity for sodium cells treated with sulphur and oxygen, and sulphur and air.

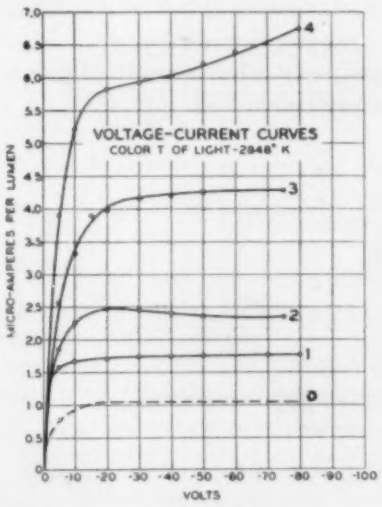

Fig. 15.

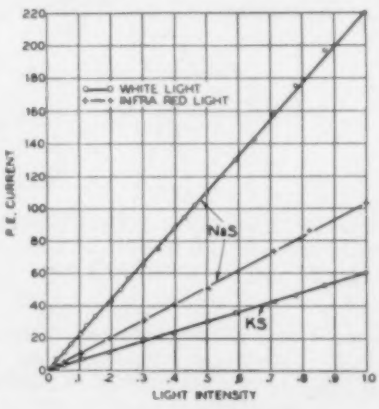

Fig. 16.

Fig. 15. Voltage-current curves for five different types of vacuum photoelectric cells when irradiated with light of color temperature 2848°K. 0—Potassium hydride cell. 1—Potassium-sulphur vapor cell. 2—Sodium-sulphur vapor cell. 3—Sodium-sulphur vapor cell with film on cathode. 4—Sodium-sulphur-air cell.

Fig. 16. Showing proportionality of response of sodium and potassium-sulphur vapor cells to white light and to infrared light.

sodium cell with a thin film deposited on top of the dielectric, and finally a sodium cell treated with both sulphur vapor and air as described above. None of these cells were gas filled so the ordinates represent true emissions from the surface. These emissions are in terms of microamperes per lumen, and the color temperature of the exciting light was 2848°K.

C. Proportionality of Response to Light

The relationship between the light intensity and photoelectric current was checked over an extensive range for both potassium and sodium surfaces sensitized by the methods described above. The results are depicted by the straight lines in Fig. 16. The variations in light intensity were effected by moving the lamp source along a photometer track. The measurements were made on a Compton electrometer, using the steady deflection method. The same linearity of response was noted when using a No. 87 EK filter (visually opaque) in the path of the light. This filter transmitted only light of greater wave-length than that to which the pure metals respond.

D. Attempts to Identify the Activating Gas in the Vapors from Sulphur

The words "sulphur vapor" have been used advisedly in the foregoing presentation, for it was early discovered that the actual sublimation of sulphur onto the surface was not essential. In fact, equally good cells were made with only the volatile gases liberated from sulphur on heating. These gases could be held in a liquid air trap between the sulphur and the cell, and then by lowering the liquid air flask properly, the amount of gas actually entering the coated cell could be accurately controlled.

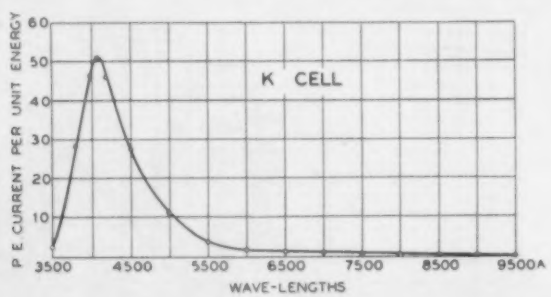

Fig. 17. Spectral response of a potassium photoelectric cell into which an unnoticeably small amount of vapor from sulphur had passed.

A surprising observation was that vapor in such small quantities as to be scarcely detectable with an ionization manometer gauge began to increase the sensitivity as soon as it entered the cell. In a way this was a fortunate discovery, for the amount of gas actually occluded or contained in commercial flowers of sulphur was decidedly small. Yet when a potassium cell with a side arm containing sulphur was sealed off the pump station, and a curve taken showing the spectral distribution of response to light (Fig. 17),

there was appreciable sensitivity out to 1μ. Evidently some gas had been liberated from the sulphur, but the amount was too small to be detected. This emphasizes the importance of taking added precautions against the presence of gas on surfaces to be used in determining the long wave limits of pure alkali metals, and suggests the likely cause for the wide discrepancies sometimes found in literature.

The question as to the nature of the activating gas contained in sulphur was a challenging one since that gas was present in such small quantities.

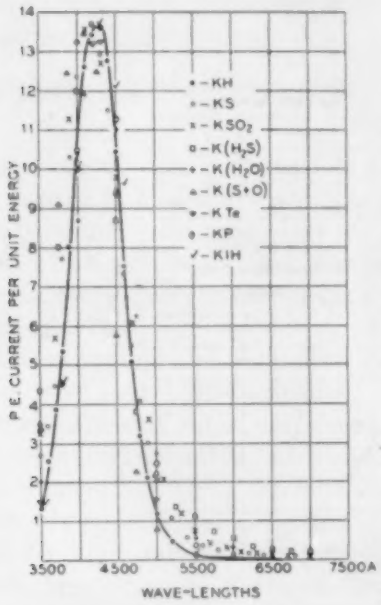

Fig. 18.

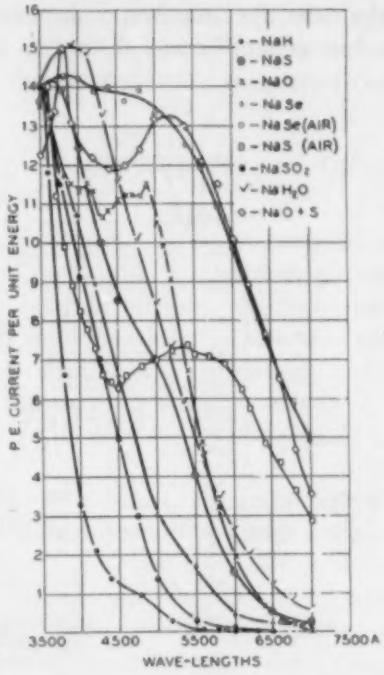

Fig. 19.

Fig. 18. Spectral response of potassium photoelectric cells, the cathodes of which were treated respectively with hydrogen, sulphur vapor, sulphur dioxide, hydrogen sulphide, water vapor, oxygen and sulphur vapor, tellurium vapor, phosphorous vapor and iodine vapor. The ordinates at the maximum are made equal.

Fig. 19. Spectral distribution of sensitivity of sodium photoelectric cells treated with hydrogen, sulphur vapor, oxygen, selenium vapor, sulphur-dioxide, water vapor, oxygen and sulphur, and selenium and sulphur with air. These curves are corrected to correspond at approximately 3500A.

It certainly was not air, hydrogen, nitrogen or oxygen, for these gases could not be condensed at liquid air temperatures. It therefore seemed plausible to suppose that it was water vapor, hydrogen-sulphide or sulphur-dioxide; and direct tests were made to find how these gases act.

A large number of potassium and sodium cells were made, the coating of each being treated with one of the mentioned gases. All of the spectral response curves for potassium cells had selective maxima in the blue at

approximately the same wave-length, and the long wave limit did not vary appreciably from one cell to another. The gas producing results on potassium most nearly like those observed when using sulphur vapor was SO_2, the only one to give the bright golden color and the one producing the most sensitive surfaces to unresolved light.

In Fig. 18 curves depicting the spectral distribution of electron emission are given for potassium cells sensitized with sulphur vapor, sulphur dioxide, hydrogen sulphide, water vapor, sulphur vapor plus oxygen, tellurium vapor, phosphorous vapor and iodine vapor. In all these cases it will be noticed that the selective maximum appeared at approximately the same wave-length, but generally was shifted to somewhat smaller values when sulphur

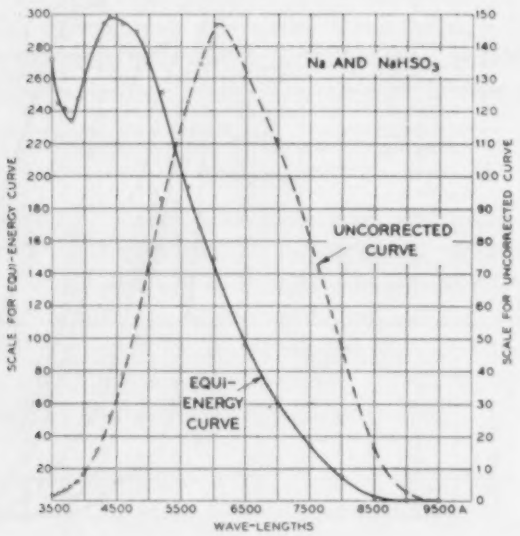

Fig. 20. Spectral response of sodium cell treated with sodium-bisulphite vapor.

was present in the activating gas. We thus find nothing to support Wiedmann's idea[8] that the position of the maximum varies with the nature of the gas. It may be, however, that the relative *magnitudes* of the newly appearing maxima are influenced by the composition of the surface films.

With sodium the different gases produced markedly different curves (Fig. 19) and this gives us a better chance of identifying the vapor proceeding from the sulphur. In this case, it turned out that water vapor yielded the curve most resembling that due to the sulphur vapors, and incidentally colored the surface with a similar tint (dull grey); while sulphur dioxide alone provided a very different curve.

There seemed only one conclusion to draw from these tests. The activating vapor liberated from commercial flowers of sulphur must have been

[8] G. Wiedmann, Verh, d. D. Phys. Ges. **16**, 343 (1915).

a combination of water vapor and sulphur dioxide,[9] and the dielectric films formed must have been sodium and potassium bisulphites. This conclusion seemed the more plausible when it was recalled that the sulphonic radical $SO_2 \cdot OH$ is an important radical in many organic dyes, and that investigators in the Eastman Research laboratory have succeeded in sensitizing photographic plates to light well into the infrared by the use of sodium bisulphite $NaHSO_3$.[10] A sodium cell was therefore made substituting sodium bisulphite for sulphur, and the spectral response of this cell (Fig. 20) was very similar to that obtained with sulphur and air. Moreover, the response was in almost identically the same spectral region to which the photographic plate treated with $NaHSO_3$ responded. The close correlation between these results in the fields of photoelectricity and photography suggests a common cause of the red sensitivity.

E. Sensitization of Sodium and Potassium Surfaces by Organic Dyes

There was no reason to suppose that sodium bisulphite is the only substance used in photography which could be applied in photoelectricity. Accordingly, other sensitizing dyes were introduced onto the light sensitive surfaces of alkali metals, and marked increases in photoelectric emission noted. In every case the amount of dye required was very small, as in plate sensitizing. The colors appearing on the cathode surfaces especially when thin films of sodium and potassium were added on top of the already treated surfaces were varied and beautiful.

Some of the side tubes containing the dyes had to be immersed in liquid air to prevent vaporization with possible decomposition under action of the pump. Others had to be warmed before they sublimed, and in such cases it is not only possible but likely that partial chemical decomposition occurred. In fact, Herndon and Reid's[11] study of the decomposition products of various alcohols, organic acids, acetates, benzenes, phenols, etc. upon heating to 400° suggests that the more complicated compounds break up into simple ones at considerably lower temperatures. Nevertheless, the well-known organic radicals which produce the absorption bands in the visible region, as the methyl group CH_3, the nitroxyl group NO_2, the amido group NH_2, the bromine group, the methoxyl group CH_3O, the carboxyl group $CO \cdot OH$ and the sulphonic group SO_2OH, and many others probably are fairly stable.

The first dyes used contained the sulphonic radical and are not commonly used in photography. They were kept in a side tube beyond a liquid air trap, and heated after the alkali metal coating was made. When they were first heated, some gas passed through the liquid air trap into the cell and was

[9] More recently Dr. G. T. Kohman of the Bell Telephone Laboratories has made a very ingenious analysis of the gases evolved from flowers of sulphur on heating and found water vapor and sulphur dioxide to be contained in greatest amounts, with also considerable hydrogen sulphide.

[10] Capstaff and Bullock, Brit. J. Phot. **67**, 719 (1920).

[11] L. R. Herndon and E. E. Reid, J.A.C.S. **50**, 3066 (1928).

pumped out. This was probably nitrogen, hydrogen, or dry oxygen, or possibly some hydrocarbon compound, for it did not react with the alkali metal. The gas retained in the liquid air trap was very effective in sensitiz-

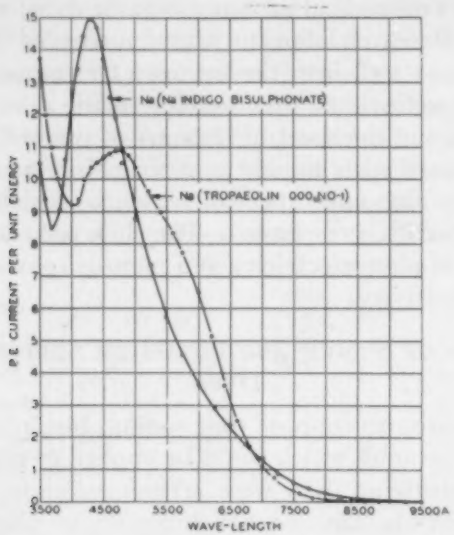
Na (Na INDIGO BISULPHONATE)
Na (TROPAEOLIN 000 NO-1)
P.E. CURRENT PER UNIT ENERGY
3500 4500 5500 6500 7500 8500 9500A
WAVE-LENGTH

Fig. 21. (a) Spectral response curves for sodium photoelectric cells treated with the vapors of tropaeolin 000 No. 1 and sodium indigo disulphonate.

ing the metallic surface of the cell when allowed to enter in small quantities. A very thin film of the alkali metal deposited on the colored surface always enhanced the emission. In Fig. 21(a) are curves showing the response, in

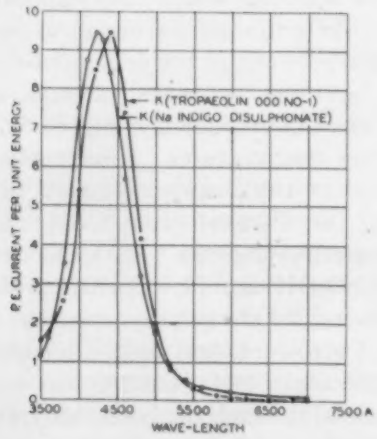

Fig. 21. (b) Spectral response curves for potassium photoelectric cells treated with the vapors of tropaeolin 000 No. 1 and sodium indigo disulphonate.

the visible and infrared, of sodium cells treated with the isomeric compounds tropaeolin 000 No. 1 [$HO \cdot C_{10}H_6 \cdot N:N \cdot C_6H_4 \cdot SO_3Na$] and sodium indigo disulphonate. Both compared favorably with the sodium-sulphur air cells

described in a previous section. Curves for the corresponding potassium coated cells, using these dyes, are given in Fig. 21(b).

To determine whether or not the sensitizing action was limited to compounds containing sulphur, a cell was made with rosaniline base [OH·C

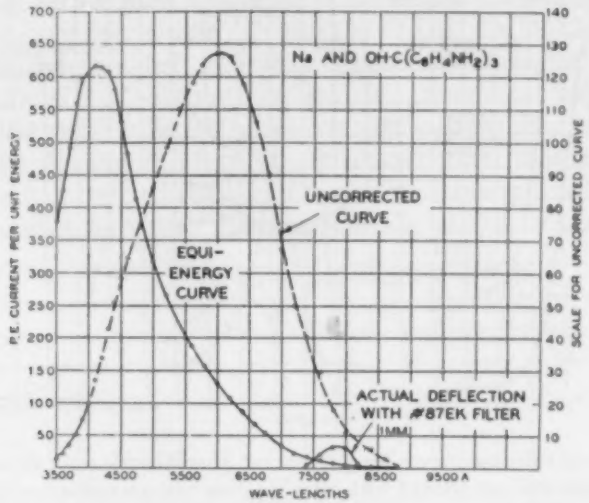

Fig. 22. Spectral response curve for a sodium cell treated with rosaniline base.

$(C_6H_4NH_2)_3$] and a sodium coating. Although no sulphur was contained in this compound, the surface treated showed a good response to light throughout the visible and near infrared, as shown in Fig. 22.

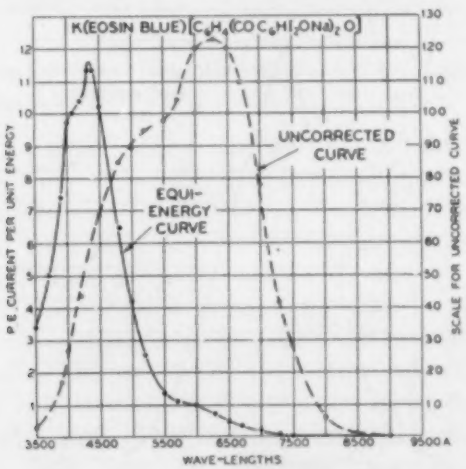

Fig. 23. Spectral response curve for a potassium photoelectric cell treated with eosin blue.

The remainder of the experiments to be reported in this section involve sensitizing dyes used in photography. Because of its historical importance, (it was first used to sensitize photographic plates to green and yellow light

in 1882) eosin [$C_6H_4(COC_6HI_2\ ONa)_2O$] was tried first. Although it brought about a decided increase in sensitivity, it was not so satisfactory as many

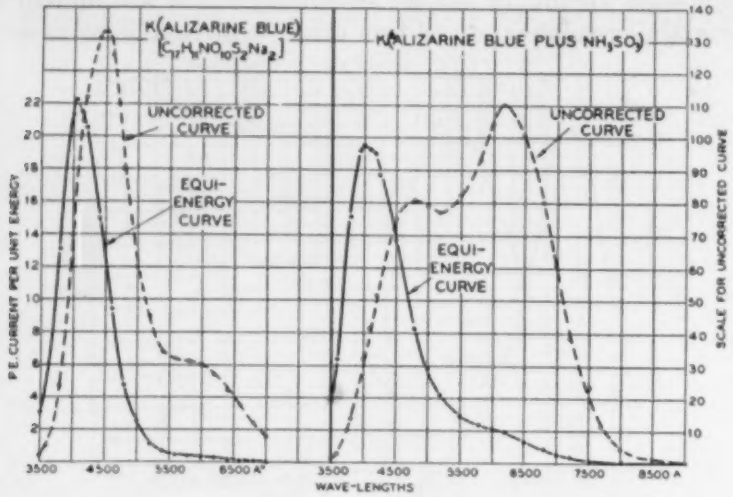

Fig. 24. (a) Spectral response curves for a potassium photoelectric cell treated with alizarine blue alone and one treated with alizarine blue plus ammonium sulphite.

others. In Fig. 23 is reproduced a spectral distribution curve for a potassium-eosin cell, showing the presence of the new maximum at longer wave-lengths very strikingly. The peculiar shape of the regular selective maximum will

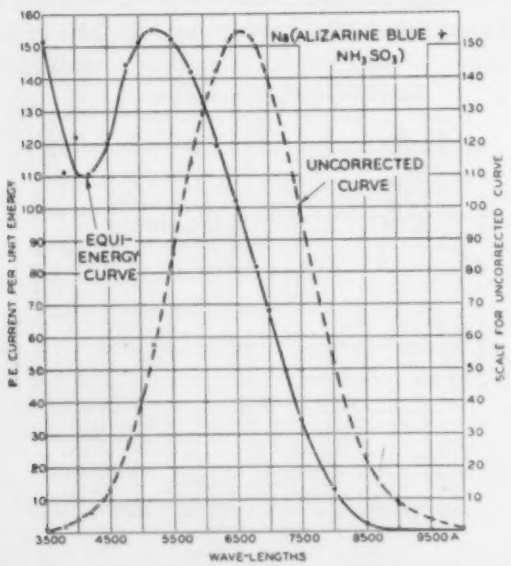

Fig. 24. (b) Spectral response curve for a sodium photoelectric cell treated with alizarine blue and ammonium sulphite.

be cited again in the discussion to follow. There appears to be a new peak at a slightly shorter wave-length.

Some have claimed astonishing results in sensitizing photographic plates to red by using alizarine blue [$C_{17}H_{11}NO_{10}S_2Na_2$];[12] and plates treated in addition with ammonia, have been reported sensitive out to about 1μ. In Fig. 24(a) is found a typical photoelectric emission curve for a potassium coating treated with alizarine blue and another curve for potassium treated also with the vapor from ammonium sulphite (NH_3SO_3). In Fig. 24(b) is a curve for sodium similarly treated. These curves show a response to light of all wave-lengths under 1 μ, with the new maxima appearing at the same position as for the sulphur vapor cells. Here again is a close correlation between results obtained in the sensitizing of photoelectric cells and photographic plates.

Similar results attended the use of dicyanine, especially with addition of ammonium sulphite, and other dyes carrying the latter part of the same word

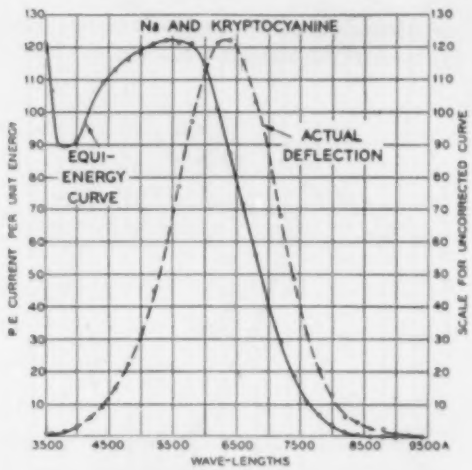

Fig. 25. Curve showing strikingly broad selective maximum in the spectral response curve for a sodium photoelectric cell treated with kryptocyanine.

in their trade names, as kryptocyanine and neocyanine. The spectral regions wherein these dyes are effective sensitizers of photographic plates is published in communication No. 255[13] of the Eastman Research Laboratories where the latter two dyes were developed. Kryptocyanine should be better in the near infrared than dicyanine which in turn should be better than cyanine ($C_{29}H_{35}N_2I$). All of these indications were borne out on photoelectric cells, the dicyanine causing a greater electron emission from alkali metal surfaces than cyanine, and very small amounts of kryptocyanine producing one of the broadest selective bands so far observed in the spectral distribution curve for sodium cells. This last mentioned curve is found in Fig. 25.

F. Sensitization by Colorless Dielectrics

The position of the new maximum seems to be characteristic of the light sensitive metal and not the dielectric on its surface. It appeared likely,

[12] Scoble, Phot. J. **46**, 190 (1906).

[13] M. L. Dundon, A. L. Schoerr, R. M. Briggs, J.O.S.A. and R.S.I. **12**, 397 (1926).

therefore, that any dielectric regardless of the peculiarities of its absorption spectrum, might bring out such a maximum. To test this, various colorless dielectrics and dielectrics practically transparent to visible light were substituted for the dyes. Most of these were liquids, but their vapors could easily be held in side tubes by means of liquid air. The technique employed in applying them was identical to that for the dyes.

Acetone ($CH_3 \cdot CO \cdot CH_3$), *acetic acid* ($C_2H_4O_2$) *carbon bisulphide* (CS_2), *methyl alcohol* (CH_3OH), *carbon tetrachloride* (CCl_4), *benzene* (C_6H_6), *chloroform* ($CHCl_3$), *phenyl mustard oil* ($C_6H_5\text{-}N\text{-}C=S$), *nitrobenzene* ($C_6H_5NO_2$), and *water-vapor* ($H_2O$) were used with more or less success. And surprising though it may seem, benzene and water vapor were the most effective, the red sensitivity of sodium surfaces properly treated with them being especially

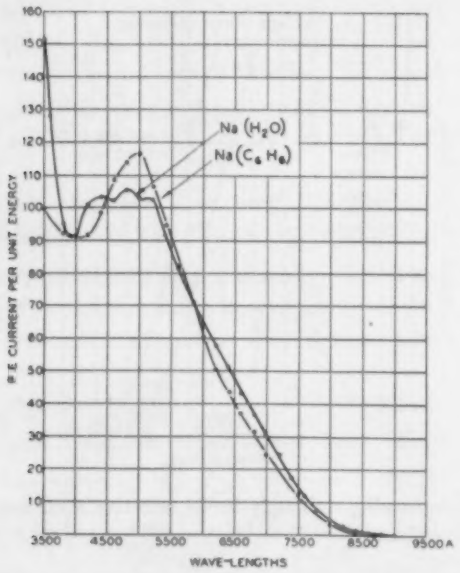

Fig. 26. Spectral response curves for sodium photoelectric cells treated with water vapor and with benzene.

marked, as shown in Fig. 26. There was absolutely no evidence of chemical action when benzene was admitted to the cell, even though a thin film of sodium was deposited on top of it. In fact, the surface of the completed photoelectric cell looked exactly like that of pure metallic sodium. This, of course, is not surprising since the alkali metals are preserved in benzene, but is cited here as evidence of the chemical purity of the sample used. In quite striking contrast to the behavior of benzene on sodium was that of water vapor, whose powerful affinity for the alkali metals makes it necessary to preserve them in benzene, oil, or sealed air-tight containers. Yet benzene and water vapor were alike in being able to increase photoelectron emissions from sodium and potassium surfaces.

In every case mentioned in the preceding paragraph, except that of CCl_4, an appreciable amount of sensitivity to red was developed. Moreover, the

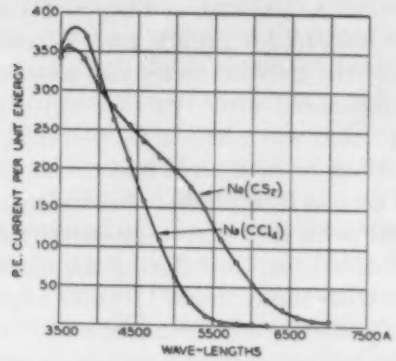

Fig. 27. Spectral response curves for sodium photoelectric cells treated with carbon bisulphide and with carbon tetrachloride.

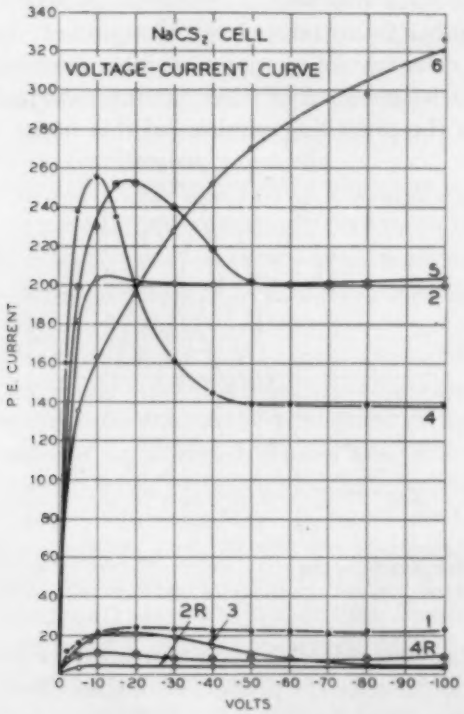

Fig. 28. Peculiarities noted in voltage-current curves for a sodium-carbon bisulphide photoelectric cell. 1—Supposedly pure sodium. 2—After first introduction of CS_2 on sodium surface. 2R—Same as 2 but for irradiation with red light only. 3—After additional CS_2 was introduced onto the surface. 4—After a film of sodium had been deposited from near the cell window. 4R—Same as 4 but for illumination with red light only. 5—Light focussed on cathode opposite cell window. 6—Light focussed on cathode adjacent cell window.

spectral distribution curves show evidence of a new maximum in the photoelectric emission curve near λ4800A for sodium and a much less pronounced peak at approximately λ6200A for potassium. When carbon tetrachloride was used no deflection of the galvanometer was observed when the exciting light was passed through a red filter, cutting out all wave-lengths under 6000A. In Fig. 27 are plotted wave-length vs. current curves for sodium surfaces sensitized with carbon tetrachloride and carbon bisulphide.

When working with carbon bisulphide (CS_2) and nitrobenzene ($C_6H_5NO_2$) the previously described peak in the voltage-current curve at low voltages was strikingly prominent. At one time during the treatment of sodium with CS_2 the current output with the cathode 15 volts negative was four to five times its value when this voltage was increased to 100 volts. A record of the change in shape of these curves as the sensitization process was carried out is included in Fig. 28. These will be discussed with those in Fig. 2 and 3 in the next section.

G. Discussion of Results

A great mass of data has been presented. It now remains to be seen whether or not they can be correlated and interpreted. In all, over two hundred photoelectric cells involving the principles and technique herein discussed have been made, and most of them carefully studied. The collection of curves presented in the preceding sections of this paper may or may not in

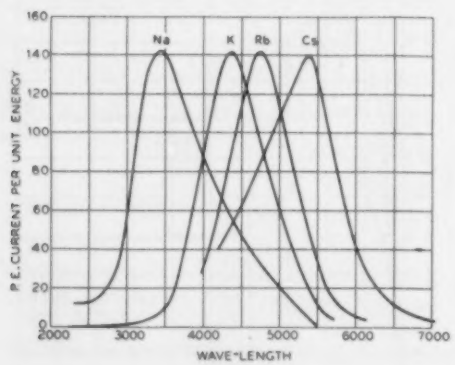

Fig. 29. Spectral response curves for the alkali metals. Curves for sodium and potassium reproduced from Pohl and Pringsheim[7] and those for rubidium and caesium from Miss Seiler.[8]

every case refer to the best cell which could possibly be made with the stated materials; but they do display the properties of the cell when made according to the best technique at that time known.

A survey of the data presented in the form of spectral response curves revealed that the properties of the cells depended very much on the metal, very little on the dielectric. As pointed out previously (Fig. 11) each curve could be represented as the sum of the "regular" curve for the pure metal and a second curve with a maximum at longer waves. Only the *relative magnitudes* of the ordinates of these two curves seemed to be a function of the

dielectric. The so-called "regular" curves for the pure alkali metals are shown in Fig. 29. Each one will be seen to resemble a resonance curve, the area underneath being more or less symmetrically located on either side of the wave-length of light producing the greatest photoelectric current. These curves are not alone characteristic of the multiply distilled metals, but are also characteristic of these metals after a glow discharge has been passed through hydrogen at a pressure of a few millimeters on the surface. This fact caused Pohl and Pringsheim[14] to refer to the metallic hydride surfaces as colloidal metal surfaces and attribute the increased response of such surfaces to light to the greater ease with which electrons might escape from tiny globules. This same fact caused Hallwachs and Wiedmann[15] to claim that the photoelectric effect was a gas-metal phenomenon and that the maxima in the curves shown in Fig. 29 were dependent on the presence of hydrogen. At this stage in our discussion it is the *existence* of these maxima in the "regular" curves rather than the *cause* to which attention is called.

The "second" curve referred to above appeared as the "regular" curve shifted to longer wave-lengths. The amount of this shift was approximately the same for all cases excepting the ones in which sulphur or selenium plus oxygen or air and certain organic dyes, as kryptocyanine, were among the activating agents, in which cases it was somewhat greater, and the new maximum broader, as illustrated in Fig. 19. Slight variations in the separations of the two maxima, when several dielectrics were used, were dependent on the relative amounts of the different materials.

1. *Role of water vapor.* This analysis of the spectral response curves suggested that there is a single activating agent common to all the dielectrics introduced onto the alkali metal surfaces, with the possibility of one or more others in a few cases. Certainly it must be conceded that water vapor may have been present in every case. Every effort was made to eliminate it, the glass bulbs being carefully and thoroughly heated during the evacuating process. But, as mentioned earlier, the substances which were evaporated or sublimed onto the cathodes may have contained water. The glass tubes containing them could not be heated sufficiently to drive out all moisture before the alkali metal coatings were made. With liquids, it was necessary to immerse the side arm containing them in liquid air to keep them from evaporating and being pumped out. Moreover, the bulky, complex organic dye compounds usually occur in the form of very fine crystalline granules, undoubtedly containing water in small quantities. Some of the substances may have decomposed with formation of water vapor. There was no assurance that the samples of liquid dielectrics were absolutely water free, even though they were obtained from a reliable chemical house as certified chemically pure material. Take, for instance, benzene, a liquid easily obtained as "chemically pure" yet Manley[16] reports experiments which seem to

[14] R. Pohl and P. Pringsheim, Verh. d. D. Phys. Ges. **13,** 219 (1911); Verh. d. D. Phys. Ges. **15,** 173 (1913).

[15] G. Wiedmann and W. Hallwachs, Verh. d. D. Phys. Ges. **16,** 107 (1914); G. Wiedmann, reference 8.

[16] J. J. Manley, Nature **123,** 907 (1929).

indicate that benzene, when exposed to air, takes up moisture and holds it tenaciously. Certainly, the difficulties involved in handling liquids in an evacuated system make it impossible to eliminate water vapor altogether from the system.

Although the amount of water that could have been present with the dielectric was admittedly always small, it may not have been negligible. As a matter of fact, many of the experiments seemed to indicate that even *minute traces of moisture* were sufficient to sensitize alkali metal surfaces. One experiment consisted in sealing an empty glass tube on the side of a bulb and then during the pumping process immersing the tube in liquid air. After the bulb was coated, mere removal of the liquid air from the side tube permitted sufficient moisture to fall onto the metal coating to increase its response greatly. The characteristic of such a sensitized surface could be represented by the spectral response curve of Fig. 26. However, the total emission was not nearly so great as in the case of the cells containing sulphur vapor or organic dyes. It appeared, therefore, that the presence of water vapor in small quantities may have been advantageous, but was certainly not alone responsible for the whole of the observed increase in the photoelectric effect.

Perhaps the water vapor present with some such dielectric as sulphur was taken up as water of crystallization as alkali metal sulphides or sulphates were formed on the cathode surface. It is rather significant in this respect that the oxides, sulphides and sulphates of sodium and potassium quite generally hydrate if water is present, and the appearance of these hydrated crystalline forms resemble those of the photoelectric cell cathodes prepared as described earlier in this paper.[17] This indicates that the surface films may have a definite configuration and the molecules a regular alignment, which really would be expected, for polar compounds in general are favorable to association, and this, as Gerlach[18] commented, is a "preliminary stage of microcrystalline character." It is a well-known observation that while water of crystallization plays a definite role in the crystal structure, it reacts toward radiant energy as water vapor in its free liquid state.[19]

In connection with these remarks on water of crystalization, attention is called to the studies of Predwoditilew and Blinow[20] concerning the photoelectric emission of finely powdered crystalline sulphates. They announced a simple relation between the photoelectric current and the water of crystallization.

It occurred to us that the dielectric substance may form a surface film which reduces the work function; the molecules may well have been so aligned as to act as tiny grids setting up powerful fields which aided in pulling electrons from the alkali metals surface. This idea has been effectively

[17] H. Bottger, Liebig's Ann. **223**, 335 (1884).

[18] W. Gerlach, "Matter, Electricity, Energy," p. 65–66.

[19] W. W. Coblentz, Publication No. 35, p. 56 Carnegie Inst. of Washington, Bull. Bur. Stand. **7**, 4, 619 (1911).

[20] A. Predwoditelew and W. Blinow, Zeits. f. Physik **42**, 60 (1927).

used in interpreting long wave shifts, such as are caused by oxide coatings on filaments of thermionic tubes;[21] but we do not see how it could explain the new selective maximum appearing simultaneously with the shift.

Richardson and Young[22] had a theory that the two peaks in their spectral response curves for potassium treated with water vapor and flashed in hydrogen were due to the presence of multiple thresholds on a spotted cathode; but there is nothing in their discussion to explain why the selective maxima occur at the same wave-length for all dielectrics on a given metal; unless, of course, water vapor be the activating agent in them and act independently of and more effectively than any other substances with which it might be mixed.

2. *Lack of correlation between selective maxima and absorption bands in the visible.* We found no relation between the absorbing power of the various dielectrics for *visible* light and the sensitization which they brought about, although this conclusion might be modified if the actual absorption of the deposited films of these substances could be observed. As an example of this might be mentioned the case of water vapor with its weak absorption in the visible, producing better results than cyanine at the particular wave-lengths where this dye has powerful selective absorption (4500–6500A).[23]

H. Theoretical Considerations

1. *Correlation of separation of maxima with infrared vibration-rotation spectra of the dielectrics.* The absorption of light by water vapor increases in the

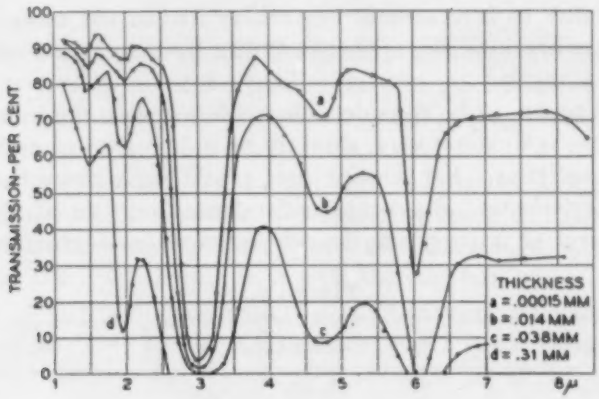

Fig. 30. Absorption spectra of thin films of water. Reproduced from Bull. Bur. Stand. **7**, 4, 631.[19]

direction of increasing wave-length, and is very strong in the near infrared. It consists of a series of lines or narrow bands so related that if the frequencies of the powerful absorption bands near 6μ and 3μ be taken as fundamentals, other bands can be regarded as the first, second, and third harmonics of

[21] J. A. Becker, Phys. Rev. **28**, 341 (1926).
[22] O. W. Richardson and A. F. A. Young, Roy. Soc. Proc. **A107**; 377 (1925).
[23] Bull. Bur. Standards No. 422 (1922).

these.[24] Also these frequencies seem to combine or add up to give other spectral lines. In general, frequencies corresponding to wave-lengths less than 1.5μ are not so strong (Fig. 30), but in the form of vapor or water of crystallization[25] the higher harmonics become sharper and more pronounced (Fig. 31), a line at 1.119μ being almost as strong as the 1.47μ line into which the 1.5μ band resolves itself. This absorption series, the "vibration-rotation

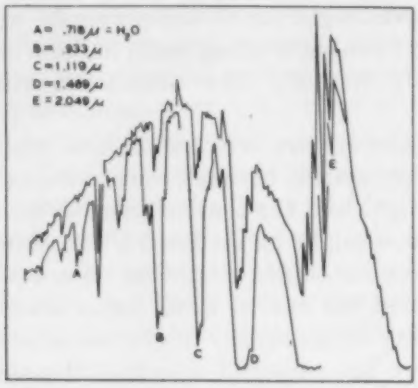

Fig. 31. Bolographic energy curves of the solar spectrum of a 60° glass prism, the upper one taken in February when the humidity was low and the lower one in September when the humidity was high. Curves reproduced after Coblentz from Fowle: Smithsonian Misc. Coll. Vol. **47**, No. 1468, (1904).

spectrum," is due to interatomic vibrations within the molecule, or more specifically to vibrations set up between the hydrogen and oxygen atomic nuclei.

Now there seems to be considerable evidence that the increased photo-electric response is in some way, directly or indirectly, connected with this or a similar spectrum. For, in the first place, such absorption bands are quite characteristic of all compounds containing an oxygen-hydrogen carbon-hydrogen or nitrogen-hydrogen linkage, as shown in Table III.

TABLE III.

O-H Linkage[26]	C-H Linkage[27]	N-H Linkage[27]
3.06μ	3.28μ	2.90μ
1.469	1.68	1.50
1.119	1.145	1.03
.933	.874	.790
.718	.713	.648

There are other important bands of longer wave-length than 3μ, the ones near 6μ being particularly strong. However, (as pointed out by Ellis in discussing the bands listed here for the N-H linkage), the ones just tabulated

[24] H. A. Rowland, Astrophys. J. **6**, (1897).

[25,26] W. W. Coblentz, reference 19.

[27] J. W. Ellis, Phys. Rev. **33**, 27 (1929), Frank. Inst. J. **208**, 4, 507 (1929).

are of particular interest, for the positions of the bands are seemingly independent of the presence or nature of the solvent.

Since a band-system of the foregoing type is found in the spectra of so many different compounds involving hydrogen, it is reasonable to suppose that the vibrations to which such bands are due, occur in the molecules formed by the vapors which we brought into contact with alkali-metal surfaces.

Now we have observed a very interesting pair of numerical agreements, which are probably more than mere coincidences. On evaluating the shift in frequency δ of the long wave limit and the selective maximum, which occurs when an alkali metal is affected by one of the vapors in question, we found:

(a) In many cases this frequency-shift is equal to the frequency corresponding to the wave-length 1.5μ, which is that of a strong band in many molecules of the stated kind;

(b) In certain other cases, notably where sodium surfaces were involved, the frequency-shift is equal to the frequency corresponding to some wave-length near 1μ, where there are other bands.

A couple of other things suggest that the presence of hydrogen may be essential to these shifts: viz. Wiedmann's[28] data which suggested to him that not only the shifts but the actual maxima themselves are due to hydrogen; and the fact that CCl_4 contains no hydrogen, has no absorption-bands in the near infrared (Abney and Festing[29]) and did not produce a frequency-shift, whereas $CHCl_3$, with its hydrogen-content and its vibration-bands, did produce one.

We make, then, the tentative hypothesis that the frequency-shifts are due to the presence of molecules having natural vibration-frequencies equal to these shifts; and attempt to explain why such molecules should have that particular effect.

It may be that when an alkali-metal atom is incorporated into a molecule having an O-H bond (for example) the resulting complex molecule possesses a natural frequency equal to that of the alkali-metal, diminished by that appropriate to the O-H bond. It is well known that two electrical or two mechanical systems with natural frequencies of their own may be coupled into compound systems having a frequency which is the difference of theirs (cf. for instance Hartley and Peterson)[30]. Something of the sort may occur here.

The newly-discovered phenomenon of the "Raman shift," however, offerred a very tempting explanation.

2. *The Raman shift as an explanation of the frequency-shift of the spectral response curves.* In the language of the quantum-theory of light, a "Raman shift"[31] occurs when a quantum or photon collides with a molecule, causes

[28] G. Wiedmann, reference 8.

[29] W. de W. Abney and E. R. Festing, Phil. Trans. **172,** III, 887 (1881).

[30] R. V. L. Hartley, Abs. 48, Bull. Am. Phys. Soc. **3,** 7 (1928); E. Peterson, Bell. Lab. Record **7,** 6, 231 (1928).

[31] C. V. Raman, Ind. Journ. of Phys. **2,** 387 (1928); C. V. Raman and K. S. Krishnan, Roy. Soc. Lond. Proc. **A122,** A-789, 23 (1929).

the molecule to pass from its initial to another of its stationary states, receives the energy which the molecule gives up (or alternatively, gives up the energy which the molecules absorb) in making this transition, and flies off with energy correspondingly increased (or diminished). In the language of the wave-theory (Hartley[32]) a Raman shift occurs when the frequency p of an incident wave-train of light is modulated by the frequency q of a natural vibration of the molecule on which the light falls, the shifted wave-trains being the "sidebands" of frequencies $p+q$, $p-q$, $2p-q$, etc.

Now suppose that some of the quanta striking the treated alkali-metal surface collide with molecules which are not in the normal, but in some excited state of vibration; and that in such a case, the molecule transfers to the quantum the amount of energy which it would release in the form of radiation, if it were spontaneously to relapse to a lower vibration-state; for instance, that it transfers the energy of one quantum of radiation of wave-length 1.5μ. Then the quanta which have made such collisions have their frequencies correspondingly augmented. If now they fall on the alkali metal and produce the photoeffect, it is the photoeffect proper to light of augmented frequency which they produce. The spectral-response curve would then be shifted because the frequency of the light itself is shifted before it reaches the photo-sensitive surface.

This idea was temporarily adopted as a working hypothesis; but a number of objections arose which are hard to surmount. In the first place, the sense of the shift is such that we must suppose the quanta to collide with molecules already excited. Now in a substance in thermal equilibrium, the proportion of molecules in any given state of excitation may be computed by Boltzmann's equation:

$$n = n_0 e^{(-\epsilon/kT)} \tag{1}$$

in which T stands for the temperature of the substance, k for the Boltzmann constant, n_0 for the number of molecules in the normal state or state of least energy, and ϵ for the energy of the given excited state referred to that of the normal state as zero. It seems unlikely that the proportion of excited molecules should be great enough to account for such results as those shown in Fig. 14 (for example) or in Fig. 32, where the "shifted" is as large as the regular maximum,—a result obtained when very thin films of potassium were flashed in hydrogen on oxidized copper plates. And it seemed doubly unlikely that the excited molecules should be numerous enough to explain the presence of such pronounced maxima at long wave-lengths as those shown in Fig. 7, where in the cases of curves (a) and (b) they are several times the magnitude of the regular maximum for caesium at λ5500A.

One would expect encounters in which quanta give energy to normal molecules to be far more abundant than encounters in which quanta receive energy from excited molecules. In other words, if p stands for the frequency of the incident light and q for that of the vibrating molecule, the $p-q$ frequency should be more intense than the $p+q$ frequency and possibly present

[32] R. V. L. Hartley, reference 30.

when the latter was not. There should then, be a new maximum, much stronger than the one which we have observed, located towards higher

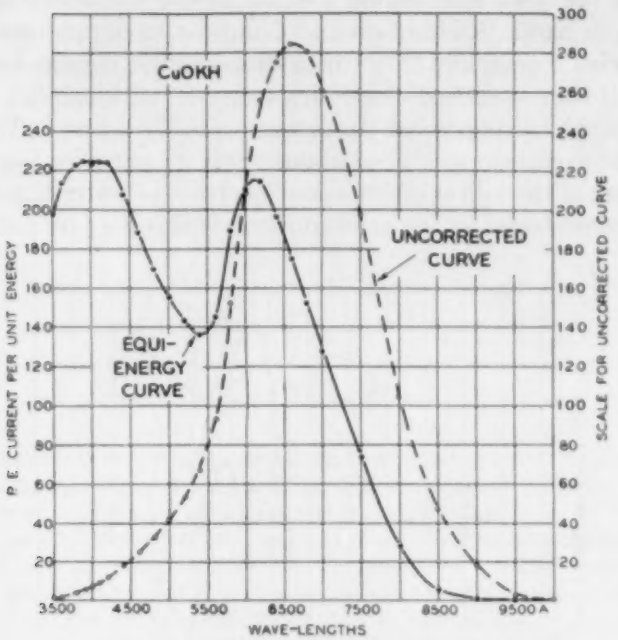

Fig. 32. Spectral response curve for a potassium film flashed in hydrogen on a copper-oxide plate

frequencies from the maximum characteristic of the pure metal. We were not fully equipped to investigate this region and so obtained no definite

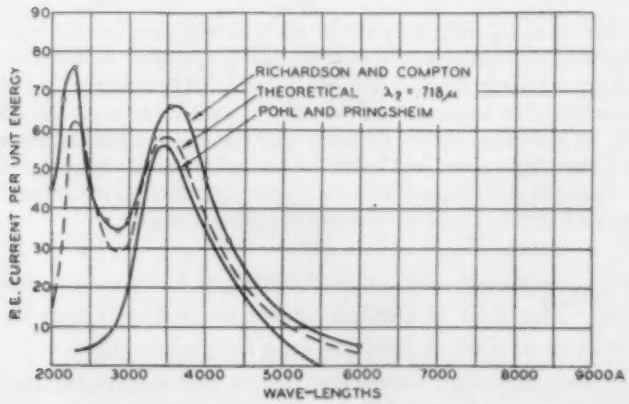

Fig. 33. Spectral response curves showing how Richardson's and Compton's observed double maxima for a sodium photoelectric cell appear as the regular selective maximum of Pohl and Pringsheim plus this maximum shifted to higher frequencies by an amount corresponding to the frequency of the λ0.718μ water vapor absorption line.

information. However, the curves for caesium cells (Fig. 7) show evidence of a maximum at higher frequencies, and also the shift of the λ4360 peak of

pure potassium to somewhat higher frequencies (Fig. 5) upon treatment with dielectrics might be explained by assuming the $p-q$ frequencies greater than the $p+q$ and taking q equal to the frequency of the intense 3μ water vapor band. Richardson and Compton have published a curve for sodium showing a peak at λ2270A in addition to the regular one at λ3600A. Since the cell they used had electrodes sealed in with cement which would prevent thorough baking, water vapor was probably present. The ultraviolet peak could be explained as a $p-q$ frequency if we put q for the frequency of the 0.718μ line of the vibration-rotation spectrum of water vapor. In Fig. 33 is plotted a curve based on the assumption that this $p-q$ frequency produces

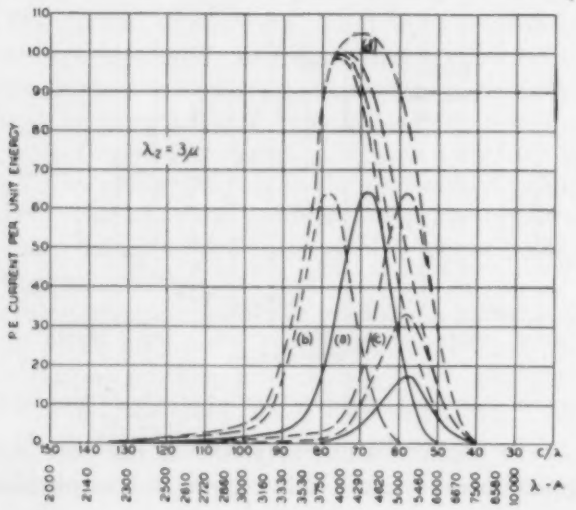

Fig. 34. Theoretical modifications of the spectral response curve for potassium photoelectric cells, assuming modulation of the incident light frequency p by the strong 3μ absorption band of water vapor. a) Curve for pure potassium (Pohl and Pringsheim). b) Curve (a) shifted to higher frequencies by an amount corresponding to $q=c/3\mu$ to show the effect of the $p-q$ side frequencies. c) Curve (a) shifted to lower frequencies by a similar amount to show the effect of the $p+q$ side frequencies. d) Composite curves assuming the presence of the incident light frequency p and the side frequencies $p \pm q$, illustrating the shift of the maximum to shorter wave-lengths with a decrease in the intensity of the $p+q$ sideband.

a maximum as strong as the unmodulated p frequency,—an assumption probably false. The shift of the long wave limit might also be taken to indicate the presence of a weak positive side frequency, also.

In Figs. 34 and 35 are plotted some theoretical curves for potassium cathodes, assuming the $p \pm q$ frequencies to be operative with varying intensities. In Fig. 36 is illustrated the close agreement between the theoretical and observed values. Similar curves for sodium may be shown.

We might avoid the need for postulating a transfer of energy to quanta from excited molecules by assuming that two quanta simultaneously strike a normal molecule and excite it, and a single quantum is then radiated having energy equal to the sum of their energies less that required to excite the mole-

cule. This seems a highly improbable event; but in any case the experiments which we are now about to describe exclude it, for if the theory were correct

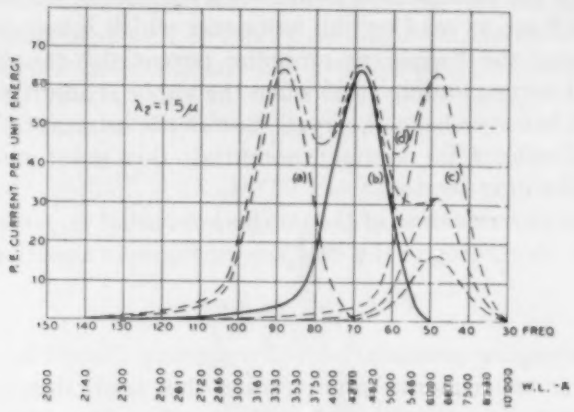

Fig. 35. Theoretical modifications of the spectral response curve for potassium photoelectric cells, assuming modulation of the incident light frequency p by the 1.5μ absorption band of water vapor. a) Curve for pure potassium (Pohl and Pringsheim). b) Curve (a) shifted to higher frequencies by an amount corresponding to $q = c/1.5\mu$ to show the effect of the $p-q$ side frequencies. c) Curve (a) shifted to lower frequencies by a similar amount to show the effect of the $p+q$ side frequencies. d) Composite curves assuming the presence of the incident light frequency p, and the side frequencies $p \pm q$, showing how the magnitude of selective maximum at λ6200A might depend on the intensity of the $p+q$ sideband.

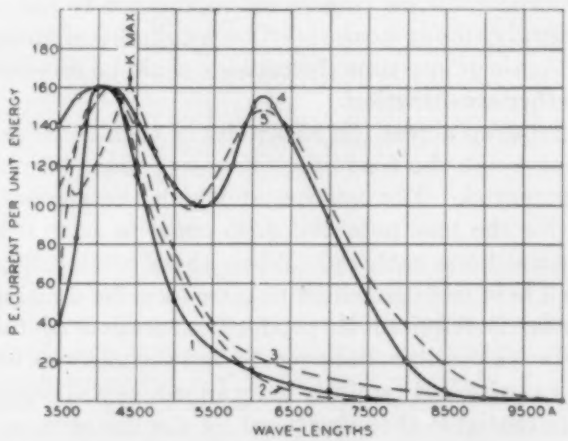

Fig. 36. 1—Experimental spectral response curve for a potassium cell after preliminary treatment with a dielectric. 2—Theoretical curve for a combination of light frequencies p and $p+q$, where $q = c/3\mu$ and the intensity of $p+q$ is considered one quarter that of the incident frequency p. 3—Theoretical curve for a combination of light frequencies p and $p+q$ where $q = c/1.5\mu$ and the intensity of $p+q$ is one-eighth that of p. 4—Experimental spectral response for a potassium film flashed in hydrogen on a copper-oxide plate. 5—Theoretical curve for a combination of light frequencies p and $p \pm q[q = c/1.5\mu]$ all of equal intensity.

the kinetic energy of the emerging electrons would be equal to $2h\nu$ minus the surface work function, instead of to $h\nu$ minus this function.

However, the gravest objection to the "Raman Shift" theory is that it requires that the electrons should receive the energy $h(\nu+\delta)$ rather than the energy $h\nu$ when the substance is illuminated by light of frequency ν; so that the adverse voltage as read on the voltmeter which is required to stop the fastest electrons, the "apparent stopping potential," should be increased by the amount corresponding to $h\delta$ when the vapor is admitted to the metal. No such effect has ever been observed; but as the interpretation of the data requires an allowance for contact potential, this point must be left for discussion in the next section.

3. *Accurate determination of the stopping-potential vs. frequency curve and evaluation of h.* According to the well-known Einstein equation

$$Ve = \tfrac{1}{2}mv^2 = h(\nu - \nu_0) \tag{2}$$

the graph of stopping potential versus frequency should be a straight line of slope h. Our experiments have verified this prediction over a range of frequencies heretofore unemployed and extending into the infrared, have led to a very precise value of h, and have incidentally eliminated the idea mentioned above that a frequency $(2p-q)$ might result from the interaction of light with the molecules; for that idea would require a slope equal to $2h$.

A photoelectric cell was specially designed to avoid the deposition of photosensitive materials on the anode, for this is fatal to accurate determinations of stopping potentials as will be explained directly. As will be seen from Fig. 37, the cathode could be coated with freshly distilled sodium in one end of the tube and then transferred in vacuum to the other end where it became a central cathode surrounded by a cylindrical anode made of soot-coated nickel. Again at any time the cathode could be removed to its original position for further sensitization.

The potential drop across the electrodes of such a cell read on the voltmeter is of course not the true one; allowance must be made for contact difference of potential. The voltage at which the current just saturates would be that for the true potential drop equal to zero, if the anode completely encompassed the cathode. When there are small openings in the anode, such as a hole through which to introduce the exciting light, a slight positive potential is required to produce saturation of the photoelectric current. It is always possible, however, to find the effective or true zero voltage if the long wave limit is carefully determined, as will soon be shown. The true stopping-potential is then measured by the distance, along the axis of voltage, from that point to the point where the current just reaches zero. This last would not be true if the cylinder emitted electrons, for then there would be a "reverse" current when the field was so directed as to drive electrons from it to the central electrode, and the net current would vanish when this just balanced the direct current, not when the direct current itself vanished. But in our experiments the cylinder was not photosensitive at all, and there were never any *reverse* currents.

The photoelectric currents were measured by means of a Compton quadrant electrometer, using the constant deflection method. The cathode

was illuminated sometimes by the highly resolved light of a glowing tungsten filament, sometimes by means of the monochromatic lines of the quartz mercury arc. The arc lines used were isolated by passing the light through a Hilger quartz monochromator and using an Eastman filter which cut out all stray light of higher frequencies. The great amount of long wave-length

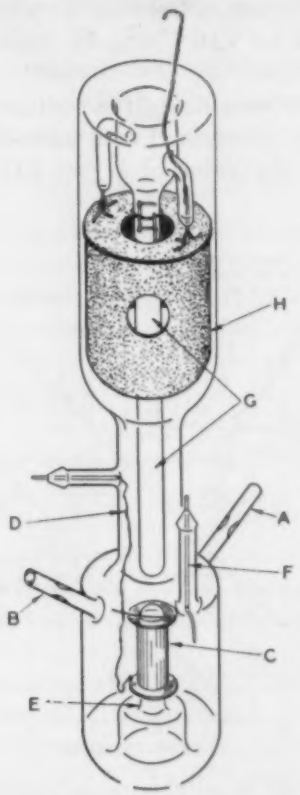

Fig. 37. Specially designed photoelectric cell for the study of stopping potentials. *A*—Tubular connection to evacuating system and entrance for sodium. *B*—Tube leading to side arm containing sulphur. *C*—Cathode of cell on which sodium is deposited. *D*—Phosphor bronze ribbon connecting cathode with external electrode. *E*—Glass stem supporting cathode while it is coated and sensitized and in which CO_2 snow was packed. *F*—Electrode forming electrical contact with coating of sodium used as temporary anode. *G*—Tube down which the sensitized cathode slides after it is sensitized and in which was kept a heating coil during the coating process. *H*—Insensitive anode to which the electrons were emitted after the tube was made.

energy radiated from a glowing tungsten filament made it easily possible to measure stopping potentials for light of wave-lengths up to 8000A with surfaces sensitized by means of dielectrics. This light was passed through a monochromator and a light filter cutting out higher frequencies, and the stopping potentials determined. Corrections for slit width were made before plotting the results. The stopping potentials were then redetermined using a

monochromator of different dispersion. The results obtained with the different instruments checked perfectly.

Both for pure sodium and sodium treated with sulphur vapor and air the curves obtained were straight lines of slope h, as shown in Fig. 38. The value of h obtained from the pure sodium cannot be considered so accurate as that obtained from the sensitized sodium surface because of the few points on the curve and the narrow spectral band to which they are confined. However, even the value $h=6.6\times10^{-27}$ can be considered a fair check of this important constant.

The curve taken after sensitizing the sodium as described earlier in this paper was very carefully determined with wave-lengths of light varying from 3500A to 8000A°, and, the value of h $(=6.541\times10^{-27})$ can be considered

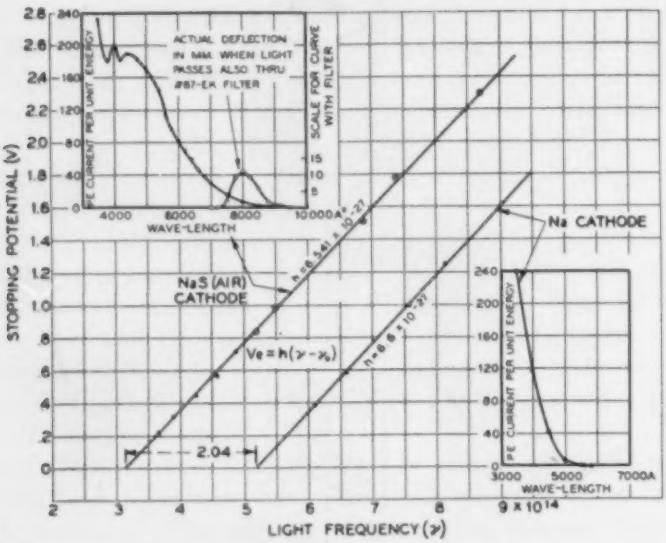

Fig. 38. Stopping potentials versus light frequencies for a sodium cathode before and after sensitizing it with sulphur and air treatments. The spectral response curves for both conditions are shown in the insets.

accurate to at least three significant figures. Perhaps this is the first time that stopping potentials for light of wave-lengths longer than λ5461A have been used in the determination of the value of h.

We never observed any line of slope $2h$. This excludes the idea of a transfer of energy to a normal molecule from two exciting quanta.

When we plot true stopping potentials (measured in the manner just described) against light frequency for pure sodium and treated sodium as is done in Fig. 38, we obtain two parallel lines displaced from one another by the frequency shift δ corresponding to 1.47μ which has already been emphasized. When we plot *apparent stopping potentials* as read by the voltmeter, the two lines fall on one another (Fig. 39). This signifies that the surface work-function of the treated surface has been diminished and the contact potential

increased by the amount corresponding in volts to δ. The electrons initially received the energy $h\nu$ from the quanta, but lose less of it in getting out through the surface, so that in effect their kinetic energy after escape is greater by $h\delta$ than it was with the pure sodium. By the Raman shift theory their kinetic energy would also have been greater by $h\delta$ after the treatment of the surface; but then the surface work function and the contact potential would have remained the same, and the apparent stopping potentials would have been shifted by δ.

To put the foregoing statements into algebraic form we may write the V of equation (2) as the sum of the P.D. registered by the voltmeter, say V_0, and the contact potential difference K:

$$(V_0 + K)e = h(\nu - \nu_0) = \tfrac{1}{2}mv^2. \tag{3}$$

Now, it is generally agreed by all investigators that when the anode is preserved unchanged, and different surfaces are used as cathodes, the stopping potential for a given wave-length of light is the same for all. Therefore, if we use primes to denote the values of V_0 and K for treated as distinguished from untreated sodium, we have,

$$(V_0' + K') - (V_0 + K) = h/e(\nu_0 - \nu_0'). \tag{4}$$

If the light frequency remains unchanged, $V_0' - V_0 = 0$, and

$$K' - K = h/e(\nu_0 - \nu_0'). \tag{5}$$

If, however, the incident light frequency is modulated, and the surface work function remains unchanged, $V_0' - V_0$ would not be zero and Eq. (7) would not explain the facts. Here was a criterion for deciding whether or not the light was modulated.

The stopping potential curves shown in Fig. 39 all refer to the same cell, one of the type shown in Fig. 37. It will be seen that the apparent stopping potentials for a given wave-length of incident light are the same before introduction of the dielectric as after.[33] The increased velocity of emission of the electrons after treatment with sulphur and air was due to a reduction of the work-function of approximately 0.8 volt which was the contact difference of potential between pure sodium and the sodium treated with the dielectric. For this particular case, then, Einstein's equation might be extended to read:

$$K' - K = \frac{h}{e}(\nu_0 - \nu_0') = \frac{h}{e}\,\frac{c}{1.47\mu}. \tag{6}$$

Here is ample evidence that the light frequencies incident on the surface are not modulated.

Referring again to Fig. 39 attention is called to the way in which all plots of the light frequency versus apparent stopping-potentials, (voltages

[33] Actually, the cathode voltage at which the current became zero was 0.5 volt more positive before admitting the dielectric than after, but this was due to the fact that the sulphur vapor and air which entered the cell had made the anode more electronegative as well as the cathode more electropositive.

at which no electrons reach the anode) fall on the same straight line which intersects the effective zero voltages at frequencies corresponding to the long wave limits of the respective cathodes. Failure of the voltage-current curves to break exactly at the effective zero is due to the fact that the anode did not enclose the cathode completely as explained above. A slight positive voltage had to be supplied to the anode before it gathered all of the emitted electrons. However, the separation of the voltages at which the currents saturate, designated by (b) and (d) and the separation of the effective zeros (a) and (c) are practically identical, and the relationship between the

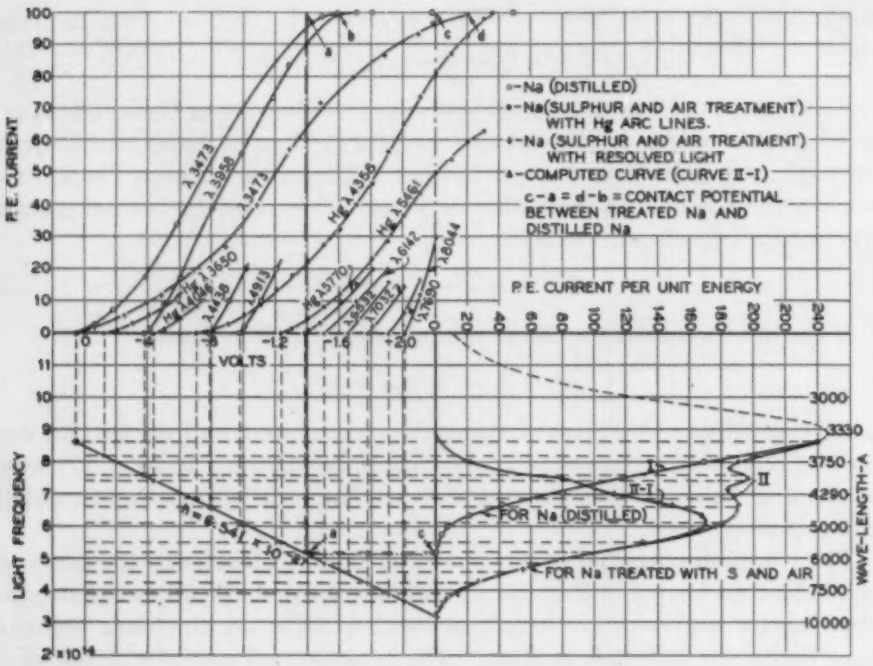

Fig. 39. Showing relationship between stopping potentials, light frequencies and photoelectric current per unit energy; and between contact potentials and long wave limits or work functions.

difference in contact potential and the shift in the long wave limit is graphically shown in the figure.

Now, contact difference of potential is generally considered a measure of the relative densities of free, conduction electrons existent in a substance. In other words, if when two conductors are electrically connected, electrons flow from one to the other, the one from which they flow is said to have a positive contact difference of potential with respect to the other. If, however, the photoelectron be considered to be the valence electron, in the atom, as has been done in this discussion, and the shift in the long wave limit be a measure of the decrease in its resonance frequency and correlate with the vibration-rotation frequencies of the surface molecules, it would appear

that contact difference of potential was a property not alone of surfaces but of molecules and, as such, a measure of the relative number of available valence electrons under excitation of light, or the relative ease with which these loosely bound electrons can be liberated by light.

I. Generalization of the Lindemann Formula

In 1911 F. A. Lindemann[34] derived, from each of two very simple models, the following formula for a natural frequency ν which he proceeded to identify with the frequency of the selective photoelectric maximum:

$$2\pi\nu = (ne^2/mr^3)^{1/2} \quad (e, m \text{ charge and mass of electron}). \tag{7}$$

This is the frequency of an electron revolving in a circular orbit of radius r (or an elliptical orbit of major axis r) about a stationary charge of magnitude $+ne$. It is also the natural frequency of vibration of a system composed of two interpenetrating spheres of continuously-distributed positive and negative charge, having radii r, and total charges $\pm ne$ and $\pm e$ respectively.

Putting n equal to unity, and putting for r the radii of the atoms of the various alkali metals (obtained from their atomic volumes in the solid state) Lindemann obtained numerical values very close to the frequencies of the chief selective maxima of these metals as then known and subsequently checked (Pohl and Pringsheim, Braun,[35] Seiler,[36] and others). See Fig. 29. His values and the experimental ones, converted into wave-lengths, are shown in Table IV.

Table IV. *Specific wave-length of selective photoelectric effect.*

Metal	By Lindemann Formula	Observed
Cs	5500	5100
Rb	4900	4800
K	4380	4350
Na	3180	3400
Li	2360	2800

Subsequently Gross[37] showed that additional maxima observed by some workers for certain of the alkali metals fall at frequencies ν agreeing well with the formula

$$2\pi\nu = (ne^2/mr^3)^{1/2}$$

provided proper integer values be assigned to n.

Some of these agreements are so noteworthy, that it seems worth while to use the Lindemann model, primitive though it may appear in the light of recent theory. Now the choice of the value unity for n, which Lindemann

[34] F. A. Lindemann Verh. d. D. Phys. Ges. **13**, 482 (1911). Verh. d. D. Phys. Ges. **13**, 1107 (1911).

[35] Braun, "Die Photoelektrischen Wirkungen der Alkali Metalle in Homogenen Licht," Boun 1906.

[36] E. F. Seiler, reference 5.

[37] F. Gross, reference 3.

made, corresponds to an electron revolving around a singly-charged ion—the sort of ion one would expect from a monovalent substance, such as the alkali metals are. Such values as 2, 3, ... for n would correspond to an electron revolving around a doubly-, triply-, ... charged ion, such as a di-, tri- . . . . valent substance would have. We might then say that in some atom-groups the alkali metals are divalent or trivalent, and that these are responsible for the maxima of higher frequencies which Gross considered.

Now in our experiments, we have checked several of the maxima to which the original Lindemann formula and the formula with Gross' modifications apply; and we have also observed maxima of lower frequency—those to which this paper is chiefly devoted—many of which are located at frequencies given by the Lindemann formula, provided that simple fractional values are assigned to the factor n.

Continuing with the model, we might say that such values of n are associated with atoms of valency $\frac{2}{3}$, $\frac{1}{2}$, and the like. To think of an electron revolving around an ion with net charge $+2e/3$ seems strange at first; but it is quite conceivable that the forces exerted on the electron by the other surrounding atoms might have the same net effect. We propose therefore to designate even the fractional values of n as "valencies".[37a]

Our data, together with those of the observers already quoted, are listed in Tables V, VI and VII, being classified according to the metals involved. The second column of each table gives the various values assigned to n; the third the corresponding wave-lengths, derived from the frequency computed by the generalized Lindemann formula; the fourth, the wave-lengths of the observed maxima; the fifth, the authorities. In the first column, we give the formulae for oxides in which the metal in question displays these valencies.

Now it is an important fact that most of these oxides are known to exist.[38]

TABLE V. *Lindemann formula* $\nu_{max} = (1/2\pi)(ne^2/mr^3)^{1/2}$.

Metal and its oxides	Valence of metal	λ_{max} (Computed)	λ_{max} (Observed)	Observer
Na	1.	3170	3400	Pohl and Pringsheim
Na_4O	0.5	4500	4700	Self (Figs. 14, 29, 42, 43.)
Na_3O	0.67	3900	4000	Self (Figs. 14, 42, 43.)
Na_2O	1.	3170	<3500	Self
Na_2O_2	2.	2250	2270	Richardson and Compton[6] (On impure Na)
$(Na_2O_3)^*$	3.	1820		

* Probably solid solutions or mixtures of R_2O_3 and R_3O_4.

Returning to the data reported in this paper, an attempt will now be made to interpret them in a way suggested by the Lindemann theory. Among

[37a] Fractional valences are recognized by the chemists by such formulae as $CdCl_2$, 2.5 H_2O, $CdSO_4$, 2.66 H_2O (I.C.T. Vol. 1, p. 120).

[38] J. W. Mellor, "A Comprehensive Treatise on Inorganic and Theoretical Chemistry," Vol. 2, p. 485, Longmans, Green and Co. Ltd., London.

the oxides of sodium are listed Na_4O, Na_3O,[39] Na_2O and Na_2O_2, showing valencies for sodium ranging from 0.5 to 2. Since the likely presence of traces of water vapor in all the dielectrics introduced onto the alkali metals has been admitted and since atmospheric air was admitted in some cases,

TABLE VI. *Lindemann formula* $\nu_{max} = (1/2\pi)(ne^2/mr^3)^{1/2}$.

Metal and its oxides	Valence of metal	λ_{max} (Computed)	λ_{max} (Observed)	Observer
K	1.	4380	4350	Pohl and Pringsheim
K_4O	0.5	6200	6200	Self (Fig. 34)
K_2O	1.	4380	4200	Self (Fig. 34)
K_2O_2	2.	3100	3130	Wiedmann
(K_2O_3)*	3.	2520		
K_2O_4	4.	2240		
K_3O_5	1.25	3920	4000 to 3500	Self (Fig. 34)
K_6O_4†	1.33	3800		
K_4O_3	1.5	3580		

* Probably solid solutions or mixtures of R_2O_2 and R_2O_4.
† Probably aggregates or mixtures of R_2O and R_2O_3.

it may well be that some oxide is formed on the cathode surface; and this may have been a suboxide. (The formation of the higher oxides should result in increasing the response to shorter wave-lengths.) As evidence that it actually was a suboxide, I cite experiments which showed that the cells

TABLE VII. *Lindemann formula* $\nu_{max} = (1/2\pi)(ne^2/mr^3)^{1/2}$.

Metal and its oxides	Valence of metal	λ_{max} (Computed)	λ_{max} (Observed)	Observer
Cs	1.	5500	5100	Braun
			5400	Miss Seiler
Cs_7O	0.29	10200		
Cs_4O	0.5	7800	7700	Self (Fig. 8(a))
Cs_7O_2	0.57	7300	7200	Self (Fig. 8(b))
Cs_3O	0.67	6700		
Cs_2O	1.	5500	5500	Self (Fig. 8 (c))
Cs_3O_5	1.25	4900		
Cs_6O_4†	1.33	4750		
Cs_4O_3	1.5	4400		
Cs_2O_2	2.	3900	3900	Richardson and Compton[6]
(Cs_2O_3)*	3.	3160		
Cs_2O_4	4.	2760	2500	Richardson and Compton[6] (On impure Cs)

* Probably solid solutions or mixtures of R_2O_2 and R_2O_4.
† Probably aggregates or mixtures of R_2O and R_2O_3.

were red-sensitive only when very small amounts of the dielectrics were used. If a certain critical amount was exceeded the response to red decreased greatly, and soon entirely disappeared. If, however at this stage a point

[39] R. de Foicrand, Compt. Rend. **127**, 364, 514 (1898).

near the cell window was heated, a vapor of sodium plus some of the dielectric was created in the cell. This lent itself to the formation of a subvalent compound on the surface and the characteristic response to light of long wavelengths was again in evidence. Moreover, the general appearance of the cathode of sodium cells so treated was exactly that of sodium suboxide, viz. a grey, porous surface crust.

Suboxides of potassium[40] and caesium[41] are also known, but they are more difficult to prepare and apparently are only obtained by limiting the amount of oxygen first coming in contact with the metal. Really this is to be expected for it is impossible to prepare oxygen sufficiently dry that it will not react with either potassium or caesium, but sodium can be distilled in dry oxygen without reaction. In the case of caesium, the suboxides are only formed by limiting the amount of oxygen present and holding the temperature at a certain value. Naturally, then, it would be expected that sodium-suboxide photoelectric cells could be made with less difficulty than potassium or caesium suboxide cells. However, by flashing hydrogen on thin potassium films deposited on oxidized copper plates in vacuum, very much as Campbell[42] has reported, a compound which apparently was potassium suboxide, was prepared. Also by proper control of the temperature, as caesium vapor came in contact with an oxidized silver plate in vacuum, caesium suboxide was formed. Each of these compounds produced a new and pronounced maximum in the spectral response curves, the former at 6200A and the latter at about 7700A. (See Figs. 32 and 7.)

There is no reason to assume, however, that such subvalent compounds are limited to the oxides. The main and limiting requirement for red sensitivity is undoubtedly the subvalent condition of the atoms in the molecules, and possibly these may be subhalides, subsulphides, or some other subvalent salts. However, not many such compounds are known; and water vapor was in all probability always present in the small amounts likely to form suboxides. The broadening of these maxima in cases when certain dyes or dielectrics were used (Figs. 12, 25) was probably due to intense absorption of these complex compounds on the long wave side of this maximum.

The work of Dima[43] on the oxides of manganese and various compounds of other metals suggests a similar theory; for using unresolved light, he found that the lower the valency of the metal in the compounds, the more photosensitive the compound. This may have been due to the shift of the maximum towards the red.

It is practically impossible to prepare a suboxide of a metal without at the same time forming some higher oxides as well. These should correspond to integer values of n in Lindemann's formula; and maxima explainable in this way have actually been observed. As in the case of the maximum for $n=1$

[40] J. J. Berzelius, Lehrbuch der Chemie, Dresden **1,** 749 (1825).
[41] E. Rengade, Compt. Rend. **148,** 1199 (1909).
[42] N. R. Campbell, Phil. Mag. **6,** 633 (1928).
[43] Dima, Compt. Rend **176,** 1366 (1913); **177;** 590 (1913).

shown by multiply distilled sodium, the additional maxima for treated sodium surfaces also generally fall at slightly greater wave-lengths than the computed values, (Table V). However, the second selective maximum observed in the ultraviolet by Richardson and Compton for sodium fits closely the maximum to be expected if $n=2$, the valence of Na in Na_2O_2. The shift of the long wave limit to greater values suggests the presence of the suboxide ($n=0.5$) in small quantities. Since their experimental conditions precluded the possibility of thoroughly eliminating moisture from the glass walls, the likelihood of these compounds being present must be admitted.

The last three oxides listed in the potassium group (Table VI) may have been responsible for the apparent shift of the regular selective maximum for that metal to shorter wave-lengths as quite generally observed after treatment with the dielectrics, (Figs. 5, 23). Moreover, for $n=2$ (the valence of K in K_2O_2) Lindemann's formula gives a maximum at almost exactly the same wave-length as that attributed to oxygen on potassium by Wiedmann.

The difficulties in preparing pure, silvery caesium in bulk form may explain why most investigators seeking to establish the presence of a selective maximum at λ5500A ($n=1$ in the Lindemann formula) for caesium, found a greater peak in the ultraviolet. For, even after multiply distilling caesium in vacuum, it usually appears slightly golden in color as if containing some oxides. If the valence of Cs in these oxides is greater than unity ($n>1$) the selective maxima should fall in the ultraviolet, as observed. As a matter of fact, experiments show that by introducing caesium onto an oxidized plate under proper temperature conditions, the regular selective maximum ($n=1$) can be made to disappear almost entirely, as shown in Fig. 7, indicating that practically all free caesium had disappeared. At the same time the maxima due to the suboxides ($n<1$) and peroxides ($n>1$) become very pronounced.

In the foregoing computations the value of the atomic radius r was left unchanged as n was modified. The alkali metal atom in the molecule was considered as an isolated atom of normal dimensions but with a different force-constant.

J. Comparison of Afore-Mentioned Hypotheses

Two seemingly different and unrelated theories have been advanced to explain the displaced selective maximum. In the first one it was assumed that there is hydrogen present, a condition not unlikely since sodium and potassium absorb great quantities of this gas without any change in their metallic appearance, much as does palladium.[44] It is further assumed that addition of some such dielectric as oxygen or nitrogen results in the appearance of characteristic vibration-rotation frequencies which were apparently subtracted from the resonance frequency of the electron in the alkali metal atom. The other theory is based on the Lindemann equation, and accounts for the reduced resonance frequency as a consequence of a decreased binding

[44] P. Hautefeuille and L. Troost, Ann. Chem. Phys. (5), **2**, 273 (1874), Compt. Rend. **78**, 809 (1874).

force on the electron correlated with a change in the valence of the alkali metals in the molecules of the compound formed on the cathode, the atoms in a subvalent condition responding to light of longer wave-lengths.

Until more is known concerning valence and molecular structure, attempts to correlate the two theories would be outright conjecture. It may be that the reason the two theories appear to explain the same phenomena is that they are both built around similar structures. For example, the very unusual molecule Na_4O may be structurally written (for want of a better formula)

On the other hand, if hydrogen is assumed present with the alkali metals the introduction of oxygen (say) into a photoelectric cell and subsequent treatment, as described above, might result in the formation of molecules which may be written:

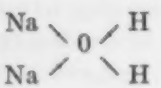

In this connection, it is significant that dry oxygen will not react with sodium. Now, the valence of the sodium atom in each of these compounds is identical, and yet the latter is shown to contain the atoms giving rise to the spectrum of water vapor. The valence of the sodium atoms being similarly reduced in each case, the resonance frequency of the valence electron would be correspondingly decreased and the response to long wave light increased.

Either theory may be made to account for the observation that for small ratios of oxygen atoms (say) to alkali metal atoms in a molecule, the response to red light becomes greater. This would be expected by the first theory, for when the atoms are attentuated, higher vibration-rotation frequencies become sharper, as pointed out previously for the case of water of crystallization.[45] It would also be expected by the second theory, for the valence of the metal and consequently the binding force on the electron would correspondingly be lessened.

K. Irregularities in Voltage-Current Curves Explained

The fact that higher voltages are required to bring about current-saturation when the surfaces are irradiated with light of large wave-lengths can be easily explained by a comparison of the contact potentials of the materials comprising the cathodes of red-sensitive cells. Experiment showed (Fig. 39) that the complex surface formed when the dielectrics were introduced onto an alkali metal cathode was electropositive with respect to the metal by as much as 0.8 volt, and since, within distances comparable to molecular diameters, both free atoms and these complex molecules were existing on the surface, electrons released from the molecules by long wave light would

[45] W. W. Coblentz, reference 19.

encounter strong opposing fields and their escape would be impeded. They would be pulled to the anode only when sufficient voltage was applied to offset these local surface fields. On the other hand, electrons released by light of shorter wave-lengths come primarily from the free atoms and since these are electronegative with respect to the molecules on the surface, the electrons encounter a helping rather than an impeding force. Consequently, the photoelectric current will saturate at lower voltages for blue light than for red light.

The phenomena, shown in Figs. 2, 3 and 28 and which might be called supersaturation, may be explained by the shape of the elements of the tube. To understand better why more electrons should reach the anode at low voltages than at high, the history of the cell will be reviewed. The first step after evacuation of the bulb was the coating of the entire inner walls with potassium or sodium. Next, by applying a fine point flame momentarily on the face of the bulb, the metal was caused to recede and form an opening through which light could enter the cell. But without thorough heating, the glass could not be made perfectly non-conducting; and on account of the

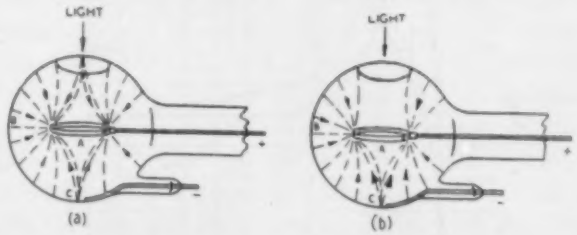

Fig. 40. Diagrams indicating the geometry of the electric fields within photoelectric cells having closed ring anodes (a) before treatment with dielectrics and (b) after such treatment.

low melting points of the alkali metals, prolonged heating of the "window" would have ruined the entire coating of the cell. Even if it were temporarily cleaned of all potassium, the high vapor pressure of the alkali metal produced by the heat of the flame would have deposited metal enough on the window to make it conducting afterward.

Now, the general shape of the electric field set up by an applied polarizing voltage within such a cell might be represented by the direction lines of diagram (a) Fig. 40. It is at once evident that the effect of increasing the polarizing voltage would be that of increasing the number of electrons reaching the anode up to complete saturation. This would result in a normal voltage-current relation. When, however, the conducting film on the glass window was destroyed by some active gas or dielectric, or by repeated heating afterward, the shape of the polarizing field changed to that illustrated by the directional lines of diagram (b). In effect the field between the window and the closed ring or anode was wiped out. From the point *C* the field spread radially toward the plane of ring *A*. For such a field there is a critical voltage at which the greatest number of emitted electrons arrive at a collector

located at some angle to the normal from an illuminated spot. These voltages have been computed for a similar case and published by Fry and Ives[46] and their computations experimentally verified by Ives, Olpin and Johnsrud[47] for central cathode photoelectric cells. The striking similarity of their curves and the voltage-current curves shown in Fig. 28, for illumination at back and side of cells treated with dielectrics, is illustrated in Fig. 41. It might also be that the greater energies of emission after treatment with the dielectric tended to augment this condition.

Apparently then, the closed ring used for the anode of these cells was responsible for these peculiarities in the voltage-current relation. Data

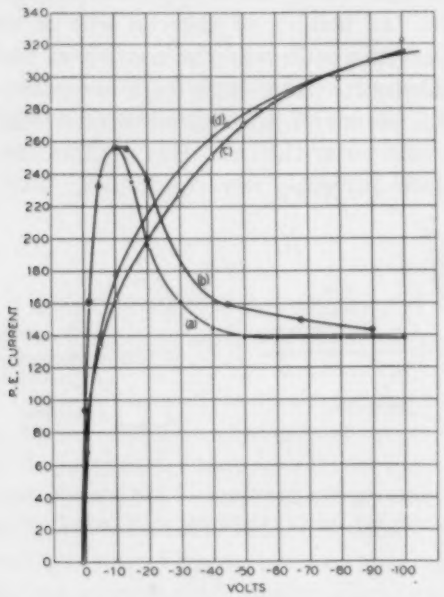

Fig. 41. Comparison of voltage-current curves obtained with photoelectric cells having closed ring electrodes as shown in Fig. 40(b) and voltage-current curves observed with anodes fixed at given angles to the normal to the cathode for cells having radial fields, as described by Ives, Olpin and Johnsrud.[47] a—Curve 4 of Fig. 28. Light incident at *C* (Fig. 40) b—Curve for a cell with a radial field when the collecting segment was located at 10° to the normal from the cathode. c—Curve 6 of Fig. 28. Light incident at B (Fig. 40). d—Curve for a cell with radial field when the collecting segment was located at 10° to the normal from the cathode.

obtained from cells having different shaped anodes, such as straight wires or grids, failed to show these peaks at low voltages. Finally a cell was made having a closed ring anode which could be rotated and set with its plane perpendicular to or parallel to the illuminated spot on the cell wall. Whenever, the plane of the ring was parallel to the back of the cell on which the light was falling, the peaks at low voltages appeared and whenever the ring was turned through 90° these maxima disappeared.

[46] T. C. Fry and H. E. Ives, Phys. Rev. **32,** 44 (1928).
[47] H. E. Ives, A. R. Olpin, A. L. Johnsrud, Phys. Rev. **32,** 57 (1928).

L. Considerations in the Realm of Photography Fluorescence and Light Absorption

While there is not space for more extensive discussions, it seems important to call attention to apparently analogous phenomena in the fields of photography, light absorption and fluorescence. It certainly seems more than a coincidence that photographic plates and photoelectric cells can be sensitized to red and infrared light by such strikingly similar methods. The presence of traces of sulphur in the gelatines obtained from some sources has been given by investigators at the Eastman Research Laboratories[48] as an explanation for their high sensitivity to light. Certainly these experiments, together with those wherein photographic plates are sensitized to red and infrared light by means of organic dyes, suggest a close relationship between photographic and photoelectric phenomena.

Saha[49] and others have already advanced theories in which fluorescence with change of wave-length is attributed to modulation of the exciting light. In general, however, his conclusions have not been enthusiastically received, many unexplainable observations standing in the way of such a theory. Certainly, however, it should not be dismissed without further consideration. Such results as Wood and Kinsey[50] reported wherein the *D* lines of sodium were excited by radiation in the region of 5100–5250A when the sodium vapor was mixed with low pressures of hydrogen, nitrogen or air, seem significant, indeed, since the wave-length region of the exciting radiation here coincides with that of the new photoelectric maximum in the spectral response curves for sodium cathodes treated with air, and the photoelectric threshold for pure sodium atoms coincides with the *D* lines.[51]

Many other closely analogous phenomena might be mentioned here; such, for instance, as the fact that the absorption lines of an absorbing medium are noticeably shifted to longer wave-lengths when the absorbing medium is dissolved in a dielectric.[52] But these are beyond the scope of this paper.

Acknowledgment

To Mr. G. R. Stilwell for invaluable contributions to the technique and art involved in the manufacture of the cells described above, to Dr. Herbert E. Ives for careful consideration of problems encountered in this investigation and for helpful suggestions, and to Dr. K. K. Darrow and Dr. Homer H. Lowry for constructive study of this manuscript, the author expresses his heartiest appreciation.

[48] A. P. H. Trivelli, Frank. Inst. J. **205,** 111 (1928).
[49] M. N. Saha, D. S. Kothari, G. R. Toshniwal, Nature **122,** 398 (1928).
[50] R. W. Wood and E. L. Kinsey, Phys. Rev. **31,** 5, 793 (1928).
[51] H.E. Ives and A. R. Olpin, Phys. Rev. **34,** 117 (1929).
[52] Aschkinass and Schaeffer, Ann. d. Physik **5,** 489 (1901).

THE INFRARED ABSORPTION OF SOME ORGANIC LIQUIDS UNDER HIGH RESOLUTION

PART II

By R. Bowling Barnes
John Hopkins University, Baltimore, Maryland

(Received June 9, 1930)

Abstract

The study of the C-H vibrations bands, which occur in organic liquids between 3.0μ and 4.0μ, has been continued and extended. A more powerful spectrometer, with which wave-lengths can be determined as accurately as $\pm 0.001\mu$, has been developed for this work. Values are given here for water-vapor, benzene and toluene.

IN A recent paper,[1] we gave an account of an attempt to obtain very accurate values for the C-H absorption bands of various organic liquids. In this discussion we stated the wave-lengths of benzene and eight of its derivatives with an estimated accuracy of $\pm 0.003\mu$. This present paper is intended primarily to outline the developments in the construction of the spectrometer, and the improvements which have been made in the technique and methods. These advances enable us to state wave-lengths now as close as $\pm 0.001\mu$.

By using an echelette grating rather than a rock-salt prism, the resolving power may be increased by a factor of 10 or more. For instance, in this region of the spectrum, a 10 cm prism has a resolving power of only about 170. So, even by using four-prism dispersion, one still has a resolving power somewhat less than 1000, neglecting any loss due to the finite width of the slits. On the other hand, in the grating spectrometer described in our last paper, the theoretical resolving power was over 10,000. In this region, this puts the theoretical limit of resolution for the two types of spectrometers at 30 A'' and 3 A'' respectively, the approximation to these values being determined by the width of the slits and the perfection of the optical systems being used.

In striving to approach these theoretical limits of resolution one uses very narrow slits. When this is done however, another factor becomes of considerable importance in determining the actual limit. In a paper at the April meeting of the American Physical Society[2] we called attention to the effects of various aberrations in this respect.

If one is not fortunate enough to have properly parabolized mirrors, one must resort to the use of spherical mirrors "off the optic axis." As long as the numerical apertures are small, and the slits are comparatively wide, the effects of the aberrations introduced are negligible. But, if we use apertures as large

[1] R. Bowling Barnes, Phys. Rev. **35**, 1524 (1930).
[2] R. Bowling Barnes and A. H. Pfund, Bulletin Amer. Phys. Soc. **5**, 2 (1930).

as $f \cdot 4$ the effects of coma become very pronounced, and the image of the first slit is broad and is accompanied by a diffuse wing. This entire image cannot go through a narrow second slit, and consequently, if the eye is placed behind S_2, or in the position of the thermocouple, it will receive light

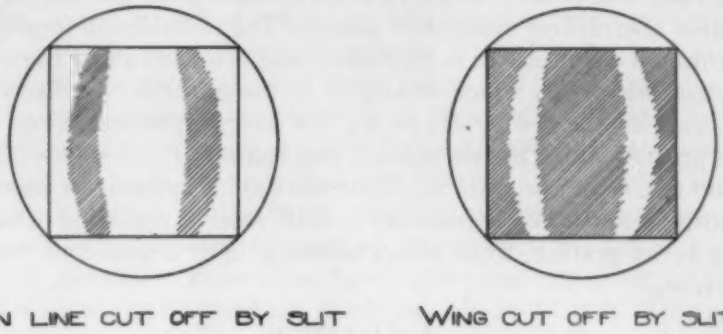

Fig. 1. Grating viewed through second slit of spectrometer when illuminated with monochromatic light. Spectral line is accompanied by a wing produced by the aberrations of the optical system.

from only a very small fraction of the grating, if the latter is illuminated with monochromatic light. Patterns such as those shown in Fig. 1 may be seen, the jaws of the slit having blocked off the light coming from some parts of the grating. However, if we use continuous radiation, such as that from a

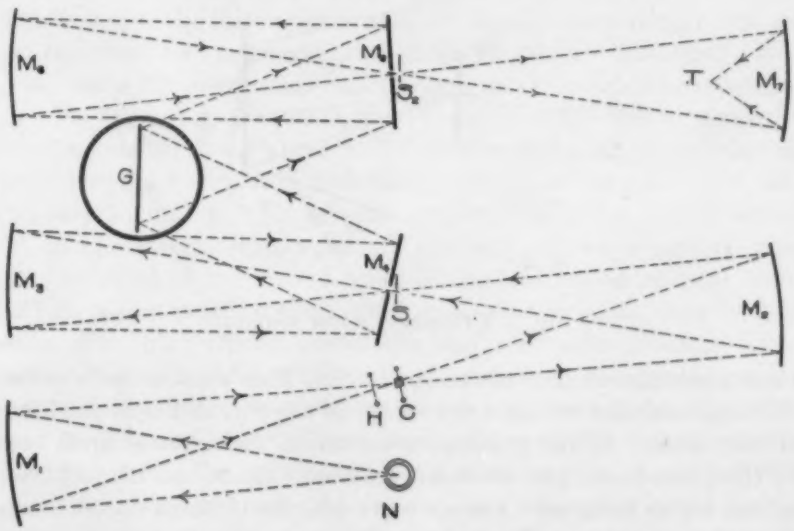

Fig. 2. Plan of spectrometer. Designed to minimize the effect of aberrations.

Nernst lamp, the spectrum falling upon S_2 will necessarily be very impure, and hence the resolving power will be correspondingly low. This diffuseness of the slit image is also a serious handicap in obtaining a very accurate calibration of the spectometer.

The apparatus which we are using at present is a grating spectrometer, the plan of which is given in Fig. 2. It makes use of about 3.5 inches of a 3600 line per inch echelette grating, which gives it a theoretical resolving power of over 12,000. By a method analogous to that described by Pfund,[3] we have been able to use $f \cdot 4$ spherical mirrors along the axis and so minimize all of these aberrations mentioned above. The radiation diverging from S_1 passes through a slot in M_4, is collimated and returned along the axis by M_3 to the plane mirror M_4 which directs it to the grating. Similarly, the diffracted beam is reflected by M_5 to M_6, the second spherical mirror, and this focusses upon S_2 which lies on the axis just behind M_5, an image of S_1 that is sharp and free from aberrations. With this optical system, we have satisfied the condition that the thermocouple shall receive radiation which comes from the entire grating, when monochromatic light is used and the slits are very narrow.

Calibration

A calibration more accurate than ± 5 A$''$, was obtained by observing the settings of the grating which would direct the various orders of the spectrum from a mercury lamp, on to the second slit. By interposing a plane mirror at 45° just behind S_2, the transmitted light could be reflected into a microscope

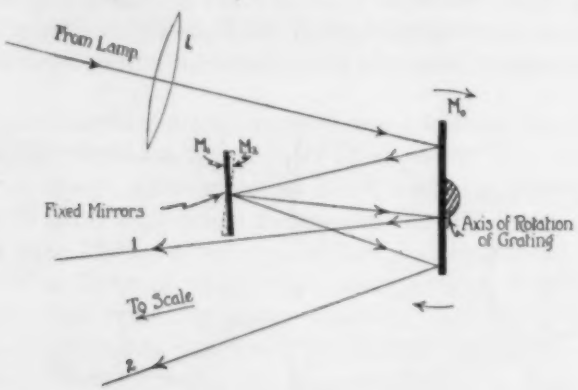

Fig. 3. Calibration mirror system.

which was a permanent part of the apparatus. This microscope was focussed upon S_2, the crosshairs set upon the center of the slit, and then the latter was opened very wide. As the grating was rotated, the spectral lines passed in turn by the cross-hairs, and an observer could thus tell accurately when the grating was set so as to send known wave-lengths through S_2. A second observer noted the grating positions by reading on a scale 3 m distant, the image of a lamp filament that had been twice reflected by a mirror which rotated rigidly with the grating. This was accomplished in the manner shown in Fig. 3. Light from an incandescent lamp after passing through a lens was reflected by M_0 to a fixed mirror M_1, which returned it to M_0. After a second

[3] A. H. Pfund, J.O.S.A. **14**, 377 (1927).

reflection by M_0 it was sent along path 1 to the scale upon which an image of the lamp filament was formed. This double reflection causes the beam of light to swing through an arc four (4) times that through which the grating is rotated. The linear displacement of the image of the filament thus becomes large. To avoid the necessity of having a very long scale, a second fixed mirror, M_2, was mounted as is shown. The angle between M_1 and M_2 was adjusted so that as the grating and M_0 were rotated image 2 came onto the scale just as image 1 was going off the opposite end. If the grating must be rotated through a large angle, a third mirror M_3 could be mounted in a similar manner causing a third image to follow image 2. A linear motion of the filament image of 1 mm at 3 m scale distance, represents a rotation of the grating of about 17 sec. of arc. If the beam of light is allowed to be reflected by M_0 three times, a displacement of 1mm would represent a rotation of only 8.5 seconds. If necessary, more than three reflections can easily be used, and also the image of the filament can safely be read to 0.1 mm. This gives us a method of handling with ease rotations of the order of 1 second of arc. In all of this work the image was moved in steps of 1 mm, this indicating a change in the wave-length falling upon the thermocouple slightly less than 10 A''. The calibration was carefully checked from time to time, and was always known closer than ± 5 A''.

Procedure

At best, the point by point method which is usually employed in making infrared measurements is a rather long and tedious process. Every step taken to improve the instruments used, in regard to sensitivity and resolving power, requires that more readings per μ be taken. Obviously, with very high resolution the problem of making such measurements becomes painfully taxing. However, we have so improved our methods that at present we can measure the absorption at over 500 different grating settings within an hour, whereas last year 50 readings constituted a full hour's work. The most fundamental step in making this possible resulted from the recent work of Dr. Pfund on controllable filters for the infrared. Since a grating superposes orders, the effect of the second order of the 1.5μ region and the third order of the 1.0μ region must be eliminated, or to say the least, must be taken into account. For this purpose, one of the MgO filters described by Dr. Pfund[4] is admirably suited. Also, a filter of a glass designed for use in solar observations was found, which was over 60 percent transparent at 3.5μ, and only 5 percent at 1.75μ and below. These filters, it is true, did not entirely eliminate the effect of the higher orders, but did succeed in reducing it sufficiently for our purposes. For instance, the one we used, though it had a transmission of only 5 percent at 1.75μ, due to the intense emission of the Nernst filament in that region transmitted enough higher order radiation to cause a contamination of the 3.5μ energy of 30 percent. It was shown separately, however, by using 100 percent 1.75μ energy, that in such small thicknesses the

[4] A. H. Pfund, Phys. Rev. July 15, 1930.

absorption of these higher orders was negligible. So, by using either of these filters, the desired results were obtained.

Further, it was found that by proper shielding the zero drift of the galvanometer could be held to a very small amount and so, instead of reading the zero between each spectrometer setting as is customary, we used the method employed in instruments which record the galvanometer deflections automatically. The zero was read before and after each series of measurements, and the results corrected for the sloping base line caused by the zero drift. Some slight discrepancies in the relative intensities of the various bands may be introduced, because of the fact that we must assume that this zero drift was linear with time. Such errors however will be small, for evidence indicates that this drift is linear. One observer changed the spectrometer setting in intervals of 10 A″, while the other read and recorded the respective galvanometer deflections. By plotting the results thus obtained we got directly a curve showing the energy transmitted (galvanometer deflections) for the various wave-lengths. The minima of these curves gave us the wave-lengths of the absorption bands.

It must be remembered that in using such a method the total energy transmitted at any wave-length is affected by many factors, namely: the emission of the source, the absorption of the atmosphere, the absorption of the empty cell, the absorption of the filter, and finally the absorption of the sample which is being studied. Separate experiments proved that the empty cell and the filter were not selective in their absorptions, but only reduced the values throughout the entire range by a constant factor. By making a series of measurements, with the absorption cell removed entirely, the combined results of the first two effects was obtained. In Fig. 4 (a) and (b) we have drawn two such curves. They are drawn from different base lines so they may be easily compared. Here we see some 65 or more weak bands, which are evidently due chiefly to the water vapor in the air. The trustworthiness and accuracy of the instrument and methods used, are shown by the manner in which the weak minima of these two curves check each other.

Results

Last year[5] readings were taken at intervals of 0.007μ on an instrument whose calibration was accurate to $\pm 0.0015\mu$ and the wave-lengths then stated were thought to be accurate to $\pm 0.003\mu$. This year readings were taken every 0.001μ, using an instrument calibrated to $\pm 0.0005\mu$, and therefore we believe that we can now state our wave-lengths to $\pm 0.001\mu$.

The absorption of benzene has been measured some 30 odd times this year, under many different conditions. We have used various cells, slit widths and thicknesses of solution. Fig. 4 (c) shows a sample curve for benzene, made with slits 0.1 mm wide (11 A″ 'slit width') and a thickness of 0.05 mm. In comparing this with a curve from last year, we find the same three strong bands located this year at 3.236μ, 3.257μ and 3.296μ. A careful study was made of the weaker indications of absorption lying on each side of the strong

[5] R. Bowling Barnes, reference 1.

group of bands. It was noticed in the work last year, that while the 3 strong bands always checked in the different curves, these weaker ones rarely ever agreed exactly. By comparing the benzene curve with those for the atmosphere, we can see the reason for this. Since we have the absorption of water vapor superposed upon that of benzene, we must expect the locations of the benzene bands to be somewhat affected by the presence of the water bands. This effect will be rather slight in the case of very strong benzene bands.

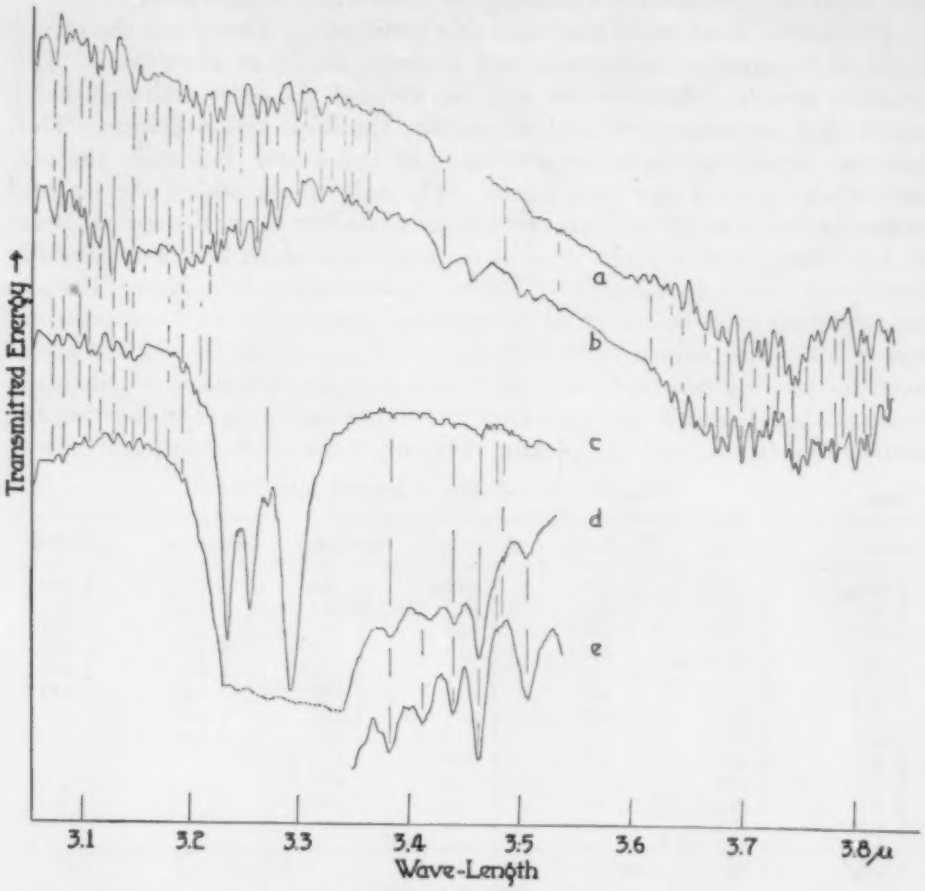

Fig. 4. Absorption curves. (a) and (b) atmospheric absorption. (c) benzene, $t=0.05$ mm. (d) benzene, $t=0.1$ mm. (e) benzene, $t=0.5$ mm.

However, in regions where the bands of the two compounds are of approximately the same intensity, a change in the partial pressure of the water vapor present in the room, may produce very noticeable changes in the absorption bands. In the previous work, since readings were taken only every 0.007μ, we always had the combined effect of benzene and water vapor, for neighboring bands could not be separated.

In order to identify further the weak benzene bands, we made measurements on benzene in 5 different thicknesses. Fig. 4 (c), (d) and (e) show a

comparison of 3 such curves, and it is easily seen that on the short wave-length side of the 3 strong bands, benzene has no absorption. However, toward longer wave-lengths several bands show decided changes as the thickness is increased. The bands which show these changes, do not correspond to any of the air bands, and thus we can say definitely just which of the weaker minima indicate benzene bands, and which, water vapor. With this process we finally arrived at the results given for benzene in Table I. Here we have also listed for reference the wave-lengths of the water-vapor bands.

Obviously, if we could eliminate this atmospheric absorption the results could be interpreted more easily and no doubt would be more exact. This could be done by taking one set of values through the compound and then a set through an empty cell, and subtracting the respective ordinates. This, however, would again require zero readings and would thus make the procedure very much longer and harder. The only course which offers a convenient solution to the problem seems to be to enclose the entire spectrometer in a vacuum, or to say the least, in an enclosure which has been carefully freed from water-vapor and CO_2. The entire instrument from Nernst lamp to thermocouple must be in such an atmosphere. Czerny[6] enclosed his spectrometer in a tin case, which contained trays of P_2O_5 and KOH. Plans are at hand for putting this instrument into just such an enclosure. Until this is accomplished however, we must continue to use our method of locating the atmospheric bands, and then picking them out of the other absorption curves.

TABLE I. *Wave-lengths of observed bands.*

Air	Air (con)	Air (con)	Air (con)	Air (con)	Benzene	Toluene
3.054μ	3.193μ	3.331μ	3.633μ	3.748μ	3.236μ	3.240μ
3.073	3.202	3.342	3.642	3.754	3.257	3.263
3.083	3.210	3.348	3.654	3.762	3.296	3.301
3.093	3.217	3.364	3.659	3.768	3.383	3.386
3.098	3.224	3.379	3.664	3.781	3.412	3.426
3.106	3.230	3.397	3.675	3.787	3.440	3.489
3.115	3.241	3.430	3.685	3.801	3.463	
3.127	3.246	3.455	3.697	3.807	3.508	
3.139	3.267	3.485	3.709	3.813		
3.146	3.270	3.498	3.715	3.825		
3.153	3.281	3.512	3.721	3.830		
3.158	3.305	3.603	3.730			
3.178	3.312	3.614	3.736			
3.180	3.321	3.626	3.743			

In this manner, the bands of toluene were also located. Curve (d) of Fig. 5 shows this absorption clearly. The air bands are easily identified. The remaining bands, whose wave-lengths are given in Table I, agree nicely with those stated in the previous paper. Again we note only a slight shift toward longer wave-lengths in the locations of the three strong bands of the benzene C-H's. These shifts are 0.004μ, 0.006μ and 0.005μ respectively. The minimum at 3.307μ shows up in the other curves for toluene to be due to air. The general intensity distribution throughout this entire region is the same as that shown previously.

[6] M. Czerny, Zeits. f. Physik **34**, 227 (1925).

Curve (b) of Fig. 5 shows an attempt to measure the absorption of cyclohexane at a thickness of 0.05 mm. As is shown in the curve the intensity of the absorption is extremely great. From 3.35μ to 3.46μ this thickness is opaque, the only energy transmitted being the 30 per cent contamination due to 1.75μ. The results were the same, using a film formed by putting one drop of the liquid between two cover glasses, which were then pressed together. Le Compte[7] gives a curve for it, but does not mention the thickness. He

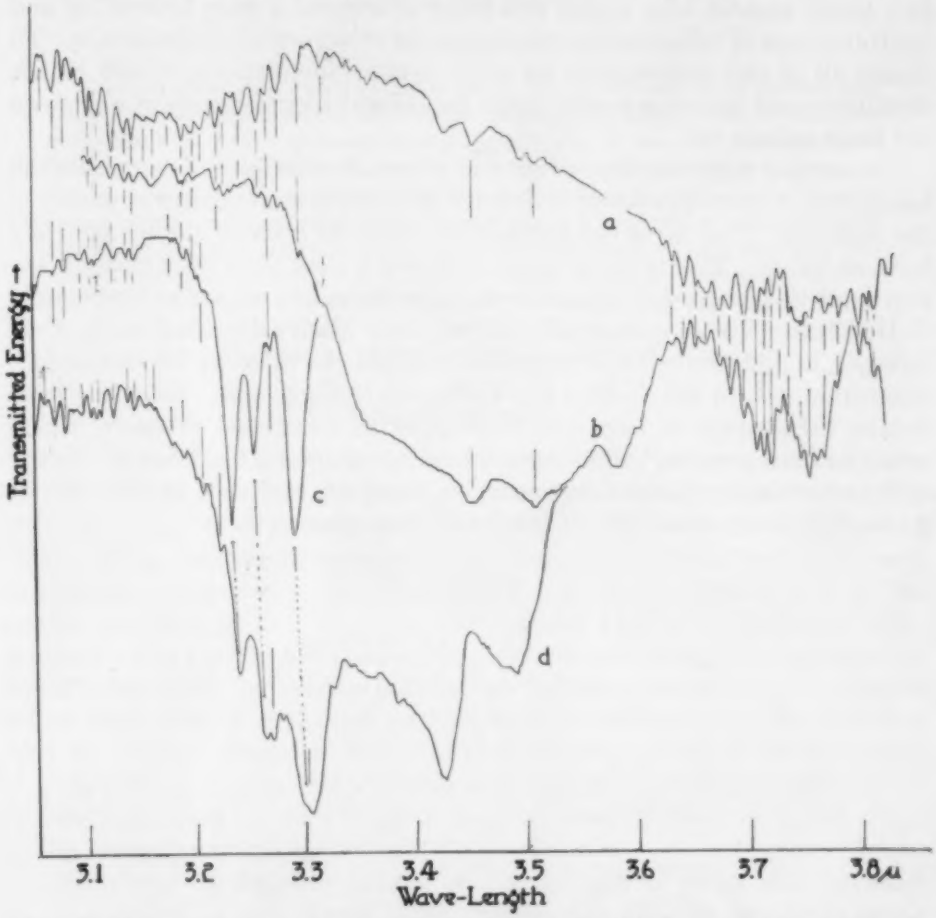

Fig. 5. Absorption curves. (a) atmospheric absorption. (b) cyclohexane, $t=0.05$ mm. (c) benzene, $t=0.05$ mm. (d) toluene, $t=0.05$ mm.

finds for it bands at 3.16μ, 3.26μ, 3.60μ and 3.90μ. We find the strong band somewhere between 3.35μ and 3.46μ. It is interesting to note that the three benzene bands are entirely absent. In this molecule no C atom has only one H atom attached as in benzene, but each has two. Apparently, the H–C–H vibrations are quite different from the C–H vibrations. Cyclohexene, also shows an extremely strong absorption in this region.

[7] J. Le Compte, Le Spectra Infrarouge., p. 218.

Conclusions

Specific heat calculations[8] and Raman photographs[9] each show definitely that the C–H linkage must vibrate with a frequency very close to 3.5μ. In most organic liquids then, we must expect to find very complex absorption bands in this region. Remembering that water also has a strong band close to 3.0μ, we see that almost every liquid will have pronounced absorption between 3.0μ and 4.0μ. The resulting fact, that so many liquids have complex bands around 3.5μ, makes this spectral interval a most interesting and fruitful source of information concerning the structure of the molecules. To obtain all of this information we must develop instruments of still higher sensitivity and resolving power. With the present spectrometers however, we can learn quite a bit.

In our first paper we showed several progressive shifts and changes in the bands, which were apparently connected with the symmetry and structure of the molecule. The curve on cyclohexane shows no trace of the three strong benzene bands. This is the first curve in which they have been entirely absent, and this is the first molecule we have examined which had no simple C–H bonds. Toluene and each of the other derivatives had some C–H linkages, in addition to their respective radicals. In these we found separate absorption due to the C–H, CH_3, C_2H_5 and C_4H_9 groups. Here in cyclohexane the absence of bands for C–H gives us additional evidence, which seems to show a mutual effect between two neighboring C–H bonds. Every shift and intensity change tells something about the molecule, and it is hoped that a theoretical discussion of these will soon appear.

[8] D. H. Andrews, Chem. Reviews **5**, 4 (1928).

[9] A. Dadieu and K. W. F. Kohlrausch, Berichte der Deutschen Chemischen Gesellschaft **2**, 251 (1930).

THE EFFECT OF HIGH PRESSURE ON THE NEAR INFRARED ABSORPTION SPECTRUM OF CERTAIN LIQUIDS*

By J. R. Collins
Cornell University

(Received June 5, 1930)

Abstract

Certain absorption bands of liquid water, methyl alcohol, amyl alcohol, and toluene were studied when the liquids were subjected to high pressures. In the case of the first three liquids, pressures up to 5000 kg/cm² were used, and pressures up to 8000 kg/cm² were applied to the toluene. No change was found either in the spectral position or in the intensity of the bands studied. The results are of interest since a change in the polymerization of polar liquids is supposed to take place with increase of pressure. The absorption bands are characteristic of the molecules and hence a change in the position and intensity should accompany the change in polymerization. As no such change was observed, it is concluded that there is no change in polymerization in the pressure range studied. The pressure necessary to solidify toluene at 20°C. was found to lie between 8100 kg/cm² and 8300 kg/cm².

Introduction

THE anomalous properties of liquid water have been explained by the hypothesis that it is composed of two or more kinds of molecules. The simplest assumption is that water consists of the molecules $(H_2O)_2$ and $(H_2O)_3$ whose relative proportions depend on the physical conditions such as temperature, pressure, etc. Sutherland[1] has made calculations as to the relative amounts of the two constituents under various conditions of temperature. The author[2] has studied the near infrared absorption spectrum of liquid water from its freezing point to its boiling point and found changes which seem readily explained on Sutherland's assumptions. Redlich[3] has used the author's results to calculate the relative amounts of the two kinds of molecules at various temperatures and finds fair agreement with similar calculations based on the change of magnetic susceptibility of liquid water as the temperature changes.

Sutherland explains the change in the viscosity of water with pressure by assuming that the degree of polymerization changes as the pressure changes. He estimates that a pressure of a few thousand atmospheres should convert all of the triple molecule into the simpler one. Hence, if one may interpret the change in the absorption spectrum as due to a change in the degree of polymerization, the absorption spectrum should show decided

* This investigation was supported by funds granted by the Heckscher Foundation for the Advancement of Research at Cornell University.

[1] Sutherland, Phil. Mag. 50, 460 (1900).

[2] Collins, Phys. Rev. 26, 771 (1925).

[3] Redlich, Proc. Akad. Wissensch. Wien 53, 874 (1929).

changes as the pressure on the liquid is increased to several thousand atmospheres. Accordingly, the present experiments were undertaken to find if such changes do occur. Although the principal interest is in the case of water, the experiments were planned to include the study of toluene as a typical nonpolymerizing liquid and as many other liquids that do show polymerization as time would permit. The experiments were performed in the Jefferson Physical Laboratory at Harvard University, and the author is under deep obligation to Professor P. W. Bridgman who kindly designed the pressure chamber which provided plane parallel glass windows through which the radiation could be passed through the specimen.

Apparatus and Experimental Procedure

The method of measurement was to pass a beam of radiation from an incandescent source through the chamber containing the liquid, to disperse the radiation by means of a spectrometer system and then to measure the intensity of the radiation at the exit slit of the spectrometer by means of a thermopile and galvanometer. On account of the impossibility of moving the absorption chamber, an indirect method of obtaining the fractional absorption of the liquid at the various pressures was used. Figure 1 illustrates

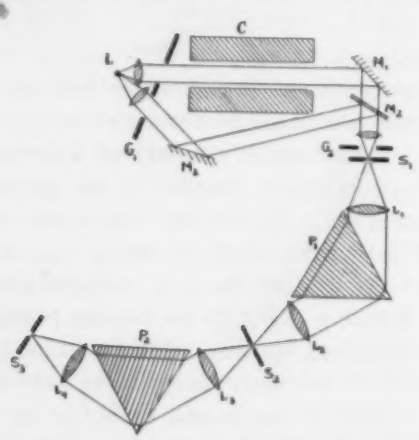

Fig. 1. Diagrammatic arrangement of apparatus.

diagrammatically the arrangement of apparatus. L is the filament of a street series incandescent lamp, from which two beams of parallel radiation are obtained. One of these beams passes through the absorption chamber C and is then focussed on the entrance slit of the spectrometer system. The other beam, after reflection from suitably placed mirrors, is also focussed on the slit of the spectrometer. By means of the shutter G_1 either of these beams may be blocked off and the intensity of the other measured by the thermopile. The beam which does not pass through the specimen serves as a standard of comparison, so that the absorption at any one pressure can be calculated if that at any other pressure is known. The absorption at atmospheric pressure was determined by a separate experiment.

The spectrometer used was a double Van Cittert spectrometer in which the slit S_2 is moved across the spectrum focussed in its plane. This movement allows any desired spectral position to be transmitted through the system. The double spectrometer is necessary to obtain the necessary purity of spectrum. The spectrometer was calibrated by means of emission lines from a mercury arc, and by means of the known positions of absorption bands of several liquids. Since the openings at the ends of the absorption chamber were only one quarter of an inch in diameter, the amount of radiation transmitted was very small. It was accordingly necessary to use a thermo-relay to magnify the galvanometer deflections. It was found that a magnification of fifty times was sufficient, and the Moll thermo-relay used was very steady at this magnification. On account of mechanical and electrical disturbances which were present in the daytime, all measurements were made at night.

Figure 2 shows the details of the mounting of the glass windows in the ends of the absorption cell. *A* is the window and was a cylinder of glass seven eighths of an inch in diameter and one and a quarter inches thick. A doubled piece of rubber tubing, *E*, was tightened around this window by

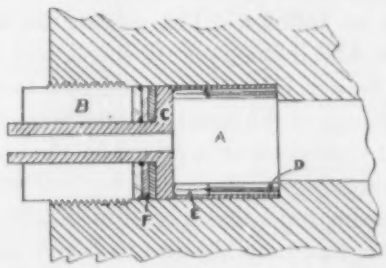

Fig. 2. Detail of mounting the windows in the pressure chamber.

means of the tube, *D*, and made a liquid tight seal between the window and holder *C*. This holder was forced in against the shoulder of the cell by means of the screw plug *B*. Packing at *F* was used to make the outside edge of the holder tight. When pressure was applied to the inside of the chamber, the window *A* was forced to a seat against the bottom of the holder. A thin washer of tin was placed between the window and bottom of the holder.

With plate glass as the material of the windows, pressures up to 10000 kg/cm² could be maintained for long periods of time. Unfortunately, however, plate glass has a strong absorption band in the spectral region being studied, and with the two windows only about one percent of the incident radiation was transmitted. Although several kinds of transparent glasses were tried, none were found which would allow pressures greater than about 5000 kg/cm² to be maintained for any length of time. Another arrangement which was used in the last part of the experiments was that described by Poulter,[4] which allowed thin windows of plate glass to be used. These windows transmitted sufficient radiation to be measured. The holder, *C*, was

[4] Poulter, Phys. Rev. **35**, 297 (1930).

made solid and the inner end ground and polished to a plane surface. Then windows five sixteenths of an inch were cemented on to the end of the holder by a very thin layer of Canada balsam.

The original plan was to have the specimen placed in an absorption cell inside the pressure chamber so that the liquid transmitting the pressure would not contaminate the specimen. However, every liquid suitable for the transmission of pressure has strong absorption bands in the spectral region being studied, and so in the final arrangement the specimen filled the whole pressure chamber and as much of the pressure chamber above the absorption chamber as was possible without affecting the manganin coil whose resistance was measured as an indication of the pressure. Kerosene was used to transmit the pressure to the specimen liquid. A capillary tube connected the absorption chamber with the pressure producing apparatus and diffusion of the kerosene through this tube was apparently slow enough to prevent harmful contamination of the specimen. The test of this was to measure the absorption of the specimen after the pressure had been on for some time and then reduced to atmospheric pressure again. No change was noticed which could be ascribed to contamination of the specimen.

The procedure was as follows. The apparatus was assembled and a small pressure applied to find if the packing was liquid tight. Then by means of the shutters G_1 and G_2 the intensity of the two beams of radiation were obtained for various settings of the spectrometer system through the spectral region desired. Then the pressure was raised to about 1000 kg/cm^2 and the process repeated. Pressures higher than 5000 kg/cm^2 were not obtained under circumstances which permitted measurements of the absorption except in the case of toluene. This was possibly due to faulty assembly, although the same care was taken in all cases. This pressure is well in excess of that estimated by Sutherland for the complete conversion of the triple molecule of water into the simpler form.

A very interesting method of obtaining the pressure necessary for the solidification of toluene at 20° C. was to observe the interior of the pressure chamber by means of a reading telescope. When the pressure was slowly increased, fine needle like crystals would begin to form, and if the pressure was maintained, the whole of the liquid would become solid. On slowly reducing the pressure, the crystals would begin to melt. As the pressure was successively raised and lowered above and below the solidification point, the pressures at which the solidification and the melting took place came nearer to each other and after a great many trials, the final values obtained were: Freezing pressure 8300 kg/cm,^{2} melting pressure 8100 kg/cm.^{2}

Results and Conclusions

The results obtained for five absorption bands of water indicate that there is no change in the spectral position or intensity of the bands. The absorption bands of water which are studied are supposed to be the overtone bands of fundamental bands farther in the infrared. It was expected that these might show even greater changes than the fundamental bands would

show. Also they are not so intense as the fundamental bands so that reasonable thicknesses of the liquid could be used. When too thin layers are used, the thickness is increased at the higher pressures on account of the packing becoming compressed and thus allowing the windows to move outward. Only a few of the curves which were obtained are shown as they are all similar in that no change in spectral position is shown and only slight changes in intensity. These changes in intensity are ascribed to the increase in length mentioned above. Account was taken of the increase in density of the liquid as the pressure was increased.

A study of the absorption of toluene was made as an example of a non-polarizing liquid and thus, presumably, of a liquid whose molecules do not

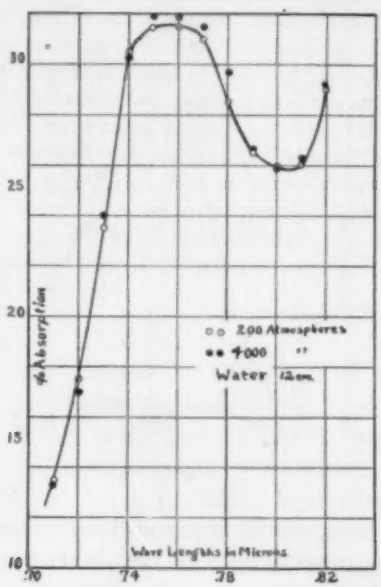

Fig. 3.

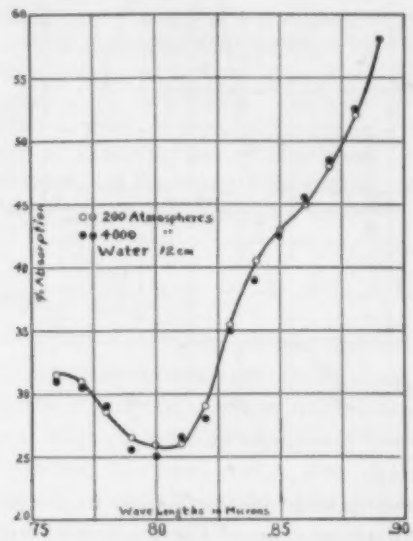

Fig. 4.

associate to produce complicated molecules. The two alcohols were studied as other examples of polymerized molecules.

Results are plotted for the lowest and highest pressures used as the results for the intermediate pressures lie intermediate between them. In the case of water several runs were taken at each absorption band and the results plotted are from one of the individual runs.

If we are to assume that changes in the absorption bands of a liquid should occur when the degree of polymerization changes, the results of these experiments indicate that no such change in polymerization occur in the pressure range used. It is difficult to imagine a process whereby an increase in pressure would cause a breaking up of the complicated molecules. Bridgman,[5] in discussing the effect of pressure on the thermal expansion of water, concluded that his results do not indicate any breaking up of the complicated

[5] Bridgman, Proc. Am. Acad. Arts, and Sci. **47**, 544 (1912).

molecules. From other considerations, he concludes that the effect of pressure should be one of increasing the complexity of the molecules.

It is interesting in this connection to note that Stewart[6] denies the existence of small molecular groups such as are postulated by Sutherland and others. His results on the x-ray diffraction halos produced by liquid water lead him to postulate the presence of very large groups of molecules with a regular arrangement, these groups having only a temporary existence to be succeeded by other similar groups. The results of the present experiments

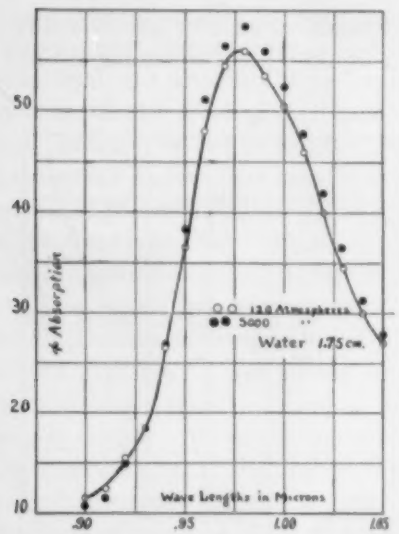

Fig. 5.

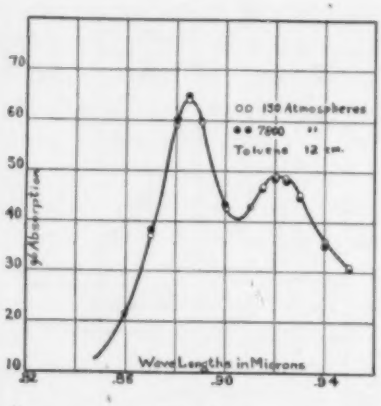

Fig. 6.

do not seem incompatible with this view of Stewart, as it seems likely that the absorption of the molecules within these groups would be different than that of the molecules not in the groups, and that there may be some effect of temperature on the number of molecules in the groups or on the time of existence of a given group.

The author wishes to make grateful acknowledgment of his indebtedness to Professor Bridgman for placing the pressure apparatus at his disposal. The author also feels under obligation to Mr. Mann, chief mechanician at Jefferson Laboratory, who helped by his skill and advice.

[6] Stewart, Proc. Am. Phys. Soc. April, 1930.

ADSORPTION OF METHYL ALCOHOL FILMS ON ROCK-SALT

By Shirleigh Silverman
Johns Hopkins University

(Received June 9, 1930)

Abstract

The optical method of Rayleigh and Drude as recently modified by Frazer and Herzfeld has been applied to the study of methyl alcohol films on rock-salt. The isothermal adsorption has been studied at pressures ranging from 10^{-5} mm to 11 cm mercury. The results indicate that a unimolecular layer is formed at a pressure between 10^{-5} and 10^{-4} mm of mercury, with no further adsorption until the region of 2–3 cm, when a second layer begins to form, with completion at 9–10 cm. The thickness of these layers is calculated to be in the neighborhood of 4.5–5.0A. The effect of thorough outgassing has been observed and the results have been interpreted to indicate that with decrease in temperature either an underlying unimolecular layer of water vapor is formed, or that there is a true increase in the natural ellipticity of the surface. In addition, it is possible to calculate the isothermal heat of adsorption from the experimental data.

Introduction

IF A beam of light be allowed to fall upon a plane surface of a transparent medium at the polarizing angle, the reflected beam is not found to be completely plane polarized, but is always elliptically polarized. Drude[1] has shown that the ellipticity of the reflected beam may be explained by assuming that there is not a perfectly sharp boundary between the two media, but that there is present a transition layer whose properties vary from the rare to the dense medium. This sheet whose index of refraction gradually changes from the value of 1 (assuming the 1st medium to be air or vacuum) to n, the refractive index of the 2nd substance, is known as the transition layer. Drude has worked out the equation which yields the relation between the observed ellipticity and the thickness of the transition layer; where we define as the ellipticity the ratio of the amplitudes of the minor and major axes of the ellipse of polarization.

The result is as follows:

$$\rho = \frac{\pi}{\lambda} \frac{(\epsilon_1 + \epsilon_2)^{1/2}}{\epsilon_1 - \epsilon_2} \int \frac{(\epsilon - \epsilon_1)(\epsilon - \epsilon_2)}{\epsilon} dz \qquad (1)$$

where ρ is the ellipticity, ϵ_1, ϵ and ϵ_2 are the dielectric constants of the first, the transition, and the second media respectively, λ the wave-length of the incident light, and z the position in the transition layer.

It is possible to determine a lower limit for the value of the thickness of the layer, L, which will not deviate very greatly from its true value. For a

[1] Drude, Theory of Optics, p. 287, Longmans (1901).

given value of ρ it is evident that L will attain its smallest value when ϵ is assumed to be a constant whose value is determined by making the factor $(\epsilon-\epsilon_1)(\epsilon-\epsilon_2)/\epsilon$ a maximum. This condition will be fulfilled when $\epsilon=(\epsilon_1\epsilon_2)^{1/2}$. Setting the refractive index equal to the square root of the dielectric constant, the expression for the lower limit of L becomes:

$$\frac{L_{min}}{\lambda} = \frac{\rho}{\pi(1+n^2)^{1/2}} \frac{n+1}{n-1} \tag{2}$$

where n is the refractive index of medium 2 with respect to medium 1.

Work by Langmuir, and later by Eucken, has formed the background for the theory that adsorption takes place in uniform monomolecular layers, and that each layer is completed before the formation of a subsequent one. Many other workers have substantiated this theory. However, many experimenters have worked with glass surfaces, with the resultant difficulty that it is very hard to describe the exact condition of the surface; to say nothing of the elaborate set-up required for the volumetric measurements on such large surfaces. Now, an adsorbed film fulfills the condition of Drude's transition layer. So, by taking a small cleavage surface of a crystal (two or three millimeters square was found to be quite large enough) which reflects nearly as well as plate glass, it is possible to calculate directly the thickness of the adsorbed layer by observing the changes in the ellipticity of the reflected light. The materials selected for this experiment were rock-salt for the transparent medium, because of the relative ease with which a perfectly clean surface may be prepared; and methyl alcohol for the vapor, because of the insolubility of rock-salt.

The equations of Drude require that the amplitude of the incident light in the plane of incidence be equal to the amplitude in the direction perpendicular to the plane of incidence. In early work on the measurement of thin films by Drude[1] and Rayleigh[2] the incident light is polarized at an angle of 45° at the plane of incidence. The ellipticity was measured by means of a Babinet compensator. Other investigators; Ives and Johnsrud[3] and Ellerbroeck,[4] have measured films; but in no case with an accuracy greater than several Angstom units. The method has been considerably improved in this laboratory by Herzfeld and Frazer,[5] and an accuracy of 3/10 to 4/10A has been attained. The essential improvements are: (1) the incident light is unpolarized, giving greater intensity while fulfilling the conditions set by the theory. (2) the ellipticity is measured photometrically with an accuracy unobtainable with a compensator. The present apparatus is very similar to that used by the above mentioned authors, with a few added refinements, particularly in the photometric arrangement.

The apparatus is shown diagrammatically in Fig. 1. The source of light wasan Ediswan 500 C. P. Pointolite which gives a very intense beam that is

[1] Rayleigh, Phil. Mag. [6] **23**, 431 (1903).
[3] Ives and Johnsrud, Journal of the Optical Soc. **15**, 374 (1927).
[4] Ellerbroeck, Arch. Neerland Sci. **111**, A10, 42–90 (1927).
[5] Frazer, Phys. Rev. **33**, 99 (1929).

quite uniform. After passing through a pin hole S_1, the image of the hot tungsten plate was brought to a focus on a second pin hole S_2 and the beam made parallel by lens L_3. A piece of clean plate glass M_1 was placed at a very slight angle to the beam, the transmitted light being allowed to fall upon the crystal and the reflected beam being used as the comparison beam in the photometer. The transmitted beam was reflected from the crystal R at the polarizing angle, passed through the analyzing nickel and brought to focus upon a piece of lightly ground glass G_1. This serves to produce a very uniform field in the photometer. The beam is then made parallel by a lens L_5, is passed by the edge of the mirror M_3 through the photometer P and the filter A, to the eye. The comparison beam was reflected successively from the mirrors M_1 and M_2, brought to focus upon a bit of ground glass G_2 which formed a pin hole S_3; behind this was placed the photometric wedge W. The beam is again made parallel, and is reflected from the photometer mirror M_3 through the filter A to the eye.

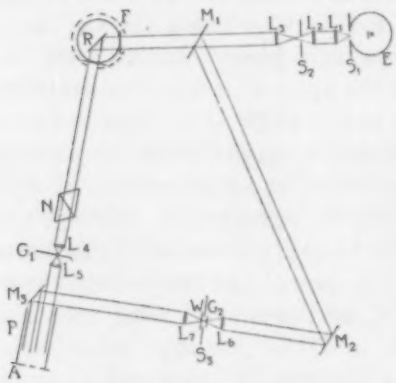

Fig. 1. Diagram of apparatus.

The photometer was of the Pfund split-field type, which consists of a mirror of a very sharp edge, set at an angle of 45° to the incident beams. One ray passes by the edge of the mirror and the other is reflected by it. The wedge was selected to give a linear transmission curve between ten percent and sixty percent; and was neutral as far as could be determined spectrophotometrically. In addition, screens were used which were calibrated against the wedge, and checked upon the same spectrophotometer. Inasmuch as the wave-length enters Drude's formula it is necessary to use a color filter. For this purpose, an aniline solution was found to be preferable to a monochromator since the intensity of the transmitted light is much greater. Such a solution was prepared by Professor Pfund, and the spectral centroid (5550A) calculated to an accuracy of about one percent.

The vacuum system itself merits a brief description. To prevent, as far as possible, contamination by stop-cock grease and occluded water vapor, a tube of activated cocoanut charcoal was placed between the crystal container and the rest of the system. The charcoal was previously outgassed by repeated heating to a dull red heat until no further gas was driven off. To make

certain that there was no backing-up on the far side of the charcoal plug, and auxiliary tube was connected to the container after the end of the main experiment. Pressure readings were found to be the same on both sides of the charcoal. The alcohol is kept in a trap and the vapor admitted as desired through a small stop-cock which was kept on the far side of the charcoal. The low pressures were read on a McLeod gauge. This was believed to be reliable as the pressure difference in the gauge at the highest pressures read was only 1.5 centimeters of mercury which is considerably below condensation pressure. As for occlusion of gases in the capillaries of the gauge, it was found that repeated pressure readings were quite consistent, so that it was not likely that our readings were affected. Higher pressures were read on the manometer.

Experimental Procedure

The experimental procedure was as follows: a piece of rock-salt which was free of cloudiness was ground and polished along one edge at an angle of about 20° to the nearest cleavage plane. It was then cracked along the nearest cleavage direction and placed immediately in the container at the polarizing angle; and the apparatus was evacuated immediately. The polishing of the back plane at this angle of 20° removed entirely any reflection from the rear surface which would have vitiated our readings. The bottle containing the crystal was then heated and pumped out at a fairly good vacuum, 10^{-5} millimeters of mercury, for some hours. Methyl alcohol was admitted and the pressure noted; the nicol prism was set for minimum and maximum transmission, and the square root of the ratio of the readings gave the value of ρ. The temperature was measured and kept constant to within 5°C. The pressure was varied, and the readings taken again. This was repeated until the whole range between 10^{-5} mm and 11 cm had been covered. The temperature was then raised to the desired value, and the set of readings repeated. The alcohol was supplied by the Chemistry Department; no traces of water vapor or of any volatile organic substances were listed among the impurities.

Certain precautions were found to be quite necessary; (1) It is exceedingly important that no water vapor be present to be adsorbed on the surface; (2) No stop-cock grease or metal should be used in the set up as they might contaminate the surface; (3) The windows of the outfit must be free of double refraction; (4) The pressure in the gauge has to be corrected to give the pressure in the container as there is a temperature difference. As for the first precaution, it is impossible to state at present whether or not all traces of water vapor can be removed, even by continued heating at temperatures around 325°C. This will be discussed more fully at the end of the article. The second contamination was avoided more readily. The crystal was imbedded in a bead of molten silver chloride at the end of a glass rod, and the upper end of the rod was ground nicely to fit into a tube; no lubricant was used. This arrangement permitted very easy adjustment of the angle of reflection, and after the crystal was set at the polarizing angle, the tube was

sealed off. The windows were of Pyrex plate glass, which were very carefully annealed and tested between crossed nicols after being sealed to the container. To further test for double refraction a specimen was taken and its ellipticity determined in air and in the apparatus. The two values were identical. Knudsen's equation for the relative pressures on the two sides of a porous plug at absolute temperatures T_1 and T_2 respectively, is:

$$\frac{p_1}{p_2} = \frac{T_1^{1/2}}{T_2^{1/2}}. \tag{3}$$

This equation fits our condition fairly closely for low pressures, and the correction was applied to all our low pressure readings; at high pressures the temperature correction is small enough to be neglected.

It was found possible to read the photometer to an accuracy of two percent. Accordingly, a group of eight or nine settings was taken for each reading, so that the probable error was quite close to one percent. Now,

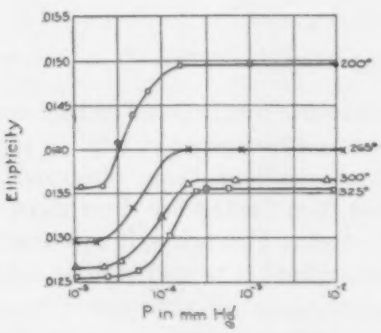

Fig. 2. Adsorption isotherms.

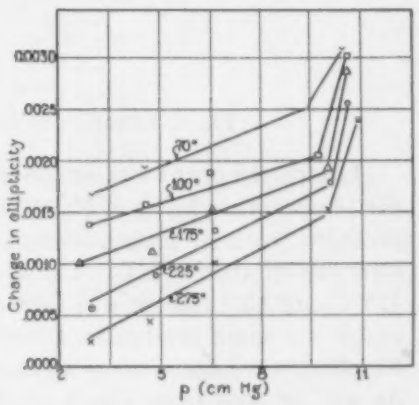

Fig. 3. Adsorption isotherms.

for $\lambda = 5550$A, a value of $\rho = 0.01$ means a layer about 45A thick. The values of ρ range from 0.0125 to 0.0170, so that the absolute error was about 0.5A. This is the same percentage error, but a slightly larger absolute error than is claimed by Frazer.[5] In all cases the adsorption is found to be completely reversible, and an adsorbed layer can be removed at will, returning the surface to its original condition.

Experimental Results

At 325°C and 10^{-5} mm pressure the ellipticity had a value of 0.01265. The value remained unchanged at twice this pressure and then increased to a value of 0.01365 at 2×10^{-4} mm from this pressure up to the neighborhood of 2 cm there was no further change in the ellipticity. From this point, the value increased linearly until 9.5–10 centimeters was reached, after which there was an abrupt increase in the ellipticity. The isothermal corresponding to 300°C showed a very similar curve, parallel and higher than the one at 325°C. At 10^{-5} mm the value was 0.0127, and above 10^{-4} mm the value was

0.0137. The same flat region extending to two or three centimeters was noticed, and the following portion proceeded as in the first case. The curves were repeated for intervals down to 75°C. In all cases the adsorption at lower pressures occured roughly between 10^{-5} mm and 10^{-4} mm, and in all cases there was no further change until the neighborhood of two to three centime ters had been reached. Further, the ellipticity following two centimeters proceeded regularly until ten centimeters was reached. These curves are shown in Figs. 2 and 3.

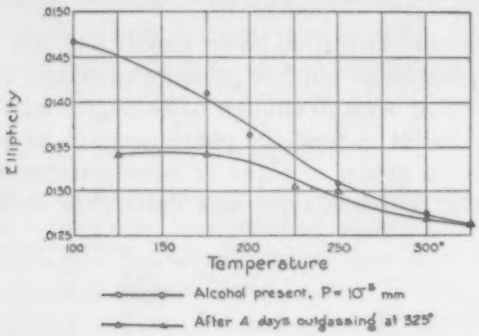

Fig. 4. Ellipticity as function of temperature. ($p = 10^{-5}$mm)

Lastly, the outfit was outgassed and the pressure was lowered to 10^{-5} mm, the temperature being 325°C. The pressure was kept constant and the temperature lowered progressively to 70°C, with readings being observed at intervals of about 50°C. The apparatus was then heated for three days at 325°C and 10^{-5} mm; it was then cooled over-night. Following, it was heated under the same conditions continuously throughout a period of four days. Readings were again taken at various temperatures as the cooling progressed. As will be seen from Fig. 4 at 325 degrees, the two curves coincide; their divergence is noticeable at 250°C, while at 100°C the increase in ellipticity for the clean surface in air is about 0.0008, and the corresponding increase for the surface in the presence of methyl alcohol is 0.00205.

Interpretation and Discussion

The results of the preceeding section are summarized in the following table:

Temp.	$\Delta\rho_1$	$\Delta\rho_2$	L_1	L_2
325	0.0009		4.1A	
300	.00095		4.3	
275	.0011	.0011	4.9	4.9A
225		.0012		5.4
200	.0014		6.3	
175		.0009		4.1
100		.0008		3.6
75		.0008		3.6

Where $\Delta\rho_1$ is the change in ellipticity in the approximate interval of 10^{-5} to 10^{-4} mm and $\Delta\rho_2$ the change in ellipticity in the approximate interval of

2–10 cm; L_1 and L_2 are the respective thicknesses in Angstroms corresponding to $\Delta\rho_1$ and $\Delta\rho_2$. The average value of L_1 is 4.9A, and the average value of L_2 is 4.3A. These values agree fairly well with values calculated by means of the kinetic theory. Pictorially, this means that the first layer of methyl alcohol molecules first begins to be adsorbed on the surface at pressures slightly above 10^{-5} mm, and that the layer is complete at pressures slightly above 10^{-4} mm. The alcohol molecule is probably oriented with its long axis perpendicular to the surface, with the OH radical adjacent to the Na ions of the lattice. From the pressure of about 10^{-4} mm until the region of 2–3 centimeters there is no further adsorption. At this point the formation of a second layer commences, and becomes complete at around 9.5–10 cm. Whether or not the second layer is oriented cannot be said definitely, as the binding forces must be considerably weaker than in the case of the first layer.

While the interpretations of the isotherms are apparently clear, it is much more difficult to explain the changes with temperature. The curves of

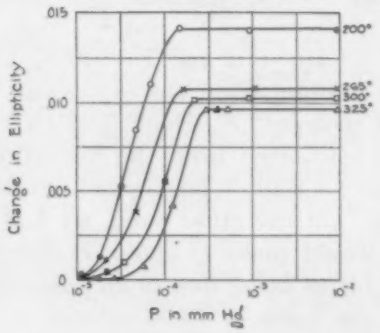

Fig. 5. Adsorption isotherms referred to a common origin.

Fig. 4 seem to show that the surface is clean at 325°C, so that the measured ellipticity must be natural to the clean surface. The increase in ρ with decrease in temperature may be explained in one of two ways. First, as the temperature is lowered, a single layer of water vapor might begin to form which is complete at temperatures around 100°C. This would mean, then, that at high temperatures there is adsorption only of methyl alcohol, but that at lower temperatures adsorption of both methyl alcohol and a layer of water vapor is observed. The second possibility is that there is no water vapor present and that the increase in ellipticity is indicative of an actual surface roughening with lowering of temperature. Very recently, Frazer[6] has observed the same type of curve with an agreement which is very encouraging. He attributes the increase in ellipticity to an adsorption of air; however, this is rather unlikely. The only possible constituent of air that would be likely to adsorb so strongly would be water vapor. However, there is nothing conclusive to be drawn from the data thus far. Certain modifications in the crystal container will have to be introduced, as it does not now appear that outgassing by heat alone is sufficient to determine whether all traces of water vapor have been removed.

If the effect is actually due to temperature directly, then we can move the curves of Fig. 2 to a common origin at their lowest points as in Fig. 5 This will then give us a family of curves of true adsorption. Then it is possible to calculate the isothermal heat of adsorption by means of the Clausius-Clapeyron equation:

$$\frac{d(\log p)}{dT} = \frac{Q}{RT^2}. \tag{4}$$

The approximate values obtained are: 7000 calories for the first layer and 2000 calories for the second layer, in the region of 250°C. However, theoretical considerations seem to be in favor of the first view as the theoretical value of Q is several times larger. If at 325°C the alcohol is adsorbed directly on the salt we could use as a rough approximation the following formula which is due to Nernst:

$$\log p = -\frac{Q}{4.51T} + 3 + 1.75 \log T \tag{5}$$

which, with a value of $p = 10^{-4}$ mm and $T = 600°$K, yields a value of 40,000 calories per mol. On the other hand one can calculate the energy between an ion and a dipole of moment[7] P, which is (PeN/r^2)ergs per mol. If we accept for r the value calculated from the hydration of the sodium ion, $r = 1.74$A, for P the value 1.7×10^{-18}; one again finds for the value of Q about 40,000 calories per mol. On the other hand, we find for 200°C almost the same pressure, which would make Q about 21,000 calories; this decrease can best be accounted for as being due to an adsorption on a partly water covered surface. But the value of 7,000 calories as found experimentally is far too small to account for the vapor pressure as small as 10^{-4} mm at 300°C. One might state the argument in another form. One can expect that the equilibrium pressure of an adsorbed monomolecular layer and the vapor pressure of the substance in bulk to be similar, if the heat of adsorption and the heat of evaporation are similar. Water, with a heat of evaporation of about 9500 calories boils at 100°C; mercury with 13000 calories boils at 338°C. As the equilibrium pressure in the present case is 10^{-4} mm at 325°C, the heat of adsorption must be considerably higher than 13000 calories.[8]

The author wishes to take this opportunity to acknowledge many useful suggestions of Professor A. H. Pfund, concerning the optical set-up; and to express his sincere thanks to Professor Karl F. Herzfeld who has suggested this problem and whose assistance and supervision during its growth have been most helpful.

[6] J. H. Frazer, Phys. Rev. **34**, 645 (1929).

[7] K. Hojendahl, Phys. Zeits. **30**, 391 (1929).

[8] K. F. Herzfeld, Kinetische Theorie der Warme, p. 298 ff. Vol. 3, Müller-Pouillets, Lehrbuch der Physik.

THE PRINCIPAL MAGNETIC SUSCEPTIBILITIES OF BISMUTH SINGLE CRYSTALS

By Alfred B. Focke
California Institute of Technology, Pasadena, California

(Received June 9, 1930)

Abstract

The Gouy method is used to determine the principal magnetic susceptibilities of bismuth single crystals grown by the method developed by Goetz. The specific susceptibility is shown to be a constant in all directions perpendicular to the principal crystallographic axis with a value of -1.487×10^{-6}. Parallel to the main axis the specific susceptibility is a minimum and has the value -1.046×10^{-6}. The mean is given then as -1.340×10^{-6}

I. Historical

RECENT investigations by Goetz,[1] Goetz and Hasler,[2] and Goetz and Focke,[3] concerning the effects of allowing one half of a single crystal of bismuth to crystallize in a strong magnetic field, have shown that different orientations are affected in different ways. The effects are a maximum if the principal axis is perpendicular to the field and a minimum if the axis is parallel to the field. This at once leads to the conclusion that if the susceptibility is a contributing factor in the effect, it must also have a maximum perpendicular to the main axis and minimum parallel to it. This supposition is sustained by the results obtained by Nusbaum.[4] There is however an objection to accepting the absolute values of the results which he has reported since the value given by him as the maximum is still below that given in tables for the susceptibility of the heterogeneous crystal aggregate. Because of this, it was felt that a new determination of the principal susceptibilities of bismuth should be made.

II. Preparation of Crystals

The bismuth used in the crystals described in this paper was obtained from the Braun Corporation and subsequently vacuum distilled in an effort to purify it.

The single crystals were made by the method developed by Goetz.[1] Crystals are grown in this method, by moving a rod of the metal which is lying in a graphite trough through a furnace at such a speed that once a crystal begins to form, it can continue its growth throughout the entire rod, the orientation of the crystal being determined by innoculation. The orientations used were P_1 (principal axis perpendicular to the length of the rod) and P_2 (principal axis parallel to the length of the rod). The

[1] A. Goetz, Phys. Rev. **35**, 193 (1930).
[2] A. Goetz and M. Hasler, to appear in Phys. Rev.
[3] A. Goetz and A. Focke, to appear in Phys. Rev.
[4] C. Nusbaum, Phys. Rev. **29**, 905 (1927).

accuracy of the orientations could be checked after magnetic observations were taken by cleaving the crystal along the basal cleavage plane. In the case of the P_1 crystals, this plane was parallel to the rod making it possible to obtain a very accurate determination of the orientation. The crystals used were all correct to less than ten minutes of arc. The P_3 orientation could not be checked so accurately in this way since the cleavage plane is perpendicular to the rod but as no error could be noticed it was probably accurate to within two degrees.

The crystals were searched for strangers and twinning lamellae before and after the observations, by etching them in nitric acid. Only those crystals which were free from these imperfections were used as any such irregularities would have destroyed the accuracy of the results.

3. Method of Measurements

The Guoy method[5] was chosen for making these measurements. The principal requirement of this method is that the sample must have a uniform cross section over the entire section in which the field gradient is appreciable. The condition of the extreme ends is not important as they are both located in uniform fields. Both of these facts were advantageous because long uniform single crystals were available and also the twinning lamellae at the ends of the crystals, which invariably are formed when bismuth is cleaved, would be in such a position as to have no effect upon the results.

The arrangement is shown in Fig. 1.

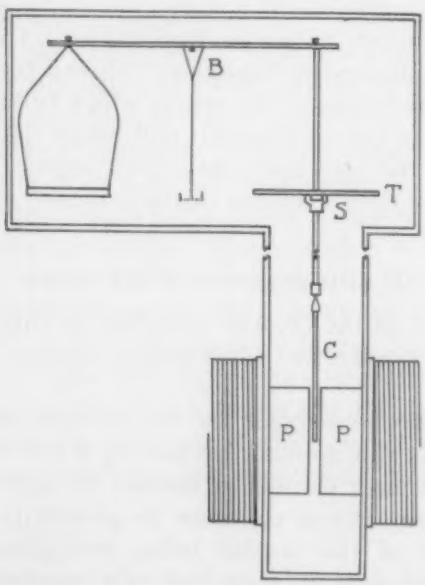

Fig. 1. Arrangement of apparatus.

An aluminum suspension S was designed to take the place of one of the regular pans of a sensitive analytical balance B. It was fitted with a divided

[5] E. C. Stoner, Magnetism and Atomic Structure, p. 40, (1926).

torsion head T so that the sample could be rotated about the vertical axis. The lower end of the suspension was about eight centimeters above the pole pieces P of the magnet. This distance was great enough so that the suspension was totally unaffected by the magnetic field. The pole pieces were flat faced and ten centimeters in diameter, giving a very uniform field between them with comparatively little stray field. The crystals C were thirteen centimeters in length, thus placing the lower end on the axis of the pole pieces while the other end was in a field of negligible intensity.

The balance, suspension, crystal and the ends of the pole pieces were enclosed in a cabinet to prevent air currents from disturbing the apparatus.

The greatest error to be expected between any two determinations of the susceptibilities was about 2 percent. The greatest single source of error was in the determination of the area of the cross section of the crystals. Due to the peculiar shape caused by the method of growth, the only practicable way of measuring the cross sectional area was by computing it from the weight, length and density of the sample under consideration. The error thus introduced was about 1 percent. The field strength was measured with a Grassot fluxmeter introducing a possible error of 0.5 percent, and the force exerted upon the crystal by the field was accurate to within 0.3 percent. The greatest deviation actually observed was less than 1.5 percent.

4. Theory of the Method

Let a crystal with principle susceptibilities k_1, k_2, k_3 be placed in a magnetic field as in Fig. 2.

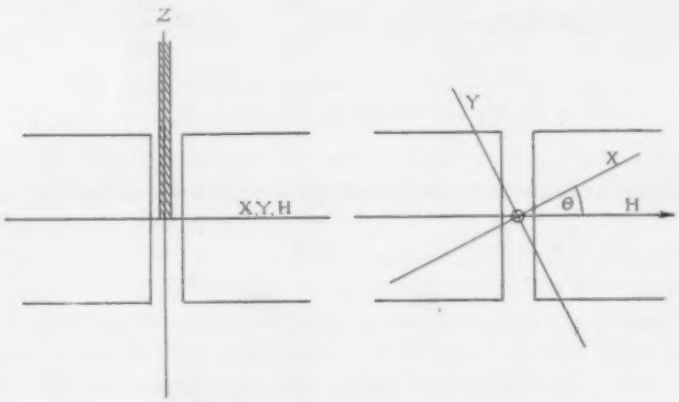

Fig. 2. Arrangement of crystal in magnetic field.

Take a set of axes parallel to the principal magnetic axes of the crystal with origin at its lower end.

Let z be parallel to the length of the crystal and let x make an angle θ with the magnetic lines of force. The boundary conditions will then be

$$H_x = H\cos\theta \qquad H_y = H\sin\theta \qquad H_z = 0$$

$$\frac{\partial H_x}{\partial x} = \frac{\partial H_x}{\partial y} = \frac{\partial H_y}{\partial x} = \frac{\partial H_y}{\partial y} = \frac{\partial H_z}{\partial x} = \frac{\partial H_z}{\partial y} = \frac{\partial H_z}{\partial z} = 0$$

if the diameter of the crystal is small in comparison to that of the pole-pieces.

The equation for the energy of a magnetic field in an anisotropic medium is given as

$$E = \frac{1}{8\pi}(\mu_x H_x^2 + \mu_y H_y^2 + \mu_z H_z^2)$$

where

$$\mu_x = 4\pi k_x,\ \mu_y = 4\pi k_y,\ \mu_z = 4\pi k_z$$

thus

$$E = \tfrac{1}{2}(k_x H_x^2 + k_y H_y^2 + k_z H_z^2).$$

The force in directions parallel to the axes is

$$F_x = \frac{\partial E}{\partial x} = \frac{k_x}{2}\frac{\partial H_x^2}{\partial x} + \frac{k_y}{2}\frac{\partial H_y^2}{\partial x} + \frac{k_z}{2}\frac{\partial H_z^2}{\partial x}$$

$$F_y = \frac{\partial E}{\partial y} = \frac{k_x}{2}\frac{\partial H_x^2}{\partial y} + \frac{k_y}{2}\frac{\partial H_y^2}{\partial y} + \frac{k_z}{2}\frac{\partial H_z^2}{\partial y}$$

$$F_z = \frac{\partial E}{\partial z} = \frac{k_x}{2}\frac{\partial H_x^2}{\partial z} + \frac{k_y}{2}\frac{\partial H_y^2}{\partial z} + \frac{k_z}{2}\frac{\partial H_z^2}{\partial z}$$

or

$$F_x = k_x H_x\frac{\partial H_x}{\partial x} + k_y H_y\frac{\partial H_y}{\partial x} + k_z H_z\frac{\partial H_z}{\partial x}$$

$$F_y = k_x H_x\frac{\partial H_x}{\partial y} + k_y H_y\frac{\partial H_y}{\partial y} + k_z H_z\frac{\partial H_z}{\partial y}$$

$$F_z = k_x H_x\frac{\partial H_x}{\partial z} + k_y H_y\frac{\partial H_y}{\partial z} + k_z H_z\frac{\partial H_z}{\partial z}$$

Substituting the boundary condition these equations reduce to:

$$F_x = 0$$

$$F_y = 0$$

$$F_z = k_x H_x\frac{\partial H_x}{\partial z} + k_y H_y\frac{\partial H_y}{\partial z}$$

$$F_z = k_x \cos^2\theta H\frac{\partial H}{\partial z} + k_y \sin^2\theta H\frac{\partial H}{\partial z}$$

$$F_z = [k_y + (k_x - k_y)\cos^2\theta]H\frac{\partial H}{\partial z}$$

If $H=H$ when $z=0$ and $H=H_0$ when $z=z$ integrating over the volume we get

$$F = \int F_z dv = \int [k_y + (k_x - k_y)\cos^2\theta]dxdydzH\frac{dH}{dz}$$

or

$$k_y + (k_x - k_y)\cos^2\theta = \frac{2}{(H^2 - H_0^2)}\frac{F}{A}.$$

If F is given in grams we have

$$k_y + (k_x - k_y)\cos^2\theta = \frac{2gF}{A(H^2 - H_0^2)}.$$

In terms of the specific susceptibility x and if $H_0 << H$, we have

$$x_y + (x_x - x_y)\cos^2\theta = \frac{2gF}{dAH^2}.$$

The similarity between this equation and that usually given for the Gouy method is seen at once by setting $x_x = x_y$ giving

$$x = \frac{2gF}{dAH^2}.$$

5. Discussion of Results

Fig. 3 shows the result obtained when the principal axis of the crystal is parallel to the rod (P_3). In this case the axis is always perpendicular to the

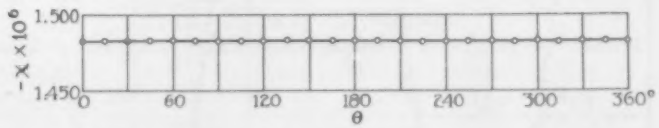

Fig. 3. Variation of specific susceptibility when major axis is parallel to length of the rod.

field and the distribution of the susceptibility in a plane perpendicular to the main axis is measured. It is seen at once that there is perfect circular symmetry about this axis.

Fig. 4 shows a compilation of five separate determinations of the variation of the susceptibility when the main axis is perpendicular to the rod, and a cosine square curve calculated from the average maximum and average minimum values of the susceptibility obtained in the cases of the five individual determinations. In the case of the maximum value the P_3 case is included. The agreement is evident showing that the variation definitely follows a cosine square law.

The principal susceptibilities of this bismuth may be given as $x_{min} - 1.046$ parallel to the main axis and $x_{max} - 1.487$ perpendicular to the main axis. The ratio of x_{max}/x_{min} is 1.425. This last point is particularly mentioned as it has been found that this ratio varies with varying amounts of impurities and an investigation of this effect is now in progress.

The susceptibility, calculated from these values, for a heterogeneous crystal aggregate is $-1.340, (^2x_{max} + x_{min})/3$ agreeing very well with the values given in various tables.

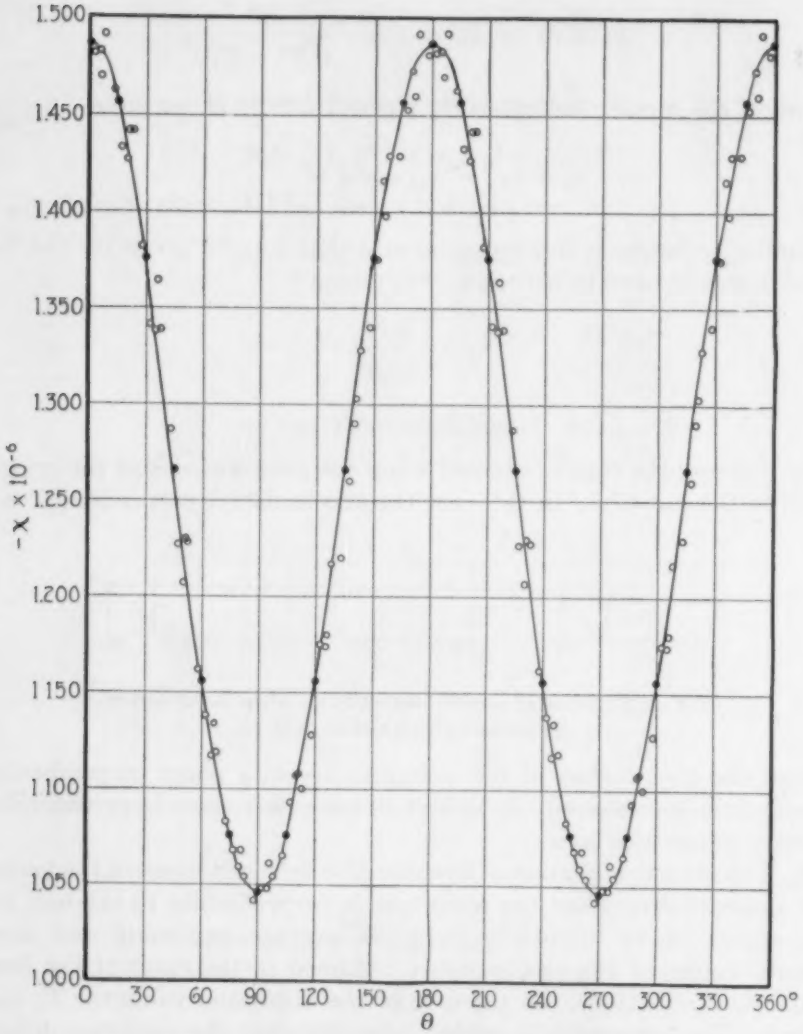

Fig. 4. Variation of specific susceptibility when major axis is perpendicular to length of the rod.

TABLE I. *Data for figure 4.*

Calculated Values		Crystal #120/11		Crystal #120/21	
θ	$-\chi\times10^6$	θ	$-\chi\times10^6$	θ	$-\chi\times10^6$
0	1.487	13	1.463	2	1.482
15	1.457	28	1.392	17	1.433
30	1.376	43	1.287	32	1.341
45	1.266	58	1.162	47	1.227
60	1.156	73	1.083	62	1.138
75	1.076	88	1.042	77	1.068
90	1.046	103	1.065	92	1.048
105	1.076	118	1.128	107	1.093
120	1.156	133	1.220	122	1.175
135	1.266	148	1.340	136	1.260
150	1.376	163	1.429	152	1.375
165	1.457	178	1.481	167	1.453
180	1.487	193	1.463	182	1.482
195	1.457	208	1.392	197	1.433
210	1.376	223	1.287	212	1.341
225	1.266	238	1.162	227	1.227
240	1.156	253	1.083	242	1.138
255	1.076	268	1.042	257	1.068
270	1.046	283	1.065	272	1.048
285	1.076	298	1.128	287	1.093
300	1.156	313	1.220	302	1.175
315	1.266	328	1.340	317	1.260
330	1.376	343	1.429	332	1.375
345	1.457	358	1.481	347	1.453
360	1.487	13	1.463	2	1.482

TABLE I. (*Continued*).

Crystal #120/51		Crystal #120/61		Crystal #120/71	
θ	$-\chi\times10^6$	θ	$-\chi\times10^6$	θ	$-\chi\times10^6$
8	1.492	5	1.483	6	1.470
23	1.442	20	1.427	21	1.442
38	1.339	35	1.338	36	1.364
53	1.228	50	1.207	51	1.230
68	1.119	65	1.117	66	1.134
83	1.054	80	1.059	81	1.068
98	1.054	95	1.048	96	1.061
113	1.100	110	1.107	111	1.108
128	1.217	125	1.174	126	1.180
143	1.328	140	1.290	141	1.303
158	1.429	155	1.416	156	1.398
173	1.492	170	1.473	171	1.460
188	1.492	185	1.483	186	1.470
203	1.442	200	1.427	201	1.442
218	1.339	215	1.338	216	1.364
233	1.228	230	1.207	231	1.230
248	1.119	245	1.117	246	1.134
263	1.054	260	1.059	261	1.068
278	1.054	275	1.048	276	1.061
293	1.100	290	1.107	291	1.108
308	1.217	305	1.174	306	1.180
323	1.328	320	1.290	321	1.303
338	1.429	335	1.416	336	1.398
353	1.492	350	1.473	351	1.460
8	1.492	5	1.483	6	1.470

DISCONTINUOUS CHANGES IN LENGTH ACCOMPANYING THE BARKHAUSEN EFFECT IN NICKEL

By C. W. Heaps and A. B. Bryan
Rice Institute, Houston, Texas

(Received May 15, 1930)

Abstract

A heterodyne beat method is described by means of which displacements as small as 9×10^{-9} cm may be measured. When a nickel wire, 1.96 cm long and 0.01 cm in diameter, is subjected to a steadily changing magnetic field there is evidence of a sudden length change at the instant of a Barkhausen discontinuity of magnetization. For a nickel wire 2 cm long and 0.002 cm in diameter these sudden length changes were larger and could easily be measured. They were associated with every Barkhausen jump observed in the specimen. The largest one measured was 4.7×10^{-7} cm. Calculations based on the measurements of these magnetostrictive jumps give 3.7×10^{-7} cc. for the minimum value of the volume of the element which suffers the jumps. Reasons are advanced for believing that the sudden change in intensity of magnetization of this volume element cannot be less than 40 units nor more than 330. A qualitative theory of the phenomenon is given.

WHEN a ferromagnetic substance is magnetized by a field which changes continuously it is found that a part at least of the resulting change in intensity of magnetization takes place in sudden discontinuous jumps. This Barkhausen effect is usually observed by means of the induced voltages in a coil surrounding the specimen. Ferromagnetic substances also undergo a change of length when magnetized. There appears to be a very close relation between the magnetostrictive effect and the Barkhausen effect. One phenomenon has so far not been observed in a substance without the other, and both are affected by heat treatment and by mechanical strain.

It seemed probable therefore, that the discontinuities of magnetization should be accompanied by discontinuous changes in length of the specimen. This conclusion follows directly from one interpretation of McKeehan's[1] theory of atomic magnetostriction and is also in agreement with a theory of the Barkhausen effect which has been discussed by one of the authors.[2] In the experiments to be described a very sensitive and quick acting apparatus has been constructed and sudden changes in the length of a nickel wire have been observed to occur simultaneously with the Barkhausen discontinuities.

Apparatus

The heterodyne beat method of measuring small capacity changes or small displacements is used. The apparatus, shown diagrammatically in Fig. 1, is a modification of that previously used by one of the authors.[3] Oscillator *A*

[1] L. W. McKeehan, Jour. Frank. Inst. **202**, 737 (1926).
[2] C. W. Heaps and J. Taylor, Phys. Rev. **34**, 937 (1929).
[3] A. B. Bryan, Phys. Rev. **34**, 615 (1929).

is maintained at 1819 k.c. by a quartz crystal. Oscillator *B*, employing a shield grid tube, is the same as in the previous work except that different condensers are used. C_1 is a calibrated General Radio precision air condenser and is used for purposes of adjustment and calibration. *C* is a small condenser with two circular horizontal plates 2 cm in diameter. The top plate is supported by a 2 cm length of the nickel wire to be examined. It is steadied and vibrations are damped out by three short sections of rubber cut from ordinary rubber bands, arranged to press downward at three points on its upper surface. The lower plate is provided with a screw adjustment so that the spacing between the plates can be made very small. *C* is mounted near the center of the large solenoid S_1, which is 15.7 cm long and has an inner diameter of 5.9 cm. The winding of S_1 and the leads to it are completely inclosed in a grounded copper shield. A field strength of 74.5 gauss per ampere is obtained.

Detector *D* includes a small loop antenna, a detector and a two stage amplifier. The radio frequency oscillations from *A* and *B* are picked up by *D* and the audible beat note between them is impressed on the telephone

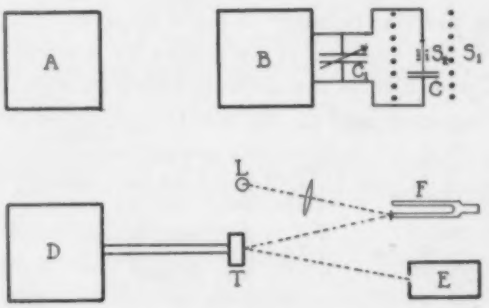

Fig. 1. Diagram of apparatus.

receiver *T*. A small mirror attached to *T* thus vibrates with the frequency of the beat note between *A* and *B*. A beam of light from lamp *L*, is reflected first from a mirror attached to one prong of a 300 cycle electrically driven tuning fork *F*. It is then reflected from the mirror attached to *T* and finally falls on a strip of motion picture film in camera *E*. The film moves downward while both mirrors are arranged to vibrate the beam of light in a horizontal plane. When the fork and heterodyne beat frequencies are about the same the combined motions of the two mirrors thus produce a sort of "photographic" beat as shown in Fig. 2. The frequency of this photographic beat is equal to the difference of the two component frequencies. When the field of S_1 produces magnetostriction in the nickel wire the capacity of *C* changes and there is a resulting change in the frequency of oscillator *B*, of the heterodyne note and of the photographic beat.

A time scale is obtained by focusing an image of the filament of an ordinary lamp on one edge of the film. The lamp carries 60 cycle alternating current and the filament vibrates with this frequency when a permanent magnet is brought near. This arrangement is not shown in Fig. 1.

The nickel wire passes through a small bakelite spool on which solenoid S_2 is wound. This solenoid is 0.65 cm in length and 1.58 cm in outside diameter and has 3960 turns. It is connected through a three stage amplifier to a second telephone receiver carrying a mirror. Light reflected from this mirror produces the third trace on the film, in this case a straight line which is broken when the sudden Barkhausen change in magnetization of the nickel wire induces a voltage in S_2. None of this equipment except S_2 is shown in Fig. 1.

Suitable rheostats are used in series with S_1 to control the magnetizing current. A spiral of fine nickel wire is also connected in series with S_1. This spiral may be heated by means of a nichrome heating coil which surrounds it, the resulting resistance change producing a slow continuous variation of current over a small range. The rheostats are so adjusted that this continuous change takes place over a range in which the Barkhausen discontinuities are largest.

Theory of the Measurements

Let the parallel plate condenser C have capacity C, area A, and plate distance d. Then $C=A/4\pi d$ and if d changes by a small amount δd we get $\delta d=-(A/4\pi C^2)\delta C$ where δC is the corresponding change in C.

Let n_0 be the frequency and C_0 the total capacity of oscillating circuit B. Then if we assume that $n^2{}_0$ is inversely proportional to C_0 it may easily be shown that a decrease δC_0 in C_0 will produce an increase δn in n_0 such that

$$\delta C_0 = C_0\left[1-\left(\frac{n_0}{n_0+\delta n}\right)^2\right] \tag{1}$$

or

$$\delta C_0 = 2C_0\delta n/n_0 \tag{2}$$

for small changes. The only change in C_0 is that produced by the nickel wire in raising or lowering the upper plate of condenser C. Thus $\delta C_0=\delta C$ and we get

$$\delta d = -AC_0\delta n/(2\pi C^2 n_0). \tag{3}$$

In this equation δd is of course the desired change in length of the supporting nickel wire. All the quantities on the right may be easily determined. The area of A of the circular condenser plate as calculated directly from its measured diameter is 3.14 cm^2. The value of n_0 differs by a negligible amount from the known frequency of the quartz crystal used and may be taken as 1819 kilocycles. The other three quantities are found as follows:

(*1*). *Determination of* C_0.—A wavemeter is used to measure n_0. Then a known large change in C_0 is produced by means of the calibrated variable condenser C_1 and the frequency $(n_0+\delta n)$ is again measured. These readings and Eq. (1) give C_0. The mean of several determinations is $C_0=597.4$ cm.

(*2*). *Determination of* C. The reading of C_1 is noted when A and B are tuned to the same frequency. Then C is disconnected and B again tuned to the fre-

quency of A by adjusting C_1. The increase of C_1 required for the retuning gives the value of C to be 41.2 cm.

(3). *Determination of* δn. Let n_A, n_B, and n_F be the frequencies of oscillator A, oscillator B, and the fork F, respectively. For simplicity assume $n_B > n_A$ and $(n_B - n_A) > n_F$. Then $(n_B - n_A)$ is the frequency of the heterodyne beat note between the two radio frequency oscillators and $(n_B - n_A - n_F)$ is the frequency of the photographic beat between this heterodyne note and the fork, as observed on the film. n_A and n_F remain constant. A decrease δd in the length of the nickel wire produces an increase δn in n_B and the frequency of the photographic beat increases to $(n_B - n_A - n_F + \delta n)$. Let $T = 1/(n_B - n_A - n_F)$ and $T' = 1/(n_B - n_A - n_F + \delta n)$ be the periods of the photographic beat before and after the change δd occurs, respectively. Then $\delta n = (T - T')/(TT')$. The periods T and T' are readily obtained from the film by means of the time scale. Obviously some care is necessary to determine whether an observed δn corresponds to an increase or a decrease in the length of the nickel wire.

To get an estimate of the smallest change in length which can be detected assume that $T = 1$ second and that a change in T of 10% can be observed. These conditions are obtained fairly easily. In this case $\delta n = 0.1$ cycle per sec. approximately, and from Eq. (3) $\delta d = 9.7 \times 10^{-9}$ cm. A higher sensitivity is obtained for larger values of T.

It should be mentioned that with this extremely high sensitivity there is always a gradual change in the beat frequency because of unavoidable temperature changes. Vibrations are perhaps an even more serious source of trouble. The condenser C was mounted on sponge rubber, a basement room was chosen for the experiment and records were taken at night; nevertheless seismic disturbances and a temperature drift were always in evidence. The sensitivity could no doubt be considerably increased by further efforts to eliminate these two disturbing factors.

Results

The first specimen was a nickel wire 0.01 cm in diameter and 1.96 cm long. The photographic record showed several Barkhausen discontinuities. A curve was drawn with the period of the photographic beat plotted against time. Since the magnetizing current varied continuously with the time the curve indicated how the length of the wire varied as the field changed continuously. It was found that the smooth course of the curve showed breaks at two of the points where Barkhausen impulses occurred. However, since these breaks were only a little larger than the apparent discontinuities due to experimental error it was felt that the evidence was not entirely conclusive.

Accordingly a new nickel wire 0.002 cm in diameter and 1.98 cm long was prepared by immersing a larger wire for a short time in nitric acid. With a fine wire it was thought that the volume which gives the Barkhausen discontinuity by its magnetization change would be a larger percentage of the whole wire and would thus produce a proportionally larger effect on the gross magnetostriction of the specimen. The results seemed to justify

this idea. The magnetizing field was decreased from a large negative value to zero and then increased to a positive value of 18.6 gauss. A further slow increase to 26.1 gauss was then produced with the hot wire arrangement previously described and the photographic records were taken during this slow increase. There were usually one large Barkhausen impulse and two smaller ones in this region. Fig. 2 shows one of the three photographic records taken of the large impulse. The break at A shows the time of arrival of the impulse. The length BC, as measured on the time scale F, shows the period T of the photographic beat before the arrival of the impulse to be (70.2/60) sec. and the length DE shows the period T' after the impulse to be (10.5/60) sec. Hence $\delta n = (T-T')/(TT') = 4.85$, and from Eq. (3) the change δd in the length of the wire is found to be 4.7×10^{-7} cm. The change in this case was a contraction, showing that the intensity of magnetization had passed through its zero value and was increasing.

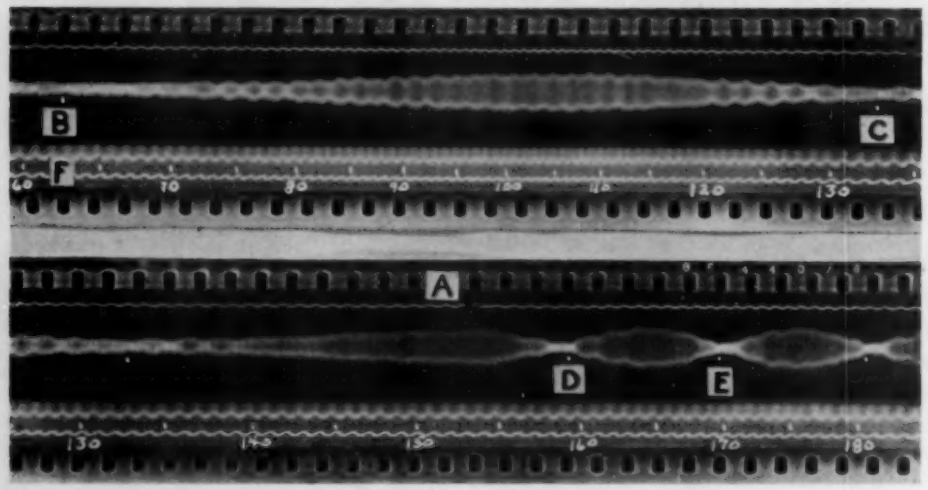

Fig. 2. Photographic record of frequency change. The lower record is a continutation of the upper with slight overlapping.

The two other records, taken in the same way, give values of 2.95×10^{-7} cm and 3.6×10^{-7} cm for this quantity. The three determinations thus give an average δd of 3.75×10^{-7} cm. The large impulse did not always occur at exactly the same magnetizing field value and it is probably not to be expected that the three determinations should be in exact agreement. Numerous additional visual observations with this same specimen showed that every Barkhausen impulse heard was invariably accompanied by a simultaneous sudden change in length of the wire.

Discussion of Results

A qualitative theory of the Barkhausen effect to which the present experiments lend support has previously been proposed.[2] This theory ascribes the effect to the presence of stresses in the specimen. To be specific,

assume that there is one small volume element in the interior of the nickel specimen which is initially under tension. The two effects of tension on nickel are to produce a decrease in magnetic permeability and a relatively larger increase in the magnetostrictive contraction for a given intensity of magnetization.[4] Consequently, when the specimen is magnetized the volume element under consideration will contract more than the surrounding material in spite of its abnormally low intensity of magnetization and the initial tension will increase until eventually there is some sort of slipping or rearrangement of the material and the tension is partially or completely released. This release causes a measurable change in length of the specimen only when the cross sectional area of the volume element is an appreciable part of that of the whole specimen. The sudden length change should thus be more prominent in fine wires, as has been observed in the present work. The release of tension also causes a sudden increase in the permeability and the intensity of magnetization of the volume element. Thus we get the Barkhausen effect. This increase in intensity of magnetization will in turn produce a secondary change in the field acting on all other parts of the specimen and in their intensities of magnetization and lengths, but this secondary effect is probably negligibly small.

The following calculation, based on the above conception of the Barkhausen effect, may be considered as a rough approximation. Assume that the volume element which has produced the experimentally observed effects has a length L parallel to the axis of the wire and a uniform cross sectional area a. Let δI be the sudden change in the intensity of magnetization I for the volume element and δL be the accompanying change in L which would result if the element were not restrained by the material around it. The actual length change, which may be identified with the observed δd, may reasonably be taken equal to $\delta L(a/a_0)$, where a_0 is the area of cross section of the whole wire. Ewing's[5] I vs H curve and an unpublished $\delta L/L$ vs H curve obtained by the present writers together give $\delta L/(L\delta I)=9.5\times10^{-9}$ for hard drawn nickel, the value being taken at a point on the hystersis loop where $H=20$ gauss and is increasing. The Barkhausen jumps for which δd was measured were near this point on the hysteresis loop. Then, assuming the magnetic similarity of the three samples of hard drawn nickel involved, the value $\delta L/L\delta I=9.5\times10^{-9}$ may be taken as correct for the volume element considered. Replacing δL by $a_0\delta d/a$, and using the experimentally found values for δd and a_0, we get $aL\delta I=1.24\times10^{-4}$. Here aL is the volume V of the volume element. The exact value of V cannot be obtained because δI is unknown. However, the maximum value of δI may be taken to be 330, this being the approximate saturation value of I for nickel. The corresponding

[4] McKeehan states, reference 1, that, "In the case of nickel the resultant orientation of atomic magnetic axes across the axis of tension, which reduces the ease of magnetization along the axis of tension, will increase the magnetostriction (contraction)." Bidwell's experiments, however, (Proc. Roy. Soc. **A47**, 469, 1890) do not seem to agree with this statement unless large magnetic fields and small tensions are used.

[5] J. A. Ewing, "Magnetic Induction in Iron," p. 87.

minimum V is 3.76×10^{-7} cc, which is roughly one sixteenth of the total volume of the specimen.

Bozorth and Dillinger[6] find that V varies over different parts of the hysteresis loop. Their value for the conditions of the present experiment is about 2×10^{-8} cc for annealed nickel, roughly a twentieth of the above found minimum value. However, they assume I to be a complete reversal from a saturation value in one direction to saturation in the other direction. With the same assumption in the present work the discrepancy between the two measurements is reduced to a factor of 10. This is not bad if we consider that the two determinations are widely different in character, that both are somewhat indirect, that the two specimens of nickel differ greatly in size and that one specimen is annealed and the other hard drawn. This last difference alone might account for the discrepancy since it is known that annealing reduces the Barkhausen effect.

The true δI is probably considerably less than the maximum of 330. An estimate may be made as follows. For a Barkhausen discontinuity to occur it is hard to see how the associated volume element could be greater than half the volume of the wire. Taking this value as a maximum for V the equation $V\delta I=1.24\times10^{-4}$ gives $\delta I=40$ as a minimum. The true δI is probably somewhere between the maximum of 330 and the minimum of 40, V having a corresponding intermediate value. The assumption of a complete reversal of the saturation value of I seems to be unwarranted. The length depends only on the magnitude of I and consequently it is difficult to see how a reversal, which involves no change in magnitude of I, could alone produce any permanent change in length, either the sudden δd of the present work or the gross magnetostriction as usually observed.

[6] Bozorth and Dillinger, Phys. Revs. 35, 733 (1930).

THE ISOTOPES OF NITROGEN, MASS 15, AND OXYGEN, MASS 18 AND 17, AND THEIR ABUNDANCES

By S. Meiring Naudé
Ryerson Physical Laboratory, University of Chicago

(Received June 9, 1930)

Abstract

I. The isotopes of nitrogen and oxygen.—The absorption spectrum of the NO γ bands, in particular that of the (0, 0) band at λ2269, the (1, 0) band at λ2154 and of the (2, 0) band at λ2052 was studied in search of isotopes of nitrogen and in order to verify the recently discovered isotopes of oxygen of mass 18 and 17.

A hydrogen continuous source was constructed which could be operated by means of a 5 K.W. transformer which gave 0.5–0.75 amps. through the secondary. It was shown that the silvering of the capillary tube joining the electrodes acts as a catalyzing agent which accelerates the recombination of the hydrogen atoms to molecules th increasing the intensity of the continuous spectrum. Owing to a chemical change in the fused quartz window on the hydrogen source which leaves the quartz coloured to a violet tint if light of shorter wave-length than λ1850 falls on it, the intensity of the continuous spectrum below λ2300 is reduced considerably. This was overcome by using a crystal quartz window which did not show this effect. The photographic plates were sensitized with vaseline.

A glass tube 92 cm long and 5 cm in diameter with quartz windows sealed onto either end was used as an absorption tube. NO was prepared by dropping a solution of $NaNO_2$ into $FeSO_4$ and H_2SO_4.

Band heads were observed in all three bands investigated corresponding to the calculated heads for the four kinds of molecules $N^{14}O^{16}$, $N^{15}O^{16}$, $N^{14}O^{18}$ and $N^{14}O^{17}$, the maximum deviation of the observed wave-lengths from the calculated values being 0.035A. The results obtained therefore provide new evidence for the existence of a nitrogen isotope of mass 15 and verifies the existence of the oxygen isotopes of mass 18 and 17.

II. The relative abundance of O^{16} and O^{18}.—From the atmospheric bands of oxygen Babcock obtained the relative abundance of O^{16} and O^{18} to be 1250 with a probable error of 25 percent. $(O^{16})_2$ is symmetric whereas $O^{16}O^{18}$ is not. This may give different absorption coefficients for the two molecules. This difficulty disappears in NO. By comparing the pressures of NO in the absorption tube at which the (1, 0) P_1 $N^{14}O^{16}$ head could be made to have the same intensity as the P_1 $N^{14}O^{18}$ head the relative abundance of O^{16} and O^{18} was found to be 1075 ± 110.

The relative abundance of N^{14} and N^{15}.—Because in the (1, 0) band the P_1 $N^{15}O^{16}$ head has the same intensity as the head Q_1 $N^{14}O^{18}$ head, the relative abundance of the N^{15} and O^{18} isotopes is inversely proportional to the relative intensity of the P_1 and Q_1 $N^{14}O^{16}$ heads. This relative intensity was found to be 0.65 ± 0.1. The relative abundance of N^{14} and N^{15} is therefore 1075×0.65 or 700 ± 140.

From the relative abundance of O^{16} and O^{18}, and O^{16} and O^{17} the mass of the O^{16} isotope was calculated to be 15.9980 ± 0.0002 if the atomic weight of the mixture of isotopes was taken to be 16.0000. Aston defines the mass of the O^{16} isotope as 16.000 and consequently his atomic weights are higher than the corresponding chemical atomic weights. The chemical atomic weights and Aston's should agree if we correct the O^{16} isotope to an atomic weight of 15.9980 ± 0.0002, that is by 1.25 parts in 10000.

The mass of the N^{14} isotope was calculated to be 14.0069 ± 0.0012 which is in close agreement with Aston's corrected value of 14.0063 ± 0.0029.

THE search for isotopes, especially among the lighter elements is important,[1] because, as is now generally believed,[2] any theory of nuclear structure will have to account for the existence or non-existence of all possible atomic species as well as for the regularities[3] which exist among the different known isotopes. The occurrence of a certain isotope provides evidence that the corresponding configuration of electrons and protons in the nucleus must be stable. The discovery of the oxygen isotopes of mass 18[4] and 17[5] by Giauque and Johnston, and of the carbon isotope of mass 13 by King and Birge[6,7] throws new light on the stability of atoms having the configurations corresponding to these atomic weights.

Recently the author[8] reported that evidence had been found from the absorption spectrum of NO of the existence of the four kinds of molecules $N^{14}O^{16}$, $N^{14}O^{18}$, $N^{14}O^{17}$ and $N^{15}O^{16}$, thus not only verifying the existence of the oxygen isotopes of mass 18 and 17 but also proving the existence of an isotope of nitrogen of mass 15. In the meantime more evidence has been found for the existence of these isotopes. The relative abundance of the isotopic species of an element is considered to be a measure of the relative stability of the different atomic configurations constituting the isotopes. Therefore special care has also been taken to find as accurately as possible the relative abundance of the O^{18} and N^{15} isotopes with respect to O^{16} and N^{14} respectively.

Part I of this paper gives the evidence that has been found for the existence of the isotopes of nitrogen and oxygen, whereas Part II deals with the experiments carried out to find the relative abundance of the isotopes and the conclusions to which the obtained results lead.

Part I. The Isotopes of Nitrogen and Oxygen

Introduction. According to the theory of the isotope effect in band spectra[9,10] a molecule containing a rarer isotope of one of the atoms con-

[1] W. F. Giauque, Nature **124,** 265 (1929). At the meeting of the "British Association for the Advancement of Science" held in South Africa in July, 1929, Sir E. Rutherford also pointed out that the determination of all the existing isotopes was one way of studying the structure of the nucleus.

[2] Cf. A. E. Ruark and H. C. Urey, "Atoms, Molecules and Quanta," McGraw-Hill Book Co,. 1930, p. 39.

[3] W. D. Harkins, J. Am. Chem. Soc. **39,** 856, 870 (1917), Phil. Mag. **42,** 305 (1926), Chem. Reviews, **5,** 371 (1928); Guido Beck, Zeits. f. Physik **47,** 407 (1928), **50,** 548 (1928), **61,** 615 (1930), H. A. Barton, Phys. Rev. **34,** 1228 (1929).

[4] W. F. Giauque and H. L. Johnston, Nature **123,** 318 (1929); J. Am. Chem. Soc. **51,** 1436 (1929).

[5] W. F. Giauque and H. L. Johnston, Nature **123,** 831 (1929); J. Am. Chem. Soc. **51,** 3528 (1929).

[6] A. S. King and R. T. Birge, Nature **124,** 182 (1929); Phys. Rev. **34,** 376 (1929).

[7] R. T. Birge, Phys. Rev. **34,** 379 (1929).

[8] S. M. Naudé, Phys. Rev. **34,** 1498 (1929); **35,** 130 (1930).

[9] R. S. Mulliken, Phys. Rev. **25,** 119 (1925).

[10] In a Symposium of the Faraday Society held September 1929 on Molecular Spectra and Molecular Structure, Birge discusses methods by which the calculation of the rotational effect can be made more accurate. In this work the approximate formula given in Eq. (2) suffices as the analysis of the NO spectrum made use of here contains relatively large probable errors.

stituting the ordinary molecule, gives rise to a displaced band which corresponds exactly to that which originates from the ordinary molecules. The position of the displaced isotopic band can be calculated accurately by taking into account firstly, the displacement due to vibration:[11]

$$\nu_2{}^r - \nu_1{}^r = (\rho - 1)[\omega_e'(v' + \tfrac{1}{2}) - \omega_e''(v'' + \tfrac{1}{2})] - (\rho^2 - 1)[\omega_e'x'(v' + \tfrac{1}{2})^2 - \omega_e''x''(v'' + \tfrac{1}{2})^2] \quad (1)$$

and secondly, the displacement due to rotation:

$$\nu_2{}^r - \nu_1{}^r = (\rho^2 - 1)\nu_1{}^r \quad (2)$$

where ν_1 refers to the ordinary molecule $N^{14}O^{16}$ and ν_2 to the isotopic molecule, e.g., $N^{15}O^{16}$, $\rho^2 = (\mu_1/\mu_2)$ where $'\mu_1 = 1/M_1 + 1/M_2$ and $'\mu_2 = 1/M_1 + 1/M_2'$, M_1 being the mass of the atom which is common to both molecules, and M_2' being the mass of the rarer of the isotopic species M_2 and M_2', and where ω_e', $\omega_e'x'$, ω_e'', $\omega_e''x''$ are vibrational constants in the initial and final states respectively, and v' and v'' are the vibrational quantum numbers in these states.

The absorption spectrum is far superior to the emission spectrum for studying the isotope effect in a gas containing a rare isotope, for by increasing the length of the absorption tube and the pressure of the gas in the tube, the number of molecules in the path of the light can be increased practically indefinitely, and hence also the number of molecules containing a rare isotope. The lower the pressure, the sharper the absorption lines that are obtained. Therefore the absorption tube is chosen as long as possible and then the pressure of the absorbing gas is raised until the expected effect, if present, is observed.

The absorption spectrum of NO, especially the (0, 0) band at λ2269, the (1, 0) band at λ2154 and the (2, 0) band at λ2052A, that belong to the γ system which is degraded towards the violet, offers a good opportunity for studying the isotope effect. This system of NO has been analyzed partly by Frl. M. Guillery[12] and partly by R. Schmid.[13] Schmid worked on the (0, 0) and (1, 0) bands mentioned. The γ system of NO has a $^2\Pi$ lower level and a $^2\Sigma$ upper level. The separation of the $^2\Pi_{3/2}$ and $^2\Pi_{1/2}$ levels has been found to be 124.4 cm^{-1}. Because the $^2\Sigma$ level is single, every band will exist of a doublet, each having a Q and a P head.[14] Of the (1, 0) band Schmid[13] was able to measure only the Q_1 heads. The position of the P_1 heads could, however, be calculated with the help of the relation:

$$Q_1(J+1) - \Delta F'(J) = P_1(J) \quad (3)$$

[11] The notation used here is in accordance with the report of Prof. Mulliken to be published in the Phys. Rev. Cf. also R. S. Mulliken, Reviews of Modern Physics **2**, 60 (1930).

[12] Frl. M. Guillery, Zeits. f. Physik **42**, 121 (1927).

[13] R. Schmid, Zeits. f. Physik **49**, 428 (1928).

[14] To avoid confusion the older notation for the heads according to Schmid is used here. The more recent nomenclature of these band heads is given by R. S. Mulliken, Phys. Rev. **32**, 413 (1928).

given by him for the final state. This calculation gives 46391.3 cm^{-1} for the wave-number of the P_1 head which agrees with the measurements made in the course of the present work. The position of the P_1 and Q_1 heads of the (2, 0) band were calculated to be 48708.6 and 48736.1 cm^{-1} respectively. The vibrational constants ω_e, $\omega_e x$, used in computing the vibrational isotopic shift of the band heads, were calculated from the ω_0 and $\omega_0 x$ given by Birge:[15] $\omega_e = \omega_0 + \omega_0 x$ and $\omega_e x = \omega_0 x$. The values thus found were $\omega_e' = 2365$, $\omega_e'' = 1902.19$, $\omega_e' x' = 13$, $\omega_e'' x'' = 13.88$. The calculated shifts with the corresponding wave-lengths are given in columns 4 and 5 of Table I.

The continuous source. As continuous light source a hydrogen lamp was constructed of Pyrex glass according to Bay and Steiner.[16] The source could be operated with a 5 K.W. transformer giving from 0.5 to 0.75 ampere through the secondary. This gave a very intense continuous spectrum. The source was provided with a quartz window at either end. The second window allowed one to sight through the hydrogen source, thus greatly facilitating the lining up of the source, the absorption tube and the spectrograph, which is very important in the case of a long absorption tube, for in this way the maximum intensity can be obtained.

Some experiments were carried out to find out what function was fulfilled by the silvering of the capillary tube which joins the electrodes and in which the discharge takes place, as no conclusions were made in this respect by Gehrcke and Lau[17] who first describe its use. It was found that, when the capillary tube was not silvered the discharge was distinctly red due to the H_α line becoming very prominent. On the other hand, when it was silvered the secondary and also the continuous spectrum of hydrogen which is emitted by the hydrogen molecule,[18] became much stronger, H_α being reduced to about the same intensity as that of the secondary spectrum. The evidence thus points to the mechanism of the silvering being to catalyze the recombination of hydrogen atoms into which the molecules dissociate on giving out the continuous spectrum back to molecules, thus strengthening the secondary spectrum and hence also the continuous spectrum.

As is well known[16] the observed intensity of the hydrogen continuous spectrum falls off rapidly below λ2400A. Experiments were carried out to determine the cause of this phenomenon. It was noticed that a fused quartz window sealed onto the hydrogen tube gave a very strong fluorescence[19] when the tube was in operation. After a window had been in use for about a week, it was replaced by a new one. It was then noticed that the used one had been discoloured to a violet tint, the pattern in it being the same as the one that was seen in fluorescence while the tube was in use. The hydrogen tube was now refilled and sealed off. Two absorption pictures were taken on the

[15] R. T. Birge, "Molecular Spectra in Gases" p. 232.

[16] Z. Bay and W. Steiner, Zeits. f. Physik **45**, 337 (1927); see also E. O. Lawrence and N. E. Edlefsen, Rev. Scientific Instruments **1**, 45 (1930).

[17] E. Gehrcke and E. Lau, Ann. d. Physik [IV] **76**, 675 (1925).

[18] J. G. Winans and E. C. Stueckelberg, Proc. Nat. Acad. Sci. **14**, 867 (1928).

[19] H. W. Webb and Miss Helen Messenger, Phys. Rev. **34**, 1463 (1929).

same photographic plate, the first with the used quartz window and the second with an unused window in the light path. It was found that the used window absorbed very strongly in the region below λ2400A. The used quartz window had to be ground down to about half the original thickness before the violet tint was removed. It is not known what the cause of this colouring is, but it seems likely that the SiO_2 constituting the quartz dissociates, giving free silicon. The wave-length causing this fluorescence must be shorter than λ1850, the shortest wave-length transmitted by quartz, because the fused quartz windows used on the absorption tube showed no fluorescence and when the windows were removed after being in use for six months, no violet colouring could be observed. A crystal quartz window was ground and polished and used to replace the fused quartz window on the hydrogen source. The fluorescence in this window was distinctly less conspicuous and the intensity of the continuous spectrum obtained was much better. This window showed no violet colouring even after being in use for three months. It is therefore advisable to use crystal quartz instead of fused quartz windows on the hydrogen source for work in the far ultraviolet.

Procedure. A tube 92 cm long and 5 cm in diameter and with two quartz windows sealed onto either end served as absorption tube. The NO gas was prepared by dropping $NaNO_2$ into a solution of H_2SO_4 and $FeSO_4$. The end of the dropping funnel was well below the surface of the liquid so that all the NO_2 formed could be reduced to NO by the $FeSO_4$. The NO gas was left over the $FeSO_4$ for about a day so that the gas obtained was practically free from NO_2. The NO gas was dried by passing it through a tube containing P_2O_5. The pressure of the gas could be determined by means of a McLeod gauge.

An E1 Hilger spectrograph was used which had a dispersion varying from 1 mm = 1.9A at λ2269 to 1.3A at λ2052. The time of exposure varied from six to twelve hours. The best pictures were taken with 2 cm pressure of NO in the absorption tube. Speedway and Eastman 40 plates were used. The copper arc lines measured by Mitra[20] and corrected by Shenstone[21] were used as comparison spectrum. In the region below λ2100 the copper lines as given by Sommer[22] are less accurately measured and consequently the measurements on the (2, 0) band are less accurate.

The insensitivity of the photographic plate in this region, λ2300 to 2000A, was overcome by using a solution of five grams of vaseline[23] in half a liter of petroleum ether[24] as sensitizer according to Beach.[25] The solution was prepared and kept in a glass bottle. Before taking an exposure the photo-

[20] S. K. Mitra, Ann. de Physique **19**, 315 (1923).

[21] A. G. Shenstone, Phys. Rev. **28**, 449 (1926).

[22] L. A. Sommer, Zeits. f. Physik **39**, 711 (1926).

[23] The vaseline used was the ordinary white product of Chesebrough Mfg. Co.

[24] The best results were obtained with petroleum ether made by the Mallinckrodt Chemical Works.

[25] A. C. G. Beach, Nature **123**, 166 (1929); Cf. also H. R. Harrison J. Opt. Soc. Am. **11**, 341 (1925).

graphic plate was dipped into the solution which had been previously poured into a flat dish. On taking it out an oscillatory movement was carried out in order to dry it in such a way that the film of vaseline formed on the surface of the plate after the petroleum ether had evaporated, should be as even as possible. An even film of vaseline was essential especially where a comparison was made between the intensity of two photographs on the same plate (as described in Part II), since the thickness of the film of vaseline determines the intensity obtained.

The plate was then inserted into the holder and the photograph taken in the ordinary way. Before the plate was developed, the vaseline was removed by rubbing its surface with cottonwool which had been soaked in acetone. The plate was then developed as usual.

Results. In all three bands bandheads are observed corresponding to the four types of molecules $N^{14}O^{16}$, $N^{15}O^{16}$, $N^{14}O^{18}$ and $N^{14}O^{17}$ except in the (0, 0) band where, owing to the smallness of shift and the proximity of the $N^{15}O^{16}$ head, the much weaker $N^{14}O^{17}$ head is not observed.

The results are tabulated in Table I being the average of the measurements on five different plates taken at different pressures.

TABLE I.

Band	Nomenclature wave-length and wave-number of $N^{14}O^{16}$ head		Type of molecule containing an isotope	Calculated shift $\nu_2-\nu_1$ in cm^{-1}	Calculated wave-length in A	Observed wave-length in A
0,0	P_1	2269.40	$N^{14}O^{17}$	−2.595	2269.53_4	—
		44050.8_{88}	$N^{15}O^{16}$	−3.375	2269.57_4	2269.56
			$N^{14}O^{18}$	−4.952	2269.65_8	2269.69
1,0	Q_1	2153.63	$N^{14}O^{17}$	−35.193	2155.26_4	2155.23
		46418.5_{77}	$N^{15}O^{16}$	−45.729	2155.75_4	2155.73
			$N^{14}O^{18}$	−67.030	2156.74_8	2156.75
	P_1	2154.90	$N^{14}O^{17}$	−34.444	2156.49_3	2156.49
		46391.3	$N^{15}O^{16}$	−44.758	2156.95_7	2156.98
			$N^{14}O^{18}$	−65.615	2157.94_9	2157.98
2,0	Q_1	2051.01	$N^{14}O^{17}$	−66.401	2054.00_5	2054.02
		48736.1	$N^{15}O^{16}$	−86.282	2054.84_8	2054.82
			$N^{14}O^{18}$	−126.482	2056.54_8	2056.54
	P_1	2052.43	$N^{14}O^{17}$	−65.646	2055.13_5	2055.15
		48708.6	$N^{15}O^{16}$	−85.304	2055.96_8	2055.97
			$N^{14}O^{18}$	−125.055	2057.64_9	2057.66

In the preliminary publication[8] mention was made of faint absorption bands appearing beyond the isotopic heads in the (1, 0) band, whose positions seemed to agree with the values calculated for a possible $N^{16}O^{16}$ head. This point has been the subject of further research. When the focus of the spectrograph was shifted so as to include the (2, 0) band, it was found that the β bands of NO[26] which originate from the same $^2\Pi$ ground state as the γ bands, but have an upper $^2\Pi$ level different from the $^2\Sigma$ upper level of the

[26] F. A. Jenkins, H. A. Barton and R. S. Mulliken, Phys. Rev. **30**, 150 (1927).

γ bands, also appear in absorption although very weakly. Now it happens that the heads of the R and P branches of the (1, 0) β band fall at λ2153.45 and 2153.68A and thus on top of the (1, 0) γ band. Consequently these heads do not interfere with the isotopic bandheads. Because the β system is degraded towards the red, its rotational fine structure appears beyond the isotopic heads. The position of these rotational lines can be calculated from the relation

$$F = \text{const} + Aj + Bj^2 + Cj^3 + Dj^4$$

given by Jenkins, Barton and Mulliken.[26] All the observed absorption lines beyond the heads of the isotopic molecules could be accounted for in this way. The isotope N^{16} does therefore not exist (unless it is less abundant

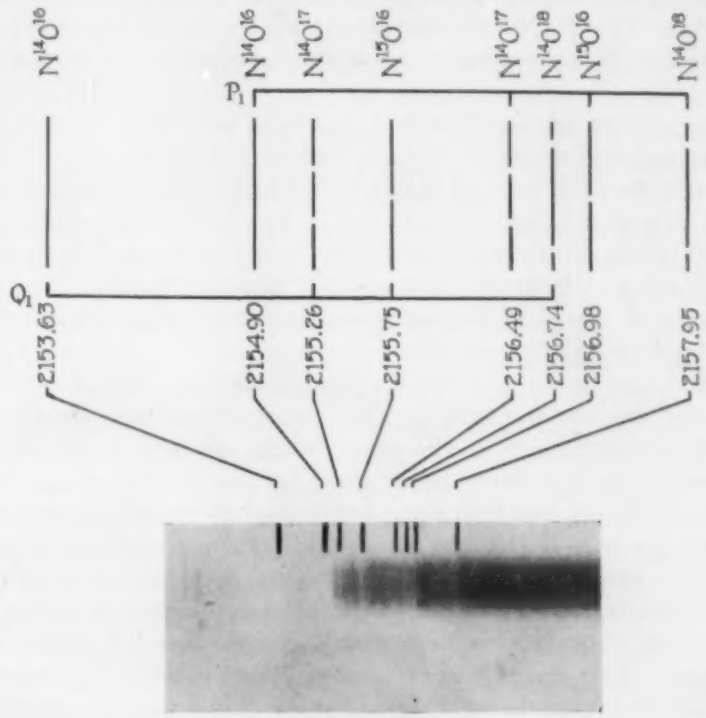

Fig. 1. The expected appearance of the band-heads of the (1, 0) band are sketched. The types of molecules giving these band-heads are given on the upper side of the figure and on the lower side the corresponding wave-lengths of the heads are given. The line on the lower side of the figure joins the Q_1 heads formed by the different types of molecules, whereas the upper line joins the corresponding P_1 heads.

Fig. 2. An enlargement of the observed appearance of the (1, 0) band. The positions of the band heads are indicated by lines which connect the heads to the corresponding heads in Fig. 1.

than O^{17}) especially since the (2, 0) band shows definitely no trace of the N^{16} isotope. The evidence the (1, 0) band gives for the other isotopes is, however, not effected by these faint absorption lines since the intensity of the isotopic heads is much greater than the rotational fine structure of the (1, 0) β band.

Because the P_1 and Q_1 heads of the (1, 0) band are separated by 27.3 cm^{-1} and the smallest displacement, namely that of the Q_1 head due to the $N^{14}O^{17}$ molecule is -35.193 cm^{-1}, one expects the six heads due to $N^{14}O^{17}$ $N^{15}O^{16}$ and $N^{14}O^{18}$ all to fall beyond the $N^{14}O^{16}$ P_1 head and to be observable as far as they do not overlap one another. In Fig. 1 a sketch is given of the expected appearance of the bandheads. In Fig. 2 a photograph (enlarged eight times) of the actual appearance of the (1, 0) band is reproduced. This photograph was taken with a pressure of 2 cm of NO in the 92 cm absorption tube, the time of exposure being ten hours.

Between the Q_1 $N^{14}O^{17}$ and $N^{15}O^{16}$ heads a faint absorption line is seen which could be shown to be due to the overlapping of three lines of the rotational structure belonging to the Q_1 $N^{15}O^{16}$, and $N^{14}O^{18}$ heads and the P_1 $N^{15}O^{16}$ head. The P_1 $N^{14}O^{17}$ head is not visible in this picture but in pictures taken at higher pressures one is able to observe and measure it accurately.

The separation of the P_1 and Q_1 heads in the (2, 0) band is 27.5 cm^{-1} The displacement of the Q_1 $N^{14}O^{17}$ head is calculated to be 66.401 cm^{-1} and will therefore fall beyond the P_1 $N^{14}O^{16}$ head. All the isotopic heads are therefore expected to fall beyond the P_1 head. As can be seen from the calculated positions of these heads in column 5 of Table I, they are widely separated and can therefore be measured more accurately. The increased insensitivity of the photographic plate, however, makes a reproduction of the obtained pictures impossible.

The fine structure of the isotopic bands could also be measured when the overlapping was not too much. This corresponded very closely with the rotational fine structure of the main heads, so that it provides further decisive evidence that these heads must be due to the isotopic molecules.

To be absolutely sure that these bands might not perhaps be due to some other molecule, e.g. $(NO)_2$, the absorption tube was replaced by a tube 1.2 cm in length and filled up to 75 cm pressure with NO. The light passing through this tube has to traverse about the same number of molecules of NO as in the case of the 92 cm tube with 1 cm pressure. If $(NO)_2$ molecules were present their concentration should increase with the square of the pressure and the path being 75 times shorter, one would expect the effect due to these molecules to be 75 times as intense. The absorption of the isotope heads observed is quite similar to that obtained with the 92 cm tube, except that they are a little more diffuse, as one might expect owing to the high pressure. The measured shift agrees accurately with the above results.

This investigation therefore definitely proves the existence of an isotope of nitrogen of mass 15 and verifies the existence of the recently discovered isotopes of oxygen of mass 17 and 18.

Part II. The Abundance of O^{18} and N^{15}

The relative abundance of O^{16} and O^{18}. The abundance of the oxygen isotope of mass 18 has been determined by Babcock[27] from the atmospheric

[27] H. D. Babcock, Proc. Nat. Acad. Sci. **15**, 471 (1929); Phys. Rev. **34**, 540 (1929).

bands of oxygen. Babcock took an absorption picture of the atmospheric bands using the sun as continuous light source and the oxygen in the atmosphere as his absorbing medium. In this way the heads of the displaced bands due to the $O^{16}O^{18}$ molecule could be photographed. On the same plate he took an absorption picture of the corresponding main bands due to $(O^{16})_2$ using a certain length of air path in the laboratory for the absorption. When the isotopic heads in the former appeared to him to be of the same intensity as the main heads in the latter picture, he concluded that the abundance of the molecules giving these bands should be inversely proportional to the number of oxygen molecules traversed in each case. The latter could be calculated from the known path lengths. In this way a relative abundance of one O^{18} isotope in every 1250 O^{16} was obtained as the weighted mean of 1175 and 1350.

The molecule $(O^{16})_2$ is symmetric whereas $O^{16}O^{18}$ is unsymmetric. These molecules may have different absorption coefficients which would affect the results obtained for the relative abundance. This difficulty disappears in the case of NO, for both $N^{14}O^{16}$ and $N^{14}O^{18}$ are unsymmetric. A redetermination of the abundance of O^{18} therefore seemed desirable.

The pressure of NO in the absorption tube could be varied thus giving different numbers of molecules in the light path, and could be measured accurately by means of a McLeod gauge. The pictures were taken on the same photographic plate, 5 mm apart, so that the condition of sensitizing and developing were exactly the same. The two pictures could be taken under the same experimental conditions and special care was taken to get the continuous background of the pictures of the same intensity.

The (1, 0) band is the best to apply this procedure to, because the intensity of the plate is still favourable and the displacement of the isotope heads is fairly large. The only displaced head to which the method can, however, be applied with certainty is the $N^{14}O^{18}$ head at $\lambda 2157.98$ corresponding to the P_1 head of $N^{14}O^{16}$ $\lambda 2154.90$. This head is displaced the farthest and consequently there is no overlapping of the fine structure of the less displaced isotopic heads. The fine structure of the (1, 0) β band mentioned above is so weak that it does not affect the accuracy with which the intensity of the displaced isotope head can be estimated.

The first pictures taken showed that the higher pressure caused the isotopic head to appear much broader than expected. Pressure broadening according to Lorentz[28] was at once suspected to be the cause. Two pictures were taken on the same plate, one with only 2.1 cm pressure of NO in the absorption tube, the other with the 2.1 cm of NO left unchanged but with 44 cm pressure of N_2 added, see Fig. 3. Since the N_2 has no absorption bands in this region it can only have the effect of pressure broadening according to Lorentz. A large number of investigators[29] have done work on the pressure

[28] H. A. Lorentz, Proc. Amsterdam **8,** 501 (1906). For a discussion of this phenomenon according to the wave mechanics cf. J. Frenkel, Zeits. f. Physik **59,** 198 (1930).

[29] Cf. W. Schütz, Zeits. f. Physik **45,** 30 (1927) and the literature given there.

broadening in the case of atoms, and Teves[30] has extended this work to bands. The pressure in the absorption tube was therefore regulated as follows: If a pressure ratio of 1 to 1000, for instance, was desired, the tube was filled to 5 cm with NO and 65 cm of N_2 added. After an exposure with this pressure was finished, the pressure in the tube was changed to 0.005 cm of NO and 70 cm of N_2, and another picture taken on the same photographic plate. In both cases therefore the total pressure was the same, viz. 70 cms, and a large excess of N_2 was present. N_2 was chosen, chiefly because it has no absorption bands above λ1520A and also because it has about the same molecular radius as NO[31], the latter factor influencing the broadening according to Lorentz and Frenkel. It was absolutely necessary to have N_2

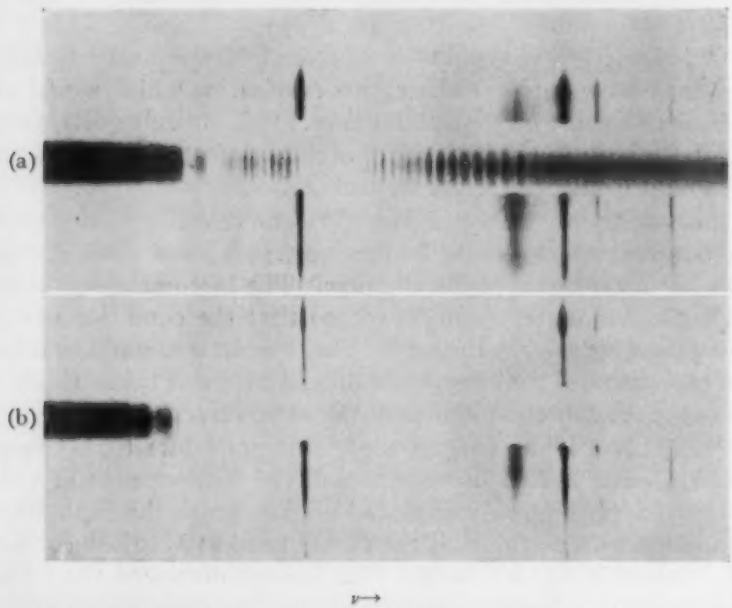

Fig. 3. (a) Absorption picture with 2.1 cm NO pressure. (b) Absorption picture with 2.1 cm NO+44 cm N_2 pressure. A comparison shows that in (b) every rotational line is broadened so much that the absorption becomes complete.

free from all traces of oxygen otherwise NO_2 would be formed in the absorption tube and this molecule gives a continuous absorption in the region in question. Pure N_2 was obtained by heating sodium azide in a flask from which all the air had been exhausted beforehand. The gas was then dried in a tube containing P_2O_5. Pictures were taken with pressure ratios varying between 1 in 1800 and 1 in 500. Definite differences in the intensity of the absorption of the main and isotopic heads were found for all ratios outside 1 in 990 and 1 in 1160. Within this region ten photographs were taken at different pressure ratios, but, as it is difficult to decide definitely about their intensities, an average is taken over all ten values giving as result a relative abundance

[30] M. C. Teves, Zeits. f. Physik **48,** 244 (1928).
[31] P. M. Morse, Phys. Rev. **34,** 57 (1929).

of O^{18} of one in every 1076 O^{16} atoms. Taking the mean of the two extreme ratios where definite differences of the same amount could be observed in the intensities a ratio 1/1075 is found for the abundance. Although the first calculation gives a probable error of only three percent, the maximum error is given as ten percent, as systematic errors might occur in the method used. The abundance ratio of O^{16} to O^{18} is therefore given as 1075 ± 110.

After obtaining the above result two comparison pictures were taken with helium instead of N_2 to make sure that no resonance effect between NO and N_2 was present. The pictures indicated that the given abundance ratio was correct.

The result differs by about 14 percent from that given by Babcock, but as Birge[32] gives a probable error of 25 percent for Babcock's values this deviation does not seem too large. Further, Babcock compares the absorption of the oxygen in the laboratory and hence at atmospheric pressure with the oxygen in the atmosphere where the pressure varies exponentially to zero. Hence the pressure broadening which, as pointed out above, is very great, is much more effective in the first case where all the oxygen is at atmospheric pressure than in the second case where only the oxygen near the ground is at atmospheric pressure. This would give a result which would differ from the one obtained with the same pressure in both cases in the sense of the result found here.

Babcock finds the relative abundance of O^{18} and O^{17} to be eight to one. If a maximum error of ten percent is allowed for this value and the relative abundance of O^{16} and O^{18} is assumed to be 1075 ± 110 as found here, the relative abundance of O^{16} and O^{17} becomes 8600 ± 1750.

The relative abundance of N^{14} and N^{15}. As stated above the overlapping of the fine structure due to the $N^{14}O^{18}$ molecule, made it impossible to determine the abundance of the $N^{15}O^{16}$ molecule in the same way. Here the circumstance that the $Q_1N^{14}O^{18}$ and $P_1N^{15}O^{16}$ heads lying close together are of the same intensity was made use of. At very low pressures practically no fine structure of the isotopic heads is present and therefore the conclusions following this observation are rigid. It was further noticed that the $P_1N^{15}O^{16}$ head was more intense than the $Q_1N^{15}O^{16}$ head. This resulted from the fact that the main $P_1N^{14}O^{16}$ head was less strongly absorbed than the corresponding Q_1 head. The ratio of the main P_1 and Q_1 heads could easily be determined by taking different pressures in the absorption tube and observing at which pressures the heads had the same intensity. The ratio of these pressures was found to be 0.65 ± 0.1 and this is evidently the intensity ratio of the main heads, the P_1 head being less intense. This result could also be verified by taking microphotometer curves of the heads with a Moll apparatus and averaging the area under each of the heads. This result agreed accurately with the above result. The fact that the $Q_1N^{14}O^{18}$ and $P_1N^{15}O^{16}$ heads are equally intense can therefore only be ascribed to the fact that the $N^{14}O^{18}$ must be less

[32] R. T. Birge, Phys. Rev. Suppl. **1**, 69 (1929).

abundant than the $N^{15}O^{16}$ in the same ratio as the Q_1 head is stronger than the P_1 head.

This result therefore gives us as relative abundance of $N^{14}O^{18}$ and $N^{15}O^{16}$ molecules the ratio 0.65 ± 0.1 and hence as the relative abundance of N^{14} and N^{15} the ratio 1075×0.65 or 700 ± 140. In this case the maximum error is given as 20 percent, since the ratio 0.65 may be affected as much as ten percent by systematic errors.

Discussion. The existence of the O^{18} and O^{17} isotopes seems to be quite certain. This, however, affects Aston's[33] atomic weights determined by means of the mass spectrograph with respect to the chemical atomic weights.[34] Aston assumes the atomic weight of the O^{16} isotope to be 16.0000, whereas the chemical method defines the average atomic weight of the O^{16}, O^{17} and O^{18} isotopes as 16.0000. The actual atomic weight of the O^{16} isotope can now be calculated by making use of the relative abundance determined above. The atomic weight of the O^{16} isotope can be computed from the following relation:

$$1074 \times 8x + 8 \times 18 + 17 = (1075 \times 8 + 1)16.0000 \qquad (4)$$

from which we get $x = 15.9980 \pm 0.0002$. We see therefore, that although the maximum error in the relative abundance of the oxygen isotopes is very large, the value of the atomic weight of the O^{16} is little affected. It is easily seen that it makes no difference in the result whether 18 or 17.991,[35] as recently found by Mecke and Wurm to be the atomic weight of O^{18}, is used. If the chemical atomic weight 16.0000 is our standard, Aston should use 15.9980 ± 0.0002 as the atomic weight of the O^{16} isotope, if he expects to obtain an agreement between his values and those obtained by chemical methods. This change in value of the O^{16} isotope used as standard by Aston corresponds to a change of 1.25 ± 0.13 in 10000. This does not mean that Aston's determinations of the atomic weights are less accurate than 1 in 10000 as given by himself, but just gives the amount by which all his values have to be corrected in order to allow a comparison with the values obtained by chemical methods.

We can now proceed to correct Aston's values by 1.25 ± 0.13 in 10000. In Table II the corrected values of Aston are compared with the chemical determinations. The elements chosen are those which have no isotopes as far as we know, or which have rare isotopes, as these are the only cases where a direct comparison is possible.

A comparison of columns 1 and 3 reveals a number of interesting points. In the case of hydrogen a correction of Aston's value makes the agreement wores, but the corrected value can be made to agree with the chemical value by assuming an error of 0.00011 which is well within the maximum error allowed for.

[33] F. W. Aston, Proc. Roy. Soc. **115A**, 487 (1927).
[34] Cf. R. T. Birge, Phys. Rev. Supplement **1**, 19 (1929).
[35] R. Mecke and K. Wurm, Zeits. f. Physik **61**, 37 (1930).

TABLE II. *Atomic weights.*[36]

Atom	Chemical method	Aston's mass spectrograph	Aston's values corrected by 1.25 in 10000
H	1.00777 ± 0.00002	1.00778 ± 0.00015	1.00766 ± 0.00016
He	4.0018 ± .0003	4.00216 ± .0004	4.00166 ± .00045
C	12.0025 ± .00019	12.0036 ± .0012	12.0021 ± .0014
N	14.0083 ± .0008	14.008 ± .0028	14.0063 ± .0030
O	16.0000 ± .0000	16.0000 ± .0000	15.9980 ± .0002
F	19.00	19.0000 ± .0019	18.9976 ± .0021
P	31.027	30.9825 ± .0046	30.9786 ± .0050
As	74.96	74.934 ± .010	74.925 ± .011
I	126.93	126.932 ± .025	126.916 ± .027

In the case of He the corrected value agrees to 1 in 30000 with the chemical value 4.0018. This correction therefore does away with a very bad discrepancy between Aston's values and the chemical values. Further, as pointed out by Birge[37] this value agrees accurately with Eddington's[38] calculated value for an ideal rigid nucleus. This agreement might be due to chance as the value still has a large maximum error and hence it cannot be assumed from this that the helium atom really has a rigid nucleus.

Birge and King have recently discovered an isotope of carbon of mass 13. One would therefore expect the chemical atomic weight to be higher than that found by Aston. The reverse is the case, however. If Aston's value is corrected one obtains a value of 12.0021 which is in close agreement with the chemical value 12.0025 and still allows for the presence of the isotope C^{13}. From these values the calculated abundance of the C^{13} isotope is 1 in 2500 but this seems to contradict Birge's[7] results according to which the C^{13} isotopt should be more abundant relative to C^{12} than the N^{15} relative to N^{14}, bu the given atomic weights still have a large probable error which may accoun for this discrepancy.

In the case of nitrogen the abundance of the N^{15} has been determined as 1 in 700 ± 140 N^{14} isotopes. From this we can determine what the expected atomic weight of the N^{14} isotope should be, for

$$700x + 15 = 701 \times 14.0083 \pm 0.0008 \qquad (5)$$

or

$$x = 14.0069 \pm 0.0012.$$

This value agrees with Aston's corrected determination 14.0063 to within 1 in 20000.

For F, P and As the chemical values are given with less accuracy, but a comparison of Aston's corrected value of P with the chemical value leads

[36] Most of the values with their probable errors given in the first column are taken from the excellent discussion by R. T. Birge, Phys. Rev. Supplement **1**, 18 (1929). The values in column 2 with their maximum errors are obtained from Aston's paper, Proc. Roy. Soc. **115A**, 487 (1927). The chemical values for F, P, As and I are taken from the Second Report of the International Committee on Chemical Elements, J. Am. Chem. Soc. **47**, 597 (1925) and the German Committee, Berichte **62**, 1 (1929).

[37] R. T. Birge, Phys. Rev. **35**, 1015 (1930).

[38] A. S. Eddington, Proc. Roy. Soc. **A126**, 696 (1930).

one to suspect the presence of heavier isotopes of P in small quantities. Although less certain, the same seems to be indicated by the corresponding values for F and As.

Until 1928 the German Committee[39] gave the atomic weight of I as 126.92 and Birge[40] finds as weighted average of Clark's values 126.926. This indicates that the real chemical value for I may still be on the lower side of 126.932—the value that is now accepted—and such a value will be in better agreement with Aston's corrected value 126.916.

Although it is difficult to draw definite conclusions from the above, it is quite clear that the sooner an agreement is reached by chemists and physicists as to the value which should be used as standard of atomic weight, the less confusion will exist as to the most accurate atomic weights.

Mr. F. Bueso-Sanlehi started this work but had to leave before obtaining any definite results. I wish to thank Professor R. S. Mulliken who suggested the search for isotopes in these NO bands and also wish to thank him and Dr. A Christy for their helpful suggestions and Professor H. B. Lemon for allowing me the use of the apparatus in his laboratory.

[39] Max Bodenstein, etc., Berichte **61B**, 1–31 (1928).
[40] R. T. Birge, Phys. Rev. Supplement **1**, 25 (1929).

THE MARGULES METHOD OF MEASURING VISCOSITIES MODIFIED TO GIVE ABSOLUTE VALUES

By Howard R. Lillie
Corning Glass Works, Corning, New York

(Received May 28, 1930)

Abstract

Measurement of absolute viscosities. A method for determining absolute viscosities in a Margules rotating cylinder type viscometer, without the aid of calibrating liquids of known viscosities, is described. This method involves the determination of true viscosity by extrapolating apparent viscosities for several lengths of inside cylinder to that viscosity corresponding to infinite length. By this method the viscosity of the commercial castor oil used is found to be 9.99 poises at 20°C, and 4.61 poises at 30°C, as compared with 9.86 and 4.51 poises quoted in the Smithsonian Tables for pure oil at corresponding temperatures.

End corrections. The additional length to be applied to the measured length to correct for finite dimensions is computed for several inside cylinders or spindles. When the radius of the outer containing cylinder is 3.2 cm, and the ends of the spindle are 1.5 cm from the upper and lower boundaries of the liquid, the corrections for spindle radii of 0.556 cm and 0.477 cm are found to be 0.62 cm and 0.52 cm respectively as long as the length of the spindle is 5 cm or greater. Accordingly, the end correction is apparently proportional to the 1.18 power of spindle radius.

Constancy of calibrating factor. Comparisons are also made between relative viscosities measured by this method and those for the same liquids measured by capillary flow. Results indicate that within experimental error these relative values are the same by both methods, for viscosities between 5 and 3500 poises, showing that the calibrating factor of the concentric cylinder system is constant over this range of viscosities.

IN A previous paper,[1] the apparatus and method were described for measuring viscosities of molten glasses (10^2 to 10^7 poises) by the use of concentric cylinders. A simple way of determining the effect of the use of cylinders of finite length was also described. However, since this determination was made for only one viscosity—that of castor oil at room temperature—the question remained as to whether one can assume that the calibrating factor is entirely independent of viscosity when the ends of the cylinders are present. Measurements were accordingly undertaken with the object of comparing the relative viscosities of two liquids differing quite widely in this property, as found by the concentric cylinders and as given by the method of capillary flow, for which a constant calibrating factor is more generally accepted.

In a majority of cases, investigators of glass viscosities[2] have found, by more or less rigorous calibration with standard liquids, that the calibrating factor is apparently independent of viscosity. On the other hand, in an

[1] H. R. Lillie, J. Am. Ceramic Soc. **12**, 505–529 (1929).

[2] S. English, J. Soc. Glass Tech. **8**, 205 (1924). Stott, Irvine and Turner, Proc. Roy. Soc. **A108**, 154 (1925). Proctor and Douglas, Proc. Phys. Soc. (London) **41**, 500 (1929). M. Volarovich. J. App. Phys. Moscow **5**, 185 (1928).

investigation of the viscosities of soda-lime glasses over a large field of compositions, Washburn[3] found that his factor existing between force per unit shear and viscosity apparently varied by a factor of about three over the range of viscosities dealt with. Comparisons made by others have shown that agreement between their results and those of Washburn can be reached only if his calibrating factor be changed to a constant or their own made variable.

Since in any rotation method the torque is simply proportional to the viscosity and to the velocity gradient at the very surface of the cylinder upon which the torque is exerted, a variation in the factor connecting torque and viscosity for a given total relative angular motion between the two cylinders, would indicate that the velocity gradient at the surface of the cylinder is not proportional to the total relative velocity alone. In other words, the velocity distribution would have to depend on viscosity. The result of this would be that if the temperature of a liquid, contained between a stationary cylinder and one rotating with a constant speed, be changed so as to alter its viscosity, some parts of the liquid would be thereby slowed down while others would rotate faster in order to change the velocity gradient to the cylinders' surfaces. This is only conceivable if centrifugal or other forces tending to disturb the regular motion of the liquid have more effect in the less viscous liquid. This may be true in the case of cylinders of finite length.

Measurement by the Concentric Cylinder Method

Mathematical procedure.

As reported in the previous papers, viscosities have been measured without the aid of actual calibration with standard liquids, simply by determining the magnitude of the "end effect" at some arbitrary viscosity and assuming a constant calibrating factor for all viscosities. The end effect was determined by first finding the apparent viscosity of the liquid, using inside cylinders or spindles of various lengths, by using the formula

$$T = \frac{4\pi\eta\Omega R_1^2 R_2^2 l}{R_2^2 - R_1^2} \tag{1}$$

where T is the torque on the inner cylinder, η the viscosity, Ω the angular velocity of the outer cylinder, R_1 and l the radius and length of the inner cylinder and R_2 the radius of the outer rotating cylinder. These apparent viscosities were then plotted against reciprocals of spindle length and the "true" value of η corresponding to infinite length found by extrapolation. A correction to l was then found for each spindle. This correction is not the same for all lengths of spindles of the same diameter, supposedly because the amount of deformation of the flow surfaces around the body of the spindle depends on the length of the spindle itself.

Some minor changes have been made in the method of computation of apparent viscosity. We have the relations

[3] Washburn, Libman and Shelton, Univ. of Illinois, Eng. Expt. Sta., Bull. No. 140 (1924).

$$T = K\theta = \frac{KZD}{2d}$$

and

$$\Omega = \frac{2\pi}{t},$$

where K is the constant of the suspension, determined as described in the previous paper, θ its angular displacement, D the deflection as read on a scale at a distance d from the mirror, Z the correction for straight scale and t the time for one revolution of the containing cylinder. Eq. (1) becomes

$$\frac{KZD}{2d} = \eta \frac{8\pi}{t}(\pi R_1^2 l)\frac{R_2^2}{R_2^2 - R_1^2},$$

or, for apparent viscosity,

$$\eta = \frac{ZDt}{d}\left[\frac{K}{16\pi V}\left(1 - \frac{R_1^2}{R_2^2}\right)\right] \tag{2}$$

where V is the total volume of the spindle. The quantity in the brackets is a constant for any one spindle since a constant value of $R_2 = 3.2$ cm was used during the whole investigation. All apparent viscosities were computed from this equation.

Fig. 1 represents diagrammatically the experimental viscometer used. A water bath is contained in a large cylindrical can placed on the rotating table V of the viscometer frame described previously. This can is surrounded by a galvanized water jacket J, the purpose of which is to maintain an external temperature below that of the bath. The outer cylinder of the measuring viscometer, C, containing the liquid under investigation, is supported at the center of the bath by a hollow pedestal of brass and is closed by a threaded top carrying a small upright tube which extends through the surface of the water bath and allows the inner cylinder or spindle E to hang into the liquid. This spindle is held by a brass connector D upon which is fastened the mirror M, all of which hangs from the calibrated steel wire suspension B. With the exception of spindle No. 53, described later, the two ends of the spindle were 1.50 cm distant from the surface of the oil and the bottom of the container.

The temperature is maintained constant by means of a vapor pressure regulator R constructed as shown. Methyl formate was found to be the most satisfactory liquid for actuating the mercury column. Various temperatures can be obtained by adjusting the pressure of air in the top part of the regulator. The contacts of the regulator are connected in series with a small flashlight dry cell and a telegraphic relay, both of which are fastened to the transite cover piece of the rotating can. This relay makes and breaks the circuit through the heater H consisting of three units of nichrome wire which can be connected in various ways depending on the temperature desired. The current for the heater is supplied through mercury cups at the extreme bottom of the viscometer frame. Circulation of the water bath is maintained

by a small toy electric motor directly connected to the shaft of the stirrer *A*. This stirrer is so built as to take water in from top and bottom and eject it tangentially at the center. Current for the motor is supplied by a large 4 volt storage battery, through brushes acting on rings around the outside of the jacket *J*. It was found necessary to house the motor completely to prevent disturbance of the spindle due to air currents from the armature. At times

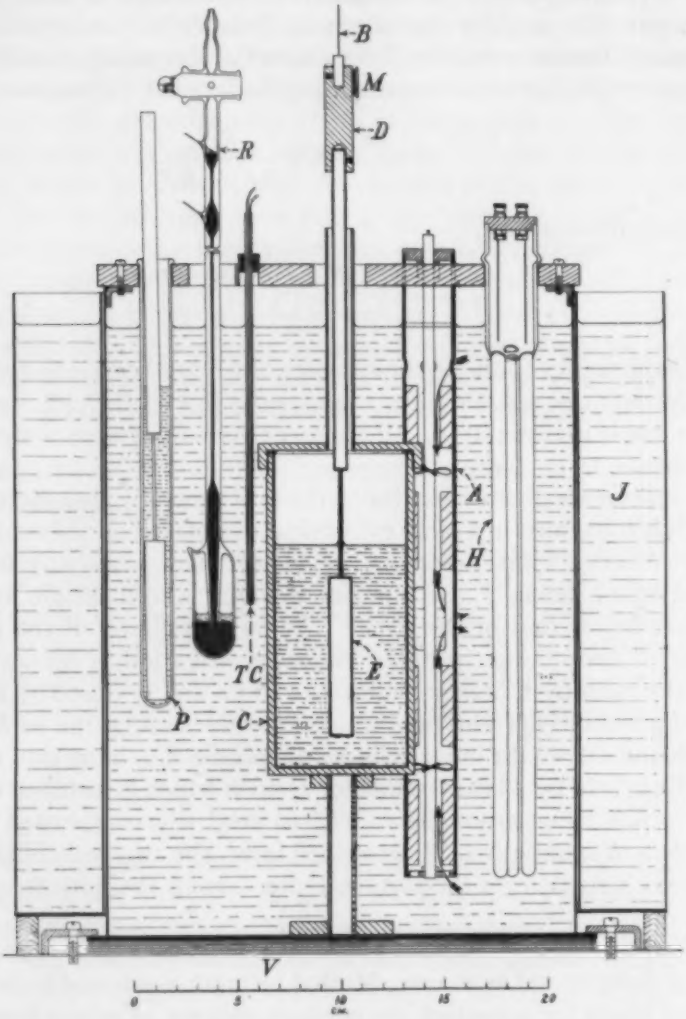

Fig. 1. Diagram of apparatus.

when various spindles were being used, one after another, a preheating tube *P* was installed containing some of the same oil as was being used in *C* so as to allow the next spindle to come to temperature before being placed in the central position. Temperatures were measured by means of three copper-constantan thermocouples placed as shown (*TC*) and connected in series through junctions kept at 0°C. A precision potentiometer accurate to less

than 1 microvolt was used for e.m.f. readings. These couples measured the average temperature of the bath to within 0.05°C and were sensitive to changes of less than 0.01°C. Their condition was checked periodically with a standard mercury thermometer to make sure that no short circuits were causing them to be far in error.

Temperature control.

Since all temperature readings made during actual viscosity measurements were for the water bath instead of for the liquid inside the viscometer proper, a few test runs were made to establish the relations between these temperatures. By placing a second set of couples in the center of the oil its temperature could be followed while the bath was cooling, heating, and just after it had come to equilibrium. In this way the following conditions were found:

Heater turned off: temperature lag 2.3°C, time lag 35 min.
Heater turned on: temperature lag 1.3°C, time lag 17 min.
(rate 0.08°C/min.)

Length of time after regulator began working, for oil to be
within 0.05°C of bath: 50 min.
within 0.01°C of bath: 70 min.

Accordingly, about two hours were always allowed, after the regulator began to function, before any viscosity readings were made. It was also observed that when the regulator had been in action for some time no periodic fluctuation of temperature in the oil could be detected.

Effective spindle length.

For determining "true" viscosities by extrapolating the apparent values for several spindles of equal radii but various lengths to the value corresponding to infinite length, five spindles of 3/8″ diameter and five of 7/16″ diameter were used. Their actual dimensions were:

No.	R_1	l	$1/l$	No.	R_1	l	$1/l$
101	0.4766 cm	10.14 cm	0.0986	106	0.5561 cm	10.22 cm	0.0979
102	.4771	7.61	.1314	107	.5562	7.60	.1315
103	.4769	5.08	.1969	108	.5564	5.12	.1953
104	.4768	3.80	.263	109	.5561	3.82	.262
105	.4770	2.53	.396	110	.5561	2.54	.394
Mean	0.4769			Mean	0.5562		

The observed apparent viscosities found by the use of these spindles (R_2 constant and equal to 3.2 cm) are shown in Table I. The ratios of viscosity at 23.40°C and 28.20°C to that at 19.97°C, as given by each spindle, are also shown. It is quite evident that over this small range of viscosities relative results are independent of the spindle used. A mean of these ratios for the two higher temperatures was accordingly taken, weighting each value according to spindle length, and all the viscosities recomputed back to the basis

TABLE I

Spindle No.	Observed Values								Mean l'	Values read from curve (Fig. 2)		
	19.97°C η=10.020		23.40 η=7.633			28.20 η=5.295						
	App. η	l'	App. η	Ratio	l'	App. η	Ratio	l'		App. η	l'	
101	10.53	0.51	8.03	0.762	0.60	5.61	0.533	0.60	0.55	10.53	0.51	
102	10.67	.49	8.15	.763	.51	5.62	.527	.56	.52	10.70	.52	0.517
103	10.99	.49	8.41	.766	.52	5.86	.534	.54	.52	11.07	.52	
104	11.29	.48	8.57	.760	.47	5.92	.525	.45	.47	11.33	.50	
105	11.72	.43	9.10	.776	.49	6.17	.526	.41	.44	11.75	.43	
106	10.63	.63	8.09	.761	.61	5.63	.529	.63	.62	10.63	.62	
107	10.85	.63	8.28	.762	.64	5.75	.529	.66	.64	10.84	.62	0.620
108	11.27	.64	8.54	.757	.60	5.90	.523	.58	.61	11.24	.62	
109	11.65	.62	8.83	.757	.59	6.09	.522	.57	.59	11.61	.60	
110	12.19	.55	9.21	.756	.52	6.43	.527	.54	.54	12.16	.53	
			Mean ratios	.7618			.5284					

of 19.97°C. This process gave the points plotted in Fig. 2. Since for a given radius of spindle the relation between apparent viscosity and reciprocal of length appeared to be a linear one for values of l greater than 5 cm, this was assumed to be true and the apparent viscosities as given by the six longest spindles were used for determining the best pair of straight lines intersecting

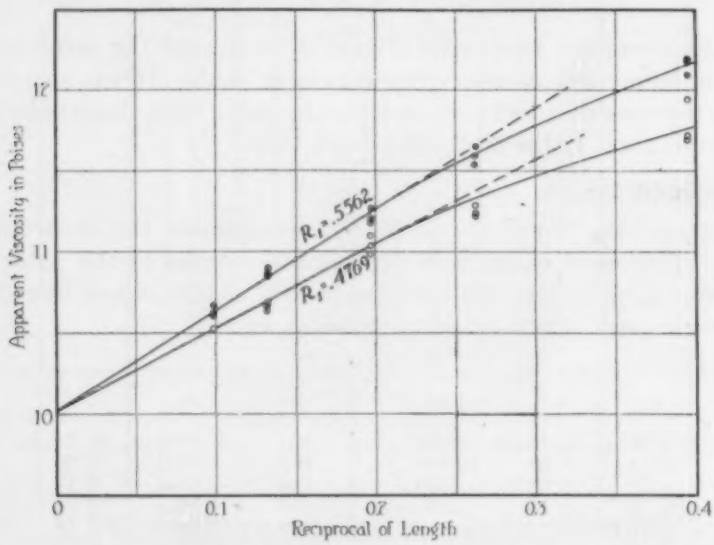

Fig. 2. Apparent viscosities of castor oil. Spindles 101–110 inclusive. Converted to 19.97°C

at $1/l=0$. In so doing it was discovered that the sum of the deviations become minimum for the two lines separately as well as collectively when the intercept was made at 10.020 poises. The average deviation in this case was about 0.3 percent, using only those spindles of length greater than 5 cm. The curved part of each line was drawn by estimate.

Using the extrapolated intercept as the true viscosity at 19.97°C and the mean ratios shown in Table I for computing the corresponding values at the

two higher temperatures, the following comparison is made with viscosities of pure castor oil as given by the Smithsonian Tables:

Temp.	Observed	Sm. T.
19.97°C	10.020 poises	9.92 poises
23.40	7.633	7.42
28.20	5.295	5.14
$\Delta \log \eta/\Delta 1/T$	297	302

Fig. 3 shows these two sets of data plotted as logarithms against the reciprocal of absolute temperature. This method of plotting was used in order to obtain a linear relation, thus facilitating interpolation. The figure includes also a similar curve for values proportional to viscosity as obtained later by capillary flow.

We now have sufficient means for computing some sort of correction to be applied to each spindle to account for the additional torque exerted by virtue of its finite length. Since others have assumed that this may be expressed in terms of an additional length of spindle which remains constant for a constant radius, it will be so computed in this case. If l' is this additional length, we have

$$l' = l\left(\frac{\text{app. } \eta}{\text{true } \eta} - 1\right).$$

Values for this correction computed from observed apparent viscosities and for those read from the curves in Fig. 2 have been included in Table I. For lengths greater than 5 cm a constant correction is obtained for each radius as follows:

$$R_1 = 0.5562 \text{ cm}, \qquad l' = 0.620 \text{ cm}$$
$$R_1 = 0.4769 \text{ cm}, \qquad l' = 0.517 \text{ cm}$$

from which we have the relation:

$$l' \text{ proportional to } (R_1)^{1.18},$$

indicating that the end correction when stated in terms of additional spindle length varies approximately as the first power of radius.

Temperature runs.

In order to determine more accurately the temperature viscosity relations for the oil, a run was made with each of four spindles, in each case leaving the spindle undistrubed while the temperature was varied. For this purpose two spindles, No. 101 and No. 107, from the previous runs were used, together with two others of special sizes.

Spindle No. 53. In a previous trial of various spindles with specially shaped ends it was found that one with conical ends showed the least variation of torque with variation of the distance from the bottom of the oil to the end of the spindle. Many subsequent determinations of glass viscosities

were made using such a spindle, consisting of platinum-iridium and having the following dimensions:

$$R_1 = 0.477 \text{ cm}, \quad l = 3.82 \text{ cm}, \quad V = 3.010 \text{ cc},$$

where l is the length of the cylindrical portion. Each end of the large portion of the spindle terminated in a 90° cone, while the whole was supported by a stem of about 0.16 cm diameter. A duplicate of this spindle was made of iron and called No. 53. Its distance of 1.5 cm from the upper and lower boundaries of the oil was measured to its cylindrical portion instead of to its pointed ends.

Spindle No. 152. Another spindle used considerably in glass is the one of "sillimanite" described in the previous paper on glass viscosities. It is nearly the same as spindle No. 101 but is held by a porcelain stem of 1/4″ double-bore thermocouple tubing. A similar one was made of brass of dimensions:

$$R_1 = 0.5151 \text{ cm}, \quad l = 10.18 \text{ cm}, \quad R' = 0.3174 \text{ cm}, \quad V = 8.960 \text{ cc},$$

where R' is the radius of the stem. This was called spindle No. 152.

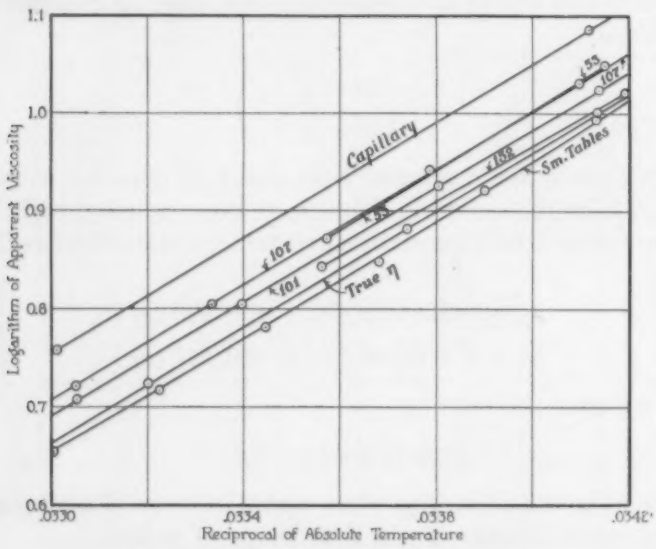

Fig. 3. Temperature runs in castor oil.

Table II gives the results for apparent viscosity of the castor oil obtained with these four spindles. The values for 20°C were interpolated on the curves in Fig. 3.

It is quite evident that the result obtained with spindle 152 at 19.47°C is in error since the slope of the curve for this spindle is less than for any of the others. Also, the similarity of No. 152 to No. 101 suggests an apparent viscosity at 20°C more nearly equal to 10.5. However, this trouble was not discovered until after the viscometer was dismantled and no redetermination was made.

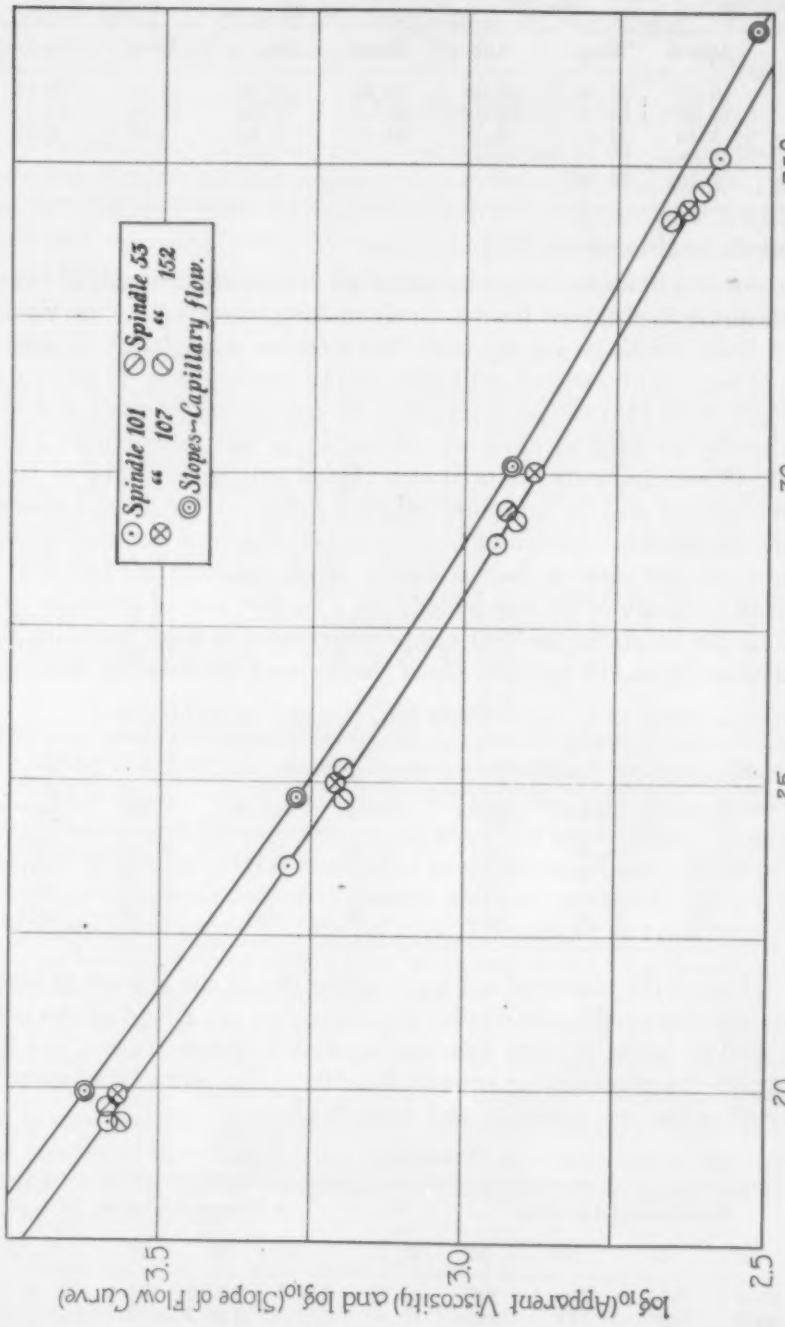

Fig. 4. Apparent viscosities of glucose solution.

TABLE II.

No. 101		No. 107		No. 53		No. 152	
Temp.	App. η	Temp.	App. η	Temp.	App. η	Temp.	App. η
19.94	10.57	20.00	10.99	19.84	11.20	19.47	10.52
20.00	10.50	20.30	10.74	20.00	11.04	20.00	10.10
22.83	8.44	23.00	8.77	24.87	7.45	24.97	6.97
26.46	6.38	26.99	6.36				
29.55	5.10	29.59	5.26				

Measurements in glucose solution.

For the purpose of measuring relatively high viscosities, a supply of heavy glucose solution was obtained from a candy making concern. At the time it was drawn from the large supply tank this solution was placed in several pint jars and kept tightly sealed until used for the various runs. It was found in preliminary tests that evaporation could be completely stopped and surface film thereby avoided by covering the surface of the glucose with a thin layer of oil. Observation also showed that the oil had no tendency to creep between the glucose and its container, while a sharp surface always showed between the two liquids. Accordingly, as soon as the glucose had been placed in the cylindrical container of the viscometer and the spindle had been put in place, a small quantity of oil was added. As a further test of constant concentration of the solution, the first temperature used in each viscosity run was repeated at the end of the run. Good checks were consistently obtained.

TABLE III.

No. 101		No. 107		No. 53		No. 152	
Temp.	App. η	Temp.	App. η	Temp.	App. η	Temp.	App. η
19.45°C	3836	19.90	3707	19.70	3842	19.45	3650
23.64	1940	25.00	1627	25.24	1576	24.74	1581
28.88	885	30.04	771	29.43	854	29.25	823
35.15	385	34.30	436	34.20	447	34.60	411

Table III gives the observed apparent viscosities of the glucose as found by the four spindles used in the similar runs in castor oil. Fig. 4 shows these results plotted in terms of their logarithms against temperature. The line drawn through the points is for spindle No. 101. The other three spindles would give three curves parallel to and near this line.

TABLE IV

Spindle No.	Apparent η for glucose				Oil at	η glucose $\div \eta$ oil at 20°			
	20°	25°	30°	35°	20°C.	20°	25°	30°	35°
101	3506	1574	760	392	10.50	334.0	150.0	72.4	37.3
107	3608	1630	777	396	10.99	328.2	148.3	70.7	36.0
53	3658	1637	789	410	11.04	331.0	148.1	71.4	37.7
152	3342	1521	744	385	10.10	331.0	150.7	73.6	38.1
					Mean	331.1	149.3	72.0	37.3
						±0.5%	±0.7%	±1.4%	±1.7%

Table IV gives values read from this family of curves corresponding to the various temperatures stated. From these values have been computed the viscosities of the glucose solution relative to castor oil at 20°C, as determined with the same spindles (Table II).

Measurement by Capillary Flow Method

The second part of the investigation consisted of measuring the relative viscosities of castor oil and glucose solution over the same range of temperatures by capillary flow. The same capillary viscometer was used for both liquids and the rates of flow so regulated as to make the maximum rates of shear as nearly as possible the same as those which prevailed in the cylinder method.

Apparatus.

The thermostat used was essentially the same as that described above for the rotating cylinder apparatus, with the exception of one slight change. A side tube was sealed into the regulator just above the top of the mercury column, this tube terminating in a large bulb immersed in the water bath. The purpose of this was to reduce further the effect of changing room temperature on the pressure over the column.

Fig. 5 is a sketch of the viscometer. Two similar reservoirs r_1 and r_2 are connected by the capillary C selected for roundness and uniformity of bore. The dimensions of the bore were found to be:

$$R = 0.1175 \text{ cm}; \quad R^4 = 1.905 \times 10^{-4} \text{ cm}^4; \quad L = 9.992 \text{ cm}$$

The ends of the capillary were ground and polished perpendicular to the axis. DeKhotinsky cement was used for fastening into the reservoirs, care being taken to have the two sides as symmetrical as possible. To avoid slipping when the higher temperatures and pressures were used, the bottom part of the viscometer was buried in plaster of Paris as shown. The reservoirs are fitted with screw tops A made of brass. The tubes t_1 and t_2 lead to a system of stopcocks which allow either tube to be connected to pressure or suction systems or to the volumetric manometer at will. This manometer is constructed as shown at the right of Fig. 5. The left-hand leg a is graduated in cm and has been calibrated for volume. The liquid used in diphenyl oxide, chosen for its low viscosity and low vapor pressure. By keeping the levels equal in tubes a and b by means of the counter columns of mercury in c and d, the volume of flow through the capillary C can be followed and measured. This flow is corrected for temperature differences between the bath and the room by the following:

$$F = V(T_1/T_2)$$

where F is the actual flow through C, V the volume registered in the manometer, T_1 and T_2 the absolute temperatures of bath and room respectively.

The pressure system contains a large carboy for holding the pressures constant during measurements.

Measurements for castor oil.

Technique: For creating such a small rate of flow as was desired, very small pressures were necessary. This meant that a difference in level in the two reservoirs would have an effect on the rate of flow. The following method was used for avoiding error from this source: Both reservoirs were first opened to

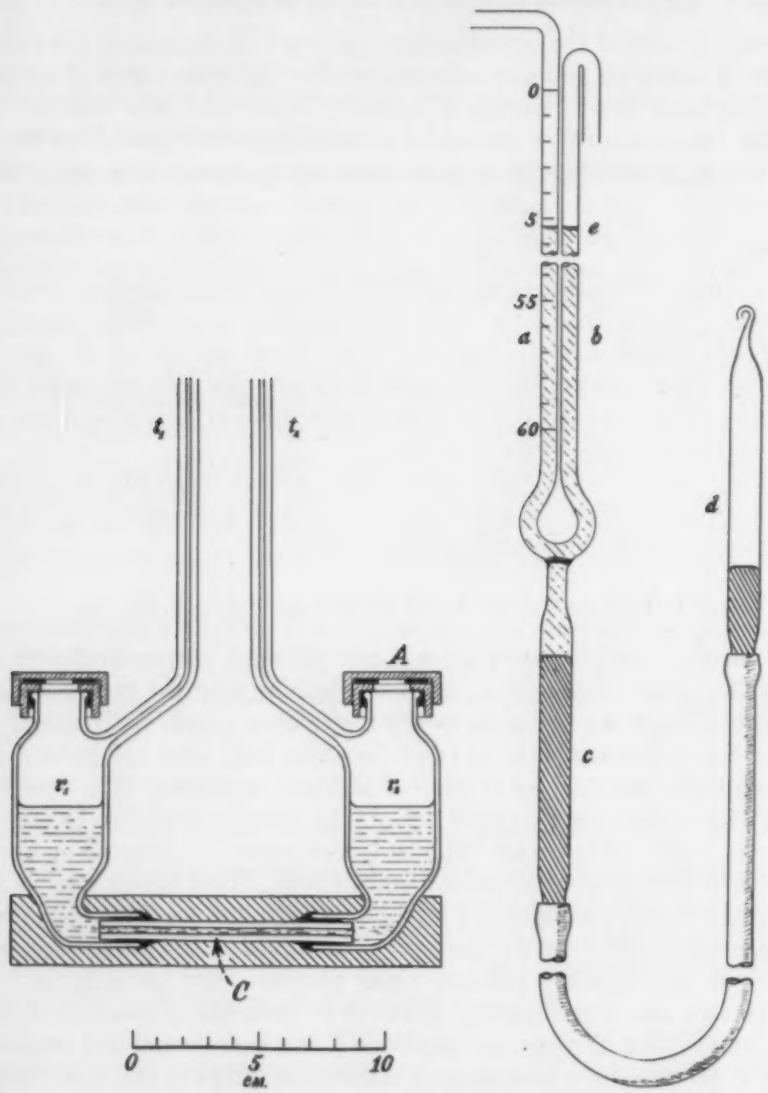

Fig. 5. Sketch of viscometer.

atmospheric pressure and the liquid allowed to come to rest. One tube, e.g. t_1, was then connected to the volumetric manometer, the columns *a* and *b* being first adjusted to about the 30 cm mark. A slight suction was then caused in r_2 and the oil made to flow back until the colunns *a* and *b* reached the 10 cm mark or thereabouts. At this time r_2 was connected to the pressure

system and, keeping atmospheric pressure in r_1 by lowering d to keep a and b on a level, time readings were made for each 2 cm drop in a by means of a split-time watch. These time readings were then plotted against the corresponding column positions, giving a slightly curved line whose slope at 30 cm was the rate of flow corresponding to zero hydrostatic pressure.

In the case of castor oil, pressures were measured by means of a Nujol manometer and later converted to the usual cm of mercury units.

Results: The actual numerical results will not be quoted here. Fig. 6 shows them graphically, the two kinds of points plotted representing the two

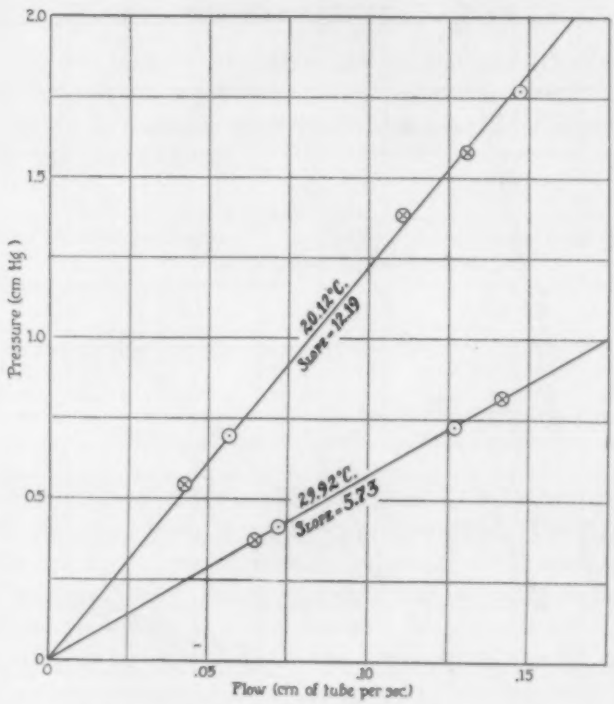

Fig. 6. Pressure-flow relations for new castor oil.

directions of flow through the capillary. It is evident that the system is quite nearly symmetrical and that the relation between rate of flow and pressure is a linear one. The slopes are:

29.92°C	5.73
20.12	12.19
20.00 (extrapolated)	12.31

These slopes, proportional to viscosity, have been plotted in Fig. 3. The value obtained in this case for $\Delta \log \eta / \Delta(1/T)$ is 297 as compared with 297 for the concentric cylinders and 302 for values from the Smithsonian Tables. This indicates that the oil itself differs slightly from that for which the viscosities in the Tables are quoted.

Measurements for glucose solution.

Technique. In order to have about the same rates of flow in the glucose solution as in the oil, very much higher pressures were used. This fact made the effect of difference of level between the two reservoirs negligible in comparison with the other forces acting. It was, therefore, unnecessary to carry out the procedures as outlined above, the flows being now measured simply by taking the total time for a certain flow—usually 10 cm in the volumetric manometer.

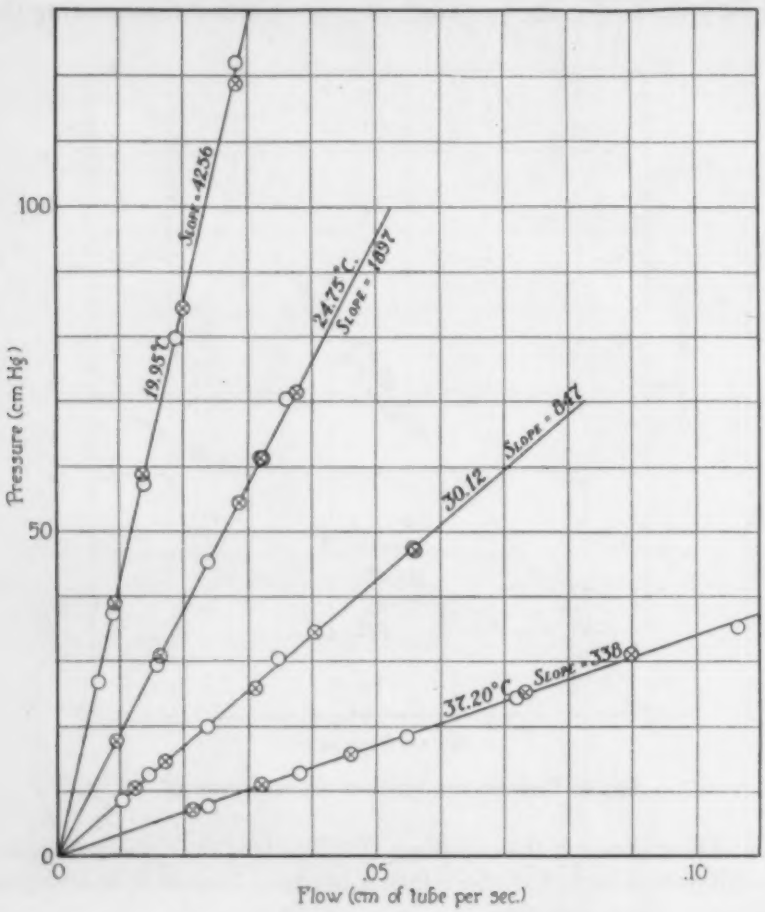

Fig. 7. Pressure-flow relations for glucose solution.

A covering of oil over the glucose was used as before and bubbles were eliminated by warming and slightly reducing the pressure for a very short time. In this case mercury was used in the pressure manometer. No suction was used over the glucose at any time during the measurements. It was found necessary to use a soft wax in the stopcocks of the pressure system. Pressure was obtained from a cylinder of nitrogen by the use of a reducing valve, a stopcock being closed between the pressure system and the reducing valve during the flow observations.

Results. Fig. 7 shows the pressure-flow relations for the glucose solution. As in the case of castor oil, it is evident that the two directions of flow agree and that the relations are represented by straight lines. It may be said in this connection that any small difference observed in apparent viscosity as the pressures were decreased seemed to be toward lower values instead of toward high ones as would be expected if plasticity were present in the glucose.

The slopes of the observed pressure-flow lines are:

37.20°C	338 ± 4	24.75°C	1897 ± 21
30.12	847 ± 11	19.95	4256 ± 53

These values, proportional to viscosity, are plotted logarithmically in Fig. 4. Values for the reference temperatures, interpolated by means of this graph, are shown in Table V, together with viscosities relative to castor oil at 20°C, as obtained by the two methods.

TABLE V.

Temp.	Interpolated slope	Oil at 20°C	η relative to castor oil at 20°		Deviation of cylinders from capillary
			capillary	cylinders	
20°C	4220 ± 53	12.31	$342.5 \pm 1.3\%$	$331.1 \pm 0.5\%$	$-3.4\% (\pm 1.8\%)$
25	1824 ± 21		$148.1 \pm 1.1\%$	$149.3 \pm 0.7\%$	$+0.8\% (\pm 1.8\%)$
30	865 ± 11		$70.3 \pm 1.3\%$	$72.0 \pm 1.4\%$	$+2.4\% (\pm 2.7\%)$
35	446 ± 6		$36.2 \pm 1.3\%$	$37.3 \pm 1.7\%$	$+3.1\% (\pm 3.0\%)$

The table also gives the deviations of values of relative viscosity as obtained by the cylinders from those by capillary flow. The figure in parentheses following each of these deviations is the sum of the estimated probable errors for the two methods taken to represent the probable error to which the final comparison is subject. The fact that this deviation is zero for about 2000 poises, while it must be zero also for the viscosity of the oil, indicates that errors in the measurements themselves, and in the various graphical interpolations made, are responsible for all the deviations. If this can be considered true it may be said that the calibrating factor of the concentric cylinders remains constant over the range of viscosities between 5 and 3500 poises. In any case the deviation from constancy is very small.

Rates of shear.

In the rotating cylinder system, the expression for rate of shear is:

$$s = \frac{2\Omega R_1^2 R_2^2}{r^2(R_2^2 - R_1^2)}.$$

This reaches a maximum when r is its minimum value R_1, or maximum rate of shear

$$S = \frac{2\Omega R_2^2}{R_2^2 - R_1^2} = 2.06\Omega \text{ approximately.}$$

The values of Ω used were from 0.233 to 0.524 radians/sec. The maximum rates of shear, then, ranged from

$$S = 0.48 \text{ to } 1.08 \text{ cm/sec/cm.}$$

In the capillary flow sytem, rate of shear is expressed by

$$s = \frac{-4rQ}{\pi R^4}$$

which reaches a maximum numerical value at $r = R$, or

$$S = \frac{-4Q}{\pi R^3}.$$

In the experiments reported above, Q was expressed in terms of cm of tube in the volumetric manometer. To convert the values to cc/sec. we must multiply the numbers by the volume of tube per cm (0.1131). This gives values of Q from 0.0045 to 0.017 for oil and from 0.0011 to 0.0113 for the glucose. Using $R^3 = 1.62 \times 10^{-3}$ we have $S = 3.54$ to 13.4 for oil and 0.86 to 8.9 for glucose. Although these limits do not correspond exactly to those found for the cylinders, they are of the same order of magnitude and actually overlap to some extent.

Capillary end correction.

The equation for viscosity by the capillary flow method is, since the kinetic energy correction is negligible,

$$\eta = \frac{\pi P R^4}{8Q}\left(\frac{1}{L+\lambda}\right)$$

where P is pressure in dynes/cm^2, Q volume rate of flow and R and L the radius and length respectively of the capillary. λ represents a length that must be added to L to give the effective length of the constriction through which the liquid must flow.

The viscosity of the castor oil at 20°C, found by the concentric cylinders is 9.99 poises. The slope P/Q found as 12.31 by capillary flow is in terms of cm of mercury per unit velocity of the column in the volumetric manometer. It is equivalent to 1.445×10^6 in c.g.s. units. Then we have

$$L + \lambda = \frac{\pi \times 1.905 \times 10^{-4} \times 1.445 \times 10^6}{8 \times 9.99}$$

$$= 10.83$$

But since $L = 9.99$ cm,

$$\lambda = 0.84 \text{ cm or about } 3.5 \text{ diameters.}$$

The experience of others has shown that λ is usually of the order of a few diameters.

Acknowledgment.

In conclusion, the writer wishes to express his appreciation for the assistance rendered by Dr. G. S. Fulcher in the preparation of this paper.

ERRATUM

THE DISPERSION FORMULA AND RAMAN EFFECT FOR THE SYMMETRICAL TOP

BY MORRIS MUSKAT

(Phys. Rev. **35**, 1262, 1930)

Exponents of the form $(2\pi i/h)\ t(W_a - W_b)$ should be preceded by a minus sign so that $\nu_{jk} = (W_j - W_k)/h$ and $\eta = +8\pi^2 A\nu/h$.

In the bracket of (21) read $[1 + \cdots]$ and in (25) $(j \mp 2m)$.

In $R(\nu + \nu_{j,\ j+1})$ the parenthesis should be $(j^4 + 3j^3 + 2j^2 + j^2m^2 + 8jm^2 + 12m^2)$ so that the numerical factor in $I(\nu + \nu_{j,\ j+1})$ becomes $128/3$.

LETTERS TO THE EDITOR

Prompt publication of brief reports of important discoveries in physics may be secured by addressing them to this department. Closing dates for this department are, for the first issue of the month, the twenty-eighth of the preceding month; for the second issue, the thirteenth of the month. The Board of Editors does not hold itself responsible for the opinions expressed by the correspondents.

Interpretation of the Visible Halogen Bands

The familiar absorption band spectra of the halogen molecules in the visible (and partly in the near ultraviolet) are commonly attributed to a $^1\Sigma \leftarrow {}^1\Sigma$ electron transition. That the lower level is $^1\Sigma$ is practically certain from the fact that Cl_2 is diamagnetic and from other considerations, while the $^1\Sigma$ character of the upper state is then indicated by the structure of the bands (one P and one R branch). Now it is known that both states dissociate into normal ^2P halogen atoms (the lower probably into $^2P_{1\frac{1}{2}}+{}^2P_{1\frac{1}{2}}$, the upper certainly into $^2P_{1\frac{1}{2}}+{}^2P_{\frac{1}{2}}$). According to the rules of Wigner and Witmer, it can be shown that two normal halogen atoms can give three $^1\Sigma$ states, namely two $^1\Sigma_g^+$ states and one $^1\Sigma_u^-$ state. The normal molecular state can in all probability be identified with one of the two $^1\Sigma_g^+$ states. Now a $^1\Sigma_g^+$ state can combine spectroscopically with another $^1\Sigma$ state only if the latter is of the $^1\Sigma_u^+$ type. Since no such state can be derived from normal atoms, and since the upper level of the halogen bands certainly *is* derived from normal atoms, it is evident that the bands cannot be of the $^1\Sigma \leftarrow {}^1\Sigma$ type. (The same conclusion would be reached if we assume $^1\Sigma_u^-$ for the normal state; this assumption is however almost certainly not appropriate.)

The upper state must then be a state of some kind other than $^1\Sigma$, fulfilling the following conditions: (1) it must be derivable from normal atoms; (2) it must be capable of combining spectroscopically with the $^1\Sigma^+$ normal state, giving a P and an R branch. The only state which fulfils these conditions is a $^3\Pi_{0u}$ state. We must, however, assume that only half of the rotational levels of the $^3\Pi_0$ state are active (in an ordinary $^3\Pi_0$ state, there are two closely adjacent rotational levels for each value of J). This at first seemingly arbitrary assumption is made plausible by a consideration of the fact that the dissociation energy of the electron level in question is of the same order of magnitude as the energy of coupling between the L and S vectors in the halogen atom. Under these circumstances the two sets of rotational levels of $^3\Pi_0$ may behave as if belonging to two separate electron levels, which we shall call 0^+ and 0^-. The halogen band can be interpreted by assuming that only combinations with the 0^+ level are observed. As for the 0^- level, it may be that it has a very small dissociation energy so that it gives only a continuous band spectrum, or it may be that its combinations with the normal state (Q branches only, they should be) are weak.

A consequence of the above interpretation is that the excited state of the halogen bands should be paramagnetic. This is in harmony with certain magnetic phenomena observed with these bands.

ROBERT S. MULLIKEN

University of Chicago,
Ryerson Physical Laboratory,
Fellow of the John Simon Guggenheim Memorial Foundation, now in Leipzig.

June 14, 1930.

Double Crystal Analysis of Scattered X-rays

A series of double crystal experiments has been completed to determine accurately the magnitude of the Compton shift. In order to do this, the angle of scattering was made as near to 180° as possible, so that variations in the scattering angle would result in small variations of the wave-length change. A metal x-ray tube of small diameter and with two

aluminum windows 0.05 mm thick was used. In a typical run, this tube carried 70 m.a. at 50 K.V., though occasionally higher currents were used. The x-rays passed through one aluminum window and were incident upon a large block of graphite placed four mm from that window. X-rays scattered from the graphite passed back through this window, and emerged from the other window on the opposite side of the tube, after which they were limited by two lead slits before striking the first crystal. This means that the x-rays were scattered at nearly 180°. The direct beam of x-rays emerging from the second window was carefully shielded, so that the only x-rays reaching the first crystal were those scattered by the graphite or by the thin windows. A test showed that no x-rays were scattered by the windows themselves.

The x-rays, after having been limited by the slits were reflected by two calcite crystals, set at the proper angle. Those x-rays, which were reflected from the second crystal, entered a carefully shielded ionization chamber, filled with methyl bromide. The amount of ionization produced at various angles of the second crystal was measured by means of an electrometer system having 6000 mm/volt sensitivity and about 35 cm capacity. The two crystals used were polished and gave a rocking curve in the parallel position, which was 20 seconds wide at half maximum.

Five different spectra were taken to determine the position of the Mo$K\alpha_1$ modified line. The $K\alpha_1$ and $K\alpha_2$ lines of the modified beam were clearly separated. Flourescent rays from Mo were used to determine the position of the unmodified $K\alpha_1$ line. The value of $d\lambda$ obtained was 0.04721A with a probable error of ± 0.00003A, on the basis of D (calcite) $=3.02904$.

The effective angle of scattering was calculated from the geometry of the slit- window system by dividing the target face into segments of area, the scattering block into small volumes and evaluating the angle between each area and each volume. The extreme values of the scattering angle ϕ were 153° and 175°. The value of 1-cos ϕ determined in the above manner was 1.9479. It is estimated that this value is accurate to ± 0.003. From the equation $d\lambda = (h/mc)$ (1-cos ϕ), one calculates for h/mc the value 0.02424 ± 0.00004A. This may be compared with 0.02417A, the value for h/mc when the mass of the electron is deduced from spectroscopic determinations, and with 0.02428A, the value for h/mc when the mass of the electron is deduced from deflection methods.

NEWELL S. GINGRICH

Ryerson Physical Laboratory,
The University of Chicago,
June 24, 1930.

A Remark on the Paper of R. C. Tolman: "Mechanical Treatment of Temperature Distribution in the Case of Radiation."

R. C. Tolman points out that heat, like every other form of energy, possesses weight, and that therefore gravitation must have an influence on the distribution of temperature throughout a system which has come to thermodynamic equilibrium. Tolman here observes: "The discovery of a dependence of equilibrium temperature on gravitational potential must be regarded as something essentially new in thermodynamics."[1]

As against this I must remark that similar ideas have previously been expressed by myself.[2] In the publication referred to I gave some formulae, which differ from the corresponding ones given by Tolman only in some unessential details.

WILHELM ANDERSON

Tartu-Dorpat (Estonia).

[1] Richard C. Tolman, Phys. Rev. **35**, 904 (1930).

[2] Wilhelm Anderson, Über den Samazustand "ertser Art" und "zweiter Art," Zeits. f. Physik **58**, 440 (1929).

A Remark on the Foregoing Letter of W. Anderson

The Editor of the Physical Review has been good enough to send me a copy of the preceding letter before publication, and Dr. Anderson has also himself kindly sent me a reprint of the article to which he refers. In this article Dr. Anderson has indeed expressed the opinion that the weight of energy should itself lead to a temperature gradient, and has thus given qualitative expression to an idea, which I believe to be essentially cor-

rect. Nevertheless, the quantitative implications of this idea can be ascertained with certainty only by a careful analysis in which the phenomena of gravitation are treated by the methods of general relativity. Such an analysis, however, is not presented by Dr. Anderson and I find myself unable to agree with the quantitative conclusions which he does obtain.

In considering the case of a system of gaseous molecules subjected to the action of gravity, Dr. Anderson does not make use of the idea that heat has weight, and comes to the conclusion that the temperature would fall to the absolute zero at levels too high for the molecules to obtain sufficient energy to reach. I should maintain on the other hand that in a treatment of thermodynamic equilibrium it was incorrect to consider the molecules separately from the radiation with which they are in equilibrium and that this radiation would have a finite temperature even at levels too high for the molecules to reach. Thus in the case of a spherical distribution of a perfect fluid, which could consist of molecules and radiation at lower levels and of pure radiation at higher levels, I should maintain that the temperature gradient would be given at all levels by my equation (54, loc. cit.)

$$\frac{d \log T_0}{dr} = -\frac{1}{2}\frac{d\nu}{dr} \tag{1}$$

and that there would be no discontinuity or drop to the absolute zero at levels too high for the molecules to reach.

In considering the case of pure radiation, Dr. Anderson does make use of the idea that energy has weight and proceeds in a manner in somewhat closer agreement with that which I should consider correct. Nevertheless, I believe that the non-relativistic treatment which he gives not only involves serious limitations but leads as well to a result which is essentially incorrect.

As to the limitations, it should be noted that this final result is expressed in terms of the quantities temperature T, height H, and gravitational acceleration g, which he does not interpret from the standpoint of the relativistic theory of gravitation. In place of his undefined quantity T he would presumably be willing to use the proper temperature T_0 which can be definitely defined as that measured by a local observer, but the ideas of height H and gravitational acceleration g are necessarily restricted in their significance to fields weak enough so that the Newtonian treatment of gravitation becomes a correct approximation and this greatly limits the generality of his result.

Turning now to the correctness of the actual result which he does obtain for the temperature gradient in a field of radiation subjected to gravitational action, namely,

$$\frac{dT}{T} = -\frac{3}{4}\frac{g}{c^2}dH \tag{2}$$

we must compare this with the approximate result which can be obtained from my Eq. (1), when the gravitational field is weak enough so that the Newtonian treatment can be to some extent introduced as a first approximation. Under such circumstances we can then approximately identify the coordinate r with the height H and approximately replace the right hand side of the equation by $-g/c^2$, where g is the acceleration that would be experienced by a *slow moving* particle in the field in question. We thus obtain the different result

$$\frac{dT_0}{T_0} = -\frac{g}{c^2}dH \tag{3}$$

The incorrect factor 3/4 appearing in Dr. Anderson's Eq. (2) is connected of course with the well-known fact, verified by the bending of light in the gravitational field of the sun, that the Newtonian approximations do not lead to correct results even in weak fields when particles are considered which are moving with velocities in the neighborhood of that of light.

At first sight it might appear as if the difference between the two formulae was an unessential detail, as suggested by Dr. Anderson. With this, however, I cannot agree since as shown in my article the formula (3) applies to matter in a weak gravitational field, and it would certainly be a thermodynamic catastrophe if a different formula (2) had to be applied to radiation, since this would force us to the conclusion that matter and the radiation in contact with it at a given level had to have *different* proper temperatures in order to be in equilibrium.

In conclusion, I am very grateful to Dr. Anderson for informing me of his earlier expression of the idea that the weight of energy should lead to a temperature gradient. Since I do not agree, however, with the con-

clusions as to temperature gradient drawn by Dr. Anderson and do not know of any other general and coherent treatment of the thermodynamic consequences of this idea, I hope Dr. Anderson will understand why I still feel inclined to maintain that the discovery of the *correct* dependence of equilibrium temperature on gravitational potential must be regarded as something essentially new in thermodynamics.

Raman Spectra of Geometric Isomers

An investigation of the Raman spectra of the geometric isomers, ethyl fumarate and ethyl maleate, has disclosed a difference between them. In the spectrum of ethyl maleate we find a broad diffuse band at 4693A to 4699A. In the case of ethyl fumarate, the band is replaced by two distinct lines at 4692A and 4698A. The frequency difference between modified and unmodified lines for the first case is from 1636 cm^{-1} to 1683 cm^{-1} and for the second case, 1633 cm^{-1} and 1661 cm^{-1}. It has been suggested by others that a shift of about 1600 wave numbers is associated with the vibration frequency along a carbon oxygen double bond. In the accepted structural formulae of the two esters,

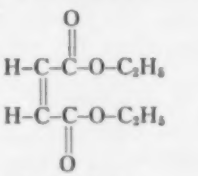

ethyl maleate

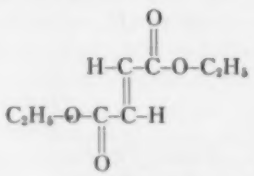

ethyl fumarate

the only C=O double bonds are exterior to the chain. In the case of the maleate, the C=O double bonds are not symmetrically arranged with regard to either the double bond connecting the two chains, or the center of mass of the molecule. In the fumarate the C=O double bands are symmetrically arranged with regard to this bond, which is also the center of mass of the system. In the spectrum of the maleate, the vibration along the two C=O double bonds may give rise to the broad band, while in the fumarate, they apparently give the separate lines.

The average value of the frequency shifts for the other lines common to both substances are,

$\Delta\nu = 865, 1169, 1212, 1732, 3033, 3061\ cm^{-1}$.

The fumarate has in addition two very faint lines corresponding to a shift of 888 and 1361 cm^{-1}.

C. F. FOLLIOTT
Rensselaer Polytechnic Institute
Troy, New York
June 13, 1930.

A Method Offered as a Means of Computing Planck's Constant without Involving the Charge on the Electron

One notes that, numerically, the magnetic moment of an electron in ergs per gauss is equal to its charge in coulombs:

$3\frac{1}{2}he/4\pi mc = e/c = 1.59 \cdot 10^{-20}$; whence

$3\frac{1}{2}h/4\pi = m$ or

$h = 4\pi/3\frac{1}{2}$.

Inserting the spectroscopic value of m, $0.9035 \cdot 10^{-27}$, one finds that $h = 6.555 \cdot 10^{-27}$ erg sec. To make the units cancel properly, one must give the spin vector the dimensions of seconds per centimeter squared, or time per unit area, dimensions which do not seem to have any obvious physical meaning. However, it passes the bounds of plausibility that the magnetic moment should be found numerically equal to the charge, or the angular momentum to the mass, without any physical basis. Two such coincidences to several significant figures in a range so enormous would have a vanishingly small possibility of occurring, were there no physical basis for such concordance.

Unfortunately, the units are different even in ultimate rational units, for in this system charge, being a world-invariant, is expressed as a pure number; whereas magnetic moment is not.

One is reminded of the theory that mass is merely the effect of self-inductance or electrical inertia. Thus the mass of the electron might be due to the self-inductance of the current representing the spin, if a spinning electron may be said to constitute a current. Thus the equating of the angular momentum of the electron to its mass is qualitatively reasonable and could doubtless be made quantitatively exact by the use of an appropriate model.

It is to be noticed that $6.555 \cdot 10^{-27}$ erg

sec. as a value of h falls just within the limit of error which Birge allows. If M_h/m_e is taken as 1840 the agreement is better, h equalling $6.552 \cdot 10^{-27}$ erg sec.

As stated, the advantage of this method of calculating h is that it does not involve the charge on the electron, since the value of the mass of the electron may be found without reference to its charge as Houston has done by the relation between the Rydberg constants for hydrogen and ionized helium. Thus we may use this value of h for computing e. According to Birge's article in the first issue of the Physical Review Supplement, by the theory of ultimate rational units, the reciprocal of the fine structure constant equals 137.3, whence, using $6.555 \cdot 10^{-27}$ as the value of h, e is found to be $4.773 \cdot 10^{-10}$ e.s.u. The uncertainty in this value lies entirely in h, and therefore in the experimental value of the mass of the electron. This is about one-twentieth of one percent, and since h occurs under a radical when one solves for e in the fine structure constant equation, the uncertainty in e is only $0.002 \cdot 10^{-10}$.

If the deflection mass instead of the spectroscopic mass of the electron is used, very disparate results are obtained for h and e.

The value of Avogadro's number obtained with the above value of e is identical with Birge's value of N.

It remains then to find some reason for the numerical equivalence of the magnetic moment and the charge of the electron, or of its angular momentum and mass, and the values of some of the more important physical constants may be established with less uncertainty than heretofore.

ALLEN LUCY

Stanford University,
May 15 to June 15, 1930.

Gas Discharge Wave-Length List in Extreme Ultraviolet

We have prepared a list, arranged in order of wave-length, of the published lines in the extreme ultraviolet (λ2500 to λ100) arising from discharges in gases. The elements included are hydrogen, helium, carbon, nitrogen, oxygen, neon, sodium, silicon, argon, and mercury. Thanks to support from the Carnegie Institution of Washington, it has been possible to publish a limited mimeographed edition of the list, copies of which have been sent to a few spectroscopists to whom we thought it might be of particular use. We should be glad to give copies to any others who may write requesting them.

JANET M. MACINNES
JOSEPH C. BOYCE
Palmer Physical Laboratory,
Princeton University,
Princeton, N. J.
June 18, 1930.

BOOK REVIEWS

Einführung in die Wellenmechanik. L. DE BROGLIE. translated (from French to German) by R. Peierls. 219 pages. Akademische Verlagsgesellschaft, Leipzig, 1929. Price RM 13.80 bound.

The discoverer of the wave nature of the electron has written here a clear account of the development of wave mechanics starting with an account of classical mechanics and building on the analogy between the principle of least action and Fermat's principle in geometrical optics. The bulk of the book is occupied with a careful discussion of free motion of a particle and its relation to the wave packets from the standpoint of the uncertainty principle of Heisenberg and Bohr. In the last chapters elementary cases of quantization of energy levels in cases of periodic motion are discussed. There is no treatment of the radiation process nor of equivalence degeneracy in problems involving several equivalent particles nor of electron spin.

E. U. CONDON

Dielectric Phenomena in High Voltage Engineering. F. W. PEEK, JR. Pp. 410, figs. 267. McGraw-Hill Book Co., New York, 1929. Price $5.00.

This is a third edition, the first having appeared in 1915. While the arrangement shows the effect of growth, involving some repetition, yet it has been thoroughly revised and brought up to date and constitutes an authoritative and exhaustive as well as very readable treatment of corona and spark-over phenomena. Mr. Peek is a leader in the field of high voltage engineering, and a large part of the material in the book is taken from his own experiments and those of his associates in the General Electric Company. Corona and spark-over in air, including lightning, are treated with great thoroughness, those in liquids and solids more briefly. The new material added to this third edition includes the results of recent studies of corona, extensive studies of the impulse breakdown of gases and insulation, cathode-ray studies of impulse breakdown in power transformers and other apparatus, and spark-over phenomena at very high voltages. Studies of artificial lightning with the author's five million volt impulse generator are of special interest.

The book contains mainly experimental data, with empirical laws and formulae, and relatively little mathematics.

ALBERT W. HULL

Elements of Electricity. ANTHONY ZELENY. Pp. xxiii+438, 267 figures, 12 appendices, McGraw-Hill Book Co., New York, 1930, Price $3.00.

This excellent elementary text is the outgrowth of many years of teaching the subject of electricity to engineering, premedical and arts students in a first course of college physics. The subject is developed in a large number (30) of short chapters, at the end of each of which are a number of questions, problems and suggested experiments for lecture demonstration. The book is profusely illustrated by line drawings and half tones, including pictures of many of the pioneers in the subject. The appendices contain tables of numerical constants, definitions of electric and magnetic units, collections of laws, important dates, answers to problems, tables of squares, cubes and reciprocals, trigonometrical functions, and logarithms.

The text being designed for a first course, the subject is developed with the minimum of mathematical detail, no analysis more advanced than elementary algebra and trigonometry being used. The electron theory is introduced in the second article, and the subject is treated from this point of view throughout. After a brief discussion of electric charges and electric forces in the first chapter, the subject of magnetostatics is taken up, after which electrostatics is treated in more detail. The characteristics of the transformer and the subject of the generation and transmission of electric power are dealt with more extensively than in the usual elementary text, and chapters are devoted to discharge in gases at low pressure; measurement of

velocity, charge, and mass of electrons, protons and isotopes; production and detection of electromagnetic waves; electrical communication; and atmospheric electricity.

The outstanding feature of the book is the adoption by the author of modern points of view which have been all too slow in finding their way into elementary texts. Consequently the student does not have to "unlearn" much of what he reads before being able to advance further in the subject. This attitude is well exemplified by the author's sensible treatment of the ether. While not discarding the term itself, he points out the difficulties which have led to the abandonment of the old elastic solid medium, and makes clear that the subject can be treated without any reference to the ether, a form of treatment which he employs throughout. Again he emphasizes the importance of the elementary electric and magnetic fields associated with each electron and proton, as against the concept of the resultant field. Altogether too few writers seem to recognize the fact that "except in electrostatics and magnetostatics) it is these elementary fields which are fundamental and not the resultant field. Lack of recognition of this important fact can all too easily lead to grievous errors.

In his treatment of currents in metallic circuits the author takes the direction of flow of electrons as fundamental instead of that of the current. Whether this is pedagogically advantageous or not seems somewhat questionable to the reviewer, since it is likely to cause confusion in determining the direction of the magnetic field due to the current. In dealing with induced electromotive forces the author explains how the field of an accelerated electron urges neighboring free electrons in the opposite direction. This gives the student a picture of the mechanism of induction far superior to the usual treatment.

While certain minor details may be criticized, the book as a whole appeals very strongly to the reviewer as one which will give the elementary student an excellent foundation in the subject of electromagnetism. It is well printed, the type being of sufficient size to facilitate reading.

LEIGH PAGE

The Size of the Universe. LUDWIG SILBERSTEIN. Pp. viii+215, figs. 11. Oxford University Press, London 1930. $3.50.

In this book Dr. Silberstein reexpresses and extends his previous treatment of the determination of the curvature radius of spacetime. The treatment presupposes the de Sitter line element for the universe in a static form, and makes no assumption as to a greater inherent probability of receding rather than approaching objects, in contradistinction to the treatment of Weyl and the corresponding non-static form for the de Sitter line element of Robertson. The estimates of radius are then based on correlations between the radial velocity and distance obtained from the consideration of five different groups of celestial objects. The groups used together with the varying values obtained for the radius were as follows:

a. Eighteen globular clusters and the two Magellanic Clouds, 3.61×10^7 parsecs.
b. Thirty-eight spiral nebulae, 7.32×10^8 parsecs.
c. Twenty-nine cepheid variables, 1.46×10^8 parsecs.
d. Thirty-five O-stars, 1.58×10^8 parsecs.
e. Four hundred and fifty-nine stars from Young and Harper's list, 1.96×10^8 parsecs.

The most recent Mount Wilson results, of Hubble and Humason, showing a linear relation between apparent velocity of recession and distance of the extragalactic nebulae out to the enormous range of approximately 2.5×10^7 parsecs, were not available to Dr. Silberstein at the time of writing. In view of these facts, however, it would now appear to the present reviewer that cosmologies such as Silberstein's which do not expressly take account of the exclusively recessional motion of all the most distant objects would have to be superseded. In addition, it would seem that the use of stars within our own galactic system would have to be abandoned in favor of extragalactic objects for any form of cosmological determination.

Dr. Silberstein expresses throughout the book a most violent and unnecessary antipathy to the Einstein line element for the universe. This antipathy leads him to devote a whole chapter to a satiric and unjustified attack on the work of Hubble, for the sole apparent reason that Hubble has once made an estimate of the average density of matter in the universe which

could then be inserted in Einstein's formula for the radius of the universe. As a matter of fact, the work of Hubble and his collaborator Humason is by far the most important of all the observational contributions to the problems of cosmogony that have been made, and the estimate of mean density which he obtained is of great interest in interpreting the new non-static line element which now appears to be more satisfactory for cosmological speculations than either that of de Sitter or of Einstein.

The book exhibits a wealth of mathematical erudition and is written in a pungent and often illuminating style, although sometimes the style becomes perhaps too extravagant as for example in the following passage:

"If $a = r^*$, we have $\theta = \infty$, and, as we see directly from (108), each star will move uniformly on a straight line, utterly asocial, as it were, that, is, disregarding the presence of all other members of this galactic community. Thus, if their instantaneous velocities are haphazard in size and direction, the crowd will sooner or later be scattered to the four winds as in spite of all visual appearances, there is nothing to hold them together. And the more so, if the galaxy has swollen up beyond that critical radius of its mass total, the orbits then degenerating, by (109), into hyperbolic branches. Is in the wording of these results an illusion implied to communities of humans, a score or so of Nation-Galaxies, now stiffly coherent, now torn asunder, not only by foreign interference but as often by internal strife, with the greed and lust of power of the 'upper thousand' to urge the territorial expansion (growing a), and a huge majority of what some modern sociologists† refer to as the 'international mob,' but too eager to profit by every tumult, to tear down all social bonds, to set out on world-wide vagabondage, and mingling with deserters of other galaxies, sweep down every civilization, like the sand-laden winds of Sahara obliterate every hillock or oasis casually formed of stray particles through long years of slow and patient toil? I prefer to leave this question to my readers, the more so as I am the last man to desire to undermine their possibly strong confidence in a steady evolution and betterment of assemblages, both human and celestial, in an ever-mounting 'progress,' that is, as opposed to the hurricane-like 'cycloism' which is (not without weighty reasons) advocated by the aforesaid group of social philosophers. At any rate, some time spent now and then on such comparisons will not be entirely lost, provided that these are tempered by caution and self-criticism, and not poisoned by passion."

RICHARD C. TOLMAN

Grundzüge der theoretischen und angewandten Elektrochemie. GEORG GRUBE. Pp. xii+495, figs. 165. Published by Theodor Steinkopff, Dresden und Leipzig, 1930. Price bound, RM 30.

This treatise will be of treat interest to chemists and can be highly recommended to their attention. The author gives a clear and adequate account of theoretical electrochemistry in the first four chapters while he devotes the eight remaining chapters to numerous technical applications. The style is clear and the point of view is strictly up-to-date. It is a very satisfactory book.

F. H. MACDOUGALL

† Namely, the advocates of the theory of *social cycloism*. See a very interesting booklet on *Sozialphilosophie*, by Prof. L. Gumplowicz, Innsbruck, 1910.

PROCEEDINGS

OF THE

AMERICAN PHYSICAL SOCIETY

MINUTES OF THE ITHACA MEETING, JUNE 19–21, 1930

The 165th meeting of the American Physical Society was held in Ithaca, New York on Thursday, Friday and Saturday, June 19, 20 and 21.

The Council authorized a $1.00 registration fee to be collected from the members attending this meeting.

The scientific sessions were all held in Rockefeller Hall. The presiding officers were Herbert E. Ives, John T. Tate, Dayton C. Miller, Ernest Merritt and Karl T. Compton.

On Wednesday, June 18, the Society was invited to be the guest of The Corning Glass Works for luncheon and an inspection trip through the Glass Works. There were 220 present at the luncheon at which we were honored by the presence of the Honorable A. B. Houghton.

On Thursday morning, June 19, from 10 a.m. to 1 p.m. the regular program for the reading of the thirty-three contributed papers was held. On Thursday afternoon a picnic was held at Buttermilk Falls and was attended by 247 persons.

On Friday morning, June 20, at 10 o'clock there were two invited papers on Astrophysics: S. A. Mitchell, Director, McCormick Observatory, University of Virginia, "Atomic Structure under Conditions of Temperature and Pressure Found at the Sun's Surface" and J. Q. Stewart, Princeton University Observatory, "The General Problems of Astrophysics with Special Reference to the Opacity of Gases." On Friday afternoon at 2 o'clock Sir William Bragg delivered an address on "Faraday's Diary." The attendance at this meeting was over 500. Among those attending this lecture were the delegates to the convention of Colloidal Chemists being held in Ithaca at the same time.

On Saturday morning, June 21, there were invited papers by F. Zwicky on "Secondary Structure of Crystals" and Arthur H. Compton on "X-ray Scattering and Atomic Structure."

In the afternoons of Thursday, Friday and Saturday informal conferences were held on the following topics: wave mechanics, dielectrics, biophysics, ionic and electronic emission, luminescence, astrophysics, electrons in metals, physical constants, molecular spectra, nuclei, quantum theory, x-rays and radio waves.

The delegates and their friends were housed in Risely Hall, one of the dormitories of the University. They all dined together in the beautiful dining room of this hall thus affording a most satisfactory opportunity to those attending the meeting to get together socially.

Meeting of the Council: At its meeting held on Friday morning, June 20, one person was elected to fellowship, one was transferred from membership to fellowship and nineteen were elected to membership. *Elected to Fellowship:* William Albert Noyes Jr. *Transferred from Membership to Fellowship:* J. J. Weigle. *Elected to Membership:* Warren F. Anderson, W. E. Bahls, Earle M. Bigsbee, Harry F. Blake, Charles P. Boner, Henry A. Boorse, Malcolm G. Colby, Ching Hsien Li, David Mann, F. L. Mears, Emerson M. Pugh, Leo J. Rysko, George H. Shortley Jr., Charles W. Sidney, Lewis K. Sillcox, Roger S. Strout, John H. Teeple, J. E. White, and Allan Williams.

The following resolution was passed by the Council and acclaimed by unanimous vote at the regular session of the Society on Saturday morning:

> "That on behalf of the Council and of the membership of the American Physical Society we express to the local committee on arrangements, and to all those who assisted them, our great appreciation of the cordial hospitality and the splendid provisions they have made to make this first summer meeting of the Society so enjoyable and successful. We recall with pleasure that the Physical Review as well as the Society of Sigma Xi had their birth on this campus and we begin to appreciate this genius for giving new movements a vital beginning."

The regular program of the American Physical Society consisted of 33 papers. Numbers 15, 25, 28, 32, and 33 were read by title. The abstracts of these papers are given in the following pages. An **Author Index** will be found at the end.

W. L. SEVERINGHAUS, *Secretary*

ABSTRACTS

1. A new type of glow-discharge tube. HERBERT J. REICH, *University of Illinois.*—Several types of glow-discharge tubes are somewhat limited in their field of usefulness by the fact that the extinction potential is considerably lower than the ignition potential, making it difficult to control or stop the current after discharge commences. This difficulty may be overcome by incorporating an electron gun in the tube, and shooting a stream of electrons at high velocity between or through the glow electrodes. The discharge may thus be completely controlled at all times by a very small variation in the potential of the control electrode of the electron gun. A study of the characteristic curves of such a tube reveals a number of very interesting operating characteristics.

2. Preliminary measurements of the mean free path of potassium atoms in nitrogen. J. J. WEIGLE AND M. S. PLESSET, *University of Pittsburgh.*—The method of Taylor (Zeits. f. Physik **57**, 242 (1929)) for the detection of beams of potassium atoms was used for a direct determination of their mean free path. A steel furnace with a single slit contained the potassium and was heated to about 150°C. At a distance of 10 cm a tungsten filament parallel to the slit, and surrounded by a slotted brass cylinder was used as a detector. The potassium atoms impinging on the hot filament are ionized and drawn to the cylinder by a suitable difference of potential. This positive ion current was measured as a function of the pressure of nitrogen filling the space between the filament and slit. Nitrogen pressures ranged from 10^{-2} to 10^{-5} cm of mercury. These ion currents are given by the equation $I = I_0 e^{-x/\lambda(p)}$ where I_0 is a constant, $\lambda(p)$ the mean free path at a given pressure p, and x the distance between the slit and filament. As λ is a known function of the average of the diameters of the potassium atom and nitrogen

molecule, this average was obtained from our measurements which gave values between 3×10^{-9} and 5×10^{-9} cm. These results are unexpectedly small. Experiments with a different apparatus are contemplated to disprove or confirm these preliminary results.

3. Organic reactions in gaseous electrical discharge. ERNEST G. LINDER, *Cornell University.*—A study of electrical discharge in a series of straight chain paraffin hydrocarbons indicates that the phenomenon is similar to that of electrolytic conduction in liquids, in so far as the amount of reaction (i.e., the amount of hydrogen liberated) appears to be proportional to the current, and independent of vapor pressure and voltage. There seems to be a simple relation between molecular size and the amount of hydrogen liberated.

4. On the recombination of electrons with caesium ions. E. H. KURTH, *California Institute of Technology.* (*Introduced by F. Zwicky.*)—An apparatus was constructed in which electrons emitted from a caesium-on-tungsten oxide surface could be accelerated into an equipotential inclosure. A beam of caesium ions generated by a tungsten filament source and projected through the electron atmosphere in the box was collected on a plate. Electron currents up to 200 microamperes could be obtained with a few volts potential difference to the box. Positive currents were measured down to 10^{-9} amperes. When the electron velocities were varied over the range in which captures by caesium ions might be expected from the work of Davis and Barnes, no measurable decrease in the positive beam current was ever observed. The apparatus is being modified to permit tests for a considerably greater ratio of electron to positive currents.

5. Potential drop-current relations of a Geissler discharge from a hollow cathode. C. H. THOMAS, *Westinghouse Lamp Co., Bloomfield, N. J.*—When a cold electrode, drilled to a depth 1/2 inch with a drill 0.076 inch in diameter was used as a cathode in neon gas at pressures between 5 and 70 mm with electrode separation of 15 mm the cathode glow concentrated almost entirely in the hole. Under these conditions the potential drop-current curve for a thorium cathode shows a maximum in potential drop at a current of about 25 milliamperes. This potential drop decreases to a minimum at 50 milliamperes and subsequently attains a second maximum at 80–90 milliamperes. At a higher current a further decrease in potential drop resulted from thermionic emission. Similar curves for iron, misch meal and throium-barium oxide cathodes in neon show a maximum at about 25 milliamperes but beyond that current their similarity to thorium curves disappears. Similar effects were observed in helium and argon. Potential drop-pressure curves for a cathode drilled with a 0.076 inch hole are given as well as the potential drop-size of hole curves which show that there is a minimum pressure for a given size hole in order that the cathode glow will concentrate in the hole. A hollow iron cathode in hydrogen at 23 mm pressure caused a decrease in the potential drop from 440 volts to 405 volts as the current was increased from 30 to 50 milliamperes.

6. The electrodeless discharge in mercury vapor. HERSCHEL SMITH, W. A. LYNCH AND NORMAN HILBERRY, *New York University, University Heights.*—The electrodeless discharge produced in Hg vapor inside the solenoid of a high frequency C. W. oscillator is studied in the pressure range between 0.004 mm and 0.8 mm of Hg. The characteristics of the two types of discharges reported by various authors (MacKinnon, Phil. Mag. Nov. 1929, Brasefield, Phys. Rev. May, 1930) are investigated in detail. Direct experimental evidence is given as to the electrostatic nature of the "glow" discharge and to the electromagnetic nature of the "arc" type discharge. Electromagnetic forces in themselves are found to be insufficient for the formation of the discharge but are sufficient for its maintenance. The "arc" type discharge is shown to be the more familiar ring discharge excited by damped oscillations. The currents in the oscillator coil necessary for the excitation of both types of discharge are examined as a function of the pressure at various frequencies. The curve for the glow discharge has a minimum within the given pressure range while that of the "arc" type discharge has both a minimum and a maximum. The form of these curves would seem to indicate the necessity for a complete revision of the present theories.

7. Effect of collisions on potential distribution in positive ion sheaths. H. P. ROBERTSON AND P. M. MORSE, *Princeton University*.—The potential distribution in a plane positive ion sheath is derived under the assumptions (1) an ion gives up a fraction θ of its kinetic energy at each collision, (2) the ions may be considered as following the lines of force and (3) the density of charge may be taken as i/v where v is the root mean square of the actual ionic velocities. The justification of assumption (2) is based on the considerations of v. Hippel, and that of (3) on the approximate agreement of dependence of potential on initial velocity for zero pressure with that obtained by previous workers (Schottky, Epstein, Fry, Langmuir). The rigorous solution of this problem gives the field strength and mean forward kinetic energy of the ions at any point in the sheath. The corresponding problem for cylindrical or spherical cathodes cannot be rigorously solved by the same methods, but can be treated by a method of approximations based on the rigorous solution for the plane case.

8. The Hall effect in tellurium amalgams. P. I. WOLD AND J. M. HYATT, *Union College*.—Certain aspects of the study of the Hall effect in crystalline materials suggested an attempt to make Te-Hg alloys. Amalgams were obtained of about 30% tellurium which were plastic when fresh but which became, in a few hours, quite hard and very friable. The plastic amalgam was placed in a mold as quickly as feasible and measurements on the Hall effect, the specific resistance and the longitudinal effect were started. The Hall effect commenced with very small values and built up steadily for two or three days. The Hall constants, after such time, were as high as 0.9, which is from 100 to 500 times the value when the amalgam was a half hour old. The authors are not aware of any previous case in which Hall effect has grown with time when temperature was constant and as a new phenomenon it seems to be of special interest. X-ray crystal photographs were taken of a sample of the amalgam as soon after making as possible and photographs taken within an hour show crystalline structure apparently as strongly as when two days old. The longitudinal effect started with very low values and increased steadily in about the same way as the Hall effect.

9. Contact resistance and microphonic action. FRANK GRAY, *Bell Telephone Laboratories, Inc.*—A mathematical theory is developed to explain the fact that conductivity of a contact between two carbon spheres changes with the force pressing the spheres together. It is assumed that the surface roughness of the carbon is equivalent to an assembly of minute spherical hills. On account of the elasticity of the material, both the macroscopic area of contact between the spheres and the microscopic areas of contact between the hills increase with contact force. The resulting relation between the contact resistance R and the contact force F is $R = A/F^{1/3} + B/F^{7/9}$ where A and B are constants. The last term of this equation, contributed by surface roughness, is almost the same as the corresponding term of the equation, $R = A/F^{1/3} + B/F^{6/9}$ which was developed by Professor P. O. Pedersen [Electrician, Feb. 4, 1916] on the assumption that carbon is covered with a thin, high resistance film. In other words, surface roughness behaves almost identically with a non-variable, high resistance film. Higher degrees of roughness increase the exponent of the last term. In the limit it becomes unity, and the roughness resistance then varies inversely as the contact force.

10. Contact resistance and microphonic action. F. S. GOUCHER, *Bell Telephone Laboratories, Inc.*—Previous work has shown that the conducting portions of contacts between single granules of microphone carbon are of the nature of carbon and that variations in contact area occur when the contact resistance is varied in a reversible resistance force cycle. An experimental study of the slopes of these reversible characteristics both for single contacts and aggregates shows them to be of the form $R = \text{const}(F)^{-n}$. The exponent n varies from cycle to cycle for equal force limits and the average value depends on the force limits. A maximum mean value independent of the force limits over a wide range, is obtained with the aggregates. This value is in agreement with the exponent in the second term of Gray's equation $R = (A/F^{1/1}) + (B/F^{7/9})$ [previous abstract] which indicates that an aggregate of contacts may, under certain conditions, behave as though it were a single contact between spheres having a rough surface. Values of n less than 1/3 are obtained with both single contacts and aggregates. This is attributed to the effect of cohesive forces the existence of which was demonstrated by the sticking of contacts.

11. Work functions and thermionic and constant "A" determined for thoriated tungsten. W. B. NOTTINGHAM, *Bartol Research Foundation.*—The work function of a type T thoriated tungsten filament was determined with a 3.5 volt accelerating potential by measuring the thermionic current as a function of temperature over the range 1045°K to 1340°K. With the filament activated to give the maximum emission at 1100°K with a 20 volt accelerating potential, the effective work function ϕ' with 3.5 volts was found to be 2.59 volts. From measurements of the current-potential relationship at 1100°K, it was found that the 3.5 volt accelerating potential had reduced the work function by $\Delta\phi = 0.56$ volt. The work function at *zero field* is $\phi' + \Delta\phi = \phi_0 = 3.15$ volts. Using this value of ϕ_0 and the measured current, the thermionic constant is $A = 59.0$. Measurements made with a thorium covering *thicker* than that required to give the maximum emission as above, gave $\phi' = 2.8$ volts with 3.5 volts accelerating potential, $\Delta\phi = 0.3$ volt and therefore $\phi_0 = 3.1$ volts and $A = 56.0$. These data indicate that abnormally low values of A previously reported can be accounted for by the fact that the work functions were not measured at zero field. Langmuir found the contact potential between thoriated tungsten and clean tungsten to be 1.46 volts. Accordingly the work function of thoriated tungsten should be 4.53—1.46 = 3.07 volts which agrees with the above.

12. The relation between the number of electrons ejected photoelectrically from the cathode and the time lag of the spark. JOHN A. TIEDEMAN, *University of Virginia.* If the ions usually present in a spark gap in ordinary air are carefully removed by sweeping potentials an impulsive field of 75,000 volts/cm can be applied for at least 10^{-6} sec. without electrical breakdown. Strong ultraviolet irradiation of the cathode reduces the time lag to less than 10^{-8} sec. By means of biasing potentials and a steady source of ultraviolet light electrons could be liberated from the cathode only during the existence of a high electric field. The time lags were measured by the Lichtenberg figure method (Pedersen, Ann. d. Physik **71**, 317 (1923)). By controlling the intensity of ultraviolet light on the cathode and the magnitude of the applied surge potential the time required for a known number of electrons to start the discharge in a field of known strength could be obtained. Between a Zn cathode and a steel anode spaced 2 mm electrons were ejected from the cathode at the rate of one in 3.3×10^{-9} sec. in an impulsive field with a maximum value of 75,000 volts/cm applied by a second spark, producing a time lag of 1.5×10^{-8} sec. while under the same conditions one electron per 9.5×10^{-9} sec. gave a time lag of 2.2×10^{-8} sec.

13. Inhibition of photoelectric emission by near infrared light. A. R. OLPIN, *Bell Telephone Laboratories, Inc.*—The response to potassium photoelectric cells to white light is greatly increased when small amounts of bromine or iodine vapor are distilled onto the cathode surface. Spectral distribution curves for cells so treated show a general increase in the response to light of all wave-lengths and a more marked increase to light at both ends of the visible spectrum. There is no measurable electron emission when the cells are irradiated with infrared light obtained by passing white light of color temperature 2848°K. through a #87 EK Wratten filter. If, however, the cathode already is emitting electrons under excitation with visible light when irradiation with infrared light occurs, a marked *decrease* in the photoelectric current is noted. Investigation shows that this decrease occurs only in the spectral regions where abnormally large increases are observed without the infrared light, and may amount to well over fifty percent for certain wave-lengths. Data showing some of the properties of this new effect, which has been observed for both potassium and sodium cells, are included. The phenomenon is closely analogous to the extinction of phosphorescence and destruction of the latent image on photographic plates by infrared radiations.

14. On chain reactions caused by physical structure. N. RASHEVSKY, *Westinghouse E. and M. Co., East Pittsburgh.*—In a previous paper (Zeits. f. Physik **59**, 558 (1930)) it has been shown that when a substance is formed as a result of a reaction in a solution and is itself soluble in the surrounding liquid, this substance may exist as a separate phase, in shape of small drops, provided the size of the drops is above a certain critical value. Such drops cannot be formed spontaneously, but will continue to grow if brought from outside into the liquid. In the present paper, the case in considered, that the drop is constituted of several substances. Due to the interaction of the phenomena of diffusion and dissolution, the formation of the different sub-

stances will follow a definite order. Below a certain size, the drop cannot exist at all. Above it, it can be constituted only by one substance. With increasing size, the number of substances constituting the drop, increases. Applications to biological phenomena are discussed.

15. The corresponding state of maximum surface tension of saturated vapors. J. L. SHERESHEFSKY, *Mellon Institute of Industrial Research.* (*Introduced by Paul D. Foote.*)—The surface tension of a liquid is given by the expression (1)$\sigma=(rh/2)(\rho_1-\rho_2)$, where h is the height of rise in a capillary of radius r, and ρ_1 and ρ_2 the densities of the liquid and vapor respectively. Writing the equation in the form $\sigma_r=rhe_1/2-rhe_2/2$ and applying Antonow s rule, $rhe_1/2$ may be conceived as the true surface tension of the liquid, σ_r the relative surface tension, and (2)$\sigma_r=rhe_2/2$ where $rhe_2/2$ is defined as the surface tension of the vapor. Combining (1), (2), McLeods equation $[\sigma_r=c(\rho_1-\rho_2)^4]$ and Goldhammer's equation $[\rho_1-\rho_2=a(1-T/T_c)^{1/3}]$, an expression is obtained relating the surface tension of the vapor with the temperature, (3) $\sigma_v=K(1-T/T_c)\rho_2$. It was found that σ_v goes through a maximum in the neighborhood of the critical temperature. Differentiating (3) the position of the maximum point is given by

$$\frac{d\log\rho_2}{dT}=\frac{0.4343}{T_c(1-T_m/T_c)}. \tag{4}$$

By means of equation (4) the values of T_m/T_c for nineteen different substances were calculated and found to equal 0.91.

16. Fundamental correspondences between geometry and thermodynamics. JOHN Q. STEWART, *Princeton University.*—Continuing interpretation of thermodynamics as a physical symbolic logic (Phys. Rev. **34**, 1289, (1929), etc.), the following equivalences exist between Euclidean plane geometry and the thermodynamics of reversible systems having two degrees of freedom. The *vector* corresponds to the working body; its magnitude, r, to volume, v; x-component to internal energy, U; y-component to entropy, S; negative slope, $-m$, to temperature, T. Summing x and y components, respectively, when vectors are added, corresponds to conserving energy and entropy. The Pythagorean relation, $x=(r^2-y^2)^{\frac{1}{2}}$, expresses the "equation of state" for the Euclidean plane. The corresponding special thermodynamic equation $U=(v^2-S^2)^{\frac{1}{2}}$, implies reckoning U, v, s, in absolute units, for dimensional equivalence. In general, when U_2 replaces S_1, and $-S_2$ replaces U_1, while v remains unchanged, $-1/T_2$ replaces T_1, and all relations of thermodynamics are preserved. This is on form of Lunn's important "principle of thermodynamic duality." (A. C. Lunn, Phys. Rev. **15**, 269 (1920)). Evidently it corresponds to the geometrical symmetry accompanying rotation of axes through $\pi/2$. The general background of these studies is the philosophy of Leibniz. His logic possesses surprisingly close affiliations with thermodynamics.

17. Entropy, elastic strain and the second law of thermodynamics, the principles of least work and of maximum probability. W. S. KIMBALL, *Michigan State College, East Lansing, Michigan.*—By relying on the geometrical expression for weight, $W=N^N(r_1r_2\cdots r_N)$, and taking strains to include unit extensions in velocity and momentum space as well as ordinary space, a relation is established between entropy and the total strain: $S=kY$, $Y=\log W$, where S is the entropy, k is Boltzmann's constant, Y the total strain and W the *apriori* probability. The Lagrange multiplier method is applied to statically indeterminate frames as well as gas theory, and shows in both cases that the principle of least work, or internal energy, is equivalent to the principle of maximum entropy, probability and strain. Furthermore the equilibrium equations which by the Lagrange method determine the equlibrium state are shown to represent balance between true stress and strain both in gas theory and in the statics of indeterminate frames, revealing the operation in these two domains of the same identical principles (not an analogy). The magnitude of the stress and strain acting in momentum space to maintain equilibrium are calculated for the case of perfect gas at temperature T, the stress being given by $(2\pi e)^{\frac{1}{2}}kT$, and the strain by $(2\pi e)^{\frac{1}{2}}/n$, and the modulus of elasticity is the familiar isothermal bulk modulus p. The outstanding experimental verification of the theory is the second law of thermodynamics. The automatic increases of entropy which it represents are explained as due to increased strain (in momentum space as well as ordinary space) under action of corresponding stresses, rather than as in statistics by the unsatisfactory ergodic hypothesis.

18. Energy changes related to the secondary structure of crystals. F. ZWICKY, *California Inst. of Technology.*—Theoretical considerations have led the author to the postulate of a secondary structure (II) of large spacing, which is superposed on the primary structure (p) of crystals. According to the theory the II-atoms are usually more densely packed than the p-atoms. It is $|E_\pi| > |E_p|$ where E_π and E_p are the respective atomic energies corresponding to the two structures. The p-atoms are therefore more easily removed from the crystal than the II-atoms. Conditions may be reversed, however, by a plastic deformation inasmuch as this process diminishes $|E_\pi|$ into $|E_\pi'|$ but dos not change E_p. These conclusions lead at once to an understanding of evaporation, etching and certain chemical reaction phenomena involving both perfect and plastically deformed crystals. As a practical criterion of the perfection or imperfection of a lattice the inequalities $|E_\pi'| \gtrless |E_\pi|$ may be used. More detailed considerations are of course required to distinguish crystals of the "metallic" type, which are both macroscopically and microscopically plastic from other types like NaCl which are macroscopically plastic but microscopically brittle. The theory further leads to the interesting conclusion that a voltaic potential difference should be found between II-planes and p-planes a mounting in general to about 0.001–0.01 volts.

19. An x-ray study of the structure of electrets. MAURICE EWING, *University of Pittsburgh. Erie, Pa.*—Electrets were prepared by allowing a molten mixture of rosin, beeswax, and carnauba wax to solidify in a strong electric field, following Adams (Frank. Inst. J. **204**, 469). These were studied by means of a pinhole camera with filtered characteristic radiation from an x-ray tube having a molybdenum target. The patterns obtained all showed three well-defined rings, which indicated spacing of $3.69 \pm .02$A, $4.15 \pm .02$A, and $4.70 \pm .03$A. The 4.15A ring was about three times as intense as the others. When the specimen was set so that the angle between the direction of the x-ray beam and the direction in which the electric field had been applied was zero, each circle was of uniform intensity over its entire circumference; but when this angle was 90°, all circles showed a marked maximum of intensity in the regions in which they would intersect a line drawn through their common center parallel to the direction in which the field had been applied to the specimen.

20. Modified line in scattered x-rays. P. A. ROSS AND J. C. CLARK, *Stanford University.*—With balanced metal foils of silver and palladium in a manner previously described, (Proc. Nat. Acad. Sci. Vol. 9, July 1923; J. A. O. S. Vol. 16, June 1928) an attempt has been made to determine the width and structure of the modified $K\alpha_1$, $K\alpha_2$ lines of antimony scattered from beryllium metal. The differences in transmission between equivalent silver and palladium foils were plotted against scattering angle. With sufficiently narrow slits the differences showed clearly the passage, first of α_2 and then of α_1 past the silver K discontinuity with increasing scattering angle. With present intensity and resolution there is no indication of any step structure or any breadth of line inexplicable by lack of homogeniety of scattering angle in the scattering of antimony $K\alpha_1$, $K\alpha_2$ from beryllium at angles between 55 and 75 degrees.

21. Apparatus for measuring absorption coefficients of soft-x-rays in gases and the absorption in air of the $K\alpha$ line of carbon. ELMER DERSHEM AND MARCEL SCHEIN, *University of Chicago.*—The apparatus consists of an x-ray tube separated by a celluloid window about 2×10^{-4} mm thick from a spectrograph into which gases at various pressures may be introduced. Within the spectrograph beams of different wave-length are isolated by means of a ruled grating. The ratio of the intensity of a given spectral line when the spectrograph is filled with gas at a known pressure to the intensity of the line when the spectrograph is exhausted to a high vacuum is measured by a photographic method. Preliminary results for the mass absorption coefficient (μ/ρ) of air have been obtained for the K_α line of carbon ($\lambda = 44.6$A). An average of 76 measures yielded the value $\mu/\rho = 5350. \pm 53$. This probable error of 1 percent compares very favorably with ionization chamber measurements of ordinary x-rays. Extrapolations of any of the various absorption formulae which are known to hold for ordinary x-rays yield values for the absorption coefficients of nitrogen and oxygen which are higher than the above but nevertheless of the same order of magnitude. The investigation is being continued with the use of pure gases and other wave-lengths.

22. Some measurements of currents through the walls of x-ray tubes. DONALD P. LEGALLEY, W. R. HAM, AND MARSH W. WHITE, *Pennsylvania State College.*—The walls of a Coolidge water cooled x-ray tube were coated with a thin layer of tin foil. The potential of this coating was varied from that of the anode, to that of the cathode in about 48 equal steps. With the walls, and the anode of the tube, at the same potential, surprisingly large currents were found to be flowing through the glass to the coating. These amounted to as much as 1 m.a., and 2 m.a. in most cases, but were found to be as large as 3 m.a. in some cases. As the potential of the walls was increased from the anode to the cathode, these currents were found to drop off rapidly, become negative, and fall to zero as soon as full retarding potential was reached. A wide range of tube voltages, and tube currents were used. Coating currents were plotted against retarding potentials, and reproducible curves secured, in which breaks occurred at certain retarding potentials time after time. It was found that the average values of these breaks corresponded to the values of the energy levels (in equivalent volts) of the material used in the anode of the tube.

23. Luminescence due to radioactivity. D. H. KABAKJIAN, *University of Pennsylvania.*—Results of several investigations on the nature and decay of luminescence due to radioactivity carried on under the direction of the author are reviewed. It is shown that the rise and decay of luminescence in various compounds, including phosphorescent zinc sulphide, cannot be explained on Rutherford's theory of "active centres." The observed facts can be explained qualitatively by assuming that the alpha, beta and gamma-rays produce excited molecules in the luminescent material. Return of these molecules to their initial state of more stable equilibrium results in emission of luminous energy. The rate at which this return takes place depends upon the thermal agitation of the molecules. The decay of luminescence is explained as due, not to the destruction of the hypothetical centres, but to the gradual increase of the absorption constant of the material for the light emitted, as evidenced by its discoloration. The disturbances produced by the exciting rays resulting in discoloration are more stable at ordinary room temperatures than those giving rise to luminescence but not necessarily so at higher temperatures. When a compound whose luminescence has decayed is brought to a temperature which removes discoloration it usually recovers its initial brightness.

24. The average life for ionized helium. LOUIS R. MAXWELL, *Bartol Research Foundation.*—The average life $T_{n,l}$ in energy states to ionized helium have been computed for levels up to $n=60$ by calculating all the transition probabilities from the level concerned. The transition probabilities can be obtained directly from known values of the (matrix amplitude)^2 as evaluated by the eigenfunctions for an electron in a Coulomb field. $T_{n,l}$ was found to increase proportional to n^3 starting with the extremely short time of 1.0×10^{-10} sec. for $n=2$. For other l values this relationship does not always hold but in general $T_{n,l}$ becomes greater for the higher states. T_n (an average mean life l not specified) has the calculated value of 1.3×10^{-10} sec. for $n=2$ which increases to 1.2×10^{-8} sec. for $n=6$. The method for measuring mean lives previously described by the writer (Phys. Rev. **33**, 721, (1928) has been applied to the 4686 series of He II. The displacements were found to become progressively greater in going from the lines 4686 (4→3) and 3203 (5→3) to 2733(6→3) and to 2511(7→3). Assuming that the excited helium ion is produced at a single collision then the lines exhibiting the greater shift must represent longer mean lives, which indicates that the average life becomes greater for the outer levels, in agreement with the theory. The above assumption has been substantiated for the line 4686 from intensity-current measurements.

25. The incomplete partial Paschen-Back effect in copper. J. B. GREEN, *Ohio State University.*—The study of the partial Paschen-Back effect in most elements has been limited to the cases in which the multiplet separation is very small compared with the normal Zeeman separation. Darwin has calculated the Zeeman effect for cases in which the magnetic separation varies from 0 to ∞. His formulas have been applied to Back's measurements on the $^2P^2D$ multiplet of Cu, 5220, 5218, and 5153. These lines, while they show the ordinary characteristics for low fields, have distortions which are due to the small value of the ^2D separation 6.90 cm^{-1} compared with the Zeeman splitting 1.74 cm^{-1}. The wave-lengths calculated on Darwin's theory are

in almost complete agreement with experiment. The calculated intensities cannot be compared since the observed intensities are only estimated, but they show qualitative agreement with experiment.

26. Interference measurements in the first spectra of krypton and xenon. C. J. HUMPHREYS, *Bureau of Standards.*—The wave-lengths of the stronger arc lines of krypton and xenon have been redetermined by the use of fixed etalons. The secondary standards of neon, photographed simultaneously with the spectrum under investigation, were used as a comparison. A sufficient number of krypton lines have been examined to permit fixing the relative values of the $1s$ terms and all the $2p$ and $3p$ terms. The accuracy of the term values is such that the average deviation of calculated combinations from the observed wave-numbers is one part in twenty million. The exact location of the combinations in the infrared region not photographically accessible can now be predicted with certainty. Such lines should prove useful wave-length standards for the infrared region. Further work is contemplated in the examination of the lines for hyperfine structure. It is apparent however from the extremely small variations of the term differences that the intensity of any satellites is too low to affect the wave-lengths. For the two strongest lines in the visible krypton spectrum, for which Perard at the International Bureau obtained wave-lengths 5570.2892 and 5870.9154A., we obtain 5570.2890 and 5870.9153A.

27. Spark spectrum of rhodium. A. G. SHENSTONE AND J. J. LIVINGOOD, *Princeton University.*—In the first spark spectrum of rhodium the following terms have been found: for the low structures, $4d^75s$, ^5F, ^3F, ^5P, among the intermediate configurations $4d^75p$, ^5F, ^5D, ^5G, ^3F, ^3D, ^3G, ^5D, ^5P, ^5S. A number of as yet unidentified levels have also been discovered in the low and middle group. The interval rule holds reasonably well for the low ^5F and ^3F, but not at all for the other multiplets. All are inverted, except the higher ^5D from d^7p, which is reinverted, and ^5F from the same structure which is partially reinverted. Preliminary investigation of the Zeeman effect indicates that the g-values do not coincide with the Landé predictions. Intensities in the multiplets show the same type of irregularity as occurs in the cobalt spark spectrum.

28. The structure of an emission line. FRANK C. HOYT, *University of Chicago.* The structure of an emission line within the frequency range of its natural width is calculated on the basis of Dirac's radiation theory as modified by Weyl. It is necessary to make use of a solution of the perturbation equations which is valid for a time long compared to the life-time of the excited state, which is in accord with the uncertainty principle. The result obtained is that the spectral distribution is that for a classical oscillator with damping constant $\frac{1}{2}A$, where A is the sum of the probabilities of spontaneous transition from the upper level to all states of lower energy.

29. Absorption and collision broadening of the mercury resonance line. M. W. ZEMANSKY, *National Research Fellow, Princeton University.*—With the assumptions that: (1) the half-breadth of the emission line $\Delta\nu_E$ from a resonance lamp is always greater than that of the absorption line, and depends on the vapor density, geometry, and the exciting line; (2) the half-breadth of the absorption line $\Delta\nu_D$ at low pressures and without any foreign gas is the Doppler breadth; (3) all five components of the λ2537 line of mercury are alike both in emission and in absorption;—the absorption for thickness l is calculated as a function of $k(\nu_0)l$ and $\Delta\nu_E/\Delta\nu_D$, where $k(\nu_0)$ is the absorption coefficient for the center of any one of the components. From experimental values, $k(\nu_0)$ is found to be $1.41\times10^{-13}\,N$ where N is the number of atoms per cc. and $\Delta\nu_E/\Delta\nu_D$ is 1.21 in these experiments, 1.6 in Orthmann's, 1.50 in Hughes and Thomas', 1.15 in Kunze s and 1.15 in Kopfermann and Tietze's. The absorption coefficient in the presence of a foreign gas is calculated as a function of the frequency and of $\Delta\nu_C/\Delta\nu_D$ where $\Delta\nu_C$ is the Lorentz collision breadth, and the absorption is calculated as a function of $\Delta\nu_C/\Delta\nu_D$ for the values of $k(\nu_0)l$ and $\Delta\nu_E/\Delta\nu_D$ that hold in these experiments and in those of Orthmann. From experimental values of the absorption of mercury vapor in the presence of H_2, N_2, A, and CO, $\Delta\nu_C$ is found as a function of pressure for each gas. From these curves the effective cross-section is found.

30. Energy distribution in the ultraviolet spectrum of skylight. BRIAN O'BRIEN, *J. N. Adam Hospital, Perrysburg, N. Y.*—Energy distribution in the spectrum of sunlight scattered from the sky was measured by a method previously described (Phys. Rev. **33**, 640 (1929)) from λ4000A to λ2994A and compared to energy distribution in the direct solar beam. For very clear sky the ratio of intensity of sky, 90° from sun 60° from zenith, to intensity of sun is proportional to $1/\lambda^4$ over the above wave-length range. For sky uniformly cloudy showing faint blurr of sun, above ratio is nearly independent of λ, and energy distribution in direct solar beam agrees with that measured on very clear days for the same elevation of sun, even when absolute intensity in direct beam is reduced by clouds to 1/100 that on a clear day. For hazy or slightly cloudy skys ratio of sky intensity to sun intensity increases with decrease in λ but less rapidly than $1/\lambda^4$, the scattering being made up of a molecular and a non-selective term. The values for the energy distribution in the spectrum of direct clear day sunlight λ3300A to λ2903A previously reported, (Phys. Rev. **33**, 1072 (1929)) (J.O.S.A. **20**, 150 (1930)), are thus applicable to sunlight through clouds or haze or scattered by clear or cloudy sky, providing the character of the scattering is taken into account. These results require that both non-selective and molecular scattering occur below the layer of atmospheric ozone, in agreement with accepted values for the height of this layer.

31. Behavior of positive ions in hydrogen. ALLAN C. G. MITCHELL, *Bartol Research Foundation.* In the present experiments, Li or Cs positive ions of various velocities are produced in a tube containing hydrogen molecules. The tube is immersed in liquid air, and the rate of decrease of pressure of hydrogen is measured as a function of the velocity of the positive ions. It is found that with no positive ions entering the tube there is a certain decrease in the pressure of the hydrogen due to its thermal dissociation on the hot filament and its subsequent condensation on the cold walls of the tube. With ions of energies from 15 to 320 volts flowing in the tube the rate of decrease of pressure is greater, showing a formation of some condensible product due to the action of the ions. The rate of pressure decrease with the voltage applied has been found to be proportional to the ion current flowing. The rate per unit current is proportional to the pressure; and the rate per unit current per unit pressure is practically independent of the voltage for Li or Cs ions of energies from 15 to 320 volts. The effect has been shown not to be due to secondary electrons. The number of hydrogen molecules disappearing per positive ion varies from 0.01 to 0.5. No critical voltage at which the effect starts has been found. A detailed account will appear shortly in the Journal of the Franklin Institute.

32. Chemical constitution and association. EUGENE C. BINGHAM AND HOLMES J. FORNWALT, *Lafayette College.* The authors have investigated the fluidities and densities and calculated the associations in several classes of homologous compounds, alcohols, acids, esters, ketones, mercaptans and hydrocarbons. In each case the association decreases as the hydrocarbon chain is increased, but a branched chain lowers the association, and the more, the closer the branch is attached to the middle of the molecule. The association is increased by certain associating groups such as hydroxyl, carboxyl etc. but these are least effective in bringing about association when they are placed at the center of the molecular chain. In the esters the association of different series e.g. the methyl esters, tends toward a definite value as the molecular weight is increased which is of course higher than the value toward which the ethyl esters approach. The association in excess of this minimum of any methyl ester has been found to be lowered quite precisely 46 percent by the addition of the methylene group necessary in going to the next higher member of the series. A recent note in Science indicated that for fifty-seven compounds the average deviation between the observed and calculated values is 0.9 percent.

33. The diffraction of hydrogen atoms. THOMAS H. JOHNSON, *Bartol Research Foundation.* The diffraction patterns which are formed when a very fine circular beam of hydrogen atoms is reflected from a cleaved 100 surface of a crystal of lithium fluoride have been photographed on a molybdenum oxide plate. Various arrangements of the crystal and plate were used. At normal incidence, with the plate perpendicular to the specularly reflected beam, the pattern consisted of two lines intersecting at right angles in the specular beam. These lines were parallel to the rows of similar ions on the surface of the crystal. The patterns for other

angles of incidence in both the 110 plane and the 100 plane have also been photographed and in each case the pattern is a set of conic sections which satisfy the two crossed grating formulae, $\cos\theta_0 - \cos\theta = n\lambda/d$; $\cos\phi_0 - \cos\phi = m\lambda/d$, where θ and ϕ are the angles between the beam and the two sets of lines of similar ions on the surface. The patterns observed correspond to $m=0$, $n=1$ and to $n=0$, $m=1$. The positions of maximum intensity correspond well with the calculated angles for the most probable wave-length in the Maxwellian distribution, if the wave-length is calculated from the velocity by the de Broglie formula, $\lambda = h/mv$.

AUTHOR INDEX

Bingham, Eugene C. and **Holmes J. Fornwalt**—No. 32

Clark, J. C.—see Ross

Dershem, Elmer and **Marcel Schein**—No. 21

Ewing, Maurice—No. 19

Fornwalt, Holmes J.—see Bingham

Goucher, F. S.—No. 10
Gray, Frank—No. 9
Green, J. B.—No. 25

Ham, W. R.—see LeGalley
Hilberry, Norman—see Smith
Hoyt, Frank C.—No. 28
Humphreys, C. J.—No. 26
Hyatt, J. M.—see Wold

Johnson, Thomas H.—No. 33

Kabakjian, D. H.—No. 23
Kimball, W. S.—No. 17
Kurth, E. H.—No. 4

LeGalley, Donald P., W. R. Ham and **Marsh W. White**—No. 22
Linder, Ernest G.—No. 3
Livingood, J. J.—see Shenstone
Lynch, W. A.—see Smith

Maxwell, Louis R.—No. 24
Mitchell, Allan C. G.—No. 31
Morse, P. M.—see Robertson

Nottingham, W. B.—No. 11

O'Brien, Brian—No. 30
Olpin, A. R.—No. 13

Plesset, M. S.—see Weigle

Rashevsky, N.—No. 14
Reich, Herbert J.—No. 1
Robertson, H. P. and **P. M. Morse**—No. 7
Ross, P. A. and **J. C. Clark**—No. 20

Schein, Marcel—see Dershem
Shenstone, A. G. and **J. J. Livingood**—No. 27
Shereshefsky, J. L.—No. 15
Smith, Herschel, W. A. Lynch and **Norman Hilberry**—No. 6
Stewart, John Q.—No. 16

Thomas, C. H.—No. 5
Tiedeman, John A.—No. 12

White, Marsh W.—see LeGalley
Weigle, J. J. and **M. S. Plesset**—No. 2
Wold, P. I. and **J. M. Hyatt**—No. 8

Zemansky, M. W.—No. 29
Zwicky, F.—No. 18